Towards a better understanding of kinetic interactions between microalgae and bacteria : from lab to large-scale high rate algal pond

Solène Jahan

THÈSE DE DOCTORAT

NANTES UNIVERSITÉ
DÉLIVRÉE CONJOINTEMENT AVEC
FLINDERS UNIVERSITY

ÉCOLE DOCTORALE N° 602
Sciences de Ingénierie et des systèmes
Spécialité : *Génie des Procédés et Bioprocédés*

Par

Solène Jahan

Towards a better understanding of kinetic interactions between microalgae and bacteria

From lab to large-scale high rate algal pond

Thèse présentée et soutenue à Saint Nazaire, le 16 septembre 2024
Unité de recherche : Laboratoire GEPEA - UMR CNRS 6144
College of Science and Engineering, Flinders University

Rapporteurs avant soutenance :

Jean-Philippe STEYER Directeur de recherche à INRAE (France)
Marco BRAVI Professeur associé à Sapienza Università di Roma (Italie)

Composition du Jury :

Président :	Jean-Philippe STEYER	Directeur de recherche à INRAE (France)
Examinateurs :	Navid MOHEIMANI	Professeur à Murdoch University (Australie)
	Gustavo Henrique Ribeiro DA SILVA	Professeur à São Paulo State University (Brésil)
	Martin JOHNSTON	Professeur associé à Flinders University (Australie)
	Mariana TITICA	Maître de conférence à Nantes Université (France)
Dir. de thèse :	Jérémy PRUVOST	Professeur à Nantes Université (France)
Co-dir. de thèse :	Howard FALLOWFIELD	Professeur à Flinders University (Australie)

Invité(s) :

Guillaume COGNE Maître de conférence à Nantes Université (France)

"If at first you don't succeed, try two more times so that your failure is statistically significant."

I certify that this thesis:

1. does not incorporate without acknowledgment any material previously submitted for a degree or diploma in any university

2. and the research within will not be submitted for any other future degree or diploma without the permission of Flinders University; and

3. to the best of my knowledge and belief, does not contain any material previously published or written by another person except where due reference is made in the text.

Solène Jahan, 15th June 2024

ACKNOWLEDGEMENT

A PhD is often regarded as a solitary work while it actually involves a significant number of people. I would like to acknowledge all the persons who supervised, examined, taught, experimented, corrected, measured, solved, re-corrected, managed, supported, re-re-corrected, talked, listened and cheered up. Your time and consideration is priceless for me.

First, I would like to acknowledge the reporters Jean-Philippe Steyer and Marco Bravi for the thorough reading and evaluation of my manuscript. Thank you also to Jean-Philippe Steyer for orchestrating the defense as the President of the jury. I am sorry for declining your postdoc offer but I hope that our paths will cross again! I would like to acknowledge as well Gustavo Da Silva, Navid Moheimani and Martin Johnston for accepting to be part of the jury members despite the important jet lag. Thank you for bringing relevant questions during the defense, always with goodwill and conciseness.

I would like to express all my gratitude to my supervisors, Jérémy Pruvost, Howard Fallowfield, Guillaume Cogne and Mariana Titica. You managed to align your visions despite your different sensitivities and perspectives regarding the topic, and it has been a real pleasure working with you all in these conditions. The collaboration you have initiated between GEPEA and Flinders University and the complementarity of your skills made the richness of this thesis.

Jérémy, thank you for your guidance, support and sound advices. Thanks also for your patience with all the paperwork that comes with a PhD in cotutelle.

Guillaume, I was lucky to have someone with so sharp knowledge and skills as you in my supervising team. Above all, I am very grateful for the time you made in your busy schedule for helping me with the model and the stoichiometric analysis. I was a beginner in modeling when we started, so thank you for your patience while explaining me the basics.

Mariana, thanks for your support and for making time to help me when I needed it. Thank you especially for your very sound comments regarding my defense presentation.

Howard, one of the things I have learned while working with you in Australia is the importance of being positive while doing research. Thanks for teaching me to be proud of my work. Thank you also for all the great moments in Peterborough or building mini-ponds!

I probably would not have started this PhD without Fabrice Béline, who offered me an end-of-studies internship position in INRAE Rennes to work on microalgae cultures on digestate in 2020. This internship opened very important doors and it was a pleasure to count you among my CSI members afterwards.

I must say I have not been the only one to struggle with lab work in this PhD. Roxane and Thibault, thank you for your dedication and reliability during your respective internships. Your results helped consolidating this thesis. Roxane, you managed to gather useful data for the model. Thibault, I remember having you on the phone while I was in Australia talking about the "failed" experiment on glucose. Eventually, these unexpected results turned out to be interesting and brought some relevant elements of discussion. This experiment was not exactly a gift but you did well! I wish you all the best now for your PhD.

None of the experiments that Roxane, Thibault and myself have conducted during this PhD would have emerged without the precious intervention, training and help of the engineers and technicians of both GEPEA lab and Flinders University. First, I would like to acknowledge Hélène for the time you spent helping me setting up the torus photobioreactor, modifying the Labview programs and solving problems with the capricious micro-GC. Thank you also to Raphaëlle, Gérard, Benjamin, Catherine, Dominique, Delphine and Raj for training me on different methods and devices. Thank you as well to Emmanuel for your help in organising the visio for the defense... and for managing the unforeseen technical issues on the D-day. I have also received some significant help from a few PhD students. Thank you Fernando for your help with the micro-GC, Samy for training Thibault while I was in Australia, Sam, Felipe and Rajina for your support in Peterborough field trips and Andreana for training me to cultivate and number MS2

virus. Thank you all for making time for me despite the big amount of work you were investing in your own PhDs at the same time. It has been a big relief to be able to count on you. I wish you all the best for the end of your PhDs and for your professional life. Thank you Pierre as well for the discussions we had on modeling and high-rate algal ponds in general. I wish you a very nice pursuit of collaboration with Flinders!

I would like to express all my gratitude and affection to the PhD students, interns and engineers of GEPEA lab, IREENA lab, Capacité, Algosolis, Algosource and Environmental Health group of Flinders University for the precious friendships we have built those last four years. Thanks to Elodie, Julie, Julien, Joris, Hugo, Flora, Samy, Romain, Thibault, Visakha, Fernando, Putty, Jack, Khadija, Abdallah, Jordan, Alexia, Anthony, Arthur, Sid, Robin, Emile and Margot for all the discussions, laughs, parties, bike rides and (long) coffee breaks. You have made the PhD road way smoother and funnier and I really hope we can stay in touch in the future.

This work also owns a lot to the unconditional support and faith of my family and my partner Christophe. Among the difficulties that punctuate a PhD journey, leaving 16 000 km away from you is one of those that marked me the most. Thanks Mom for your dedication and support, thanks for being an example of rigor, hard work and organisation. Thanks Dad for passing me your convictions for the protection of the nature, without which I might not have pursued this path. Thanks to my little brother Baptiste, who was often told to follow his big sister's example as a child. Now we are adults, it is me who sometimes follow your example, for your sense of friendship, your spontaneity and your capacity to think by yourself. As an adult, thinking out of the box like you do is sometimes the most fruitful way to go.

Finally, thank you Christophe. Thank you for helping me, supporting me and waiting for me on this road that is way more beautiful with you.

Solène

LIST OF SCIENTIFIC COMMUNICATIONS

Publications

• JAHAN (S.), PRUVOST (J.), TITICA (M.), COGNE (G.) et FALLOWFIELD (H.) Synergy between carbon sources and light in microalgal culture from the perspective of wastewater treatment in high rate algal ponds In Algal Research, vol. 79, (2024) 10.1016/j.algal.2024.103466

• JAHAN (S.), K C (R.), SABATTE (F.), BUTTERWORTH (S.), PRUVOST (J.), TITICA (M.), COGNE (G.) et FALLOWFIELD (H.) 3D characterisation of a large high rate algal pond for wastewater treatment - In Algal Research, vol. 80, (2024) 10.1016/j.algal.2024.103537

• JAHAN (S.), PRUVOST (J.), TITICA (M.), COGNE (G.) et FALLOWFIELD (H.) Couplage vertueux d'épuration des eaux et de culture de microalgues - In Techniques de l'ingénieur

Oral communications

• Abstract accepted for an oral presentation: "Role and fate of carbon and oxygen in high rate algal pond system implying microalgae and bacteria in interaction for wastewater treatment", 19th Congress of the French Bioprocess Engineering Society (Deauville, France), 15^{th}-17^{th} October 2024.

• "Microalgae impact on inactivation of indicator virus in a large-scale wastewater treatment system using microalgae", 8th Congress of the International Society of Applied Phycology (Porto, Portugal) on 18^{th} June 2024.

• "Relevance of using laboratory photobioreactors to simulate large-scale wastewater treatment systems using microalgae", International Conference "Water & Wastewater Management with special focus on Developing Countries" in Murdoch University (Perth, Australia) on 5^{th} December 2023.

• "Modeling and optimising wastewater treatment processes using microalgae", GEPEA annual seminar, May 2022.

Résumé

Environ 80% des eaux usées dans le monde sont déversées dans le milieu naturel sans traitement adéquat. Or, un assainissement insuffisant conduit à des risques de diffusion de maladies graves comme le choléra, la dysenterie, la typhoïde, les infections par vers intestinaux et la polio. La contamination des eaux domestiques due à des systèmes d'épuration inadéquats a ainsi causé plus de 1 000 décès d'enfants chaque jour dans le monde en 2012, principalement en Afrique et en Asie de l'Est. Le déversement dans le milieu naturel des substances nutritives contenues dans les eaux usées comme l'azote et le phosphore favorise également le développement excessif d'algues, qui finissent par asphyxier les masses d'eau qu'elles envahissent et causer la mort de la faune aquatique. S'il existe des systèmes efficaces pour l'élimination des polluants et des pathogènes, ceux-ci sont souvent trop onéreux et énergivores pour être utilisés durablement dans les pays les plus pauvres, où la part des eaux usées non traitées est la plus élevée dans le monde. Dans le cas des pays développés, l'assainissement pose toujours des problèmes de coût, d'impact environnemental et de valorisation des polluants issus des eaux usées sous la forme de nutriments.

Des solutions à faible coût, nécessitant peu de maintenance et consommant peu d'énergie sont donc nécessaires. Pour répondre à ces besoins, les systèmes de traitement des eaux usées utilisant des microalgues ont vu le jour dans les années 1950 en Californie. Des bassins opérés en extérieur, appelés High Rate Algal Ponds (HRAPs), sont utilisés pour le traitement biologique secondaire des eaux usées domestiques ou industrielles. Ils permettent de s'affranchir de l'aération artificielle utilisée dans les systèmes classiques à boues activées en utilisant des organismes photosynthétiques comme les microalgues pour produire l'oxygène nécessaire à la dégradation des polluants. Les microalgues consomment également une partie des polluants ciblés par le traitement des eaux comme le carbone, l'azote, le phosphore et le soufre, nécessaires au bon

fonctionnement et aux éléments structuraux des cellules de microalgues.

Néanmoins, des éléments clefs pour la compréhension des interactions microalgues-bactéries autour de la source de carbone et de l'oxygène dans les HRAPs manquent encore dans la littérature.

Cette thèse aborde le sujet des interactions dans les consortiums microalgues-bactéries pour l'amélioration de l'abattement de la matière organique, des minéraux et des pathogènes en HRAP en utilisant une approche intégrative confrontant des études à échelle réelle et à échelle laboratoire couplées à des travaux de modélisation, explorant ainsi différents systèmes d'étude afin de creuser les interactions complexes entre les microalgues et les bactéries. Ce projet de thèse a été conduit en cotutelle entre le laboratoire GEPEA (Saint Nazaire, France) et Flinders University (Australie), les deux premières années ayant été réalisées au GEPEA et la dernière année à Flinders University. Cette collaboration a permis de réaliser cette étude en utilisant différents systèmes à différentes échelles. Alors que le laboratoire GEPEA possède des photobioréacteurs de laboratoire opérés en conditions contrôlées, Flinders University a accès à un HRAP industriel de 5000 m^2 localisé à Peterborough, offrant ainsi l'opportunité d'étudier un système HRAP en conditions réelles.

L'objectif, dans un premier temps, était d'établir un état des lieux de l'activité des microorganismes, des conditions physico-chimiques et de la pénétration des radiations solaires dans le HRAP à large échelle de Peterborough en réalisant une caractérisation 3D. La caractérisation 3D du HRAP de Peterborough a démontré le mélange efficace d'un HRAP de forme sinueuse d'1 km de long, illustré par une homogénéité de la composition chimique et microbienne de l'eau usée. Notamment, les indicateurs de l'activité microalgale et bactérienne tels que l'oxygène dissous, le carbone organique et le carbone inorganique étaient répartis de façon homogène dans le HRAP. L'oxygène requis pour la dégradation de la matière organique par les bactéries était produit par photosynthèse et homogénéisé efficacement dans le HRAP par la roue à aubes. En général, les substrats principaux pour la croissance microalgale et bactérienne étaient disponibles sur la longueur (1 km), la largeur (4 m) et la profondeur (0.3 m) du HRAP.

Différentes questions émergent de ce premier état des lieux, incluant la disponibilité du

carbone organique pour les microalgues, la contribution des microalgues et des bactéries aux cycles de l'oxygène et du carbone, ainsi que l'impact des microalgues sur la désinfection solaire au regard de l'atténuation des UVs mesurée dans ce HRAP à large échelle.

L'hypothèse selon laquelle le carbone organique est consommé uniquement par les bactéries a été discuté dans la littérature. Le recoupement d'informations sur la composition des eaux usées et l'affinité des microalgues avec les molécules organiques a permis d'estimer qu'une faible fraction des molécules organiques présentes dans les eaux usées (10-15%) était potentiellement disponible pour les microalgues. Cette fraction est cependant probablement plus importante en aval d'un pré-traitement en bassin anaérobie où des acides gras volatiles facilement assimilables par les microalgues sont produits. Ces informations soulèvent l'hypothèse d'une croissance microalgale hétérotrophe significative susceptible d'impacter les interactions avec les bactéries. Au regard de la complexité des interactions trophiques dans le consortium microalgues-bactéries, une étude en photobioréacteur (PBR) de laboratoire torique en conditions contrôlées intégrant des mesures en ligne au long du cycle jour-nuit couplée à une approche théorique en modélisation a été choisie pour apporter une meilleure compréhension des interactions microalgues-bactéries. Les cultures de la microalgue *S. obliquus* en photoautotrophie, photohétérotropie et mixotrophie réalisées dans le cadre de cette thèse ont démontré que l'acétate apporté pour simuler le carbone organique des eaux usées n'était pas suffisant pour couvrir les besoins en carbone des microalgues et qu'une source intrinsèque de CO_2 issu de la respiration bactérienne était nécessaire. Cette étude a également démontré que la production d'oxygène par les microalgues dépendait du carbone inorganique disponible.

De façon significative, la co-culture de *S. obliquus* et *E. coli* utilisant de l'acétate comme source de carbone organique a démontré une forte compétition pour l'acétate entre les microalgues et les bactéries au lieu de la symbiose attendue. L'analyse stoechiométrique a démontré que l'acétate était majoritairement consommé par les microalgues et que la photohétérotrophie était le mode de croissance principal de *S. obliquus*. Au contraire, dans les simulations où le carbone organique était consommé uniquement par les bactéries ainsi que dans la co-culture utilisant du glucose comme source de carbone, les bactéries dominaient la culture et la croissance

des microalgues était très faible. Ces résultats montrent que la contribution photohétérotrophe dans le consortium microalgues-bactéries dépend de la source de carbone utilisée. De plus, les similarités dans le comportement de l'oxygène et du carbone inorganique dissous dans le modèle et dans la co-culture expérimentale sur acétate ont démontré que la croissance des microalgues était impactée par une limitation par le carbone inorganique dans la co-culture sur acétate alors même que l'acétate était la source principale de carbone pour les microalgues selon l'analyse stoechiométrique. Alors même que les microalgues et les bactéries étaient en compétition pour l'acétate, la croissance des microalgues était donc également impactée par la production de CO_2 par les bactéries. Par conséquent, l'oxygène dissous consommé par la suite par les bactéries s'est révélée dépendante de l'apport de CO_2, ce qui s'avère cohérent avec les résultats issus des cultures de *S. obliquus* en photoautotrophie, photohétérotrophie et mixotrophie.

Cependant, les systèmes excessivement simplifiés comme le modèle ou les expériences dans le photobioréacteur de laboratoire torique utilisant une seule source de carbone organique, une seule espèce de microalgue et une seule espèce de bactérie n'a pas permis de recréer la symbiose attendue dans le HRAP. Comme montré dans nos résultats, l'affinité pour la source de carbone s'est révélée très importante dans les échanges créés par la suite entre les populations. Il est recommandé pour la suite d'utiliser un mélange complexe de sources de carbone organique et des populations mixtes de microalgues et de bactéries afin de simuler le HRAP.

Néanmoins, le PBR torique et le consortium microalgues-bactéries simplifié se sont néanmoins avérés être des outils pertinents pour étudier le comportement du HRAP. Premièrement, les mesures en ligne ont fourni des informations clef sur les dynamiques d'O_2 et de CO_2 au long du cycle jour-nuit. Deuxièmement, alors qu'une des hypothèses posées en amont de ce travail questionnait la représentativité d'un PBR de laboratoire efficacement mélangé tel que le PBR torique comparé à un raceway à large échelle potentiellement hétérogène, la caractérisation 3D du HRAP de Peterborough a montré un très bon mélange. Cela a justifié l'utilisation d'un PBR de laboratoire homogène tel que le torique pour simuler le système à échelle réelle. Le travail de recherche présenté ici a démontré qu'un modèle cinétique couplé à un modèle radiatif constituait un outil précieux pour comprendre les dynamiques d'O_2, de CO_2, de biomasse microalgale

et de biomasse bactérienne au long du cycle jour-nuit. Malgré la sursimplification du modèle dans cette thèse, les concentrations en oxygène dissous étaient en accord avec celles mesurées en HRAP. Les tendances étaient cependant différentes et ont permis de mettre en lumière une limitation par le carbone inorganique dans le modèle alors que le HRAP paraissait être plutôt limité par la lumière. Cette tendance tend à souligner que les hypothèses et phénomènes sous-jacents supposés dans notre modèle étaient proches du fonctionnement réel du HRAP (c'est-à-dire un carbone organique consommé essentiellement par les bactéries), mais que certains phénomènes complexes sous-jacents impliqués dans le devenir du carbone dans le consortium microalgues-bactéries sont toujours à élucider (c'est-à-dire l'absence de limitation par le carbone inorganique dans le HRAP qui serait potentiellement associé à des mécanismes synergiques plus complexes).

En outre, la modélisation du comportement d'un HRAP et de ses performances en termes d'abattement des polluants et des pathogènes est extrêmement complexe car elle implique la prise en compte de l'hydrodynamique, du transfert de la lumière, des transferts de gaz, des interactions cinétiques entre les microorganismes et des mécanismes de désinfection. Généralement, ces facteurs sont étudiés indépendamment. Ce travail de recherche présente l'avantage de développer et d'évaluer une approche intégrative de laboratoire pour mieux comprendre les interactions physiques (caractérisation 3D d'un HRAP en termes de vitesse d'écoulement et de mélange de l'oxygène et des polluants), chimiques et biologiques (interactions microalgues-bactéries et impact des microalgues sur les mécanismes de désinfection) en HRAP.

La mesure des radiations solaires dans le HRAP de Peterborough a prouvé que leur pénétration dans le HRAP était très faible, questionnant l'impact relatif des microalgues sur la désinfection solaire. Au final, des expérimentations en laboratoire dans une cabine UV sur l'inactivation du virus indicateur MS2 ont permis de mettre en avant le rôle majeur des microalgues non seulement dans les interactions trophiques avec les bactéries mais également dans les mécanismes de désinfection en produisant significativement des espèces réactives à l'oxygène sous l'action des UV.

Perspectives de recherche

• Explorer les corrélations entre le mélange d'un raceway, la turbulence, les flocs, les zones micro-anaérobies, la disponibilité O_2/CO_2 et la nitrification.

• Caractériser les molécules organiques présentes dans les eaux usées après prétraitement anaérobie et leur affinité avec les groupes de microorganismes présents dans le HRAP.

• Complexifier les expériences de laboratoire et les modèles en termes de source de carbone et de populations.

• Explorer l'intérêt d'un système en couche mince ciblant la désinfection des pathogènes.

Table of Contents

List of figures **33**

List of tables **36**

List of abbreviations **37**

Introduction **39**

1 State of the art **51**

1.1 Generalities about wastewater treatment 51

1.1.1 A brief history of wastewater treatment 51

1.1.2 Composition of wastewater 53

1.1.3 Legislation: required water standards quality 55

1.1.4 Activated sludge: mechanisms, issues and alternatives 57

1.2 High Rate Algal Pond technology: functioning of a promising alternative solution 62

1.2.1 Primary treatment 63

1.2.2 Secondary treatment: the central process in the HRAP 65

1.2.3 Tertiary treatment: the separation of recoverable biomass and treated wastewater 67

1.2.4 Valorisation of the water treated and of the biomass produced in the HRAP 68

1.3 Sustainability and performances of HRAP systems 73

1.3.1 HRAP systems performances in real conditions 73

1.3.2 Optimisation of HRAP performances through engineering parameters . . 79

1.3.3 Modeling HRAP systems 83

1.3.4 Environmental and economical impact of HRAP 85
1.3.5 Conclusion: HRAP versus activated sludge and improvement perspectives 89
1.4 Microalgae and bacteria in HRAP systems 91
1.4.1 Microalgae 92
1.4.2 Bacteria 107
1.4.3 Interactions between microalgae and bacteria in HRAP systems 112
1.5 Disinfection processes in HRAP and the role of microalgae 122
1.5.1 Generalities on viruses 122
1.5.2 Disinfection processes 123
1.5.3 Conclusion on potential microalgae impact on pathogens solar inactivation 131
1.6 Conclusion 131

2 Studied systems and analytical methods 133

2.1 Peterborough HRAP: study on the large-scale pilot 133
2.1.1 Objective of the study 133
2.1.2 Study site and data collection in the pond 133
2.1.3 Analysis of wastewater composition 137
2.1.4 Statistics and data visualisation 139
2.2 Torus photobioreactor: experiments at laboratory scale 139
2.2.1 Objective of the study 139
2.2.2 Torus PBR 140
2.2.3 Simulation of day-night cycles 143
2.2.4 Inoculum 143
2.2.5 Culture monitoring 144
2.3 Modeling microalgae-bacteria interactions in the torus PBR 160
2.3.1 Principle 160
2.3.2 Modelling of light transfer and light limitation 161
2.3.3 Modeling of gas-liquid transfer 163
2.3.4 Modelling of algal growth, bacterial growth and gas exchanges 165

2.3.5 State variables . . . 168
2.4 Characterisation of microalgae impact on virus inactivation . . . 169
2.4.1 Objective of the study . . . 169
2.4.2 UVA cabinet . . . 169
2.4.3 Preparation of the culture mediums . . . 170
2.4.4 MS2 and *E. coli* stock and MS2 quantification . . . 173

3 Overview of microorganisms' activity in HRAP by Peterborough HRAP 3D characterisation 177

3.1 Introduction . . . 177
3.2 Material and methods . . . 179
3.2.1 *In situ* measurements . . . 179
3.2.2 Normalisation between sensors . . . 180
3.2.3 Normalisation of diurnal changes in wastewater DO and pH . . . 180
3.3 Results . . . 183
3.3.1 Environmental conditions . . . 183
3.3.2 Flow velocity . . . 183
3.3.3 Suspended solids . . . 185
3.3.4 Chlorophyll *a* and dissolved oxygen . . . 185
3.3.5 Total organic carbon (TOC) . . . 188
3.3.6 Nitrifying activity . . . 189
3.3.7 Turbidity and attenuation of solar radiations . . . 194
3.4 Discussion . . . 195
3.4.1 Flow velocity . . . 195
3.4.2 Suspended solids . . . 197
3.4.3 Dissolved oxygen . . . 198
3.4.4 Nitrification . . . 198
3.4.5 Sun radiations . . . 200
3.4.6 Power consumption . . . 200

3.5 Conclusion 201

4 Synergy between carbon source and light in microalgal culture from the perspective of wastewater treatment in high rate algal ponds 203

4.1 Introduction 203

4.2 Relevance of microalgal consumption of organic and inorganic carbon in wastewater 206

4.2.1 Organic carbon 206

4.2.2 Inorganic carbon 207

4.2.3 Synergy between organic and inorganic carbon consumption 208

4.3 Impact of light on microalgae in HRAP under autotrophic, heterotrophic and mixotrophic conditions 210

4.3.1 Light availability in HRAP 210

4.3.2 Impact of day-night cycles on biomass growth 211

4.3.3 Effect on light stress 214

4.3.4 Effect on pigments 214

4.3.5 Effect on cell composition 215

4.3.6 Effect on RuBisCO and citrate synthase activities 216

4.3.7 Effect on carbon uptake 217

4.4 Lab-scale experiments representativity of HRAP actual conditions 218

4.5 Conclusion 223

5 Relative contributions of photoautotrophy and photoheterotrophy to mixotrophic growth of *Scenedesmus obliquus* in synthetic wastewater 225

5.1 Introduction 225

5.2 Materials and methods 227

5.3 Results 229

5.3.1 Contribution of photoautotrophy and photoheterotrophy to biomass productivity in mixotrophy 229

5.3.2 Organic carbon, inorganic carbon and oxygen fate and their contribution to algal growth . . . 231
5.3.3 Oxygen balance . . . 237
5.3.4 Pigments . . . 237
5.4 Discussion . . . 239
5.5 Conclusion . . . 241

6 Fate and role of carbon sources in microalgae-bacteria interactions in synthetic wastewater under simulated solar conditions 243
6.1 Introduction . . . 243
6.2 Material and methods . . . 245
6.3 Results . . . 247
6.3.1 Theoretical approach of microalgae-bacteria interactions . . . 247
6.3.2 Experimental investigation of microalgae-bacteria interactions . . . 254
6.4 Discussion . . . 272
6.4.1 Investigation of carbon and oxygen fate in a coculture in day-night cycle . 272
6.4.2 Relevance of using torus PBR to simulate HRAP . . . 276
6.5 Conclusion . . . 280

7 Impact of microalgae on indicator viruses solar inactivation in HRAP in the perspective of improving pathogens removal in HRAP systems 283
7.1 Introduction . . . 283
7.2 Material and methods . . . 287
7.3 Results . . . 292
7.3.1 Effect of UVA attenuation by wastewater and microalgae on MS2 inactivation . . . 292
7.3.2 Effect of ROS from wastewater and microalgae on MS2 inactivation . . . 294
7.3.3 Balance between positive and negative impact of microalgae and wastewater on MS2 inactivation . . . 298

7.3.4 MS2 inactivation in a 30 cm depth wastewater column 299
7.4 Discussion 300
7.4.1 Effect of UVA attenuation 300
7.4.2 Effect of ROS production 301
7.4.3 Impact of microalgae in 30 cm depth columns 304
7.5 Conclusion 306

General conclusion **307**

A Culture medium composition **315**

B Schumpe coefficients for the effect of salinity on O_2 solubility **317**

C UVA intensity variation in the waterbath **318**

D MS2 concentration curves **319**

Bibliography **323**

List of Figures

1 Aerated pond in an activated sludge wastewater treatment plant 41

2 Different designs of photobioreactors for microalgae culture 44

3 5000 m^2 HRAP in Peterborough, South Australia 47

4 Global structure of the thesis 50

1.1 Timeline of wastewater treatment history in environmental and sanitary context (Steichen 2011, Barraqué 2014, Bird 1992) 52

1.2 Origin and concentration of domestic wastewater components 54

1.3 Water quality standards in France 56

1.4 Water quality standards in Australia 57

1.5 Principle of activated sludge (Wang et al. 2008, Cébron 2004, Deronzier et al. 2001) 60

1.6 Aerial view of Peterborough wastewater treatment site 63

1.7 Main chemical and biological processus occurring in pretreatment anaerobic pond (Fallowfield and Garrett 1985, Kang et al. 2020, Park et al. 2013, Delfosse 2014) 64

1.8 Valorisation routes for treated water and biomass after secondary treatment in HRAP 71

1.9 N-NH_4^+, P-PO_4^{3-}, BOD_5 and COD concentrations in HRAPs outlet operating in real conditions compared to French and Australian standards for rejection of treated wastewater in natural environment 75

1.10 *E. coli* concentrations in HRAPs outlet operating in real conditions compared to French and Australian standards for irrigation of non-food crops 77

1.11 Velocity profiles in a 500m^2, 0.2m depth raceway obtained by CFD modelling . . 80

1.12 Energy consumption per cubic metre of treated water for HRAP compared to activated sludge, Sequencing Batch Reactor (SBR) and constructed wetlands . . 86
1.13 CO_2, N_2O and NH_3 emissions per cubic metre of treated water for HRAP compared to activated sludge, Sequencing Batch Reactor (SBR) and constructed wetlands 87
1.14 Area per cubic metre per day of treated water for HRAP compared to activated sludge and constructed wetlands 88
1.15 Capital and operation cost for HRAP compared to activated sludge, Sequencing Batch Reactor (SBR) and constructed wetlands 89
1.16 Repartition of particulate carbon among HRAP microorganisms and organic detritus 91
1.17 Microalgae structure 92
1.18 Representation of electron transport chain in thylakoid membrane 94
1.19 Reactions occurring in Calvin cycle in chloroplast stroma 95
1.20 Reactions occurring in mitochondria and cytosol as part of aerobic respiration . . 96
1.21 Evolution of productivity as a function of MRPA 100
1.22 Mechanisms of inorganic carbon transport through algal cell 102
1.23 Bacteria cell structure 108
1.24 Aerobic respiration in heterotrophic bacteria 109
1.25 Ammonium and nitrite oxidation and CO_2 fixation in nitrifying bacteria 111
1.26 Main chemical and biological processus occurring in HRAP during the day (Fallowfield and Garrett 1985, Cébron 2004, Canziani 2010) 113
1.27 Main chemical and biological processus occurring in HRAP during the night (Fallowfield and Garrett 1985, Cébron 2004, Canziani 2010) 114
1.28 Potential carbon fluxes in microalgae-bacteria consortium in presence of organic carbon (Fallowfield and Garrett 1985) 121
1.29 MS2 virus structure (Golmohammadi et al. 1993) 123
1.30 Infection of *E. coli* by MS2 virus 124

1.31 Links between parameters involved in microorganisms and viruses inactivation in HRAP (red arrows corresponds to negative effects on inactivation and green arrows corresponds to positive effects on inactivation) (Bolton 2012) 132

2.1 Peterborough HRAP (Photo: Rajina K C) 134
2.2 Localisation of the cross sections in the pond and their distance from the paddle-wheel 135
2.3 Gantry equipped with multiparameter sensors and wastewater sampling hoses . . 136
2.4 Gantry equipped with flowmeters 136
2.5 Torus PBR equipment and instrumentation 140
2.6 Light attenuation profile in (a) 4 cm depth torus PBR (b) 30 cm depth HRAP . 141
2.7 Light attenuation profile in microalgae culture with nutrient supply equal to anaerobically pretreated wastewater composition in: (a) 4 cm depth torus PBR (b) 30 cm depth HRAP 142
2.8 Functioning of micro gas chromatograph 490 145
2.9 Principle of radiative properties measurement 151
2.10 Correlation curve between turbidity and dry weight for *E. coli* 152
2.11 Method for *E. coli* CFU determination 153
2.12 Correlation curve between turbidity and CFU for *E. coli* 154
2.13 Block diagram of the kinetic model aiming at simulating photoautotrophic growth of *S. obliquus*, chemoheterotrophic growth of *E. coli* and gas exchanges 160
2.14 UVA cabinet 170
2.15 Calibration curve predicting the power value to apply depending on the UVA incident irradiance 171
2.16 Cultures of microalgae isolated from Peterborough HRAP (a) Isolated species (b) Final mixture 172
2.17 Dissolved organic carbon in microalgae culture before and after sonication, freezing-defreezing and heating 172
2.18 Anaerobic pond upstream Peterborough HRAP 173

2.19 MS2 plate count 175

3.1 Global view of Peterborough HRAP (Photo: Howard Fallowfield) 178

3.2 DO diurnal variation and resulting polynomial regression 182

3.3 Flow velocity (m.s^{-1}) in Peterborough HRAP throughout channel length, width and depth 184

3.4 Suspended solids (g.L^{-1}) in Peterborough HRAP throughout channel length, width and depth 186

3.5 Dissolved oxygen (mg.L^{-1}) in Peterborough HRAP throughout channel length, width and depth 187

3.6 Chlorophyll a concentration (mg.L^{-1}) at different cross-sections along the length of the channel 188

3.7 Total organic carbon (mgC.L^{-1}) in Peterborough HRAP throughout channel length, width and depth 189

3.8 Ammonium (mgN-NH_4^+.L^{-1}) in Peterborough HRAP throughout channel length, width and depth 191

3.9 Nitrites (mgN-NO_2^-.L^{-1}) in Peterborough HRAP throughout channel length, width and depth 192

3.10 Nitrates (mgN-NO_3^-.L^{-1}) in Peterborough HRAP throughout channel length, width and depth 193

3.11 Microscopic observation of the HRAP wastewater during the first campaign in November 2022 (a) and during the second in June 2023 (b). 194

3.12 Total inorganic carbon (mgC.L^{-1}) in Peterborough HRAP throughout channel length, width and depth 195

3.13 Orthophosphates (mgP-PO_4^{3-}.L^{-1}) in Peterborough HRAP throughout channel length, width and depth 196

3.14 (a) PAR attenuation (μmol.m^{-2}.s^{-1}) and (b) UVA attenuation (W.m^{-2}) over the pond depth. 197

3.15 Effect of the distance from the paddlewheel on different microorganmisms' populations in Peterborough HRAP 202

4.1 Overview of carbon sources assimilable by microalgae in domestic wastewater . . 209

4.2 Impact of irradiance on microalgae in presence and absence of assimilable organic carbon 218

4.3 Overview of factors influencing light and organic carbon availability for microalgae and the different trophies occurring depending on variations in those conditions . 220

5.1 Energy source, carbon source and electron donor for microalgae in photoautotrophy, photoheterotrophy, mixotrophy and chemotrophy. 226

5.2 Surface microalgal productivities in autotrophy, photoheterotrophy and mixotrophy limited and non-limited in N and P 231

5.3 Carbon balance deduced from carbon flux in the inlet and the outlet of autotrophic, photoheterotrophic and mixotrophic *S. obliquus* cultures 232

5.4 Carbon, oxygen and nitrogen fluxes in mol/m^3/h in photoautotrophic, photoheterotrophic and mixotrophic *S. obliquus* culture 236

5.5 Net productions rates of O_2 and CO_2 in autotrophy, photoheterotrophy and mixotrophy (normalised by the biomass concentration) 238

5.6 Chlorophyll a, chlorophyll b and carotenoids content in the biomass in autotrophy, photoheterotrophy, mixotrophy limited and non-limited in nutrients 239

5.7 Overview of O_2 and CO_2 dynamics in autotrophy, photoheterotrophy and mixotrophy 241

6.1 Diurnal variation of the incident PFD 247

6.2 Experimental (black dots) and modeled (dotted line) biomass concentration C_{XT}, pigment concentration C_{pig} and pigment content w_{pig} for 2 batch cultures of *S. obliquus* (a) at 100 μmol.m^{-2}.s^{-1} (b) at 800 μmol.m^{-2}.s^{-1} 248

6.3 (a) Modeled microalgal and bacterial biomass in coculture in day-night cycle, D=0.008 h^{-1}, C_{org}=260 mgC.L^{-1} (b) Modeled biomass in day-night cycle, D=0.008 h^{-1}, C_{org}=260 mgC.L^{-1} when microalgae were grown alone (left) and when bacteria were grown alone (right) 250

6.4 First column: modeled DO, microalgal O_2 production rate $r_{O2_{alg}}$ and microalgal growth rate μ_{alg}; second column: TIC and microalgal CO_2 production rate $r_{CO2_{alg}}$ 252

6.5 Modeled O_2 and CO_2 volumetric transfer rates NO_2 and NCO_2 253

6.6 Surface biomass productivities in Peterborough HRAP and in torus PBR supplied with synthetic wastewater with 130 mgC.L^{-1} of acetate, 260 mgC.L^{-1} of acetate and 130 mgC.L^{-1} of glucose 255

6.7 Organic carbon consumption rate in the torus PBR supplied with synthetic wastewater with 130 mgC.L^{-1} of acetate, 260 mgC.L^{-1} of acetate and 130 mgC.L^{-1} of glucose 256

6.8 Microalgal and bacterial productivities in synthetic wastewater supplied with 130 mgC.L^{-1} of acetate, 260 mgC.L^{-1} of acetate and 130 mgC.L^{-1} of glucose 256

6.9 Diurnal variations of total, microalgal and bacterial biomass in synthetic wastewater supplied with 260 mgC.L^{-1} of acetate. Black line is the irradiance, orange dots the total biomass, green dots microalgal biomass and purple dots the bacterial biomass 257

6.10 Diurnal variations of dissolved oxygen in a coculture supplied with synthetic wastewater with 260 mgC.L^{-1} of acetate (in red) compared to the model (in grey) 258

6.11 Diurnal variations of total inorganic carbon (TIC) and total organic carbon (TOC) in a coculture supplied with synthetic wastewater with 260 mgC.L^{-1} of acetate 259

6.12 Net O_2 and CO_2 volumetric production rates along the diurnal cycle in a coculture supplied with synthetic wastewater with 260 mgC.L^{-1} of acetate 262

6.13 Carbon balance showing the repartition of carbon supplied between the biomass, the liquid phase and the gas phase in the coculture supplied with (a) SWWx1 (130 mgC.L^{-1} of acetate) (b) SWWx2 (260 mgC.L^{-1} of acetate) 263

6.14 Acetate, TIC, O_2 and NH_3 fluxes (in mol.m^{-3}.h^{-1}) in *S. obliquus-E. coli* coculture with 130 mgC.L^{-1} of acetate supply during the daytime and the nighttime . . . 268

6.15 Acetate, TIC, O_2 and NH_3 fluxes (in mol.m^{-3}.h^{-1}) in *S. obliquus-E. coli* coculture with 260 mgC.L^{-1} of acetate supply during the daytime and the nighttime . . . 269

6.16 Dissolved oxygen concentration in Peterborough HRAP over 24h 271

6.17 Factors determined by experimental conditions influencing O_2, CO_2 and organic carbon availability in a laboratory PBR 279

7.1 Interactions of factors influencing disinfection in HRAP 286

7.2 Experimental plan for investigation of effect of UVA attenuation by microalgae and wastewater on MS2 inactivation by UVA 288

7.3 Experimental plan for investigation of effect of ROS from microalgae and wastewater on MS2 inactivation by UVA - Determination of depth-averaged irradiance . 289

7.4 Experimental plan for investigation of the effect of ROS from microalgae and wastewater on MS2 inactivation by UVA - Irradiation of MS2 290

7.5 Mode of action of L-histidine for the inhibition of the effects of singlet oxygen . . 290

7.6 Composition of the different media used in experiments investigating the effect of ROS from wastewater and microalgae on MS2 inactivation 291

7.7 Experimental plan for investigation of the effect of microalgae on MS2 inactivation in a 30 cm depth wastewater column 292

7.8 UVA attenuation in a 30 cm-depth column of (a) RO water (b) anaerobically pretreated wastewater (c) microalgae culture. Dotted lines correspond to the averaged UVA irradiance. 293

7.9 MS2 inactivation rates K in h^{-1} obtained in RO water at UVA incident irradiances equivalent to the respective depth averaged irradiance obtained at an incident irradiance of 22 $W.m^{-2}$ within 30 cm-depth columns of RO water, wastewater and a microalgal suspension. 294

7.10 MS2 inactivation rates K in h^{-1} with and without L-histidine in RO water, 0.45 μm filtered wastewater, BBM, heated and 0.45 μm filtered microalgae culture and microalgae culture irradiated respective depth averaged UVA irradiances $G_{0_{RO}}$ = 8.8 $W.m^{-2}$, $G_{0_{WW}}$ = 16.8 $W.m^{-2}$, $G_{0_{BBM}}$ = 8.8 $W.m^{-2}$, $G_{0_{EXTR}}$ = 12.4 $W.m^{-2}$ and $G_{0_{ALG}}$ = 27.7 $W.m^{-2}$ 295

7.11 Dissolved organic carbon in RO water, 0.45 μm filtered wastewater, BBM, heated and 0.45 μm filtered microalgae culture and microalgae culture 296

7.12 Contribution of water + MS2 inoculum and BBM to the total MS2 inactivation (without L-histidine) in filtered wastewater, microalgae extract and microalgae experiments 297

7.13 Negative impact of microalgae and wastewater on inactivation rate due to UV attenuation (in red) and positive impact of microalgae and wastewater on inactivation rate due to ROS production (in green) 298

7.14 MS2 inactivation rates K with and without L-histidine in wastewater and wastewater added with microalgae, irradiated with 22 $W.m^{-2}$ UVA 300

7.15 UVA attenuation in 30 cm depth wastewater columns containing or not microalgae 300

C.1 UVA intensity variation in the waterbath inside the UV cabinet and position of the 6 samples 318

D.1 MS2 concentration over 50h irradiated with (a) G_{dark} = 0 $W.m^{-2}$, (b) $G_{mean_{RO}}$ = 12.9 $W.m^{-2}$, (c) $G_{mean_{WW}}$ = 2.5 $W.m^{-2}$, (d) $G_{mean_{algae}}$ = 2.1 $W.m^{-2}$ 319

D.2 MS2 concentration over 50h in (a) RO water, $G_{0_{RO}}$ = 8.8 $W.m^{-2}$, (b) Filtered wastewater, $G_{0_{WW}}$ = 16.8 $W.m^{-2}$, (c) BBM, $G_{0_{BBM}}$ = 8.8 $W.m^{-2}$, (d) Microalgae extract, $G_{0_{EXTR}}$ = 12.4 $W.m^{-2}$, (e) Microalgae, $G_{0_{ALG}}$ = 27.7 $W.m^{-2}$ 320

D.3 MS2 concentration over 50h under $G_0 = 22$ W.m^{-2} in a 30-cm depth column of (a) Wastewater (b) Wastewater + microalgae 321

List of Tables

1.1 Average wastewater composition after anaerobic pond treatment according to Assemany et al. (2015), Buchanan et al. (2018a), El Hamouri et al. (1995), El Hamouri (2009), El Hamouri et al. (2003), Paing et al. (2003), Sutherland et al. (2017), Zhao et al. (2018) 65

1.2 N-NH_4^+, P-PO_4^{3-} and BOD_5 removal performance results on HRAP >25m^2 treating real domestic wastewater in outdoor conditions 76

1.3 Compilation of HRAP faecal coliforms removal performance results on pilots >25m^2 treating real domestic wastewater in outdoor conditions. UASB = Upflow Anaerobic Sludge Blanket reactor 77

1.4 Comparison of activated sludge and HRAP performances, surface, costs and energy consumption 90

1.5 Elemental composition of *Chlorella vulgaris* (Souliès 2014) 97

1.6 Carbonate equilibria equations and corresponding pH ranges (Pobernik et al. 2008) 101

1.7 Synthesis of previous studies on algae-bacteria interactions in effluent treatment (ANOB=Ammonium and Nitrite Oxidising Bacteria, HB=Heterotrophic Bacteria, PAO=Phosphorus Accumulating Organisms, AS=Activated Sludge, SWW=Synthetic Wastewater) 118

1.8 Respective euphotic depth for UVB, UVA and visible light in Waste Stabilisation Pond and in freshwater, whicg is the depth at which 1% of the incident surface irradiance is recorded (Bolton et al. 2011) 126

2.1 Values and units for constants used for the calculation of net volumetric production of O_2 and CO_2 145

2.2 Values and units for constants used in light transfer modelling equations (Urbain 2017) 163

2.3 Values and units for constants used in gas-liquid transfer modelling equations (Urbain 2017) 166

2.4 Values and units for constants used in gas-liquid transfer modelling equations . . 167

2.5 Values and units for constants used in the calculation of the derivatives of the state variables (Urbain 2017) 169

2.6 Purpose and preparation of each media 173

3.1 Characterisation of anaerobically pre-treated wastewater (inlet). 180

3.2 Variability of pH and DO measurements between left, center and right sensors and resulting corrections to apply 181

4.1 Impact of low irradiance and high irradiance on algal cell in autotrophy 212

5.1 Culture conditions for autotrophic, photoheterotrophic, mixotrophic limited and non limited experiments 229

5.2 Carbon balance showing the repartition of carbon supplied between biomass, liquid phase and gas phases for photoautotrophic, photoheterotrophic and mixotrophic cultures 233

6.1 Culture conditions for experiments imitating HRAP conditions 246

6.2 Carbon balance showing the repartition of carbon supplied between the biomass, the liquid phase and the gas phase in the coculture supplied with 130 and 260 $mgC.L^{-1}$ of acetate 263

6.3 Dissolved oxygen, total inorganic and organic carbon measured during the day in Peterborough HRAP and cocultures in the torus PBR 270

7.1 UVA irradiance (in W.m^{-2}) over 4 cm-depth RO water/BBM, microalgae, microalgae extract and filtered wastewater after adjusting incident UVA irradiance (at depth = 0 cm, in red) to obtain similar average irradiance over the 4 cm depth (in bold) 289

A.1 Composition of BBM-nitrate medium 315

A.2 Composition of additive 1 315

A.3 Composition of additive 2 315

A.4 Composition of M9 medium for *E. coli* cultivation 316

A.5 Composition of synthetic wastewater, classical (SWWx1) and concentrated (SWWX2) 316

B.1 Schumpe coefficients H_i at 23°C for each ion 317

List of abbreviations

AA: Amino Acids

ADP: Adenosine diphosphate

AMO: ammonia monooxygenase

AOB: Ammonium Oxidising Bacteria

AOM: Algal Organic Matter

AS: activated sludge

ATP: Adenosine triphosphate

BBm: Bold Basal Medium

BNR: Biological Nutrient Removal

BOD_5: Biological Oxygen Demand over 5 days

CCM: Carbon Concentration Mechanisms

CEC: Contaminants of Emerging Concern

CFD: Computational Fluids Dynamics

CFU: Colonies Forming Units

COD: Chemical Oxygen Demand

CS: cross section

DNA: deoxyribonucleic acid

DO: Dissolved Oxygen

EBPR: Enhanced Biological Phosphorus Removal

EPS: Exopolysaccharides

ETC: Electron Transport Chain

GEPEA: Génie des Procédés Environnement Agroalimentaire

HAO: hydroxylamine oxidoreductase

HB: heterotrophic bacteria

HRAP: High Rate Algal Pond

HRT: Hydraulic Retention Time

LB: Lysogeny Broth

MRPA: Mean Rate of Photons Absorption

NOB: Nitrite Oxidising Bacteria

NPQ: Non-photochemical quenching

NXR: nitrite oxidoreductase

PAO: Phosphate Accumulating Organism

PAR: Photosynthetically Active Radiations

PBR: Photobioreactor

PFD: Photons Flux Density

PFU: Plaque Forming Unit

PID: Proportional Integral Derived

PSI, PSII: photosystems I and II

RNA: Ribonucleic acid

RO: Reverse osmosis water

ROS: Reactive Oxygen Species

RuBisCO: -1,5-bisphosphate carboxylase/oxygenase

SRT: Solid Retention Time

SWW: synthetic wastewater

TC: total carbon

TKN: Total Kjeldhal Nitrogen

TIC: Total Inorganic Carbon

TOC: Total Organic Carbon

TSA: Tryptone Soy Agar

TSB: Tryptone Soya Broth

TSS: Total Suspended Solids

UASB: Up-flow Anaerobic Sludge Blanket

UV: Ultraviolet

VFA: Volatile Fatty Acids

VSS: Volatile Suspended Solids

WHO: World Health Organisation

WSP: Waste Stabilisation Pond

INTRODUCTION

An overview of current wastewater treatment systems

The first wastewater management systems composed of cesspits and clay pipes appeared around 4000 BC and prefigured the sewage systems we know today (Khaire 2020). Later, wastewater management and treatment technologies have evolved throughout history with the discoveries in bacteriology, the progress of the techniques and the evolution of the legislation.

Wastewater treatment is crucial for protecting public health and preserving the environment. Poor sanitation is linked to the transmission of diarrhoeal diseases such as cholera and dysentery, as well as typhoid, intestinal worm infections and polio. It also contributes to the spread of antibiotic resistance. In developing countries, the contamination of domestic-use water due to inadequate wastewater system sanitation caused more than 1 000 child death per day in 2012, mainly attributed to Africa and South-East Asia (World Health Organisation 2022).

Nowadays, pathogens removal remains the biggest challenge of wastewater treatment in the world. Wastewater also contains large amounts of nutrients, principally ammonium, nitrates and phosphates. When discharged in significant quantities into the environment, those nutrients lead to eutrophication of the system, characterised by excessive algal growth called algal blooms. During their degradation, algae consume the oxygen available in the water, causing the asphyxia of the aquatic environment and fauna death. The decomposition of algal biomass is also associated with the production of hydrogen sulfide (H_2S), a toxic gas. Moreover, cyanobacteria, a phylum able to produce toxins, are likely to develop in the algal blooms. Those toxins could be dangerous for fauna, flora and human health (Chislock et al. 2013). Besides, the daily use of personal care products and pharmaceuticals implies the presence of emerging contaminants in domestic wastewater. Emerging contaminants are substances that recently appeared in the

environment and are often non-regulated or monitored and presenting a potential treat for the health and the environment (Norvill et al. 2016). Other micropollutants such as heavy metals and pesticides are found in significant concentrations in raw wastewater and are susceptible to cause serious diseases if not removed efficiently.

Because of the risk associated with untreated wastewater for the health and the environment, national guidelines and standards for treated wastewater were established worldwide. Treated wastewater must reach acceptable quality before being rejected in rivers or used for human activities in order to protect the environment, the users health and safety and the drinking water resource (Steichen 2011). Wastewater treatment systems adapted to the available area and the origin of the wastewater have been implemented worldwide to reach these national guidelines and standards.

Wastewater can be of industrial, agricultural or domestic origin. While small industries are usually connected to the domestic sewage network, bigger companies use their own wastewater treatment system. In urban areas, the great majority of domestic wastewater is treated in collective plants. On the contrary, in remote areas, very isolated houses cannot be connected to the general wastewater network and must be equipped with individual wastewater treatment systems such as septic tanks. Rainwater can flow in the same network as wastewater in the case of unitary network. Otherwise, when a separate network is present, rain water is collected and treated in a different place than wastewater. This system limits wastewater flow rate and dilution and makes either wastewater and rain water treatment easier.

In average, in Europe, a person produces between 44 and 126 L of wastewater per day. The wastewater production is especially important in the morning, in the evening and during the weekend (Eme and Boutin 2015). The concept of population-equivalent has been established as a base to evaluate the organic pollution present in wastewater, based on the average production per person per day. One population-equivalent corresponds then to an average daily discharge of 60 g of BOD_5 (Biological Oxygen Demand over 5 days), BOD_5 representing the biodegradable organic load (note that the total organic load corresponds to the Chemical Oxygen Demand COD) (Bird 1992).

Collective wastewater treatment systems must then be scaled to store and treat variable quantities of wastewater. The activated sludge system, based on bacterial aerobic degradation of organic matter and flocculation (Figure 1) and often completed by chemical disinfection, is the most widely used system for treating wastewater in developed countries. This compact system that allows to treat large volumes of wastewater turned out to be efficient for organic matter removal for a wide range of population-equivalent.

Figure 1 – Aerated pond in an activated sludge wastewater treatment plant. Source: https://cpe.rutgers.edu/water-wastewater/microbiology-of-activated-sludge

However, the activated sludge system is often too expensive and energy-consuming for being used sustainably in developing countries, where the part of untreated wastewater being discharged into the environment is the highest in the world. 2.6 billion humans still cannot access sanitation services, even while it is considered as a fundamental right by the United nations organization (Steichen 2011). In the case of developed countries, sanitation still raises issues regarding the cost, the environmental impact and the valorisation as nutrients of the pollutants from the wastewater. Activated sludge implies the use of costly and energy-consuming artificial aeration for providing oxygen to the bacteria. In order to maintain dissolved oxygen concentrations, a mechanical (the air is mixed with the liquid phase) or diffused (pressurized air is diffused at the bottom of the tank) aeration system is used in the tank (Tuser 2021). In addition, the significant amount of sludge produced by this system presents a high water content that needs to be drastically reduced before valorisation for sanitisation and for reducing handling and transport costs. When solar drying is not possible, the water content must be reduced by thermal drying which is energy-consuming and costly. After drying, sludge can be spread on

agricultural lands as a fertilizer, be incinerated or converted into gas for energy recovery. These valorisation routes are however expensive and submitted to strict regulations (Nazari et al. 2018, Gomes et al. 2023). For reducing the risks of eutrophication, the legislation does not allow to apply the totality of the sludge produced on agricultural lands. The remaining sludge cannot be valorised and must be incinerated. Finally, activated sludge is underperforming for phosphorus removal, meaning that a tertiary chemical treatment is necessary for reaching the standards for phosphorus applied by different countries.

Secondary alternative treatments are already setup to replace or complete activated sludge systems, like natural lagoon systems where water is simply stocked in shallow ponds or planted bed of reed. Activated sludge process can also be completed by bacterial filters: after the clarifier, water is brought to a filtering mater where bacteria are developing. Those bacteria help to degrade the remaining pollutants in the water (Moulin et al. 2013). Discharging vegetated areas can also be introduced between the wastewater treatment plant and the receiving environment, allowing to complement treatment for suspended material, nutrients, metals and micropollutants (Boutin and Prost-Boucle 2012). Anaerobic reactors also enable comparable removal rates as activated sludge, with lower sludge production, lower energy consumption and lower space requirements. However, higher retention times are required, odors can be emitted and an aerobic post-treatment is often required to meet standards rejection (Pavlostathis 2011). Whatever the technology, a real need for improving accessible, low energy-consuming and robust alternative system is emerging.

High rate algal ponds: a promising alternative technology

In order to meet the needs in proposing alternative process for water treatment, wastewater treatment systems using microalgae emerged in 1950's in California (Benemann et al. 1978). Those outdoor ponds called High Rate Algal Ponds (HRAP) are used for the biological secondary treatment of wastewater of domestic or industrial origin. In these paddlewheel-mixed shallow raceways (30-50 cm depth), oxygenation of the HRAP by photosynthetic organisms such as microalgae replaces artificial aeration for aerobic degradation of organic matter. Microalgae and

bacteria consume the nutrients targeted by wastewater treatment such as carbon, nitrogen, phosphorus and sulfur, which are necessary for the prosper functioning and for the structural elements of microalgal and bacterial cells. Several studies have demonstrated the ability of microalgae to consume and remove nutrients and organic matter from wastewater (Mehrabadi et al. 2015, Hernández et al. 2016, García et al. 2000), together with bacteria that benefit from microalgal oxygen production and provide inorganic carbon to the microalgae. In other words, microalgae-bacteria consortium turn the dissolved pollutants into biomass that can be subsequently separated from the treated water.

Algal biomass constitute a promising source of molecules of interest for agriculture, food, pharmaceutic and cosmetic. Generally, microalgae are cultivated in photobioreactors (PBR) of different designs, among others tubular, raceway, inclined plan or columns, presented in the Figure 2, that aim at optimising light utilization by microalgae. However, production costs are currently very high due to the need for artificial continuous light, freshwater and nutrients. Yet, in HRAP, light is supplied by the sun and water and nutrients are brought by the wastewater, removing the need for artificial light, clean water or synthetic nutritive mediums. According to Mehrabadi et al. (2015), producing 1 ton of microalgae requires 40-100 kg of nitrogen and 3-12 kg of phosphorus, which would correspond to around 2500 m^3 of wastewater. However, reusing algal biomass produced in wastewater presents limitations. The high level of contamination of the biomass does not permit applications in health, animal or human feeding. However, biogas, fertilizers or biofuel production remains possible (Mussgnug et al. 2010, Álvarez-González et al. 2023, Heredia et al. 2022).

In the end, the low environmental footprint and the low cost associated with HRAP systems could favour the replacement of some existing non-optimal technologies for wastewater treatment or the equipment of areas that does not have one. Sparsely limited by space while housing small populations, rural areas are especially adapted for the setting up of wastewater treatment systems including microalgae. Since the first experiments on wastewater treatment with microalgae in California in 1950's, some rural communities chose this wastewater treatment system and, since 1970s, microalgae have been used as a tertiary water treatment (Wang

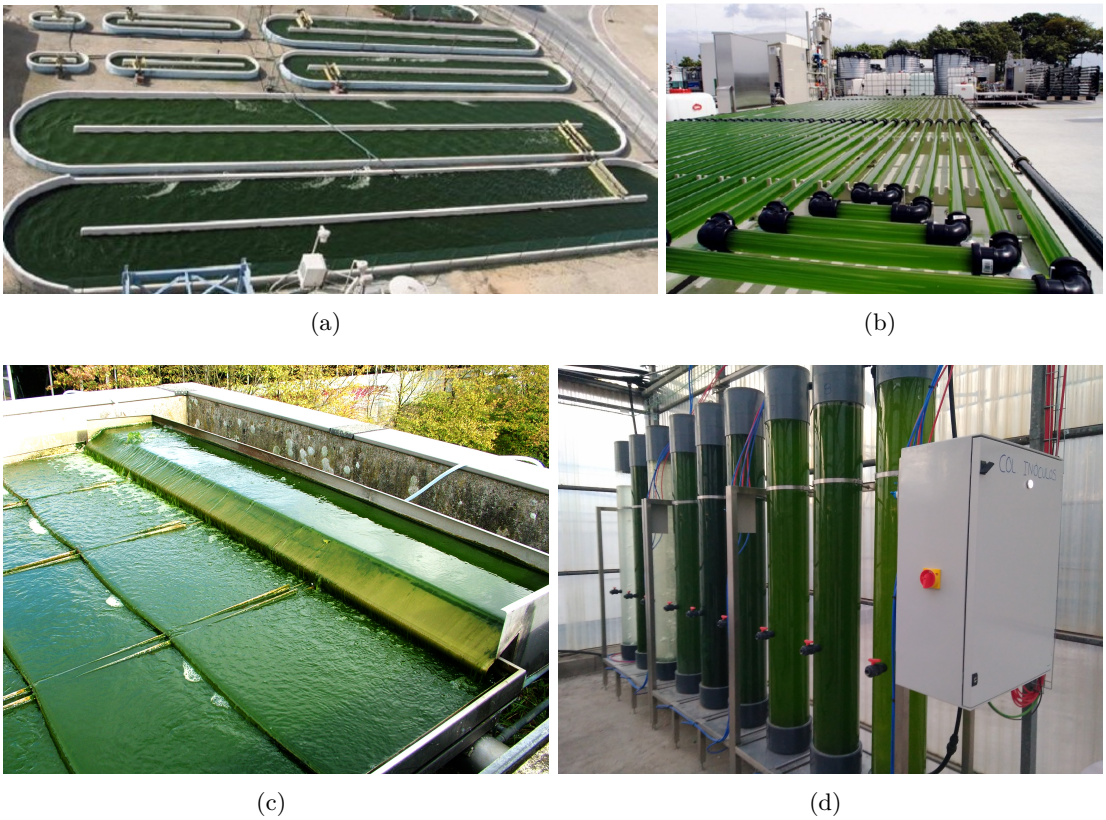

Figure 2 – Different designs of photobioreactors for microalgae culture (a) Raceway (Kumar and Jain 2014) (b) Tubular (Abert Vian et al. 2013) (c) Inclined plan (http://www.phytosystems.ulg.ac.be/fr/infrastructures/bioreacteurs) (d) Columns (https://www.besustainablemagazine.com/cms2/sabana-project-launched/)

et al. 2016). Several studies in outdoor HRAP have reported satisfying pollutant removal from municipal, agro-industrial, pharmaceutical, textile-dye or even petrochemical effluents (Pereira et al. 2017, Wang et al. 2016). Nevertheless, outdoor HRAP systems are sunlight-dependant, inducing variable although significant performances along the seasons and the time of the day. In addition, even while a pre-treatment pond can act as a buffer, wastewater composition is also likely to vary depending on the period of the day or the year. While optimising a system submitted to such environmental conditions, modeling is of interest to consider the varying parameters in the perspective of implementing the HRAP at industrial scale. Numeric simulations allow to run a great amount of scenarios in a short time and also to generate data that can be used for a better understanding of the experimental data. In the case of wastewater treatment processes, using a model is useful to predict removal performances and then scale the system.

In order to implement a realistic model, a better understanding of the HRAP system and the trophic interactions between microalgae and bacteria is however needed.

The rising interest of scientists for microalgae-bacteria consortium for wastewater treatment is relatively recent. While this type of system has been studied since 1970, 65% of the publications written between 1970 and 2021 were done after 2018 (Oviedo et al. 2022). Numerous studies have already investigated the impact of hydraulic retention time (HRT) and solid retention time (SRT), depth, geometry, pre-treatment, inoculated algal species or CO_2 injections on organic and mineral pollutants and pathogens removal, allowing to determine a range of optimal engineering parameters for the operation of HRAP (Ruas et al. 2020, Young et al. 2019a, Sutherland et al. 2014b, Inostroza et al. 2021). Numerous technico-economic studies have also demonstrated the economic and environmental interest of HRAP for wastewater treatment (Garfí et al. 2017, Kohlheb et al. 2020, Arashiro et al. 2018). According to these studies, the paddlewheel mixing system used in HRAP is very energy-efficient compared to the activated sludge systems. However, mixing and heterogeneity of large-scale HRAP has been rather understudied.

As a key aspect of HRAP functioning, organic molecules are present in significant quantities in domestic wastewater. In classical wastewater treatment systems, those molecules represent the carbon and energy source for heterotrophic bacteria. In HRAP system where microalgae and bacteria are in interaction, organic molecules could also play a role in microalgal growth. While microalgae are mainly photoautotroph, utilizing then CO_2 as a carbon source and light as an energy source, they are also able to use organic carbon as both their carbon and energy source, in photoheterotrophy (in the presence of light) or chemoheterotrophy (in darkness). They are also able to use simultaneously light and organic carbon as their energy source and CO_2 and organic carbon as their carbon source, in mixotrophy. Nevertheless, in wastewater, bacteria is expected to play a major role in organic depollution. Indeed, their growth kinetic is quicker than microalgae and organic carbon is their unique source of carbon and energy. Because of this, bacteria should be the major consumer of organic molecules, but could also compete with microalgae for nutrients (nitrogen, phosphorus, sulfur). Large-scale HRAP is then a complex system composed of a diverse population with intricate trophic interactions. Yet, there is still

some debate on the necessity to add carbon dioxide to HRAPs to improve microalgal growth and wastewater treatment, potentially increasing their capital and operating costs and limiting wider application. As microalgae may also use organic molecules present in wastewater as a carbon source simultaneously with inorganic carbon produced from both algal and bacterial oxidation of organic carbon, the need for external carbon dioxide addition can be questioned. However, interactions between microalgae and bacteria are still unclear due to the difficulties of separating microalgae, bacteria and other suspended solids and to discriminate the contributions of each element to the carbon and oxygen production and consumption.

Besides, pathogens removal in HRAP also calls on complex mechanisms as it relies on the synergistic disinfecting action of ultraviolet (UV) radiations, dissolved oxygen, pH and Reactive Oxygen Species (ROS) for killing bacteria and viruses. The current debate implies the contribution of dark and sunlight-driven mechanisms (Chambonniere et al. 2020) and the interest of separating microalgae from the water for improving tertiary treatment. In HRAP, pathogen removal mainly relies on UV radiation from the sun. UV radiation induces photochemical modifications of DNA (deoxyribonucleic acid) and RNA (ribonucleic acid), leading to pathogen inactivation. However, high turbidity due to microalgae and detritus from the wastewater reduces UV penetration in HRAP. Microalgae are expected to contribute significantly to turbidity in HRAP, however, they are also responsible for high oxygen concentration, high pH and production of Reactive Oxygen Species favouring disinfection, questioning the relative impact of microalgae on pathogen inactivation.

An integrative approach for understanding HRAP

This PhD thesis addresses the topic of microalgae-bacteria consortium for the improvement of organic matter, minerals and pathogens removal in high rate algal ponds by a global approach linking large-scale studies and laboratory-scale experiments coupled to numerical simulations, thus exploring different study systems for delving into the complex interactions between microalgae and bacteria. This PhD thesis was conducted in cotutelle between GEPEA (Génie des Procédés Environnement Agroalimentaire) laboratory (Saint Nazaire, France) and Flinders Uni-

versity (Adelaide, South Australia), with the two first years spent in GEPEA and the last year in Flinders University. This collaboration allowed to complete the present study using different systems at different scales. While GEPEA laboratory holds laboratory photobioreactors operated in controlled conditions, Flinders University has access to an industrial scale HRAP of 5000 m^2 in Peterborough (South Australia) (Figure 3) that offers the opportunity to study HRAP system in real conditions.

Figure 3 – 5000 m^2 HRAP in Peterborough, South Australia

In a first time, the thesis aims at drawing up an overview of microorganisms activity, physicochemical conditions and penetration of sun radiations inside the large-scale HRAP of Peterborough. Different questions emerge from this first study, including the availability of organic carbon for microalgae, the contribution of microalgae and bacteria to carbon and oxygen cycle, and the impact of microalgae on solar disinfection regarding the UV attenuation measured in this large-scale HRAP.

Considering the complexity of wastewater-microalgae consortium, investigations at laboratory scale in a 1.4 L torus PBR were conducted in a second time in order to understand carbon fate and role in microalgae-bacteria interactions in HRAP systems. Laboratory PBR using sterile synthetic wastewater allow consortia cultivation in axenic, controlled conditions, avoiding po-

tentially confounding factors like suspended solids or toxic compounds, enabling a focus only on microorganisms populations dynamics. Adapting the carbon supply and/or choice of inoculated species permits discrimination of the relative contributions of different trophic modes or microorganisms to the systems' oxygen and carbon balance, while collecting data online on both liquid and gas phases during a simulated day-night cycle. Data analysis was based on a mass balance on carbon, oxygen, hydrogen and nitrogen calling for stoichiometric analysis and reconciliation of experimental data. A kinetic model coupled to a radiative model was also implemented to explain and support the outcomes obtained experimentally. All those information contributed to a better understanding of carbon and oxygen dynamics during microalgae-bacteria co-culture.

The use of different systems during the PhD thesis also questions to what extent laboratory photobioreactors can inform population interaction dynamics in the HRAP. The Peterborough HRAP and laboratory PBR differ indeed in size and geometry, impacting heterogeneity and light transfer, which are characterised and compared through experimental and simulation work. The relevance of the choice of the carbon for the synthetic wastewater used in laboratory photobioreactors and its impact on oxygen and carbon balance and dominance of species in the reactor has then been discussed. In conclusion, data collected in PBR is expected to bring further understanding of the contribution of heterotrophy to microalgal growth in wastewater and its impact on the symbiosis with bacteria. Evaluating total carbon availability was for example of interest to determine the likelihood of growth limitation which would occur in such culture system, emphasizing the role of bacteria to provide inorganic carbon to microalgal culture but also possibly of a direct uptake of organic carbon source by microalgae.

Finally, the penetration of UV radiations in Peterborough HRAP, measured during the first phase of the study, questions the relative impact of microalgae on solar disinfection in HRAP system. The last part of the thesis has then estimated the impact of microalgae on indicator viruses inactivation, in terms of UV attenuation (inhibition of inactivation) and production of ROS (enhancement of inactivation), in a laboratory UV cabinet in Flinders University. This might bring elements for discussing the relevance of separating microalgae from wastewater as part of a tertiary treatment targeting pathogens.

This PhD thesis also reveals a few limits. Notably, the simulation at lab scale of a complex system such as HRAP implies a simplification step in order to focus on the main mechanisms. First, as wastewater is pre-treated in an anaerobic pond upstream Peterborough HRAP, the synthetic wastewater used in the torus PBR presented the same average composition as a classical anaerobically pre-treated wastewater. Nevertheless, in order to facilitate the modeling work and to understand the interactions between microorganisms, a sole organic carbon source, acetate, was used to simulate the organic load of the wastewater in the synthetic wastewater, which might affect the outcome. Moreover, considering the crucial importance of carbon in microalgal growth, this study focused on carbon fate and the interactions between microalgae and heterotrophic bacteria, neglecting the effect of nitrifying bacteria and the fate of nitrogen in the consortium.

The thesis is organised by chapters as follows. Figure 4 illustrates the links between the chapters:

• Chapter 1 draws up a state of the art of current knowledge on HRAP, focusing particularly on microalgae-bacteria interactions and disinfection processes.

• Chapter 2 presents the studied systems and the analytical methods.

• Chapter 3 draws up an overview of microorganisms activity, physicochemical conditions and sun radiations inside the large-scale HRAP of Peterborough, through a 3D characterisation of the pond.

• Chapter 4 is a literature review questioning the carbon sources available for microalgae in HRAP, investigating the synergy between carbon source and light and the relevance of using lab-scale PBR for investigating the mechanisms occurring in a large-scale HRAP.

• Chapter 5 investigates at lab-scale the impact of the carbon source on microalgae by estimating the relative contribution of photoautotrophy and photoheterotrophy in mixotrophic growth of the microalgae *S. obliquus*.

• Chapter 6 studies the fate and role of carbon source in microalgae-bacteria interactions in synthetic wastewater and simulated solar conditions at lab scale using the microalgae *S. obliquus* and the bacteria *E. coli*.

• Chapter 7 focuses on solar disinfection for pathogens removal and follows the observations

made in Chapter 3 about mixing and UV radiations penetration in Peterborough HRAP. This chapter investigates the impact of microalgae on indicator viruses solar disinfection in HRAP systems.

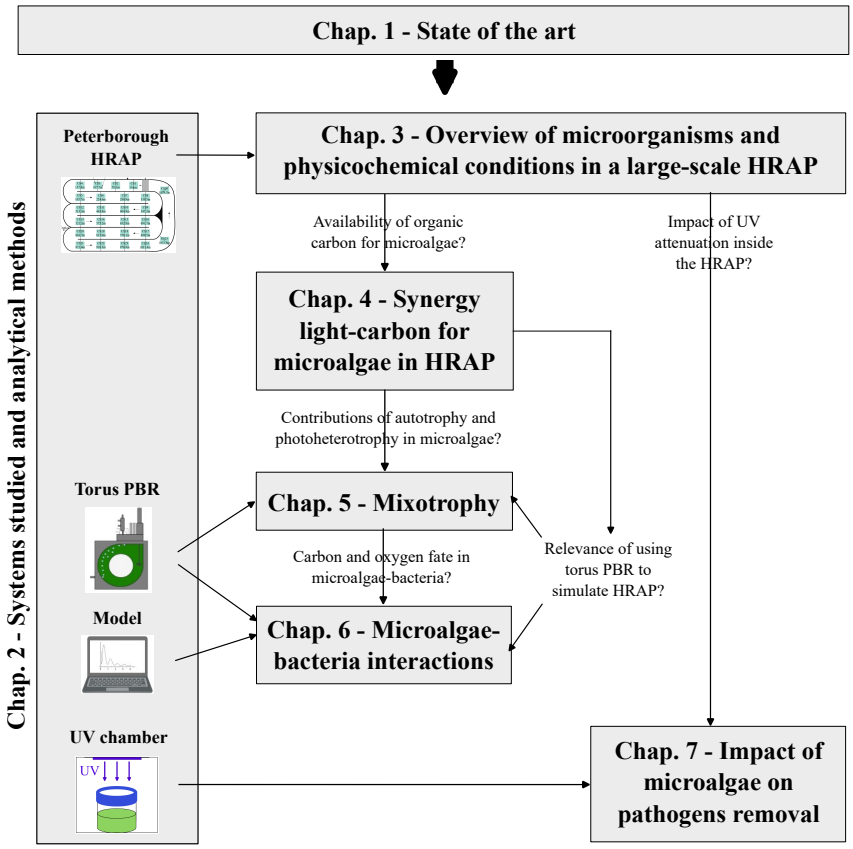

Figure 4 – Global structure of the thesis

Chapter 1

State of the art

1.1 Generalities about wastewater treatment

1.1.1 A brief history of wastewater treatment

Until the end of the 19th century, few houses had access to a cesspool. In cities at this time, wastewater evacuation infrastructures did not exist, and excrement was often disposed of directly into the streets. Raw wastewater was also commonly spread directly onto agricultural land. These practices facilitated the propagation of cholera and typhoid epidemics. Subsequently, public health concerns prompted a reevaluation of sanitation practices, leading to the initiation of the first wastewater collection and treatment operations (Figure 1.1). The aim was to take away stagnant water as far as possible from the city center (Deutsch and Vullierme 2003). Urbanisation also resulted in soil sealing, necessitating the collection of rainwater, which became indispensable. Later, drinking water became directly accessible from the tap, leading to increased water consumption and the need for larger volumes of wastewater to be evacuated. As the discharge of wastewater into water bodies quickly exceeded the self-purification capacities of rivers, wastewater treatment plants became necessary. Modern activated sludge treatment plants, as we know them today, began operating in the mid-20th century (Figure 1.1). In parallel, bacteriology made great progress at the beginning of the 20th century, highlighting the necessity of wastewater treatment (Barraqué 2014). These advancements were followed by further studies on wastewater treatment systems and sanitary risk evaluation in the 1960s. The 1970s and 1980s were characterized by growing environmental awareness, culminating in the First United Nations Water Conference held in 1977 (Steichen 2011). In 1973, the World Health Organisation

(WHO) declared that water quality for irrigation had to meet drinking water standards. This requirement was revised downward in 1989, with water quality thresholds adapted to the type of crop, wastewater treatment system, and irrigation method (Akissa and Inrgref 1992).

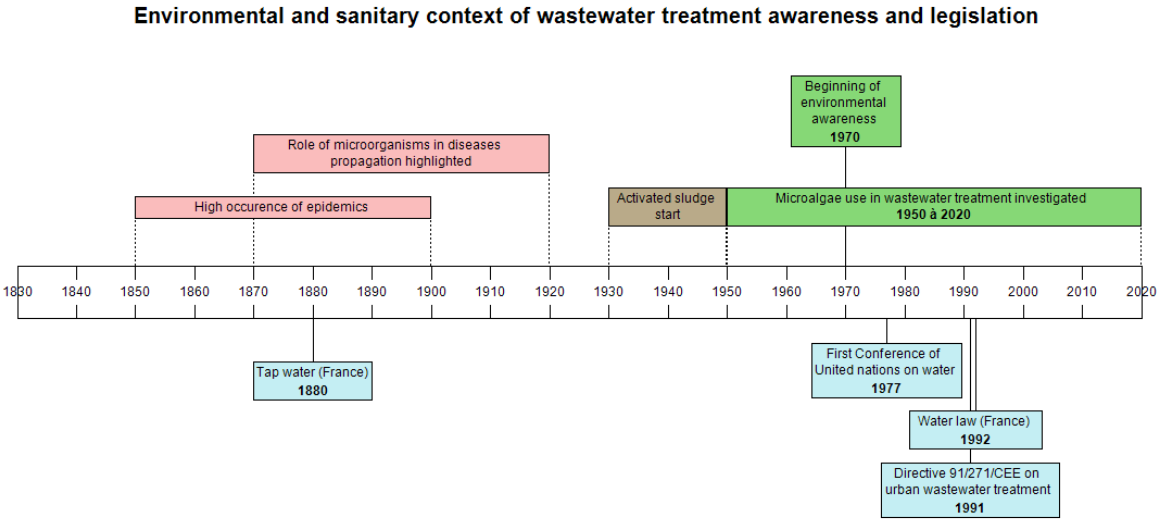

Figure 1.1 – Timeline of wastewater treatment history in environmental and sanitary context (Steichen 2011, Barraqué 2014, Bird 1992)

In 1991, the European Directive 91/271/CEE concerning urban wastewater treatment defined a population equivalent as a daily discharge of 60 g of BOD_5, representing the biodegradable organic matter in wastewater. This unit expresses the pollutants load produced per day by one inhabitant (Bird 1992). The Directive mandated that wastewater treatment plants in European states receiving more than 2 000 population equivalents must provide a biological secondary treatment system for organic load removal. According to this directive, European states are required to designate sensitive areas within their territory. Agglomerations with more than 10 000 population equivalents discharging into these sensitive areas were then obliged to implement tertiary phosphate and nitrogen removal in their sanitation system, to complement secondary treatment. However, a collective sanitation systems was not mandatory for cities with less than 2 000 population equivalents (Steichen 2011).

The introduction of the Directive led to the installation of new wastewater treatment plants to meet its obligations. Simultaneously, there was a desire to reduce the space required for

wastewater treatment plant, leading to the adoption of compact methods. However, the issue of sludge valorisation arose: 60 % of the mass produced by wastewater treatment was used for agricultural spreading, but this practice was found to exacerbate eutrophication problems by allowing excess sludge nutrients to runoff into natural water bodies. Consequently, a significant portion of the sludge was either incinerated or buried (Deutsch and Vullierme 2003).

Moreover, even in developed countries, and despite legislation, discharged water does not always comply with standards that protect the receiving environment. The 1991 European Directive led to the establishment of the Water Law in France in 1992, which translated the directive into legislation and measures adapted to the French territory. Nevertheless, French State was brought before The Court of Justice of the European Union in 2009 for non-compliant water treatment (Steichen 2011). Beyond this lack of compliance, new pollutants are continuously discovered in wastewater, and its treatment is far from ideal from economic, environmental, and sanitary point of view, even in developed countries. Nowadays, wastewater treatment remains a major public health problem in developing countries where sanitation systems are often nonexistent.

1.1.2 Composition of wastewater

The volume of wastewater to treat has increased sharply since tap water arrived in households. In 2016, 160 liters of water per person were delivered to French households every day, compared to 200 liters per person for Australian households (IWA 2016). Although these figures do not exactly reflect domestic wastewater production as they also include water used for car washing and garden watering, they provide an estimate of the volume treated daily by wastewater treatment plants in developed countries. Wastewater contains water from toilet flushing, bathing, food waste from the kitchen, as well as clothes and dishwashing. Residues from these activities consist of solids (suspended material) or dissolved components (ions, urea, diverse organic molecules, microorganisms). The main pollutants found in domestic wastewater, their origin, and their average concentrations are synthesized in Figure 1.2 below.

In wastewater, organic matter is frequently referred as COD (Chemical Oxygen Demand)

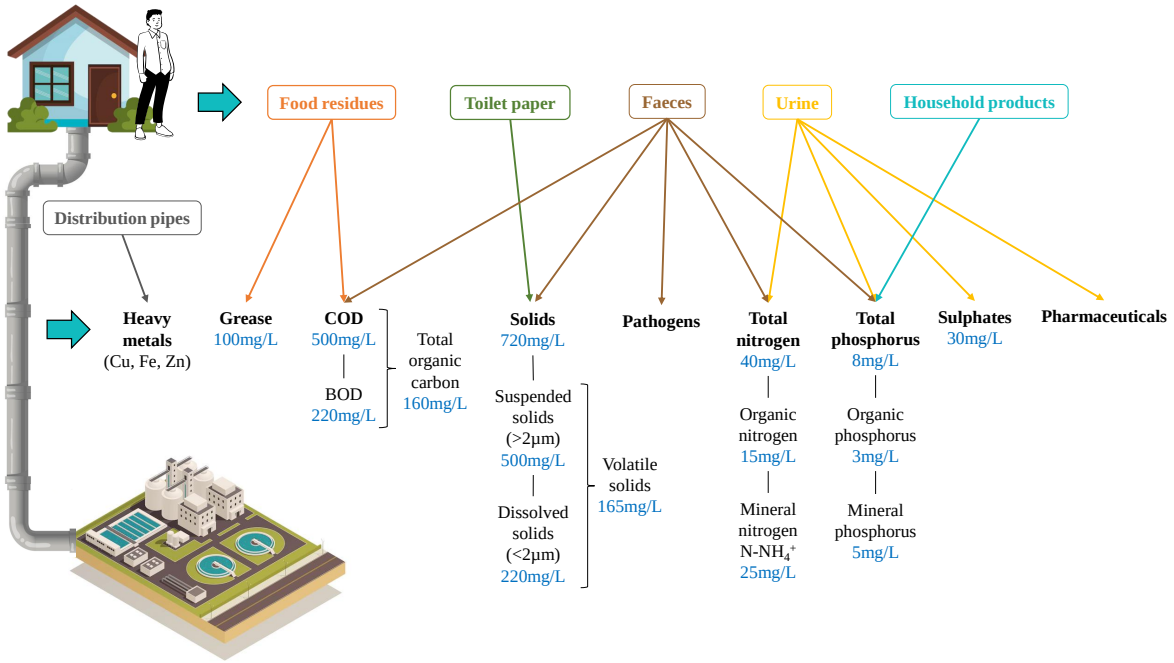

Figure 1.2 – Origin and concentration of domestic wastewater components (Rawat et al. 2016, Eme and Boutin 2015). Drawings from Freepik

and BOD (Biological Oxygen Demand). The composition of COD in raw domestic wastewater comprises 10-40 % lipid, 17-65 % protein, and 12-67 % carbohydrate (Lester 2001, Owusu-Agyeman et al. 2023, Chipasa and Mdrzycka 2006, Xu et al. 2023, Huang et al. 2010, Ravndal et al. 2018), with values varying greatly depending on the effluent's origin. Although the organic load (500 mgCOD.L^{-1} in average, Rawat et al. 2016) is mainly due to feces and, to a lesser extend, to food residues, minerals such as nitrogen (averaging 40 mgN.L^{-1} [1], Rawat et al. 2016) and phosphorus (averaging 8 mgP.L^{-1}, Rawat et al. 2016) mainly come from urine: an average person produces 12.8 gN.day^{-1} and 1.9 gP.day^{-1}, of which 11.2 gN and 1.1 gP are from urine and 1.6 gN and 0.8 gP are from feces (Eme and Boutin 2015). It's important to note that even through the organic nitrogen portion is non-negligible in total nitrogen in raw wastewater, its concentration will decrease during pretreatment due to rapid urea hydrolysis to ammonium (mineral nitrogen). In addition to these dissolved components, feces and sanitary products also

1. Units such as "mgN.L^{-1}", "mgP.L^{-1}", "gN.day^{-1}", "gP.day^{-1}" express nutrients quantities in terms of elementary nitrogen (N) or phosphorus (P)

bring solids to the effluent, with on average of 70 % of suspended solids (>2 μm) and 30% of dissolved solids (<2 μm) (Rawat et al. 2016). Low concentrations of heavy metals are also found in wastewater and mainly comes from distribution pipes.

1.1.3 Legislation: required water standards quality

1.1.3.1 In France

Water quality is monitored using organic and mineral (N and P) pollutants as well as bacteriological reference indicators such as *Escherichia coli*. The maximal values that can be reached for suspended solids, BOD_5, COD, N, P, and *E. coli* in treated wastewater destined to discharge and irrigation waters in France are synthesised in Figure 1.3. Note that the legislation was last updated in July 2021 for rejection water and in December 2023 for irrigation water. Treated water must have a nitrogen concentration <15 $mg.L^{-1}$ and a phosphorus concentration <2 $mg.L^{-1}$ before being discharged into natural water bodies. There is no mandatory bacteriological quality requirement for water exiting a wastewater treatment plant, unless it is used for irrigation of food crops or discharged into bathing areas. It's important to note that suspended solids and BOD requirements are the same for water destined for discharge into natural environment and for irrigation (35 $mg.L^{-1}$ of suspended solids and 25 $mg.L^{-1}$ of BOD), excepted for water intended for the irrigation of commercial food crops that can be consumed raw or unprocessed, which must attain a maximal concentration of suspended solids of 10 $mg.L^{-1}$ and a maximal concentration of BOD of 10 $mg.L^{-1}$.

The reuse of treated wastewater for irrigation in France is regulated since 2010 and was revised in 2023. The French decree of December 18, 2023, regarding the use of wastewater-treated water for irrigation of crops or green areas, establishes the maximal values required for BOD, suspended solid, and *E. coli* indicators for irrigation water. These values depend on the type of crop, the irrigation method, and the exposure of the public or workers. Bacteriological requirements for irrigation water vary based on the presence or absence of elements that could interrupt the transmission chain: for example, sprinkler irrigation poses a higher risk of contamination than drip irrigation and may correspond to stricter bacteriological standards. Similarly,

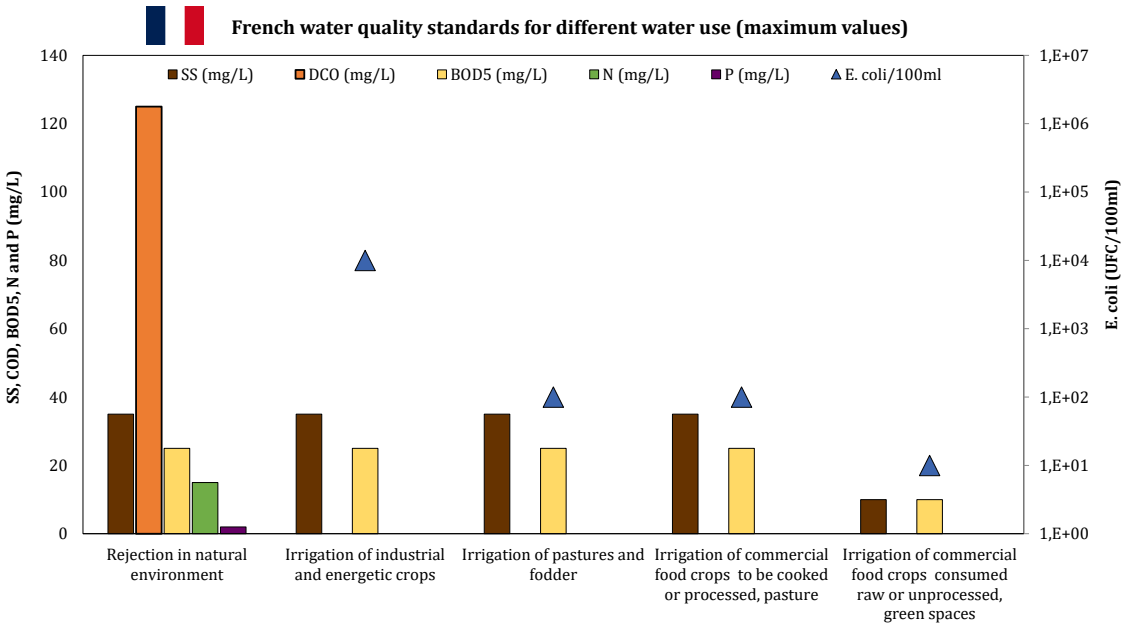

Figure 1.3 – Water quality standards in France for rejection in natural environment and irrigation. Note that values for rejection in natural environment are for plants with a capacity >120kgBOD_5/d (Legifrance 2021, Legifrance 2023)

non-food crops can be irrigated with water that does not meet any bacteriological standard, but only if the public is not exposed, excluding areas such as public gardens or stadiums. Cooking or processing food typically results in the inactivation of most microorganisms before consumption. Therefore, crops intended for cooking or processing after harvesting can be irrigated with water containing a maximum of 100 *E. coli* per 100 mL, compared to 10 *E. coli* per 100 mL for food crops that can be consumed raw or unprocessed.

1.1.3.2 In Australia

Wastewater reuse for irrigation is regulated since 2000 in Australia and was revised through a risk management approach in 2006 (Natural Resource Management Ministerial Council 2006). Maximum allowable values for suspended solids, BOD_5, N, P, and *E. coli* in wastewater effluent and irrigation water in Australia are summarized in the Figure 1.4. While the requirement for BOD_5, suspended solids, N, and P are similar to those in France, the bacteriological requirements are higher: wastewater treatment plant effluent should not exceed 10^6 *E. coli*/100 mL for

discharge into natural environment. Additionally, stricter standards apply to irrigation water, where the complete removal of *E. coli* is required for water used to irrigate commercial crops for raw consumption. Purification requirements for irrigation of non-food crops also include a 1-log reduction of viral pathogens (LGA 2020). However, specific BOD_5 and suspended solids requirements for irrigation of commercial food consumed raw or unprocessed are not available.

In the end, since the French legislation for wastewater reuse for irrigation was strengthened in 2023, restrictions applied are similar in France and in Australia.

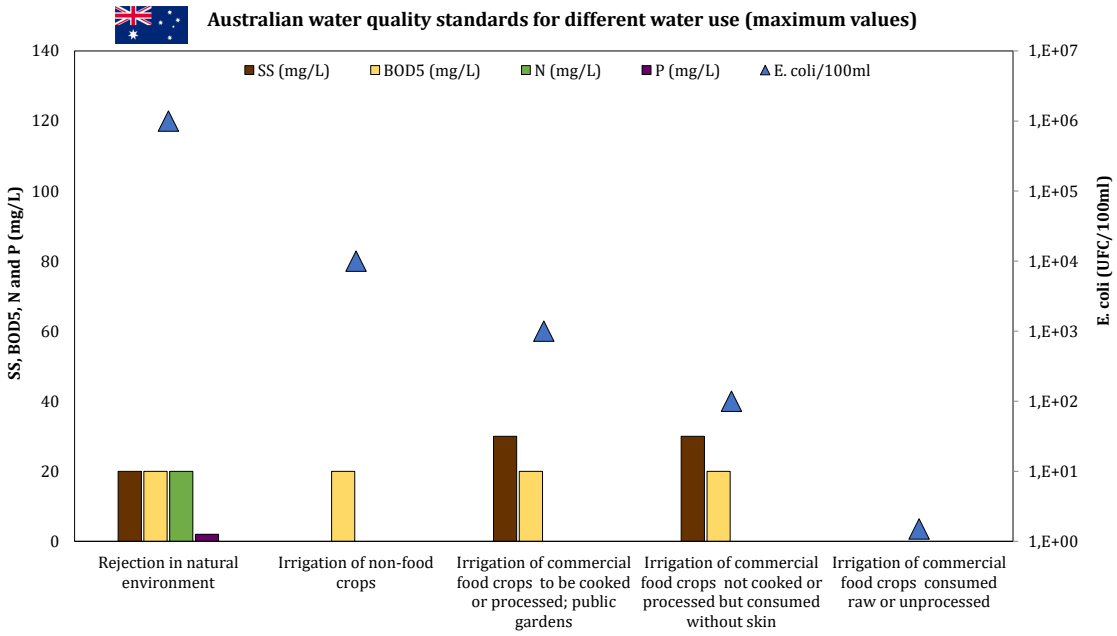

Figure 1.4 – Water quality standards in Australia for rejection in natural environment and irrigation (ARMCANZ 1997, NRMMC 2006)

1.1.4 Activated sludge: mechanisms, issues and alternatives

Globally, in developed countries, the quality requirements mentioned above are commonly achieved through the use of activated sludge treatment plants. This system is widely used due to its compactness, efficiency in removing organic matter, and suitability for handling variations in organic load.

1.1.4.1 Primary treatment

In most wastewater treatment systems, primary treatments are essential to safeguard downstream processes by removing the largest solids from the wastewater. These solids are separated from the water through screening and grit removal, utilizing successive grids with gauges ranging from 8 cm to a few millimeters. Adequat water velocity (0.5 to 1 $m.s^{-1}$ even if the grid is obstructed) is necessary to facilitate the deposition of solids on the grid (SUEZ). This first grid removal accounts for 35 % of the total pollutants in the wastewater. Subsequently, fats are eliminated through flotation (Moulin et al. 2013).

1.1.4.2 Secondary treatment

After this initial step, the activated sludge process commonly serves as the secondary treatment for removing organic pollutants. As depicted in Figure 1.5, the pretreated water enters an aerated pond. The suspended solids or sludge, containing a complex consortium of microorganisms, are settled in a clarifier and a proportion recycled to the aeration basin. This "activated sludge" maintains the active consortium in the aeration basin to effect treatment. Heterotrophic bacteria degrade organic molecules in the wastewater through aerobic respiration, wherein oxygen is consumed and carbon dioxide is produced (Eq. 1.1):

$$C_6H_{12}O_6 + 6\,O_2 \rightarrow 6\,H_2O + 6\,CO_2 \tag{1.1}$$

In addition to this mineralisation process, bacterial biomass can form flocs with organic matter present in the water, aiding in the sedimentation of sludge in the subsequent pond, known as the clarifier. After passing through the clarifier, some of the sludge is recirculated back into the aerated pond to maintain the concentration of heterotrophic bacterial (Wang et al. 2008).

While this process efficiently removes organic carbon, it is also essential to eliminate mineral nitrogen compounds such as ammonium and nitrate. This removal is achieved by biological nutrient removal (BNR) using activated sludge plants with extended aeration to complete the ni-

trification process which is followed by denitrification. Nitrification occurs in two steps involving two types of autotrophic bacteria: Ammonium Oxidising Bacteria (AOB), typically represented by the genus *Nitrosomonas*, oxidize NH_4^+ to NO_2^- (Eq. 1.2), and Nitrite Oxidising Bacteria (NOB), usually represented by the genus *Nitrobacter*, further oxidize NO_2^- to NO_3^- (Eq. 1.3) (Cébron 2004). The resulting nitrate molecules are then converted into atmospheric gas N_2 by denitrifying bacteria, such as those from the genus *Pseudomonas*. This anaerobic process removes nitrogen from the water, transferring it to the atmosphere. The overall conversion process can be represented by the Eq. 1.4:

$$NH_3 + 1.5\,O_2 \rightarrow H_2O + NO_2^- + H^+ \tag{1.2}$$

$$NO_2^- + 0.5\,O_2 \rightarrow NO_3^- \tag{1.3}$$

$$2\,NO_3^- + 10e + H^+ \rightarrow N_2 + 6\,H_2O \tag{1.4}$$

The sludge is subsequently dried, stabilised with soda, and either spread on agricultural lands as fertiliser or incinerated. The sludge can also be composted or digested to CH_4.

1.1.4.3 Tertiary treatment

After activated sludge treatment, complementary tertiary treatments are often needed to remove phosphate and remaining pathogens. Phosphorus can be precipitated in particulate form by adding chemicals such as iron, aluminium, or lime to the activated sludge-treated water. This step must occur after organic matter removal to prevent adverse reactions of the chemicals with organic molecules. The precipitate is then harvested by filtration or decantation (Deronzier and Choubert 2004).

Excessive pathogen concentrations can persist in the water after the activated sludge process, even though most bacterial biomass has flocculated. Remaining pathogens can be removed from the water through adsorption of bacteria and viruses onto larger aggregated particles, which

are then separated from the treated water by sedimentation, membrane filtration, enzymatic degradation, UV irradiation, chlorination, or ozonation (Corpuz et al. 2020).

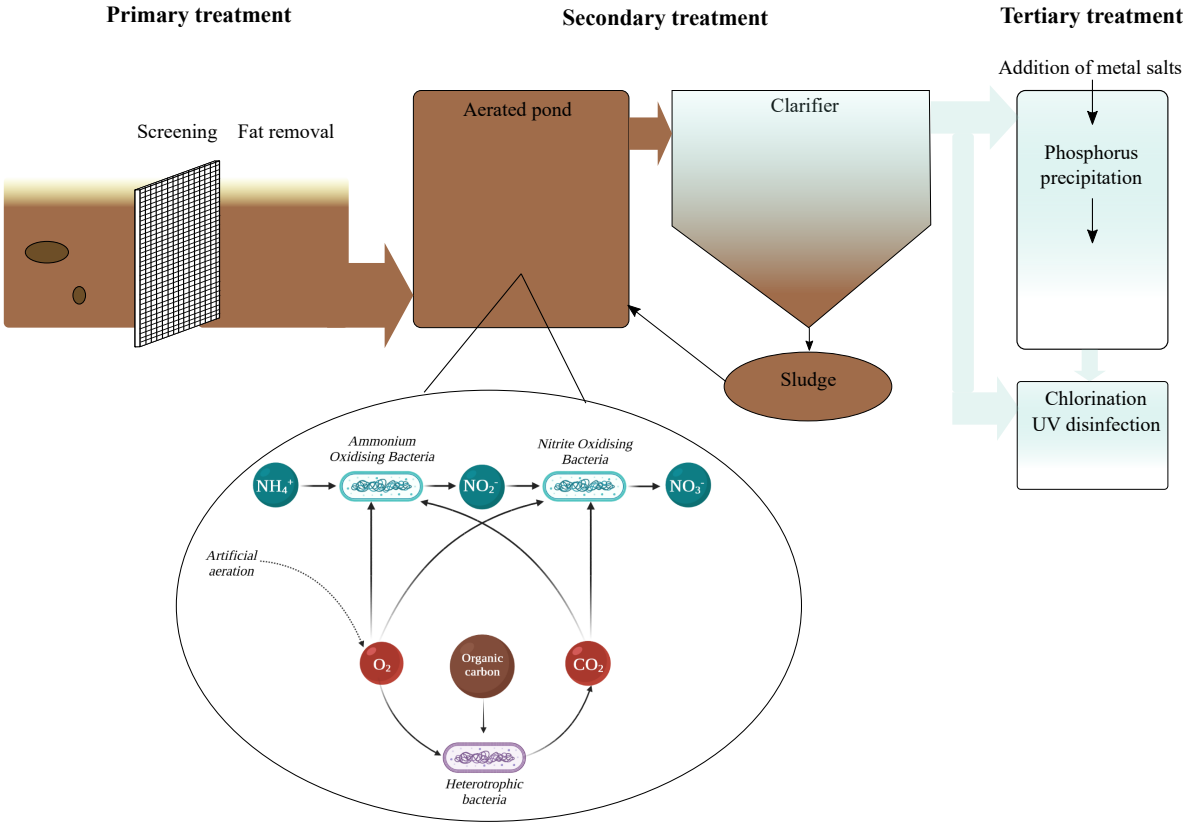

Figure 1.5 – Principle of activated sludge (Wang et al. 2008, Cébron 2004, Deronzier et al. 2001)

1.1.4.4 Toward more sustainable methods for wastewater treatment

Activated sludge constitutes a relatively efficient method for treating organic matter and nitrogen substances in wastewater, with most effluents meeting the quality standards set at the national scale worldwide. However, this system is far from ideal from both ecological and economical perspectives. Continuous oxygen supply to aerated pond is essential for bacterial respiration and efficient pollutant degradation. However, this process is energy-intensive and costly, often constituting a significant portion (50 % to 90 %) of the total energy consumption of activated sludge treatment plants (Oviedo et al. 2022). In Melbourne in 2009-2010, 3 075 GJ of

energy per GL of wastewater were consumed and the production of greenhouse gases associated with wastewater pumping and treatment in Melbourne was 277 335 tons of CO_2-equivalent over one year in 2013-2014 (Cook et al. 2012).

Moreover, nitrogen present in the influent cannot be valorised as it is lost to the atmosphere after denitrification. Additionally, activated sludge as wastewater treatment systems face challenges regarding the valorisation of sludge, the solid waste produced during the treatment. Typically, sludge is spread on agricultural lands, leading to eutrophication problems due to the high levels of nitrate and phosphate contained in the sludge, which can runoff into water bodies during precipitation events (Quilbé et al. 2005).

Despite being the most widely used sanitation system, there are less expensive and less environmentally impactful pond-based alternatives that can also be used for secondary and tertiary treatment.

- **Secondary treatments:**

— **Waste Stabilisation Ponds (WSP):** These consist of three unmixed successive ponds with a total Hydraulic Retention Time of 20 to 60 days. The first pond, known as the anaerobic pond, is characterized by its depth (2 to 5 m) and removes approximately 70 % of the organic load. The remaining organic matter undergoes degradation in the shallower facultative pond (1-2.5 m), which facilitates significant oxygen exchanges with the atmosphere and allows for light penetration, promoting algal growth and oxygen production. Sunlight disinfection occurs in the last and shallowest pond, referred to as the maturation pond (0.5-1.5 m depth, Natural Resource Management Ministerial Council 2006).

— **Aerated ponds:** These ponds differ from WSP by their artificial aeration and are also commonly used as a secondary treatment option (Renou et al. 2008). WSP and aerated ponds aim to replace activated sludge with their efficient organic load removal capacity. However, a major drawback is the very long HRT required to achieve pollutants removal, leading to a significant land footprint and high evaporation rates (LGA 2020).

- **Tertiary treatments:**

— **Vegetative areas:** Alternative tertiary treatments are also available to further pollutant removal without the use of chemicals. These methods include discharging water through vegetative areas or planted reed beds between the wastewater treatment plant and the receiving environment. This allows for additional treatment of suspended materials, nutrients, metals, and micropollutants.

— **Bacterial filters:** Another option involves passing water through a filtering medium where bacteria develop and aid in degrading remaining pollutants after the clarifier (Moulin et al. 2013).

— **Inoculation with dephosphating bacteria:** Water can also be inoculated with bacteria capable of uptaking phosphorus in large quantities, not only to meet their metabolic needs but also by accumulating phosphorus into their biomass (Deronzier and Choubert 2004). This method, known as Enhanced Biological Phosphorus Removal (EBPR) by Phosphate Accumulating Organisms (PAO), enhances phosphorus removal by 80 to 90 % (Fallahi et al. 2021).

— **Nutritive Biological Displacement:** In this approach, water circulates through a tank containing bacteria that accumulate phosphorus (Wainaina 2021).

1.2 High Rate Algal Pond technology: functioning of a promising alternative solution

The current operation of wastewater treatment systems reveals significant environmental and economic challenges, highlighting a genuine need for alternative methods. High Rate Algal Ponds offer a potential solution for secondary wastewater treatment in remote areas, being more cost-effective and energy-efficient than activated sludge, yet more intensive than Waste Stabilisation Ponds and lagooning ponds. HRAPs consist of shallow raceways typically 30-50 cm in depth, mixed with a paddlewheel. This design allows a good light penetration throughout the pond depth, promoting photosynthesis and microalgal growth (Fallowfield and Garrett 1985). As a

result, photosynthesis enables self-sustaining oxygen production for degradation of organic matter by heterotrophic bacteria (Young et al. 2017), eliminating the need for artificial mechanical aeration in HRAPs.

The efficiency of microalgae-based systems in achieving acceptable pollutants concentrations for the receiving environment or irrigation, while minimizing environmental impact, has already been demonstrated in numerous studies. The Peterborough HRAP in South Australia serves as a prime example of a successful large-scale HRAP treating actual wastewater (Figure 1.6). The following sections aim to outline the pond design and the functioning of the successive biological treatment steps of Peterborough HRAP.

Figure 1.6 – Aerial view of Peterborough wastewater treatment site

1.2.1 Primary treatment

The primary treatment preceding the HRAP system varies depending on the installation. At the Peterborough plant, wastewater undergoes pretreatment in an anaerobic pond with a depth of 4 meters and a HRT of 4 days before entering the HRAP. This first step involves the settling of larger particles in a deep pond, contributing to the reduction of wastewater turbidity and enabling better light penetration in the HRAP thereafter. Approximately 50 % of BOD_5 is removed during pretreatment in the anaerobic pond through the mineralisation of the organic matter present in the wastewater (Figure 1.7).

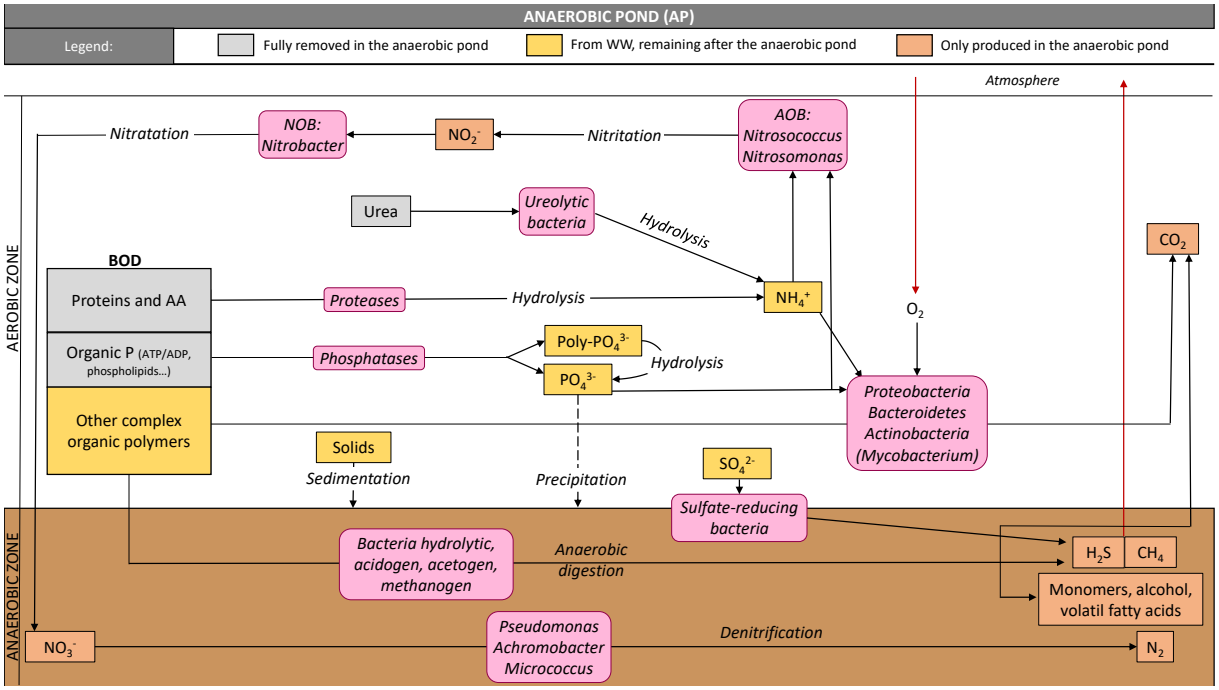

Figure 1.7 – Main chemical and biological processus occurring in pretreatment anaerobic pond. WW=wastewater; AP=anaerobic pond; AA=amino acids (Fallowfield and Garrett 1985, Kang et al. 2020, Park et al. 2013, Delfosse 2014)

The anaerobic pond comprises both an aerobic zone near the surface and an anaerobic zone at the bottom, creating different abiotic conditions conducive to various processes during pretreatment. Anaerobic bacteria facilitate the anaerobic digestion of organic matter at the pond's bottom, where oxygen concentration is minimal. During anaerobic digestion, organic molecules undergo hydrolysis to form volatile fatty acids (VFA), CO_2, NH_3, and H_2. Subsequently, under alkaline conditions, these smaller molecules are converted into CH_4 (Fallowfield and Garrett 1985). In contrast, near the surface, gas exchanges with the atmosphere and photosynthesis occur, resulting in higher oxygen concentrations, allowing aerobic bacteria to oxidise organic matter. After passing through the anaerobic pond, proteins and urea are almost entirely mineralised into NH_4^+ through the action of proteases and urea hydrolysis (Table 1.1). Nitrates produced by nitrification in the aerobic zone are consumed by anaerobic denitrifying bacteria and converted into N_2. Organic phosphorus is also mineralised into phosphates and polyphosphates by the action of phosphatases. Hydrolysis of polyphosphates leads to the formation of

simple phosphates, which are likely to precipitate under high pH conditions. Sulphate-reducing bacteria consume sulphates to produce H_2S. Ammonium, phosphates, and sulfates are consumed by heterotrophic and autotrophic bacteria.

Concentrations of mineral and organic pollutants after pretreatment in an anaerobic pond (Table 1.1) are significantly reduced compared to the composition of raw wastewater (Figure 1.2). Only nitrates and nitrites show a slight increase due to nitrifier activity. Solids sedimentation significantly contributes to pollutant removal and raises questions about the fate of the sludge accumulated at the bottom of the anaerobic pond. A gradual compaction of the bottom sludge is expected, resulting in only a few millimeters of sludge thickness gain annually (Nelson et al. 2004). This reduction in solid waste accumulation facilitates pond maintenance.

Components	**Average concentration ± SD** (mg/L)
Total suspended solids (TSS)	107 ± 57
Volatile suspended solids (VSS)	81 ± 54
Chemical Oxygen Demand (COD)	206 ± 56
Biological Oxygen Demand (BOD)	129 ± 58
Organic carbon	19 ± 7
Inorganic carbon	14 ± 13
N-NH_4^+	46 ± 32
N-NO_3^-	9 ± 9
N-NO_2^-	0.4 ± 0.6
P-PO_4^{3-}	14 ± 8
SO_4^{2-}	57 ± 33
Chlorophyll *a*	0.8 ± 1

Table 1.1 – Average wastewater composition after anaerobic pond treatment according to Assemany et al. (2015), Buchanan et al. (2018a), El Hamouri et al. (1995), El Hamouri (2009), El Hamouri et al. (2003), Paing et al. (2003), Sutherland et al. (2017), Zhao et al. (2018)

.

1.2.2 Secondary treatment: the central process in the HRAP

1.2.2.1 Design of an HRAP according to South Australia guidelines

After its passage through the anaerobic pond, pretreated wastewater exits by overflowing and is discharged by gravity into the HRAP. Peterborough HRAP inlet is located a few meters downstream the paddlewheel in order to ensure efficient mixing with the microalgae in the HRAP.

Engineering guidelines essential for efficient removal of organic matter, minerals, and pathogens, based on previous studies, are outlined in the High Rate Algal Pond Design Guideline from the Local Government Association of South Australia (LGA 2020). According to this document, an 8-bladed paddlewheel must rotate at 12 rpm to provide continuous mixing and maintain a flow velocity of 0.2 $m.s^{-1}$ in the channel to prevent the sedimentation of suspended solids.

The channel can consist of a single loop or a series of loops with central channel dividers. The ratio of total channel length to channel width must be at least 6:1 (LGA 2020). In the case of Peterborough, the channel meanders through a series of 6 channels (Figure 1.6). At the end of the 5^{th} channel, an outlet allows the transfer of the treated wastewater mixed with microalgae to storage ponds by gravity. Guidelines specify that the hydraulic retention time in the pond should be at least 10 days to achieve a 1-log reduction in viral pathogens before exiting the pond. To ensure sufficient light penetration for pathogens disinfection and photosynthesis, the depth of HRAPs is limited to a maximum of 50 cm and is more often operated at a depth of 30 cm. Additionally, guidelines require a freeboard of at least 30 cm.

1.2.2.2 Principle of biological pollutants and pathogens removal in HRAP

The availability of photons for microalgae in the pond is ensured by both the shallow depth and the mixing provided by the paddlewheel (Demory et al. 2018). This enables natural microalgal consortia to achieve relatively high productivities in outdoor conditions using sunlight as an energy source (Artu 2016). The dissolved oxygen produced through photosynthesis is utilized by heterotrophic bacteria present in wastewater. These bacteria oxidise organic pollutants such as volatile fatty acids, sugars, polycyclic aromatic hydrocarbons, organic solvents, or phenolic compounds (Rawat et al. 2016). CO_2 produced by the mineralisation of organic carbon by heterotrophic bacteria is then consumed by microalgae. A consortium is formed between heterotrophic and photosynthetic microorganisms. Both the dissolved oxygen produced by microalgae and the inorganic carbon produced by heterotrophic bacteria are consumed by nitrifying bacteria. These bacteria utilize ammonium to produce nitrites and then convert nitrites to nitrates, which are a less harmful molecules, similar to the process in an activated

sludge system (Evans et al. 2005). Microalgae, heterotrophic bacteria and nitrifying bacteria consume dissolved wastewater mineral pollutants, primarily NH_4^+, NO_3^-, PO_4^{3-}, and SO_4^{2-}, converting them into biomass and facilitating the separation of these pollutants from water (Sforza et al. 2018). Additionally, phosphorus can be removed by precipitation when the pH rises above 11, which frequently occurs in a HRAP during the day due to photosynthesis.

The HRAP system enables compliance with national standards for irrigating non-food crops in terms of pathogen removal, which constitutes the main challenge of wastewater treatment (Young et al. 2016). This is because HRAP is exposed to sunlight and consequently to UV radiation, which is highly energetic and damages microorganisms' DNA. High dissolved oxygen and pH levels resulting from photosynthetic activity also create favorable conditions for microorganisms inactivation and synergize with UV radiation (Benchokroun et al. 2003).

1.2.3 Tertiary treatment: the separation of recoverable biomass and treated wastewater

In the case of Peterborough, treated wastewater mixed with microalgae flows into two storage ponds where the microalgae is partially separated from the treated water through sedimentation. The HRT in these storage ponds is 25 days, as required for helminth removal (LGA 2020). Generally, biomass is not separated from the treated water due to low biomass concentration. Moreover, due to the similar density between biomass and water, harvesting microalgae can become a challenging step (Fallahi et al. 2021). In the case of biomass separation from the treated water, various methods can be employed, such as sedimentation or flotation. Several studies have also demonstrated that recycling harvested biomass by recirculating a portion of the harvested microalgae into the HRAP significantly improves settleability and harvesting efficiency (Gutiérrez et al. 2016a, Park et al. 2011).

1.2.4 Valorisation of the water treated and of the biomass produced in the HRAP

1.2.4.1 Valorisation of the treated water

Generally, the fate of treated water depends on its quality after treatment and on the interests and risks associated with its intended use. Legal standards and guidelines for the discharge of treated wastewater into the natural environment and for its reuse or irrigation in France and Australia were presented in section 1.1.3. This section aims at presenting and discussing the various options for wastewater fate after treatment in HRAP (Figure 1.8).

1.2.4.1.1 Discharge in the natural environment

Discharging treated water into natural water bodies can help achieving the minimum ecological river flow required for local fauna habitat conservation, especially during warmer months (Yan et al. 2018). However, even through the water undergoes treatment, its discharge into the natural environment has been reported to impact river quality. For instance, 47.6 % of 84 organic micropollutants found in river water were also detected in the effluent from industrial wastewater treatment plants (Liu et al. 2022). In Shanghai's river, treated wastewater contributed of 68.3 % of the nitrate (NO_3^-) content, followed by soil nitrogen (15.7 %) and fertilizers (15.5 %), despite Shanghais high urban domestic sewage recovery rate of 92 % (Zhao et al. 2023a). In contrast, treated wastewater did not contribute to parasitic contamination by *Cryptosporidium spp.* and *Giardia duodenalis* in the Seine river upstream of Paris due to efficient removal of those organisms in the treatment plant (Moulin et al. 2010).

1.2.4.1.2 Irrigation

70 % of abstracted water is used for agricultural irrigation in arid and semi-arid regions of the globe. Utilizing treated wastewater for irrigation could diminish the necessity for water abstraction and aid in protecting water resources. The benefits of treated wastewater for soil enrichment and microbial activity was demonstrated by several studies. After six years of irrigation with treated wastewater, an increase in NO_3^-, K, P, and micronutrient concentrations was

reported in arable soil, thereby improving soil quality and agricultural productivity (Ganjegunte et al. 2017). Moreover, N and P are available in a mineralised form in treated wastewater, facilitating their uptake by the crops (Yalin et al. 2023). Using treated wastewater, which contains fewer nutrients than traditional fertilisers, can help prevent excessive nutrient application and subsequent runoff into natural water bodies. However, attention should be paid to suspended solids in treated wastewater, as they may clog soil pores, reduce water infiltration, and increase runoff. Wastewater irrigation also enhances the of soil microbial populations, which is advantageous considering that 80 to 90 % of processes occurring in soils are facilitated by microbes. Additionally, the growth of microorganisms in soil is supported by organic molecules found in wastewater (Ofori et al. 2021).

Improvements in soil quality also lead to enhanced plant growth. A study by Zema et al. (2012) found that irrigating three different types of crops with treated wastewater for two years resulted in significant increase in plant growth compared to conventional water irrigation. Pooja et al. (2022) conducted a study comparing the growth of tomato plants irrigated with wastewater treated using *Chlorella vulgaris* (then separated from the biomass after treatment) versus chemical fertilizer. They found no significant differences in tomato productivity between the two conditions, indicating that HRAP treated wastewater can be efficiently utilized as irrigation water.

However, irrigation with wastewater could also have detrimental effects on soil. High conductivity levels measured in treated wastewater can lead to soil salinisation. When salinity levels are too high, plant water uptake is affected depending on the plant's tolerance to high salinity. Ayers and Westcot (1985) recommend slight to moderate irrigation restrictions when wastewater conductivity exceeds 700 μS.cm^{-1}, and severe restriction when it surpasses 3000 μS.cm^{-1}. Moreover, wastewater is likely to contain micropollutants such as endocrine-disrupting compounds, pharmaceuticals, or heavy metals, which could be uptake by the plants and have toxic effects on their growth. However, Soleimani et al. (2023) reported that among treated wastewater effluent, well water with fertilizer, and river water, treated wastewater effluent transferred the lowest amount of heavy metals to the soil, making it the most suitable source for irrigation due to

its low heavy metal concentration and high nutrient content. In addition, heavy metals tend to accumulate in surface soil due to their low solubility and limited plant uptake, leading to accumulation primarily in roots rather than in the edible parts of the plant.

Although treated water still contains significant remaining pathogens, raising concerns about the public health impact of irrigation with treated wastewater, no pathogenic contamination of plants occurs if there is no direct contact between the edible parts of the plants and the irrigation water (Ofori et al. 2021).

In conclusion, utilizing treated wastewater for irrigation offers considerable advantages for agriculture, which are also reflected in economic benefits. Studies have shown that using treated wastewater can lead to significant reductions in the usage of chemical fertilizers, with potential savings ranging from 45 % to 94 % in various crops such as wheat, alfalfa, and tomatoes (Ofori et al. 2021). For instance, in wheat and alfalfa cultivation, chemical fertilizer usage could be reduced by up to 94 %. Similarly, for tomato cultivation, potential savings of 280€ per hectare were identified (Vergine et al. 2017). However, it's essential to acknowledge that there are additional costs associated with wastewater transportation, including infrastructure such as reservoirs, piping, and pumping facilities.

Finally, while HRAP systems offer promising wastewater treatment capabilities, one of the primary challenges for utilizing treated wastewater in irrigation is ensuring consistent disinfection performance. This variability in disinfection efficacy may restrict the reuse of treated water to irrigation purposes for non-food crops only unless additional disinfection measures are adopted (Yalin et al. 2023).

1.2.4.2 Valorisation of the biomass

The production of microalgal biomass has raised the interest of scientists across various fields, including agriculture, energy production, cosmetics, and human and animal nutrition. However, the high cost of microalgae production, ranging from 20 to 200 $ per kilogram (Robles et al. 2020), has been a limiting factor. Microalgae cultivation in HRAP systems offers a potential solution to reduce production costs by eliminating the need for additional water, nutrients, and

artificial light sources. Despite the benefits of microalgal biomass production in HRAP systems, contamination of the biomass by pollutants and pathogens from wastewater restricts its use in cosmetics or food applications. However, the biomass remains valuable for processing into bio-fertilisers, biofuels, or biogas (Figure 1.8). Even if the microalgal biomass has potential interest, the primary objective of HRAP systems is water treatment, with biomass production being a secondary consideration. As a result, process parameters, particularly hydraulic retention time, are optimized to achieve the lowest possible pollutant concentrations in the treated water. This optimization may lead to nutrient limitation for microalgae, resulting in lower biomass productivity compared to systems focused solely on biomass production.

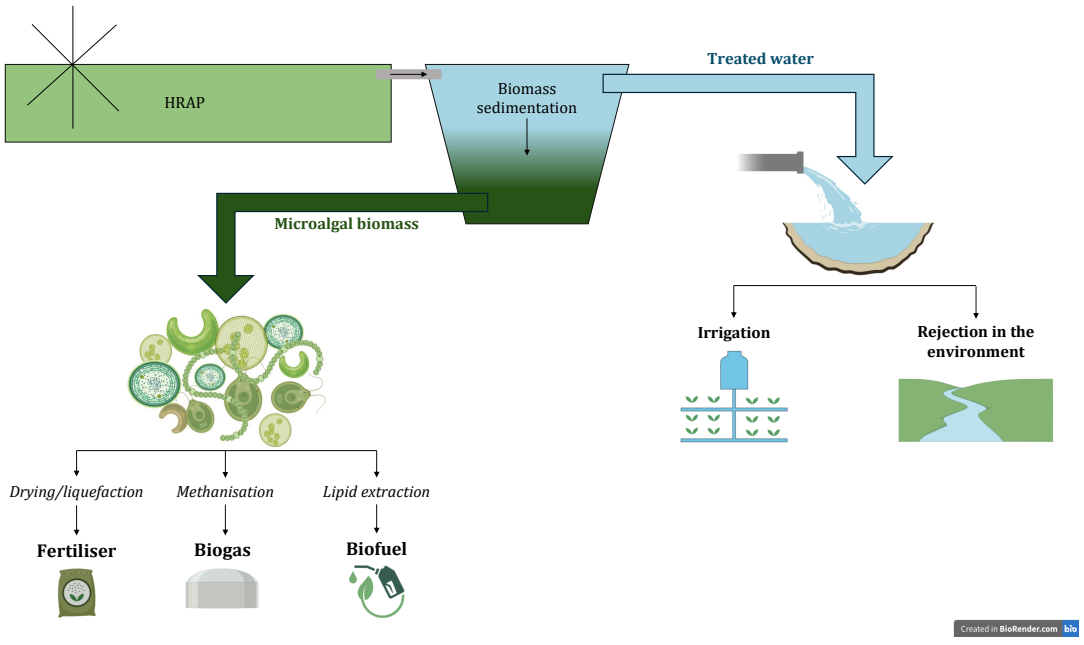

Figure 1.8 – Valorisation routes for treated water and biomass after secondary treatment in HRAP

1.2.4.2.1 Bio-fertilizers

The interest in algae as fertilizers lies not only in the nutrients contained in the biomass but also in the biostimulant properties of algal products. Biostimulants can also be derived from algae amino acids through enzymatic hydrolysis of the biomass.

Compared to traditional spreading of wastewater treatment plant sludge for agricultural fer-

tilization, the use of microalgae as fertilizers also reduces the risk of eutrophication because N and P are contained within algal cells and are less likely to runoff in soil and water. Research by Álvarez-González et al. (2022) found that basil crops fertilised with microalgae showed comparable plant growth to crops fertilised with traditional inorganic fertilisers, as well as a mix of both. Simlarly, Álvarez-González et al. (2023) examined the impact of using microalgae grown in municipal wastewater as a fertiliser on lettuce and reported similar fresh shoot weights between microalgae fertilisers and traditional fertilisers. However, the use of microalgae grown in wastewater as a fertilizer raises concerns about biomass contamination and its potential impact on crops contamination. Álvarez-González et al. (2023) found that pathogen and heavy metal concentrations in microalgal biomass grown in municipal wastewater were below the thresholds established by the European regulation for fertilizing products (UE 2019), except for cadmium. Cadmium and contaminants of emerging concern (CECs) were also detected in traditional fertilisers.

1.2.4.2.2 Biofuels

Microalgae are also raising increasing interest for biofuel production due to their ability to accumulate energy-rich metabolites (lipids, carbohydrates) within their cells, which can be converted into biofuels. Through the use of simulation tools, Heredia et al. (2022) demonstrated from an energetic perspective that coupling intensified photobioreactors for microalgae production with photovoltaic panels, solvent-free metabolite recovery processes, and high biomass concentration treatments contributed to increasing the energy return on energy invested in producing bioethanol and biodiesel liquid fuels from microalgae. Depending on these variables, this valorisation route could become cost-effective in the future, especially considering that the energetic cost associated with microalgae production in HRAPs is reduced compared to traditional photobioreactors. This suggests that integrating intensified photobioreactors with renewable energy sources and efficient downstream processing techniques could enhance the viability of microalgae-based biofuel production.

1.2.4.2.3 Biogas

Microalgal biomass digestion can indeed result in the production of biogas, primarly methane. The biogas can then be utilized for various applications such as electricity generation, fuel cells, and liquid fuel production. For example, according to Mussgnug et al. (2010), microalgae species like *Chlamydomonas reinhardtii* exhibit promising characteristics for biogas pproduction, with a yield of 587 mL of biogas per gram of volatil solids, compared to 287 mL for *Scenedesmus obliquus*.

1.3 Sustainability and performances of HRAP systems

1.3.1 HRAP systems performances in real conditions

Analyzing the performance data of large-scale HRAPs is crucial for assessing their compliance with wastewater treatment regulations. To conduct this evaluation, data from 14 studies obtained from the literature were compiled (see Table 1.2 and Table 1.3 for all the references). These studies focused on HRAP systems treating real wastewater continuously in outdoor ponds for a minimal duration of one year. Additionally, only HRAPs with a surface aera greater than 25 m^2 were included in the analysis. The gathered data will be utilized to assess the removal performance of macropollutants and pathogens in the following sections.

1.3.1.1 Mineral and organic macropollutants removal

The compilation of HRAP performance data for the removal of N-NH_4^+, P-PO_4^{3-}, BOD_5, and COD from pilots with surface areas greater than 25 m^2, treating real domestic wastewater in outdoor conditions, is summarized in Table 1.2. These data reveal significant pollutant removal achieved by the microalgae-bacteria consortium within HRAP systems. On average, HRAPs achieved removal efficiencies of 67 % ± 20 % for N-NH_4^+, 41 % ± 19 % for P-PO_4^{3-}, 55 % ± 19 % for BOD_5 and 39 % ± 24 % for COD. However, the performance varies and is influenced by seasonal factors, and may not always ensure compliance with regulations for effluent discharge into the environment in France or Australia. Figure 1.9 illustrates the concentrations of N-NH_4^+,

P-PO_4^{3-}, and BOD_5 in HRAP effluents compared to the maximum allowable concentrations for effluent discharge into the environment in France (representated by the dark blue line) and Australia (represented by yellow line). Among the 25 analyzed HRAP effluents, 18 complied with French regulations for N-NH_4^+, and 20 complied with Australian regulations. For P-PO_4^{3-}, 6 HRAP effluents out of 23 complied with both French and Australian regulations. Regarding BOD_5, 3 HRAP effluents out of 9 complied with French regulations, while 2 complied with Australian regulations. Finally, 2 HRAP effluents out of 8 complied with French regulations for COD.

It's noteworthy that the limits for BOD_5 (in Australian regulations) and COD (in French regulations) are applicable to both effluent discharge into the environment and irrigation of food and non-food crops. As per the analysis presented earlier, only 2 HRAP effluents out of 9 would meet the criteria for irrigation in Australia, and 2 out of 8 would meet the standards for irrigation in France, considering only macropollutant concentrations.

In HRAP, higher removal of P-PO_4^{3-} appears to be correlated with higher microalgal productivities. Microalgal productivity is typically measured based on total suspended solids (TTS), as shown in Table 1.2. The microalgal productivity in HRAP ranges from 12.5 and 54 g of TSS/m^3/d, with the highest values observed during the summer months. These productivities are relatively low compared to those achieved in thinner photobioreactors (typically 2-10 cm depth), where productivities can reach around 500 gTSS/m^3/d. However, the productivities obtained in wastewater in HRAP are consistent with the maximum productivities theoretically achievable in a 30 cm depth photobioreactor. This suggests that microalgae growth in HRAP is primarly limited by light availability rather than nutrient availability, confirming the suitability of using wastewater as a nutrient source for microalgae (Pruvost et al. 2012). It's important to note that the suspended solids in HRAP comprise not only microalgae but also organic matter flocs, so the productivities based on TSS may be slightly overestimated.

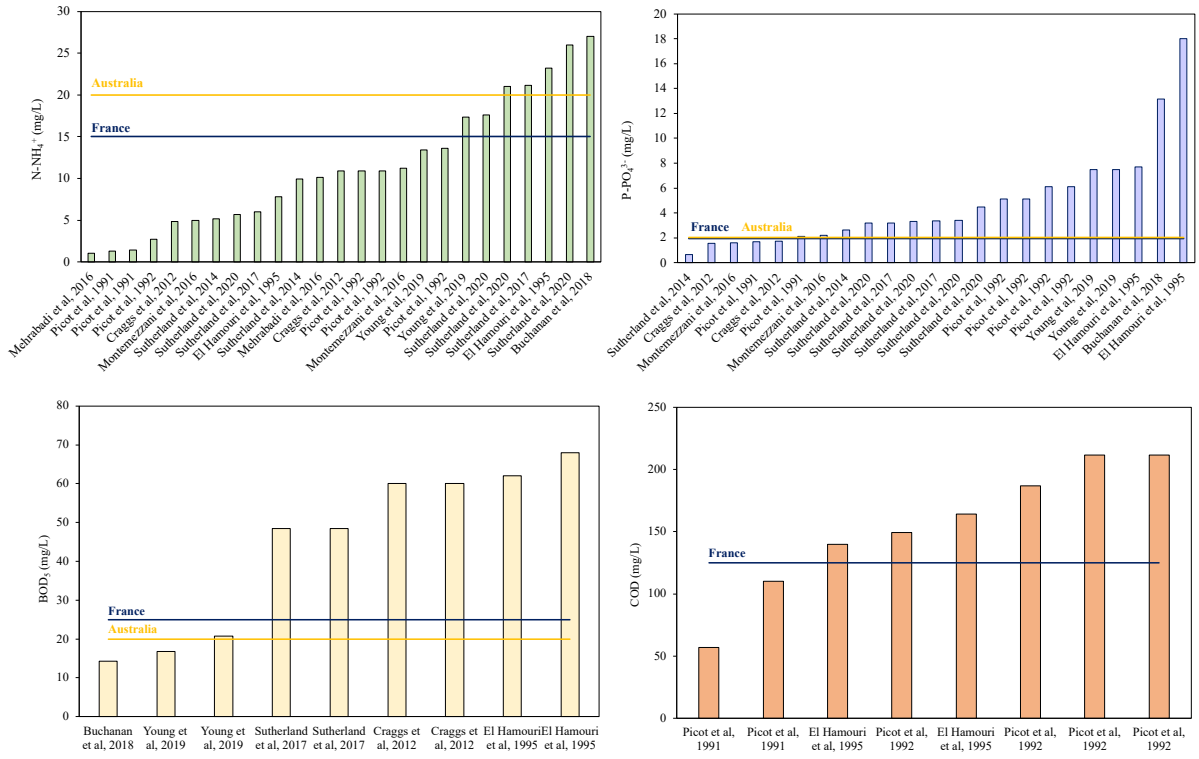

Figure 1.9 – N-NH_4^+, P-PO_4^{3-} BOD_5 and COD concentrations in HRAPs outlet operating in real conditions compared to French and Australian standards for rejection of treated wastewater in natural environment

1.3.1.2 Pathogens removal

Pathogens removal efficiency is typically assessed by measuring the reduction in faecal coliform bacteria, such as *Escherichia coli*, between the influent and effluent of the treatment system. A significant log reduction of 1.9 for faecal coliforms was achieved by averaging the performance data from 12 HRAPs operated under real conditions. The results are synthesised in Table 1.3. Figure 1.10 illustrates the faecal coliform concentrations in the HRAP effluents compared to the standards set by France and Australia for irrigation of non-food crops. It's important to note that while the faecal coliform concentrations in the HRAP effluents meet the regulations for discharge into the natural environment (with no limit in France and a limit of 10^6 *E. coli*/100 mL in Australia), the authorised maximum faecal coliform concentration for treated wastewater reused in the irrigation of non-food crops is lower. Figure 1.10 demonstrates that 6

Reference	Place	Pretreatment	CO_2 injection	Season	Depth (m)	Surface (m^2)	HRT (days)	N-NH_4^+ % removal (influent mg/L)	P-PO_4^{3-} % removal (influent mg/L)	BOD_5 % removal (influent mg/L)	COD % removal (influent mg/L)	TSS productivity ($g/m^2/d$)
Young et al. (2019a)	Australia	Anaerobic + facultative lagoon	No	Average on the year	0.30	223	4	76% (56)	17% (9)	37% (33)		4.1
			Yes					69% (56)	17% (9)	49% (33)		4.8
El Hamouri et al. (1995)	Morocco	Anaerobic pond	No	Summer	0.40	3023	4.2	79% (37)	53% (16.4)	32% (100)	31% (238)	21.9
				Winter				22% (29.7)	31% (25.9)	45% (113)	36% (220)	16.4
Picot et al. (1992)	France	Clarifier	No	Summer	0.35	100	4	60% (27.3)	40% (10.2)		15% (249)	
				Winter			8	50% (27.3)	40% (10.2)		40% (249)	
		Facultative pond		Summer			4	90% (27.3)	50% (10.2)		15% (249)	14
				Winter			8	60% (27.3)	50% (10.2)		25% (249)	7
Sutherland et al. (2020)	New Zealand	Covered anaerobic pond	No	Summer	0.30	330	8	90% (56.8)	38% (5.5)			8.9
						10000		69% (56.8)	42% (5.5)			6.3
				Winter		330		45% (38.2)	50% (6.6)			4.7
						10000		32% (38.2)	32% (6.6)			4
Sutherland et al. (2017)	New Zealand	Covered anaerobic pond	No	Summer	0.30	10000	8	82% (33.9)	42% (5.8)	48% (94)		5.7
				Winter				38% (34.2)	42% (5.6)	48% (94)		5.7
Craggs et al. (2012)	New Zealand	Primary effluent	Yes	Summer	0.30	14000	8	80% (24.2)	20% (1.92)	69% (195)		10
				Winter				55% (24.2)	10% (1.92)	69% (195)		5
Mehrabadi et al. (2016)	New Zealand	Primary settler	Yes	Summer	0.30	32	5	86% (7.6)				10
				Winter			8	50% (20.3)				4
Picot et al. (1991)	France	Primary settler	No	Summer	0.35	48	4	94% (21.6)	71% (7.3)		68% (344)	17
				Spring	0.35	48	8	92% (18.2)	71% (5.8)		80% (285)	9.3
Montemezzani et al. (2016)	New Zealand	Primary settler	Yes	Summer	0.30	27	4	80% (25)	61% (4)			15.8
				Winter			4	53% (24)	34% (3.4)			3.8
Sutherland et al. (2014b)	New Zealand	Primary settler	No	Summer	0.30	32	4	75% (39.7)	58% (6.3)			13.8
		Primary settler + dilution x2						74% (19.9)	79% (3.2)			17.4
Buchanan et al. (2018a)	Australia	Septic tank	No	Average on the year	0.32	200	4.5	70% (90)	6% (14)	93% (204)		

Table 1.2 – N-NH_4^+, P-PO_4^{3-} and BOD_5 removal performance results on HRAP >25m^2 treating real domestic wastewater in outdoor conditions

out of 12 HRAP effluents comply with for this specific use in both France and Australia.

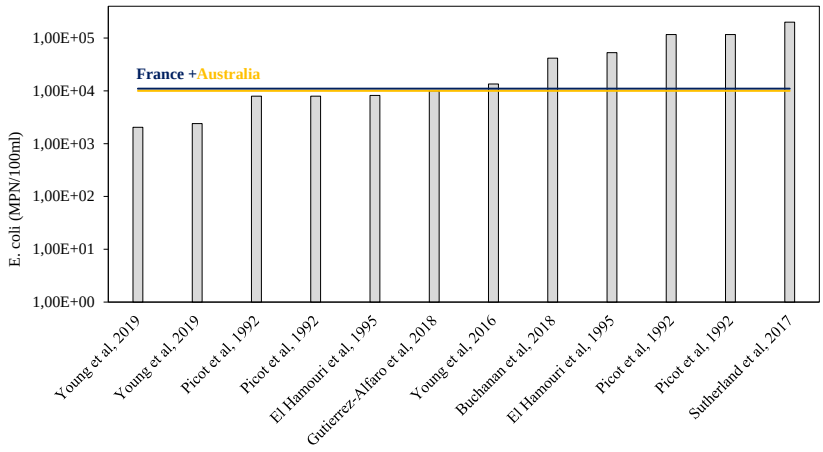

Figure 1.10 – *E. coli* concentrations in HRAPs outlet operating in real conditions compared to French and Australian standards for irrigation of non-food crops

Reference	Place	Pretreatment	CO_2 injection	Season	Depth (m)	Surface (m^2)	HRT (days)	Faecal coliforms or *E. coli*/100ml in the inlet	Faecal coliforms removal
Young et al. (2019a)	Australia	Anaerobic + facultative lagoon	No	Average on the year	0.30	223	4	$2.51.10^4$	1.2log
			Yes					$2.51.10^4$	1.2log
El Hamouri et al. (1995)	Morocco	Anaerobic pond	No	Summer	0.40	3023	4.2	$8.60.10^5$	2.5log
				Winter				$2.70.10^5$	1.9log
Picot et al. (1992)	France	Clarifier	No	Summer	0.35	100	4	$1.10.10^7$	3.3log
				Winter			8	$1.10.10^7$	1.5log
		Facultative pond		Summer			4	$1.10.10^7$	2.8log
				Winter			8	$1.10.10^7$	1.75log
Sutherland et al. (2017)	New Zealand	Covered anaerobic pond	No	Year average	0.30	10000	8	$2.50.10^6$	1.0log
Young et al. (2016)	Australia	Septic tank	No	Winter	0.30	200	10	$1.70.10^6$	2.13log
Buchanan et al. (2018a)	Australia	Septic tank	No	Average on the year	0.32	200	4.5	$2.40.10^6$	1.7log
Gutiérrez-Alfaro et al. (2018)	Spain	UASB	No	Unknown	0.30	32	6	$1.90.10^5$	2.0log

Table 1.3 – Compilation of HRAP faecal coliforms removal performance results on pilots >25m^2 treating real domestic wastewater in outdoor conditions. UASB = Up-flow Anaerobic Sludge Blanket reactor

1.3.1.3 Micropollutants removal

The term « micropollutant » refers to compounds present in wastewater at concentration on the order of magnitude of micrograms per liter ($\mu g.L^{-1}$), including pharmaceuticals, personal care products, nanomaterials, perfluorinated compounds, or heavy metals. Initially derived from faeces and urine, these micropollutants can lead to endocrine disruption, chronic eco-toxicity, or the promotion of antibiotic resistance once they are discharged into the environment (Norvill et al. 2016). However, the vast diversity of these contaminants, the ongoing discovery of new emerging pollutants in wastewater, and the formation of metabolites and transformation products pose significant challenges for their identification and removal, both in HRAP systems and traditional treatment methods. Due to a lack of data on micropollutants in large-scale HRAP systems, the following paragraph considers studies conducted in smaller ponds and synthetic wastewater.

In HRAP systems, micropollutants can undergo removal through processes such as sorption, biodegradation, or photodegradation. Sorption onto suspended solids is influenced by factors like pH, temperature, and physicochemical properties of the micropollutants. While micropollutants are typically not biodegradable, some may undergo biodegradation through enzymatic processes, albeit at low rates due to their low concentrations. However, biodegradation can be facilitated by sorption onto solids. In contrast, photodegradation is a significant pathway for micropollutant removal in HRAP systems. This process involves the oxidation of contaminants by radicals generated through the interaction of sunlight, particularly UV radiation, with organic matter present in the wastewater (Norvill et al. 2016). Additionally, research by García-Galán et al. (2020) indicated that certain emerging contaminants were detected in significant concentrations within HRAP biomass but at very low levels in the water, suggesting potential removal through bioaccumulation processes.

Recent studies on HRAP systems treating real wastewater from primary settlers at pilot scale have shown relatively high removal rates for model molecules (caffeine) and common contaminants (ibuprofen). Matamoros et al. (2015) reported removal rate of 86-99 % for ibuprofen and 85-98 % removal rate for caffeine (HRT 4-8 days), with higher removal rates observed during

warmer seasons and lower rates during colder seasons, such as the 21% removal rate observed for diclofenac. Similarly, Vassalle et al. (2020) found slightly lower rates for caffeine (59 %) with an HRT of 4.5 days, while García-Galán et al. (2020) reported a removal rate of 70% for ibuprofen with an HRT of 4.5 days. The efficiency of antibiotics removal in HRAP systems appears to be more variable. Vassalle et al. (2020) reported a 4 % removal efficiency for the antibiotic sulfapyridine compared to 100 % for sulfathiazole. In another study by García-Galán et al. (2020), five out of six antibiotics were removed at more than 80 %, with the remaining antibiotic removed at 45 %. Furthermore, Shi et al. (2010) showed efficient degradation of estrogen (52-56 %) by a mixture of four algae in synthetic wastewater. These findings highlight the potential of HRAP systems for the removal of a range of micropollutants from wastewater.

Algal wastewater treatment demonstrated effectiveness in removing specific heavy metals. In a study by Sekomo et al. (2012), three successive algal ponds with a total HRT of 7 days achieved significant removal rates for various heavy metals. Specifically, the treatment process achieved 98 % removal for chromium (Cr), 40-70 % removal for zinc (Zn), 33 % removal for lead (Pb), 21% for cadmium (Cd), and 29% removal for copper (Cu). These results underscore the potential of algal ponds as a viable method for the removal of certain heavy metals from wastewater.

1.3.2 Optimisation of HRAP performances through engineering parameters

Given the significant challenges in achieving satisfactory pollutant removal in HRAP, numerous studies have focused on assessing the impact of engineering parameters on HRAP performance to enable a better control and optimisation of the process.

• **Dead zones reduction:** The presence of bends at the extremities of the raceway creates dead zones where flow velocity is very low, nil, or negative, leading to the appearance of vortices. Figure 1.11a shows the result of Computational Fluids Dynamic (CFD) modelling of a 500 m^2, 0.2 m depth raceway mixed with a paddlewheel (Inostroza et al. 2021), where dead zones can be observed at the exit of the bends. As accumulation of solids is likely to occur in those areas,

different geometries have been tested to avoid settling zones, represented in Figure 1.11b and c. In Figure 1.11b, the central divider of the raceway has been modified to follow the shape of the dead zones, and in Figure 1.11c deflectors have been installed inside the bends. In this study, the utilization of deflectors was reported to provide the best performance in terms of fluid velocity and reduction of dead zones (Inostroza et al. 2021).

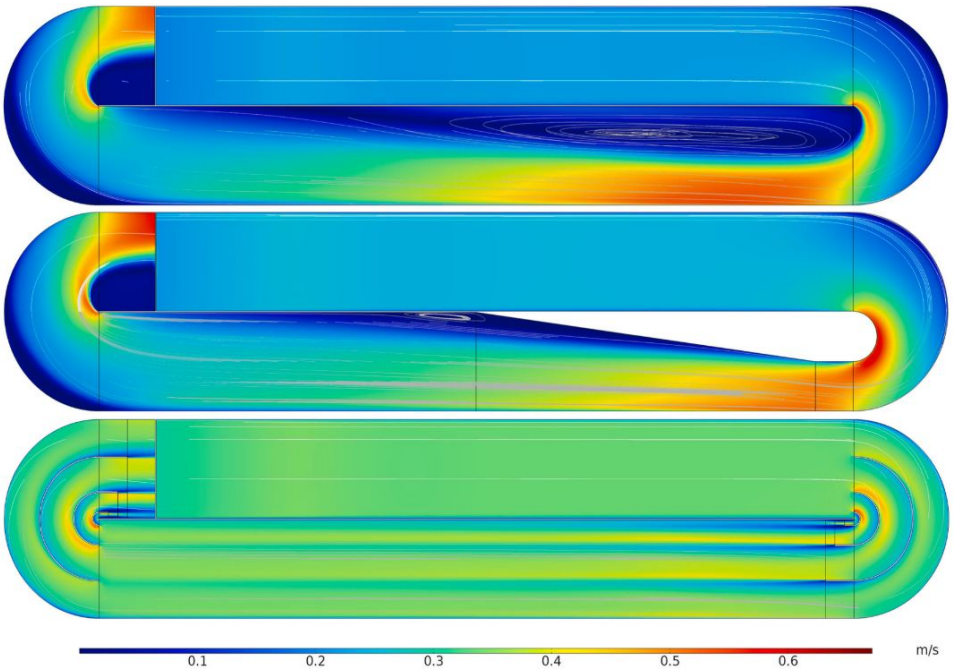

Figure 1.11 – Velocity profiles in a 500m^2, 0.2m depth raceway obtained by CFD modelling. Top: Traditional. Middle: Isle Partition. Bottom: Baffles Partition. (Inostroza et al. 2021)

• **HRT:** Increasing the HRT from 5 to 7 days significantly improved pollutants removal in HRAP system according to Ruas et al. (2020). There was an increase from 34 to 67 % in COD removal, from 36 to 69 % for Total Organic Carbon (TOC) removal, from 80 to 90 % for total nitrogen removal, and from 58 to 87 % for total phosphorus removal. Total suspended solids (including microalgae) also increased from 89.9 to 184.5 mg.L^{-1}, suggesting that higher removal rates were due to higher algal biomass consuming pollutants. These results were confirmed by Cromar and Fallowfield (1997), where an increase in HRT from 4 to 7 days resulted in an improvement of N removal from 89 to 95 % and an improvement from 44 to 55 % for P removal. Here again, chlorophyll *a* increased with HRT, confirming that higher HRT promotes nutrient

removal by allowing higher algal biomass. Several studies adjusted the HRT depending on the seasons to adapt to lower algal growth rates in winter due to lower irradiance. Lower HRT can then be applied in summer (4 days) compared to winter (8 days) (Picot et al. 1991, Picot et al. 1992).

• **Depth:** Considering the high nutrient load in HRAP, microalgae are likely to be limited by light availability in the culture depth. However, light availability decreases along the pond depth, and higher pond depths are expected to inhibit algal growth and consequently pollutants removal. This was confirmed by Kim et al. (2018), which reported decreasing N and P removal rates with increasing pond depth: N removal was 83 % and P removal 90 % for a pond depth of 20 cm, compared to 43 % and 36 % for a 30 cm depth pond, and 19 % and 33 % for a 40 cm depth pond. However, the reverse effect was obtained in a similar study (Sutherland et al. 2014b). Generally, most large-scale HRAPs are operated at 30 cm depth, which seems to be a compromise between light availability and the volume of wastewater treated per land area. The depth of the pond can also be varied to adapt to seasonal variations and manage peaking flow, for example (LGA 2020).

• **Pond size:** High volumes of wastewater to treat imply large ponds. However, upscaling was reported to negatively impact nutrient removal. For the same HRT, influent load, and environmental conditions, lower daily nutrient removal and biomass production occurred in a 1-ha HRAP pond compared to 330 m^2 and 5 m^2 ponds, questioning the mixing efficiency in larger ponds (Sutherland et al. 2020).

• **CO_2 addition:** Numerous studies have investigated the addition of CO_2 to HRAP to provide an inorganic carbon source for algal growth and to lower and control pH. pH naturally tends to increase during the day due to photosynthesis until reaching potential lethal values for algae and bacteria. Some studies have focused on the effect of sparging extra inorganic carbon as CO_2 into raceway ponds containing wastewater-microalgae consortiua on microalgal growth. Significant increases in biomass productivity and nutrient removal were reported when

CO_2 was sparged, either pure or in a mixture with 70 % of N_2, into raceway ponds treating raw or anaerobically digested abattoir wastewater compared to non-enriched ponds (Shayesteh et al. 2021; Ruas et al. 2020). The study on raw wastewater demonstrated that adding 30 % CO_2 mixed with 70 % N_2 increased biomass productivity by 60 %, resulting in a 20 % increase in COD removal and a 25 % increase in total organic carbon removal (Ruas et al. 2020). In contrast, adding CO_2 (recovered from anaerobic pond biogas, without pH control) to secondary treated wastewater in large-scale outdoor raceway ponds did not impact microalgal productivity nor nutrient removal according to Young et al. (2019a). This could be due to the quality of the biogas and the presence of potential toxic compounds, considering that CO_2 injections actually allowed significantly higher dissolved inorganic carbon concentration in the enriched pond. While high pH and the absence of CO_2 supply are generally unfavourable for microalgal growth, the high pH reached when pH is not controlled by CO_2 injections favours nitrogen removal by volatilization. Indeed, the pKa of the NH_4^+/NH_3 pair is 9.2, meaning that above this value most of the ammoniacal N is in the gaseous form NH_3. In an HRAP with a pH of 9, nitrogen removal by stripping of NH_3 then produced was reported to be significant (32-47 % for García et al. (2000) and 36-46 % for Picot et al. (1991)). High pH also favours disinfection (Chambonniere et al. 2020, Sebastian and Nair 1984) and limits the establishment of zooplancton communities that graze on microalgae (Arauzo and Valladolid 2003). Thus, not controlling the pH by CO_2 injections can also increase effluent microbiological quality.

• **Pretreatment:** Typically, HRAP influent undergoes pretreatment in settling tanks, anaerobic or facultative ponds, depending on the raw wastewater pollutant load and the required water quality at the HRAP outlet. Pretreatment is necessary to reduce suspended material concentration, which can make the culture medium turbid and reduce light availability for algae. Arashiro et al. (2019) reported no significant effect of primary treatment in settling tanks on N and COD removal. However, further pretreatment in a facultative pond (1.5 m depth, HRT = 8 days) was found to improve water quality at the HRAP outlet: the removal efficiency was 60 % for N and 40 % for P for the HRAP that received effluent from a clarifier (HRT = 2 hours), compared to

90 % for N and 50 % for P for the HRAP that received effluent from the facultative pond (Picot et al. 1992). Similarly, reducing nutrient load in HRAP influent by dilution by a factor of 2 resulted in a lower algal productivity but higher effluent quality (Sutherland et al. 2014a), highlighting the importance of further nutrient removal upstream of the HRAP when the primary goal is water treatment.

1.3.3 Modeling HRAP systems

Modeling constitute a key tool for optimizing HRAP performances by considering the variations of the parameters that are not constant (wastewater composition, climate). In the case of wastewater treatment processes, using a model is useful to predict removal performances and then scale the system. Modeling is then a crucial step for the implementation of HRAP at industrial scale.

Shoener et al. (2019a) reviewed 300 published models of phytoplankton in water resource recovery facilities. This study synthesized the different strategies used for the prediction of growth, nutrient uptake, carbon uptake and storage, and respiration. Among the different growth models, the Monod formulation, that implies maximum specific growth rate and half-saturation constant of the substrate, was used in 48% of the models reviewed, making it the most widely used notably due to the ease of calibration. However, the authors stated that the Droop model, used in only 19% of the models, was more adapted because it allows to decouple nutrient uptake and growth by considering internal nutrient content in the cell. Cells metabolism can be modeled at different levels of complexity. Metabolic flux analysis permits a thorough representation but turns out to be very complex, with more than 100 reactions to consider. Consequently, this formulation was used in only 3% of the models reviewed. On the contrary, the empirical method, consisting in converting the substrate into biomass using a yield determined experimentally, was widely used in the models reviewed. However, the yield is sensitive to environmental conditions and the reproductibility of this approach is poor. The authors recommended a compromise between empirical approach and metabolic flux, the lumped pathway, that necessitates approximately 10 groups of reactions instead of more than 100 individual reactions needed in the metabolic flux

analysis. Light is the source of energy for photoautotrophic microalgae and should always be considered while modeling HRAP. Light was considered in 66% of the models reviewed, which mostly used Monod-like formulations. Light attenuation through depth by microalgal cells was considered using Beer-Lambert law in 35% of the models reviewed. Only 6.8% of the models considered photoinhibition and photoacclimation. However, regarding the strong variations of light occurring in HRAP due to solar conditions, photoinhibition and photoacclimation are crucial mechanisms and should not be neglected. Temperature can also take extreme values in HRAP and have a great influence on microorganisms activity and should always be considered. Temperature was included in 34% of the articles reviewed. Models mostly used the difference between HRAP temperature and the optimal temperature of the microorganism considered, with no growth below a minimal temperature of tolerance and above a maximal temperature of tolerance. Besides, the authors stated that gas-liquid mass transfer should be included if dissolved gases CO_2 and O_2 are expected inhibitory or limiting. In the same way, pH should be considered if the system is not buffered or pH-controlled or when pH takes values that can cause inhibition of the growth. Moreover, HRAP comprise of paddlewheel-mixed raceway ponds that implies heterogeneous flow velocity in the pond, especially in large-scale systems. Mixing impacts crucial parameters such as light availability for microalgae, gas-liquid transfer and the occurrence of anaerobic zones in the pond. CFD models (Inostroza et al. 2021) should then be coupled to growth models to accurately predict HRAP behaviour.

A few models simulating microalgae-wastewater systems have already been validated in outdoor conditions. BIO_ALGAE model (Solimeno and García 2019) accurately predicted total biomass concentration, pH, dissolved oxygen and nutrient concentrations in a 1.54 m^2 outdoor pilot raceway pond fed with facultative pond effluent, both in summer and in winter. Later, the ALBA model (Casagli et al. 2021) was validated in a 56 m^2 outdoor raceway fed with synthetic wastewater throughout the four seasons. The model was able to predict accurately the growth of microalgae, heterotrophic bacteria and nitrifying bacteria as well as pollutant removal. Finally, the model ABACO-2 (Nordio et al. 2024) was validated in a 80 m^2 outdoor raceway operated in a semi-continuous mode fed with urban wastewater from May to November. While most of

models simulating HRAP behaviour focus on microalgal growth, COD, BOD, N and P removal, modeling of disinfection mechanisms and pathogens removal is relatively understudied. A model (Craggs et al. 2004) took into consideration both sunlight disinfection and dark inactivation of *E. coli* in HRAP and obtained a good fitting between the model and experimental data. This disinfection model was validated in a 35.7 m^2 outdoor raceway operated in batch using dairy farm effluent following pre-treatment in an anaerobic pond.

These studies demonstrated that models could accurately predict microalgal growth and pollutants removal even while the systems were exposed to variable environmental conditions throughout the day, however robustness of the models should be improved in order to fit different types of influent and different climates.

1.3.4 Environmental and economical impact of HRAP

HRAP systems differ from classical systems in terms of energy consumption, nature and quantity of emitted gases, required area, and associated costs. Life cycle analysis enables a detailed evaluation of the environmental impacts of a system over its lifetime, considering aspects such as material acquisition, production, transportation, usage, and waste disposal. This section draws upon five studies on the life cycle analysis of large-scale HRAP systems compared to classical systems to estimate the range of energy consumption, greenhouse gas emissions, required area as well as capital and operational costs associated with operating an HRAP system (see Figures 1.12, 1.13, 1.14 and 1.15 for references).

1.3.4.1 Energy consumption

According to Arashiro et al. (2018) and Garfí et al. (2017), activated sludge systems consume approximately 0.9 and 1.3 kWh/m^3 of treated wastewater, respectively, whereas HRAP systems consume significantly less energy, ranging from 0.09 to 0.25 kWh/m^3 (Figure 1.12, Arashiro et al. 2018, Kohlheb et al. 2020, Garfí et al. 2017, Vassalle et al. 2023). Given the low power requirements of HRAP, energy can be readily supplied by solar panels, especially in sunny areas (LGA 2020).

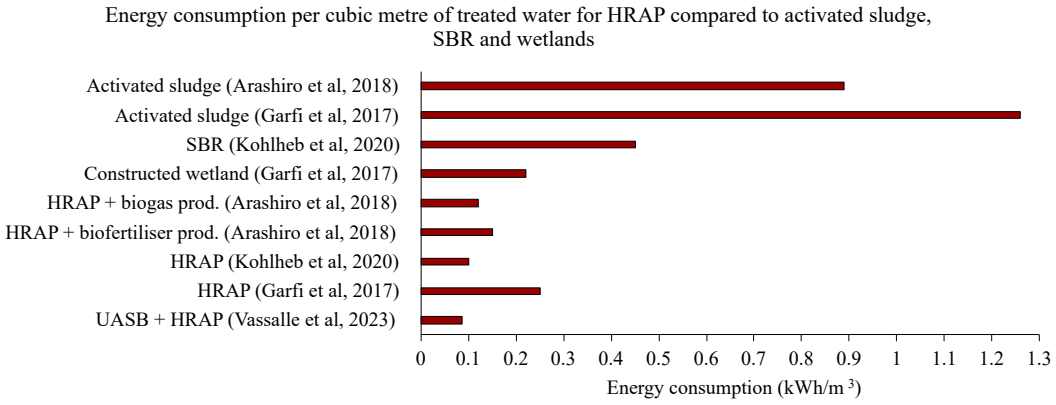

Figure 1.12 – Energy consumption per cubic metre of treated water for HRAP compared to activated sludge, Sequencing Batch Reactor (SBR) and constructed wetlands

Like HRAPs, constructed wetlands also exhibit low energy consumption compared to activated sludge systems, typically around 0.45 kWh/m^3. Constructed wetlands consist of shallow ponds ($<$ 2 m depth) of standing water where pollutants are removed through various processes such as sedimentation, filtration, UV exposure, precipitation, adsorption, volatilization, microbial degradation, or uptake from macrophytes roots (Vymazal 2011).

Due to lower energy consumption, the oxygenation capacity per kWh consumed is higher in an HRAP (measured at 8.2 kgO_2/kWh in the Peterborough HRAP during winter mornings, attributed to photosynthetically produced dissolved oxygen) compared to an aerated pond in an anaerobic sludge treatment plant (measured at 2.56 kgO_2/kWh, determined at laboratory scale in a 28 L pond, Vaxelaire et al. 1995).

1.3.4.2 Greenhouse gas emissions

Garfí et al. (2017) reported CO_2 emissions of 1.27 kgCO_2/m^3 for activated sludge, 0.69 kgCO_2/m^3 for constructed wetlands, and 0.57 kgCO_2/m^3 for HRAP. Additionally, Vassalle et al. (2023) even reported negative CO_2 emissions due to CO_2 uptake by microalgae (Figure 1.13). However, HRAP tend to emit more N_2O and NH_3 than activated sludge systems. While Arashiro et al. (2018) and Garfí et al. (2017) reported 0.11 gN_2O emitted per m^3 of treated water and nil NH_3 emissions for activated sludge, HRAP emitted from 0.06 gN_2O/m^3 (HRAP coupled

with biofertilizer production) to 0.26 gN_2O/m^3 (HRAP coupled with biogas production) and 6-10 gNH_3/m^3. The high pH induced by photosynthesis in HRAP leads to significant NH_3 formation and volatilisation.

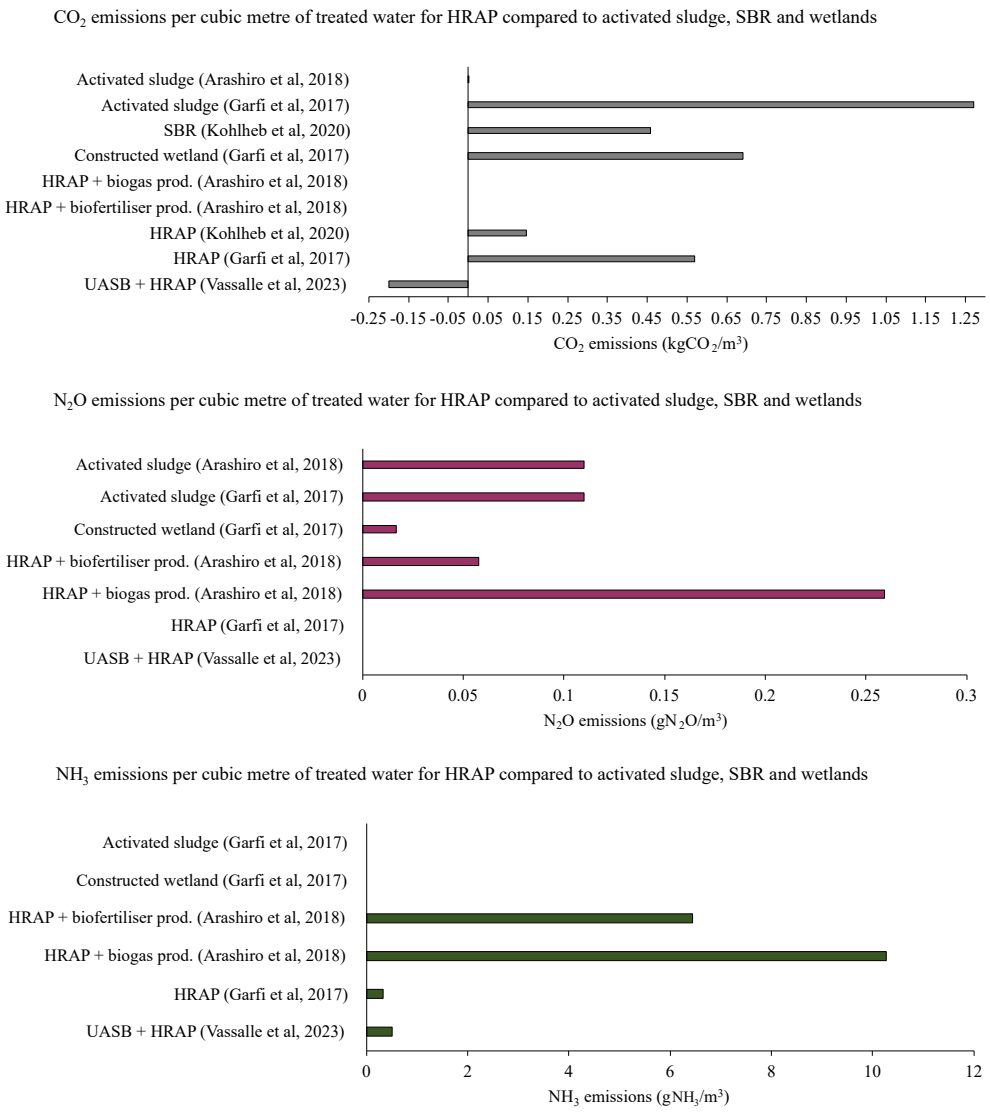

Figure 1.13 – CO_2, N_2O and NH_3 emissions per cubic metre of treated water for HRAP compared to activated sludge, Sequencing Batch Reactor (SBR) and constructed wetlands

1.3.4.3 Area

Due to their lower depth, HRAPs require a larger area than activated sludge to treat an equal volume of water. According to Arashiro et al. (2018), the area needed per m^3/day of treated water is 0.46 m^2 for activated sludge, whereas it ranges from 10 to 30 m^2 for HRAPs (Figure 1.14, Craggs et al. 2015, Vassalle et al. 2023, Garfí et al. 2017, Kohlheb et al. 2020, Arashiro et al. 2018). Consequently, HRAP systems are more suitable for remote areas, sometimes not serviced by classical water sanitation network (LGA 2020), than for cities where available area is usually limited. It's worth noting that the footprint of HRAPs in terms of surface aera is still 50 % lower than that of facultative ponds used in those remote areas due to the lower HRT of HRAPs (LGA 2020).

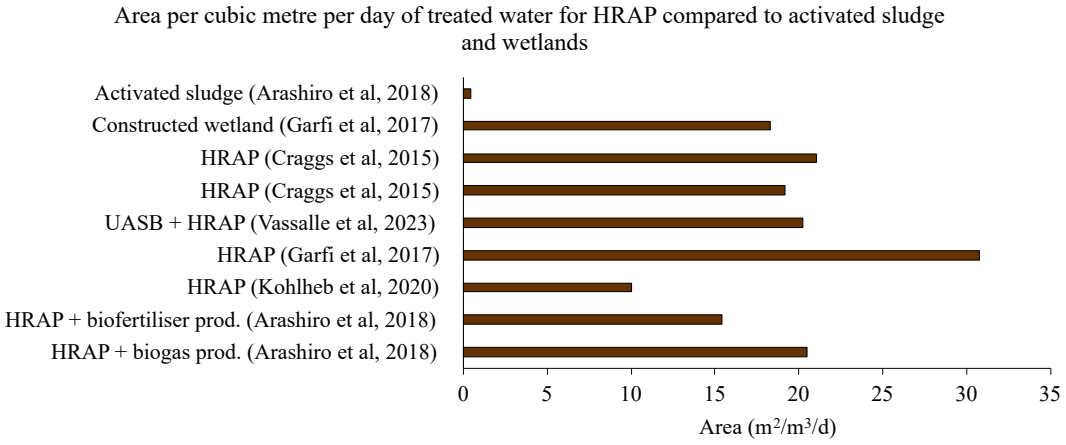

Figure 1.14 – Area per cubic metre per day of treated water for HRAP compared to activated sludge and constructed wetlands

1.3.4.4 Capital and operation cost

Due to their simpler facilities and the reduced need for operator actions on-site (LGA 2020) as well as the absence of artificial aeration which typically contributes to 50 to 90 % of the operational cost in an activated sludge wastewater treatment plant (Oviedo et al. 2022), both investment and operational costs are lower for HRAP compared to activated sludge systems. Garfí et al. (2017) reported a capital cost of 2774 € per cubic metre of water treated per day for

activated sludge plants, compared to 600 to 1000 € for HRAPs. Similarly, the operational cost for an activated sludge treatment plant was estimated around 0.79 € per cubic metre of treated water, while it ranges from 0.02 to 0.4 € for HRAPs (Figure 1.15, Garfí et al. 2017, Kohlheb et al. 2020, Vassalle et al. 2023, Arashiro et al. 2018).

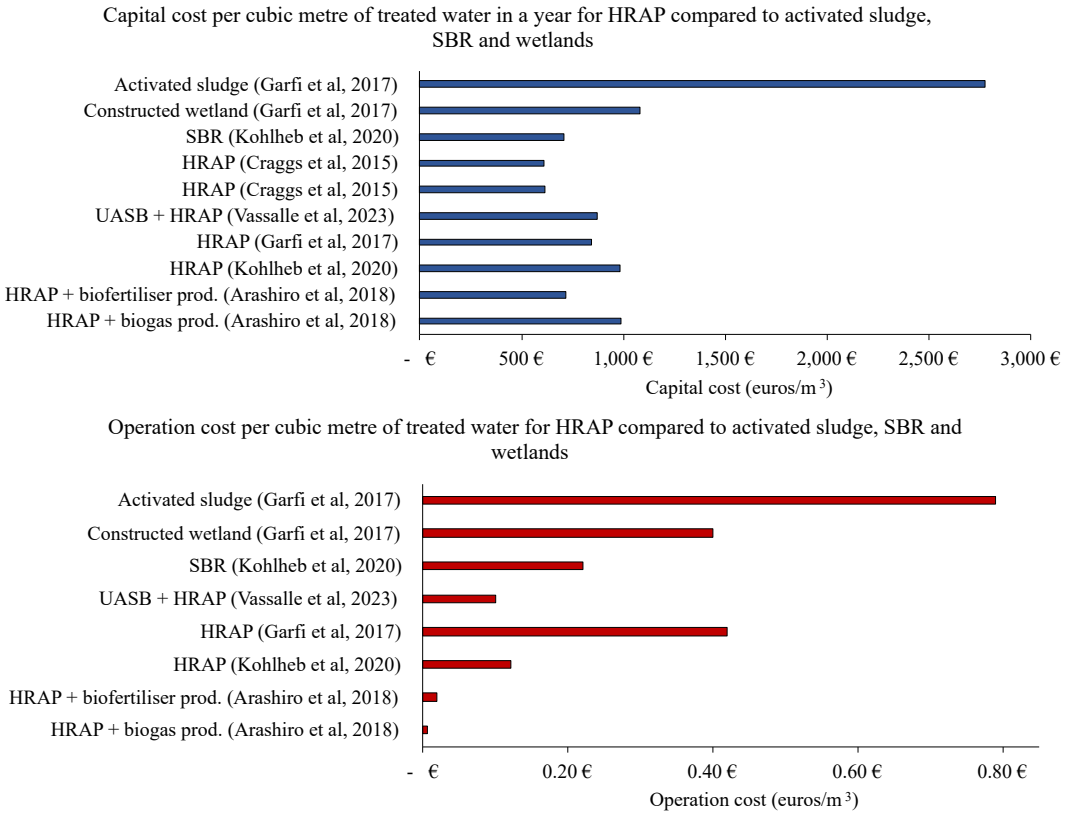

Figure 1.15 – Capital and operation cost for HRAP compared to activated sludge, Sequencing Batch Reactor (SBR) and constructed wetlands

1.3.5 Conclusion: HRAP versus activated sludge and improvement perspectives

Pollutants removal performance, as well as the environmental and economic impact of HRAP, has been assessed worldwide, across a wide range of biotic and abiotic conditions. Table 1.4 summarizes the advantages and drawbacks of HRAP compared to classical activated sludge systems, which are currently used for wastewater treatment in most parts of the world. Generally, acti-

vated sludge demonstrates slightly better pollutant removal rates than HRAP, albeit requiring a smaller surface area, but to a much higher energetic and economic cost.

	References	**Activated sludge**	**References**	**HRAP system**
BOD_5 removal efficiency	AERM (2007)	90%	Young et al. (2017)	69%
N removal efficiency	AERM (2007)	80%	Young et al. (2017)	61%
P removal efficiency	AERM (2007)	55%	Young et al. (2017)	21%
Energy consumption	Garfí et al. (2017)	1.3 kWh/m^3	Vassalle et al. (2023)	0.09 kWh/m^3
Capital cost	Garfí et al. (2017)	2774€/m^3/d	Garfí et al. (2017)	842€/m^3/d
Functioning cost	Garfí et al. (2017)	0.79€/m^3	Kohlheb et al. (2020)	0.18€/m^3
Area needed	Arashiro et al. (2018)	0.46 m^2/m^3/d	Kohlheb et al. (2020)	10 m^2/m^3/d

Table 1.4 – Comparison of activated sludge and HRAP performances, surface, costs and energy consumption

While HRAPs are more suitable for remote communities with large area available and a need for low-cost systems, compact systems like activated sludge are more suitable for cities that can afford higher treatment costs and where available area is limited. Each system is also suitable for a particular treated water reuse. While effluent from an activated sludge plant can be discharged into the natural environment due to its high removal efficiencies for N, P, and BOD_5, treated water from HRAP would be more suitable for irrigation of non-food crops, considering slightly lower removal efficiencies of macropollutants. When considering water reuse for irrigation of food crops, chemical disinfection after both HRAP and activated sludge treatment may be necessary to meet strict regulatory requirements and address public health concerns. Finally, while the separation of the sludge from the treated water in activated sludge systems is relatively efficient, separating the biomass from the treated water in HRAP is more challenging. However, algal biomass from HRAP is more interesting than sludge in terms of valorisation.

The wide range of microorganisms and their interactions, combined with uncontrolled populations and variable solar conditions, contribute to the complexity and performance variability

of HRAP systems. While HRAP systems hold promise as wastewater treatment technologies, a deeper understanding of microbial functions and interactions is necessary for optimisation, especially to compete with activated sludge systems in terms of sanitation efficiency.

1.4 Microalgae and bacteria in HRAP systems

As open systems rich in nutrients, HRAP systems provide a conducive environment for a diverse array of microorganisms, including microalgae, bacteria, viruses, and zooplancton (Figure 1.16). According to Safi et al. (2016), microalgae constitute the majority of particulate carbon in the pond, accounting for 61 %, with variations across seasons reaching a maximum of 69 % in summer and a minimum of 48 % in winter. Bacterial particulate carbon comprises 13.5 %, exhibiting lower seasonal variability, with a maximum of 19 % in winter and a minimum of 7.5 % in summer. Grazers (zooplancton) contribute 4 % of the particulate carbon, increasing to 14 % during spring zooplankton blooms. The remaining 21.5 % of particulate carbon consists of dead algae, detritus, and mucilage (Safi et al. 2016).

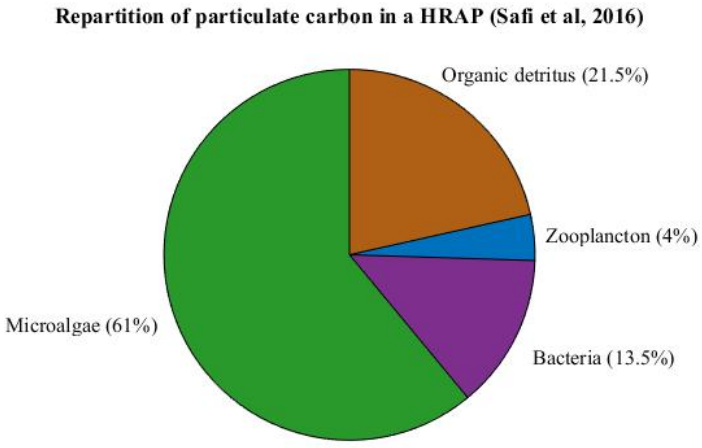

Figure 1.16 – Repartition of particulate carbon among HRAP microorganisms and organic detritus (Safi et al. 2016)

While certain microorganisms such as microalgae and bacteria play a beneficial role in pollutant removal within HRAP systems, others pose challenges. For instance, zooplankton can proliferate to the extent of threatening microalgal populations, while the presence of human pathogens like viruses and certain bacteria raises concerns about water safety and public health.

1.4.1 Microalgae

1.4.1.1 Generalities about microalgae

Microalgae are unicellular photosynthetic microorganisms characterized by their lack of specialized organs such as roots, stems, or leaves, unlike macroalgae. They encompass both microscopic eukaryotic algae and cyanobacteria, which are photosynthetic prokaryotes. Typically ranging from 10 to 20 μm in size, a microalgal cell contains a nucleus enclosed within a double membrane, housing the organism's genetic material. Within the cytosol, chloroplasts serve as the primary sites for photosynthesis, featuring thylakoid structures where pigments like chlorophyll *a*, chlorophyll *b*, and carotenoids are located, facilitating light absorption (Jacob-Lopes et al. 2020). Additionally, mitochondria, also present in the cytosol, are responsible for cellular respiration processes. This cellular organites depicted in Figure 1.17, enables microalgae to efficiently harness energy from sunlight and perform essential metabolic functions.

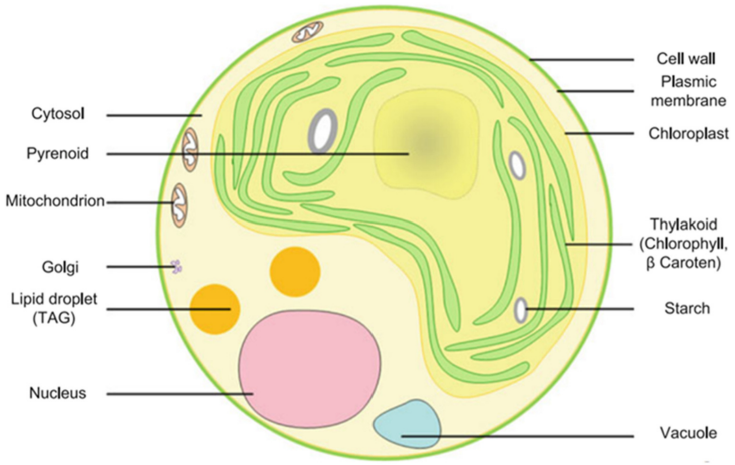

Figure 1.17 – Microalgae structure (Pignolet et al. 2013)

As photosynthetic organisms, microalgae produce organic molecules for their growth from inorganic compounds in the presence of light (Hall and Rao 1992). During this process, carbon dioxide and water are converted into carbohydrates, rich in energy, and dioxygen (Equation 1.5).

$$CO_2 + H_2O \rightarrow CH_2O + O_2 \tag{1.5}$$

Photosynthesis occurs in two steps, a light phase occurring in presence of light, and a dark phase independant of light:

• **Light phase - the electron transport chain:** In the light phase, photons excite the chlorophyll *a* molecules located in the photosystems II and I (PSII and PSI), which consist of pigments and proteins. Upon returning to a stable state, chlorophyll *a* emits fluorescence. While chlorophyll *a* is the primary pigment in photosystems, carotenoids also contribute to photosynthesis and photoprotection by dissipating excess energy as heat at this stage (Jacob-Lopes et al. 2020, Benedetti et al. 2018). Light energy is then converted into NADPH and ATP through electron transfer. Electrons are derived from H_2O molecules, which are initially converted into O_2, H^+, and electrons in photosystem II (Figure 1.18). Subsequently, in photosystem I, $NADP^+$ is reduced to NADPH. The H^+ ions generated from the conversion of H_2O molecules into oxygen in PSII are then utilized by ATP synthase to convert ADP into ATP (Li et al. 2023).

• **Dark phase - the Calvin cycle:** In the dark phase, which occurs in the stroma, the NADPH and ATP produced during the light phase drive the Calvin cycle. This cycle converts CO_2 from the cell environment or from the respiratory process into carbohydrates (Hall and Rao 1992).

ATP produced during the light phase is insufficient to meet the cell's energy demands. Therefore, alongside photosynthesis, respiration reactions provide most of the ATP required by Calvin cycle (Bonnanfant 2020). During respiration, carbohydrates and O_2 are converted into CO_2 and H_2O (Equation 1.6), as follows:

$$CH_2O + O_2 \rightarrow H_2O + CO_2 \tag{1.6}$$

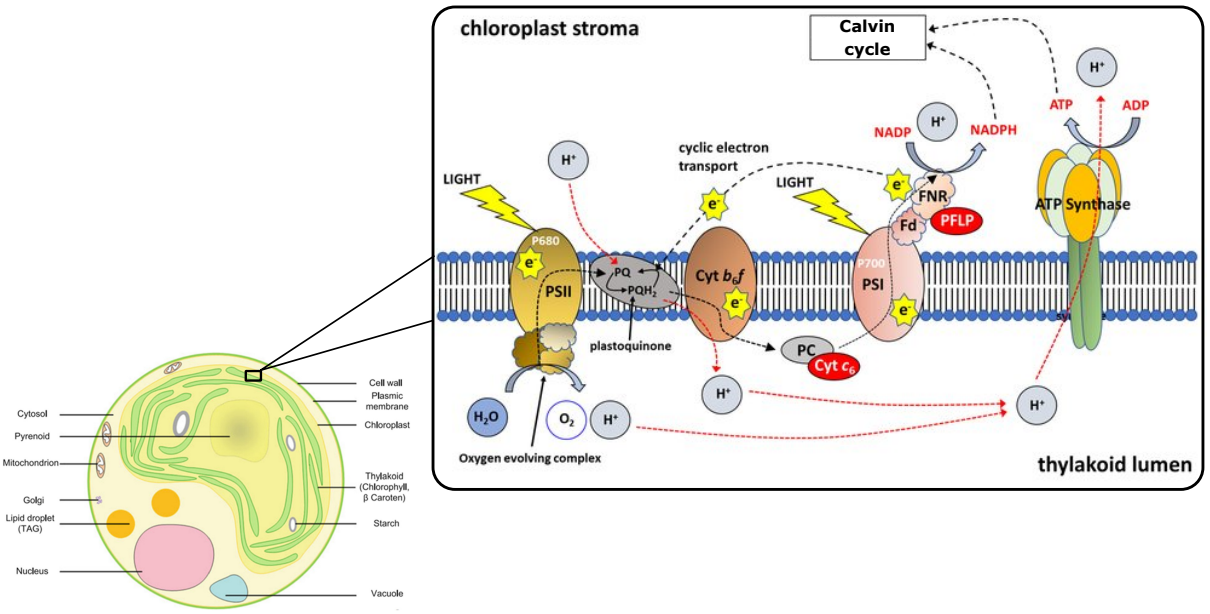

Figure 1.18 – Representation of electron transport chain in thylakoid membrane (modified from Pignolet et al. 2013 and Simkin 2019)

Microalgae cultivated in HRAP systems typically experience 10 to 14 hours of darkness within a 24-hour cycle, depending on the seasons (Casagli et al. 2021). During periods of darkness, respiration becomes the primary process for providing ATP to the cell, occurring in three steps presented in Figure 1.20 (Kazbar et al. 2019, Cecchin 2020). Mitochondrial respiration comprises glycolysis, the Krebs cycle (citric acid cycle), and oxidative phosphorylation. First, glucose is degraded in the cytoplasm via glycolysis. Then, pyruvate, the end product of glycolysis, is converted into acetyl-CoA in the Krebs cycle, accompanied by the production of CO_2 and H_2O. Finally, ATP is generated through oxidative phosphorylation, which utilizes the H^+ ions produced during the Krebs cycle. Consequently, microalgae can utilize glucose derived from photosynthesis, along with oxygen, to produce ATP during periods of darkness (Kazbar et al. 2019, Cecchin 2020) (Figure 1.20).

In terms of stoechiometry, Abiusi et al. (2020) reported that 1 gram of algal biomass (*Chlorella sorokiniana*) consumed 0.53 grams of carbon from CO_2 through photosynthesis. The

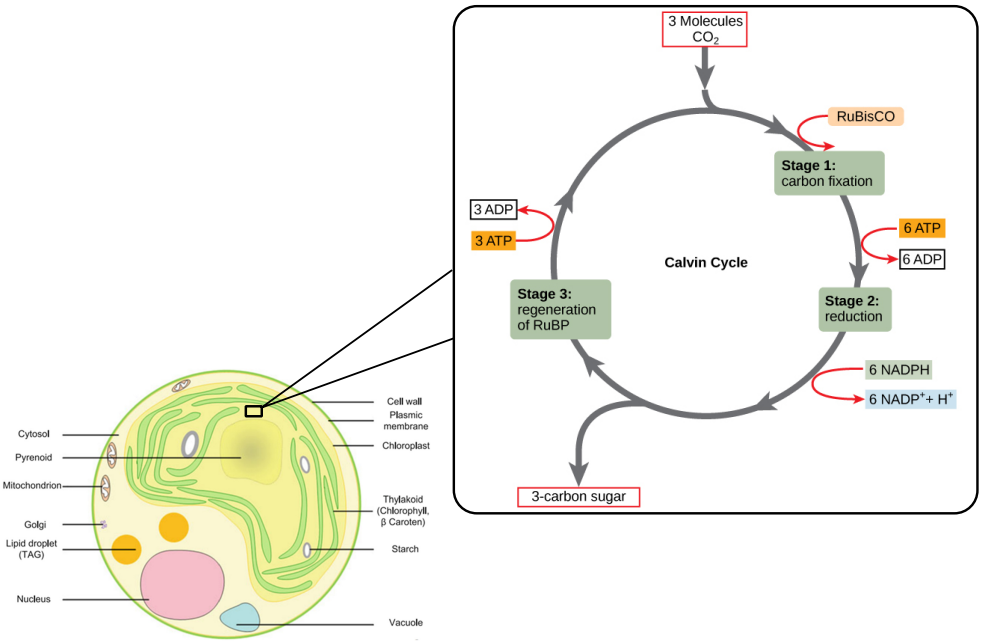

Figure 1.19 – Reactions occurring in Calvin cycle in chloroplast stroma (modified from Pignolet et al. (2013) and Molnar and Gair (2015))

same 1 gram of algal biomass consumed 1.27 grams of O_2 and produced 0.53 grams of carbon from CO_2.

1.4.1.2 Microalgal population in HRAP systems

HRAPs are open systems where the microalgal species present are influenced by contamination from aerosols and wastewater. Some recurrent microalgae species in HRAP natural consortia include *Chlorella sp., Scenedesmus sp., Mucidosphaerium sp., Micractinium sp., Pediastrum sp., Desmodesmus sp., Stigeoclonium sp., Pseudanabaena sp., Chlamydomonas sp.*, and *Ankistrodesmus sp.* (Ruas et al. 2020; Young et al. 2019a; Sutherland et al. 2014b; Gutiérrez et al. 2016a; Mehrabadi et al. 2016; Montemezzani et al. 2016, 2017; Pham et al. 2020; Arashiro et al. 2019; Passos et al. 2014; Galès et al. 2019; Sutherland et al. 2017; Gutiérrez et al. 2016b; Assemany et al. 2015; Vassalle et al. 2020; Plouviez et al. 2019).

However, the microalgae population in HRAP is subject to variations in environmental con-

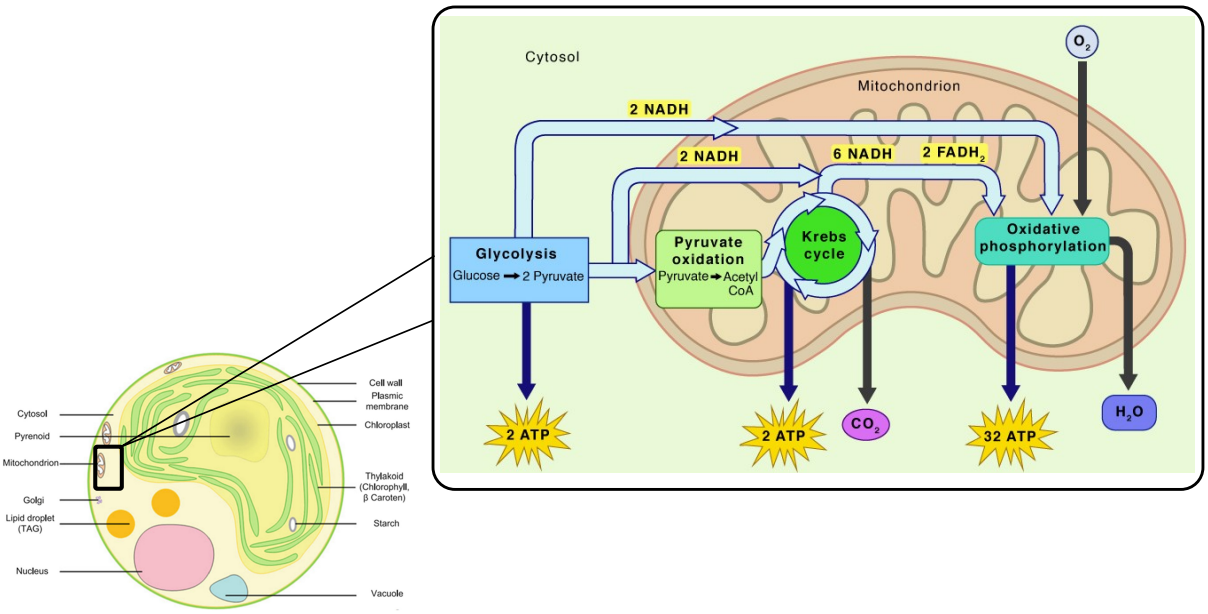

Figure 1.20 – Reactions occurring in mitochondria and cytosol as part of aerobic respiration in darkness conditions (modified from Pignolet et al. (2013) and https://www.sciencefacts.net)

ditions. Therefore, different species dominate the culture depending on the season, grazing pressure, or on HRAP location. For example, Fallowfield and Garrett (1985) observed *Chlorella vulgaris* as the dominant species from September to November in a HRAP in Scotland, whereas genera *Chlamydomonas, Ulotrix, Ankistrodesmus*, and *Nitzschia* were dominant from May to September. The composition of the algal population could also depend on nutrient availability: Marcilhac (2014) reported that, in the case of phosphorus limitation, *Scenedesmus sp.* tends to dominate the culture compared to *Chlorella sp.*.

1.4.1.3 Parameters influencing microalgal growth in HRAP system

Microalgae require light and nutrients, mainly carbon, nitrogen, phosphorus, and sulfur, for their growth. The nutrients requirements depend directly on the elemental composition of microalgae as presented in Table 1.5 for *Chlorella vulgaris* (Souliès 2014). Typically, in HRAP systems, nutrients are present in excess, so the culture is mainly limited by light availability

(Voltolina et al. 2005). Microalgae are also affected by physico-chemical conditions and predation.

Elements	C	H	O	N	S	P	K	Mg	Ca
Mass fraction	0.480	0.070	0.264	0.089	0.008	0.009	0.011	0.003	0.002
C molar composition	1	1.742	0.413	0.158	0.006	0.008	0.0073	0.0036	0.0013

Table 1.5 – Elemental composition of *Chlorella vulgaris* (Souliès 2014)

1.4.1.3.1 Light

Microalgae are photosynthetic microorganisms that rely on capturing light energy to perform photosynthesis. They can only utilize light within the Photosynthetically Active Radiation (PAR) wavelengths, typically between 400 and 700 nm (Mehrabadi et al. 2015). In open systems exposed to sunlight, such as HRAPs, irradiation levels vary depending on factors such as day-night cycles, sun trajectory, cloud cover, and the specific characteristics of culture systems (Bonnanfant 2020). For instance, in a study conducted in New Zealand, average diurnal photon flux densities of 116 μmol.m^{-2}.s^{-1} in winter and 700 μmol.m^{-2}.s^{-1} in summer were reported for an HRAP (Sutherland et al. 2021). However, it's essentiel to note that the photon flux density (PFD), which characterizes the light received onto the illuminated surface of the culture system, may not accurately represent the light received by cells within the culture volume. This is because light attenuation occurs due to self-shading of cells. When the microalgae culture is concentrated or the culture medium is highly turbid, a dark zone can form in the depth of culture where light penetration is insufficient, even during the daytime. This can lead to increased respiration activity in microalgae rather than photosynthesis. Biomass concentration in the pond and microalgae pigmentation, among other factors, are key parameters influencing light availability and algal productivity in microalgae cultures (Bonnanfant 2020):

• **PFD:** PFD represents the amount of photons reaching the surface of the culture per unit of time and aera. For instance, incident PFD can range from 0 μmol.m^{-2}.s^{-1} at night to exceeding 2000 μmol.m^{-2}.s^{-1} on a sunny day (Artu 2016). Incident PFD is commonly used parameter to characterize the light conditions in a culture. However, it alone doesn't fully represent the availability of photons for microalgal cells. The mean rate of photon absorption (Artu 2016) is

a more relevant parameter for discussing light availability, as it depends on a complex set of interdependent parameters such as biomass concentration, pigment content, and reactor depth.

• **Biomass concentration:** Higher biomass concentration leads to increased turbidity and reduced average light availability for microalgae in the pond, a phenomenon known as self-shading. Biomass concentration depends on the microalgal growth rate, which in turn is influenced by light and nutrient availability in the pond, as well as the dilution rate. HRAPs, like many microalgae production systems, are operate continuously, where the continuous inlet volumetric flow rate equals the harvesting flow rate, keeping the reactor volume constant. The liquid flow rate Q (in $m^3.h^{-1}$) is determined based on the reactor volume ($V_{reactor}$) in m^3 and the desired HRT in hours (Equation 1.7):

$$Q = \frac{V_{reactor}}{HRT} \tag{1.7}$$

The dilution rate (D) in h^{-1} is the reciprocal of the HRT (Equation 1.8):

$$D = \frac{1}{HRT} \tag{1.8}$$

The dilution rate directly impacts the volume of culture harvested and replaced by inlet water within a given period, as well as the microalgal concentration in the culture. If the dilution rate is too high, the growth rate of microalgae may not compensate for the harvested biomass, leading to culture washout. Conversly, if the dilution rate is too low, microalgae cells may accumulate, resulting in significant self shading and potentially light limitation. Additionally, low renewal of culture medium could lead to nutrient limitation. Optimizing the dilution rate is essential to achieve the highest biomass productivity. This optimal rate balances the need for sufficient renewal of culture medium to prevent nutrient limitation and maintain favorable growth conditions, while avoiding excessive dilution that may lead to culture washout (Pruvost et al. 2012). In wastewater treatment, the aim is not necessarily to optimise algal biomass productivity and a balance must be reached between retention time and pollutant removal required for wastewater reuse.

• **Pigment content:** The pigment content within a microalgal cell typically ranges from 3-5%. Chlorophyll *a* predominates in green algae and tends to increase in concentration when light availability decreases, a strategy aimed at optimizing light capture (Bonnanfant 2020). As the pigment content of a cell increases, its absorbance also increases, resulting in reduced light availability within the culture.

• **Microalgal cell shape:** A microalgal cell has the ability to absorb, reflect, and refract incident light. The ability depends on the cell's shape and pigment composition, and it is quantified through radiative properties, which can vary among species. However, light absorption is the main process occurring in algal cells, and scattering processes such as reflection and refraction are typically negligible (Legrand et al. 2016). The specific light absorption coefficient of a microalgal cell Ea is expressed in kg.m^{-2} and depends on its pigment content, primarily chlorophyll *a*. This coefficient is also wavelength-dependent and exhibits higher values at wavelengths corresponding to the absorption peaks of chlorophyll *a*, typically around 450 nm and 650 nm.

The Mean Rate of Photons Absorption (MRPA) in the culture, represented in $\mu mol.m^{-2}.s^{-1}$, depends on both the algal mass absorption coefficient Ea (in $kg.m^{-2}$) and the local fluence rate G (in $\mu mol.kg^{-1}.s^{-1}$), integrated over the PAR region. This relationship is described by Equation 1.9):

$$MRPA = \int_{PAR} Ea_\lambda \cdot G_\lambda \, d\lambda \tag{1.9}$$

This equation represents the integration of the product of the algal mass absorption coefficient and the local fluence rate over the PAR region, yielding the MRPA.

• **Depth:** The fluence rate G (in μmol.m^{-2}.s^{-1}) in the pond decreases exponentially as depth z (in m) increases, as described by the Beer-Lambert law (Legrand et al. 2016), Equation 1.10), where $G(0)$ can be approximated by the incident PFD:

$$G(z) = G(0) \cdot e^{-Ea \cdot C_x \cdot z} \tag{1.10}$$

MRPA is crucial for algal productivity. Productivity increases with MRPA until it reaches the light saturation point. Beyond this limit, algal productivity starts to decrease with MRPA due to photoinhibition processes (Figure 1.21).

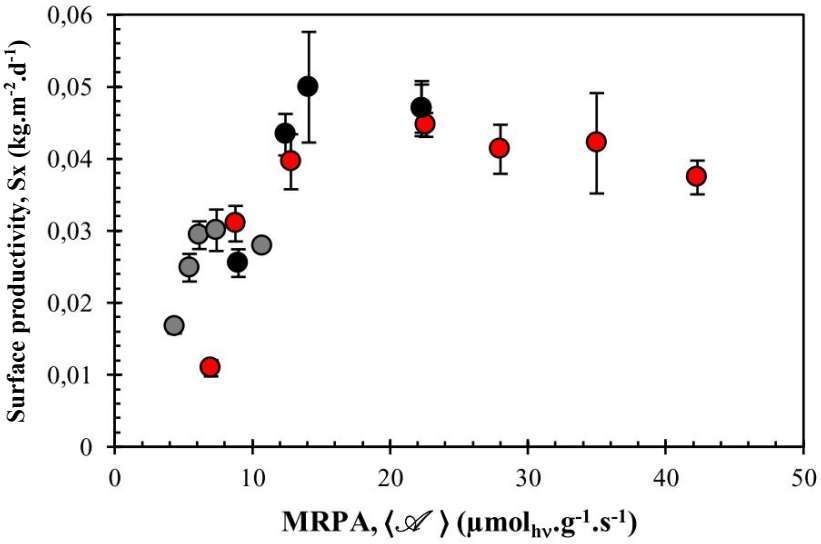

Figure 1.21 – Evolution of productivity as a function of MRPA (in red dilution rate D=0,05 h^{-1}, in grey incident irradiance q_0=270 μmol.m^{-2}.s^{-1} and in black q_0=760 μmol.m^{-2}.s^{-1}) (Artu 2016)

1.4.1.3.2 Carbon

- **Inorganic carbon**

Microalgal cells are composed of approximately 50 % of carbon (Souliès 2014). CO_2 is the most common carbon source for microalgae, as it is fixed by photosynthesis after dissolution in the liquid medium. In HRAP, the availability of inorganic carbon for microalgae primarily depends on CO_2 produced by respiration, as well as the pH of the culture and the gas-liquid mass transfer coefficient (K_La), which is influenced by pond agitation and geometry. Biomass production is generally enhanced by a higher Total Inorganic Carbon (TIC) concentrations up to a certain threshold where it becomes non-limiting. For instance, this concentration was estimated to be around 1 mM for *Chlorella vulgaris* (Pruvost et al. 2022). In HRAP, the mineralisation of organic matter by heterotrophic bacteria results in CO_2 production (Russel et al. 2020),

leading to TIC concentrations typically ranging between 1 and 3 mM (Sutherland et al. 2021). However, it's important to note that pH in HRAP often fluctuates between 8 and 11 (Sutherland et al. 2021). At these pH values, TIC is mainly present in the form of HCO_3^- and CO_3^{2-} ions (Table 1.6). Free CO_2 is not likely to be present at this pH range, and the mass transfer of carbon dioxide from the liquid to the gas phase can often be considered negligible, contributing to an increase in TIC concentration.

pH range	Equilibrium equation
pH < 4.3	$CO_2(g) + H_2O = H_2CO_3$
4.3 < pH < 8.2	$H_2CO_3 + H_2O = HCO_3^- + H_3O^+$
pH > 8.2	$HCO_3^- + H_2O = CO_3^{2-} + H_3O^+$

Table 1.6 – Carbonate equilibria equations and corresponding pH ranges (Pobernik et al. 2008)

Microalgae have the ability to uptake inorganic carbon using transporters located in the cell membrane and in the chloroplast (Figure 1.22). These transporters facilitate the movement of inorganic carbon molecules, such as bicarbonate (HCO_3^-) and carbon dioxide (CO_2), across the cell membrane and into the chloroplast, where they can be utilized in photosynthesis. The presence of specific transporters allows microalgae to efficiently utilize the available inorganic carbon in their environment, even at varying pH levels and concentrations.

As a result, inorganic carbon, primarily in the form of HCO_3^-, , accumulates in the chloroplast and in the stroma of microalgae cells, where the intracellular pH is typically around 7 to 8 (Lane and Burris 1981). Within the chloroplast, bicarbonate is converted to CO_2 by the enzyme carbonic anhydrase. This conversion occurs in the stroma before the carbon dioxide enters the thylakoid lumen. In the thylakoid lumen, the CO_2 is utilized in the process of photosynthesis. Specifically, it diffuses through pyrenoids tubules, which are structures within the thylakoid membrane, to the pyrenoid matrix located in in chloroplast stroma. In the pyrenoid matrix, the CO_2 is assimilated into the Calvin cycle by the action of the enzyme ribulose-1,5-bisphosphate carboxylase/oxygenase (RuBisCO) (Basu et al. 2013a).

When TIC is present in limiting concentrations, microalgae activate Carbon Concentration Mechanisms (CCMs) to enhance their carbon uptake efficiency. These mechanisms involve active

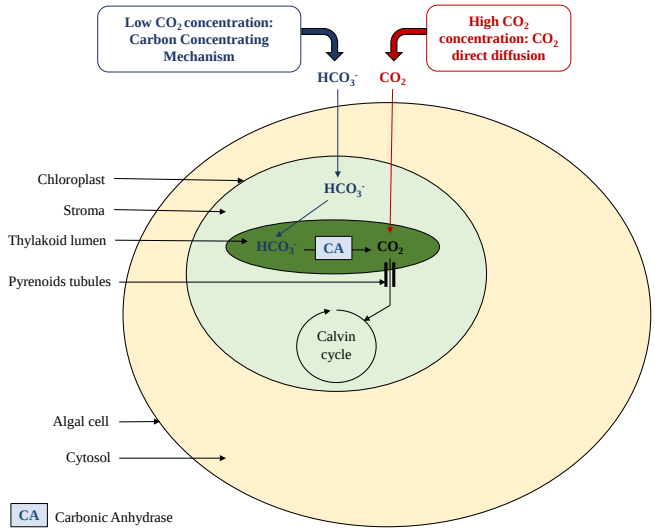

Figure 1.22 – Mechanisms of inorganic carbon transport through algal cell. Adapted from Nair and Chakraborty (2020)

transport systems that enable the uptake of bicarbonate from the surrounding medium into the cell, where it is then concentrated around the enzyme RuBisCO. However, these CCMs require energy for operation, which can impact the overall growth rate of the microalgae (Price et al. 1998). In the context of HRAPs, the relevance of CCMs may be questionable, especially considering that the concentration of inorganic carbon typically ranges between 1 and 3 mM in HRAPs (El Ouarghi et al. 2003, Sutherland et al. 2021). This concentration level is close to or slightly above the threshold for carbon-limited growth. Consequently, microalgae in HRAPs may not necessarily require the activation of CCMs to maintain adequate carbon uptake rates, as the TIC concentration is generally sufficient to support their growth and metabolic processes.

Maintaining an adequate concentration of CO_2 within the cell is crucial for efficient photosynthesis in microalgae. When the CO_2 concentration is too low relative to O_2, there is a risk of photorespiration, where RuBisCO fixes O_2 instead of CO_2, leading to metabolic inefficiency and biomass loss (Zeng et al. 2021). The ratio of CO_2 to O_2 is a critical determinant of the likelihood of photorespiration. Studies have shown that significant photorespiration occurs when this ratio falls below a certain threshold. For example, for *Chlorella vulgaris*, photorespiration becomes significant when the CO_2/O_2 ratio is less than 0.4 (Kazbar 2019). In contrast, when the CO_2/O_2

ratio exceeds 0.6, the contribution of photorespiration to overall metabolism is considered negligible. Therefore, maintaining an appropriate balance between CO_2 and O_2 concentrations is essential for optimizing microalgal growth and photosynthetic efficiency in HRAPs and other cultivation systems.

The interplay between oxygen and carbon dioxide concentrations is critical for the metabolic processes of microalgae. High oxygen levels can promote respiration over CO_2 fixation (Manhaeghe et al. 2020). Conversely, high concentrations of CO_2 can decrease the affinity of RuBisCO for CO_2 and may lead to the inactivation of photosystem PSII, resulting in reduced photosynthetic efficiency and lower yield (Nair and Chakraborty 2020). In HRAP systems that are fed with anaerobically pre-treated wastewater and non-sparged with CO_2, the concentrations of inorganic carbon typically range from 1 to 3 mM, while dissolved oxygen concentrations can be relatively high, ranging from 0.6 mM in winter to 2.5 mM in summer) (Sutherland et al. 2021). However, even at these elevated dissolved oxygen levels, considering the ratio CO_2/O_2, significant photorespiration is unlikely to occur in the pond. Therefore, while oxygen concentrations may influence metabolic pathways, the likelihood of photorespiration in HRAP systems is low given the prevailing conditions..

- **Organic carbon**

In HRAP systems, organic carbon can serve as an alternative carbon source for microalgae. A large variety of microalgae species are able to grow photoheterotrophically in the presence of light or chemoheterotrophically in the dark, utilizing organic carbon compounds as a carbon source, either instead of or in addition to inorganic carbon. However, it's important to note that while heterotrophic bacteria can degrade large organic molecules like polysaccharides, cellulose, starch, or proteins, microalgae have limitations in utilizing these complex compounds. Instead, they are typically capable of utilizing smaller organic molecules such as sugars, sugar alcohols (Lin and Wu 2015), sugar phosphates, amino acids, and organic acids (Abeliovich and Weisman 1978, Abreu et al. 2022, Sforza et al. 2018). The relevance of organic carbon consumption by microalgae in HRAP systems and the potential synergy between different carbon sources uptake are topics that are further discussed in Chapter 4. Understanding how microalgae utilize

organic carbon sources in HRAPs could provide insights into optimizing nutrient utilization and improving overall system efficiency.

1.4.1.3.3 Nitrogen

As a component of the structural and functional proteins and nucleic acids, nitrogen is a crucial nutrient for microalgae growth, constituting approximately 9 % of their total biomass (Abiusi et al. 2020). Microalgae have the capability to utilize inorganic nitrogen in the form of ammonium (NH_4^+) or as nitrate (NO_3^-), with ammonium being preferred due to its easier assimilation. In wastewater, ammonium is typically derived from hydrolysis of urea and other organic nitrogen molecules, while nitrate is a product of nitrification, a process we will discuss in more detail later. Although high concentrations of ammonium in the culture medium has been reported to inhibit ATP production in the chloroplast and photosynthesis (Kazbar 2019), the concentrations of ammonium typically found in wastewater are well below this toxic threshold. On the contrary, in cases of nitrogen depletion, the production of proteins becomes limited, prompting microalgae to produce more lipids and carbohydrates. However, in HRAP systems, total mineral nitrogen is usually present in excess, ranging from 1.2 to 6.3 mM (Buchanan et al. 2018a, Young et al. 2019a, Sutherland et al. 2014b, Sutherland et al. 2020).

1.4.1.3.4 Phosphorus

Phosphorus plays a vital role in microalgae as a component of ATP and DNA, constituting approximately 1 to 2 % of their total biomass. Microalgae assimilate phosphorus primarily in the form of phosphates (PO_4^{3-}). When phosphate concentrations are too high, they can precipitate with carbonates, leading to the formation of solid particles that increase turbidity. This reduction in light availability can inhibit algal growth (Mehrabadi et al. 2015). Moreover, precipitated phosphorus is not readily available to support algal growth (Bonnanfant 2020). In cases of phosphorus depletion, microalgae adapt by producing non-phosphorus lipids. However, a lack of phosphorus can induce photorespiration, leading to a loss of biomass (Kazbar 2019). Moreover, the absence of phosphorus can halt the synthesis of phycobilisomes, the light energy collectors, further impeding growth (Beccerra-Celis 2009). In HRAP systems, total mineral phosphorus

typically ranges from 0.2 to 0.4 mM (Buchanan et al. 2018a, Young et al. 2019a, Sutherland et al. 2014b, Sutherland et al. 2020).

1.4.1.3.5 Sulphur

Sulphur constitutes approximately 0.4 to 0.6 % of the total biomass of microalgae (Luther and Soeder 1991). While a complete absence of sulphur would completely inhibit algal growth, even small amounts of sulphate can have a significant impact on growth. Sulphate concentrations typically range around 0.6 mM in HRAP systems (Paing et al. 2003).

1.4.1.3.6 Microelements

Microalgae also require trace amounts of micronutrients such as magnesium (Mg), iron (Fe), manganese (Mn), copper (Cu), cobalt (Co), zinc (Zn), and boron (Bo) to synthesize compounds or facilitate redox reactions. Iron, in particular, plays a crucial role in electron transport during photosynthesis and is considered as a catalyst for chlorophyll synthesis (Beccerra-Celis 2009; Kazbar 2019). While these micronutrients represent less than 1 % of the algal composition, they are are essential for various metabolic processes (Bonnanfant 2020). Studies, such as that by Daneshvar et al. (2018), have indicated that wastewater contains sufficient levels of these elements to support microalgal growth, with some of these micronutrients deriving from plumbing materials used in wastewater transport systems.

1.4.1.3.7 Dissolved oxygen

Dissolved oxygen (DO) present in microalgae culture is mainly produced by photosynthesis. However, a too high O_2 concentration can induce photorespiration phenomena, leading to a loss in productivity. For instance, O_2 concentration above 0.94 mM can result in a 30 % reduction in biomass productivity. Additionally, excess O_2 can exacerbate the negative effects of excessive light, causing a decrease in pigment concentration and photochemical damage (Kazbar et al. 2019). Nevertheless, a minimal dissolved O_2 concentration is necessary in the cell environment to maintain proper functioning of RuBisCO (Bonnanfant et al. 2019). Moreover, in the presence of potentially assimilable organic molecules, microalgae consume oxygen as part of the

oxidation process of these organic molecules during respiration. In HRAP systems, dissolved oxygen concentration typically drops to 0 mM at night and can reach 0.3 mM to 1.3 mM during the day, respectively in winter and summer (Sutherland et al. 2021, Chambonniere et al. 2020).

1.4.1.3.8 Temperature

Algal cells need a minimal apparent activation energy to initiate their growth, and at an adequate temperature, enzymes associated with the Calvin cycle can become activated (Kazbar 2019). For example, Hodaifa et al. (2010) found that the maximal growth rate for *Scenedesmus obliquus* occured at a temperature of 29.7 °C, with maximal BOD_5 removal observed at 15 °C, and growth stopping at 38 °C. Generally, the optimal temperature for microalgae growth falls between 25 and 35 °C, depending on species. At too low temperature, algae are more sensitive to nitrogen limitation and increase the synthesis of unsaturated fatty acids and omega-3 fatty acids involved in membrane composition. Conversely, excessively high temperature can induce photorespiration, protein degradation, and enzyme denaturation, leading to reduced photosynthetic productivity or even cell death (Bonnanfant 2020; Kazbar et al. 2019; Rawat et al. 2016). Additionally, at high temperatures, CO_2 is less soluble and less readily diffused in the medium (Hodaifa et al. 2010). Moreover, elevated temperatures favour the production of free ammonia, which can be toxic (Wang et al. 2016). However, microalgae can adapt to different thermal conditions through processes involving enzyme reactions, cell permeability, and cell composition (Hodaifa et al. 2010). In HRAP, temperatures can drop to less than 10 °C at night and reach 20 °C or higher in summer (Evans et al. 2005, Sutherland et al. 2021, Chambonniere et al. 2020).

1.4.1.3.9 pH

pH levels in microalgae cultures regulate acid/base pairs, thereby influencing the form in which nutrients are present in the medium. An increase in pH can promote the precipitation of carbonates and phosphates of Ca, Mg, or Fe (Beccerra-Celis 2009), as well as the formation and volatilization of NH_3, highly toxic for microalgal cells, making these nutrients less available for microalgae growth. pH also plays a crucial role in establishing the internal protons gradient of microalgae. In a HRAP, pH levels were reported to vary diurnally between 7 and 8 during

winter, while reaching up to 10.5 in summer (Sutherland et al. 2021, Chambonniere et al. 2020). These fluctuations can significantly impact nutrient availability and metabolic processes within the microalgae culture.

1.4.1.3.10 Predation

The abundance of microalgae in HRAP systems often lead to frequent contamination of the pond by zooplancton that feed on them. Grazers in these systems include ciliates, oligotrichs, rotifers, cladocerans, copepods, and ostrapods, typically larger than 200 μm size (Safi et al. 2016, Montemezzani et al. 2016). While low dissolved oxygen concentrations, high organic matter concentrations, and high pH (that implies the presence of toxic NH_3) generally keep grazers away from the pond (Rawat et al. 2016), HRAP systems with CO_2 addition allowing to control the pH tend to have close-to-neutral pH that favour the development of grazers (Montemezzani et al. 2016). As a result, just two or three days of predation can lead to a 10 % loss in biomass (Mehrabadi et al. 2015). Additionally, the establishment of zooplancton can impact the dominance of microalgal species, rapidly reduce algal productivity and nutrient removal rates, and increase colony size, the number of cells in colonies, and biomass settleability (Montemezzani et al. 2016). This increase in settleability under grazing pressure has been observed by Lürling (2003) as well. Settleability is a characteristic of interest for biomass harvesting, and predation has been considered a natural solution to select algae species or induce behaviours that facilitate biomass harvesting (Li et al. 2015). However, the increased settleability induced by predation can also enhance light attenuation, potentially negatively impacting algal biomass productivity (Lürling 2003).

1.4.2 Bacteria

1.4.2.1 General bacterial cell structure

Bacteria are unicellular prokaryotic organisms, typically smaller than microalgae, with sizes ranging between 0.1 and 1 μm. As depicted in Figure 1.23, bacterial cells contain DNA and ribosomes for proteins synthesis in their cytoplasm. The cell is bounded by a membrane where

respiration occurs, a cell wall composed of peptidoglycans, and an external capsule made of polysaccharides (Molnar and Gair 2015).

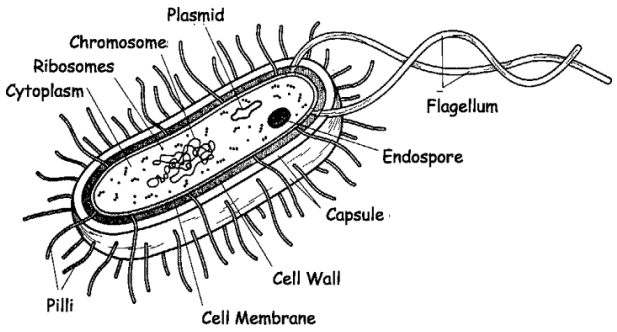

Figure 1.23 – Bacteria cell structure (Hiremath et al. 2012)

Wastewater naturally contains a significant amount and diversity of bacteria. Additionally, open ponds rich in nutrients, like HRAP, are subject to external contamination by microorganisms. While a few bacteria can be pathogenic to humans, the majority of them are harmless (Rogers 2011). In wastewater, the abundance of human pathogenic bacteria has been estimated to be 0.06-3.20 % of the total bacterial population (Cai and Zhang 2013). However, they can have great adverse effect on human health where wastewater reuse might expose the population (irrigation and consumption of irrigated crops for example).

1.4.2.2 Heterotrophic bacteria

Acinetobacter, *Pseudomomas*, and *Enterobacter* are three of the dominant genera of heterotrophic bacteria found in wastewater (Lotter and Murphy 1985). Heterotrophic bacteria utilize organic molecules as sources of energy and carbon. In HRAP systems, they are able to degrade polysaccharides, cellulose, starch, or proteins and to convert them into smaller molecules like glucose and in CO_2, which are available for algae (Abeliovich and Weisman 1978). Aerobic respiration in these bacteria occurs in three steps, as illustrated in Figure 1.24:

- **Glycolysis:** Carbohydrates are first converted into pyruvate in the cytoplasm.

- **Krebs cycle:** In prokaryotic microorganisms like bacteria, the Krebs cycle occurs in the cytoplasm since they lack mitochondria. In this cycle, pyruvate from glycolysis is converted into

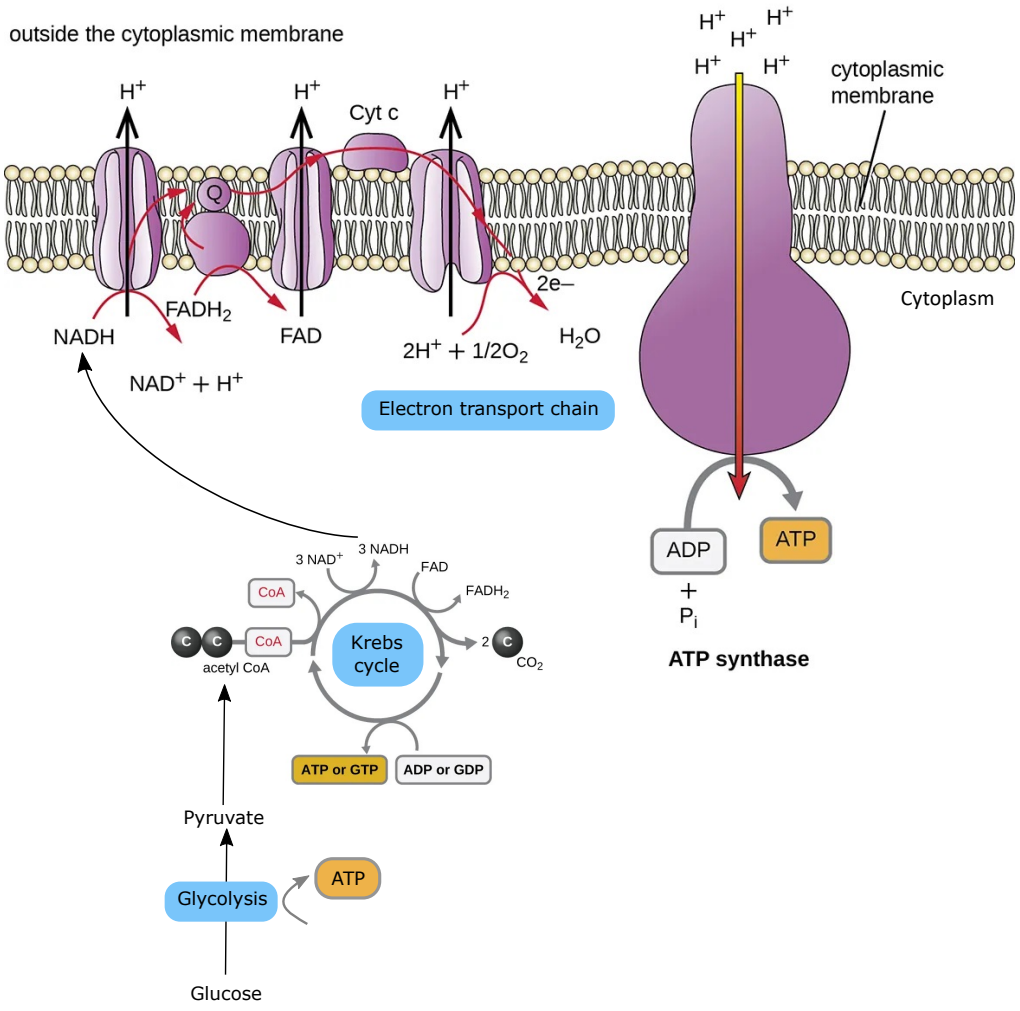

Figure 1.24 – Aerobic respiration in heterotrophic bacteria (modified from Parker et al. (2016))

acetyl-CoA, which serves as the starting point. During the Krebs cycle, CO_2 and NADH are produced.

- **Electron transport chain (ETC):** In the ETC, which occurs in the cell membrane of bacteria, NADH produced in the Krebs cycle is utilized. The conversion of NADH into H^+ releases an electron, which is transferred through an enzyme complex. This process leads to the consumption of O_2 and the production of H_2O. ATP is then generated in ATP synthase as a result of this electron transfer process (Parker et al. 2016).

Globally, aerobic respiration in *E. coli* bacteria results in the consumption of 0.55 g of O_2 per gram of bacterial biomass, while producing 0.20 g of carbon in the form of CO_2 (Roeva et al. 2015, Guardia and Calvo 2001).

1.4.2.3 Nitrifying bacteria

Nitrifying bacteria are aerobic autotrophic bacteria that derive their energy from oxidizing mineral nitrogen compounds. There are two types of nitrifiers depending on the molecule they oxidise:

• **Ammonium Oxidising Bacteria (AOB):** AOB achieve nitritation by converting NH_4^+ into NO_2^-. Typically, *Nitrosomonas sp.* is an AOB. As illustrated in Figure 1.25, the enzyme ammonia monooxygenase (AMO) of the respiratory chain forms NH_2OH and water from NH_3, O_2 and H^+. The enzyme hydroxylamine oxidoreductase (HAO) uses NH_2OH and water to form NO_2^- and H^+.

• **Nitrite Oxidising Bacteria (NOB):** NOB achieve nitratation by converting NO_2^- into NO_3^-. Typically, *Nitrobacter sp.* is a NOB. As illustrated in Figure 1.25, the enzyme nitrite oxidoreductase (NXR) uses NO_2^- and water to form NO_3^- and H^+.

As autotrophic microorganisms, nitrifying bacteria fix CO_2 through the Calvin cycle (detailed in the section about microalgae), as illustrated in Figure 1.25. Additionally, the Krebs cycle also operates in parallel to provide ATP for cell maintenance.

Oxidising NH_4^+ and NO_2^- provides low energy to nitrifiers, and consequently, they need to consume a large amount of these compounds to cover their energy needs. Godos et al. (2009) reported that 86 % of the Total Kjeldhal Nitrogen (TKN) was nitrified in a HRAP. Additionally, Ebeling et al. (2006) reported that 5.85 g of inorganic carbon were needed to nitrify 1 g of N-NH_4^+.

Nitrosomonas sp. exhibit a better affinity for O_2 compared to *Nitrobacter sp.*, giving them a competitive advantage in oxygen-rich environments. This preference for O_2 can lead to nitrite accumulation, particularly in conditions of oxygen excess (Poughon et al. 1999). Also, *Nitrobac-*

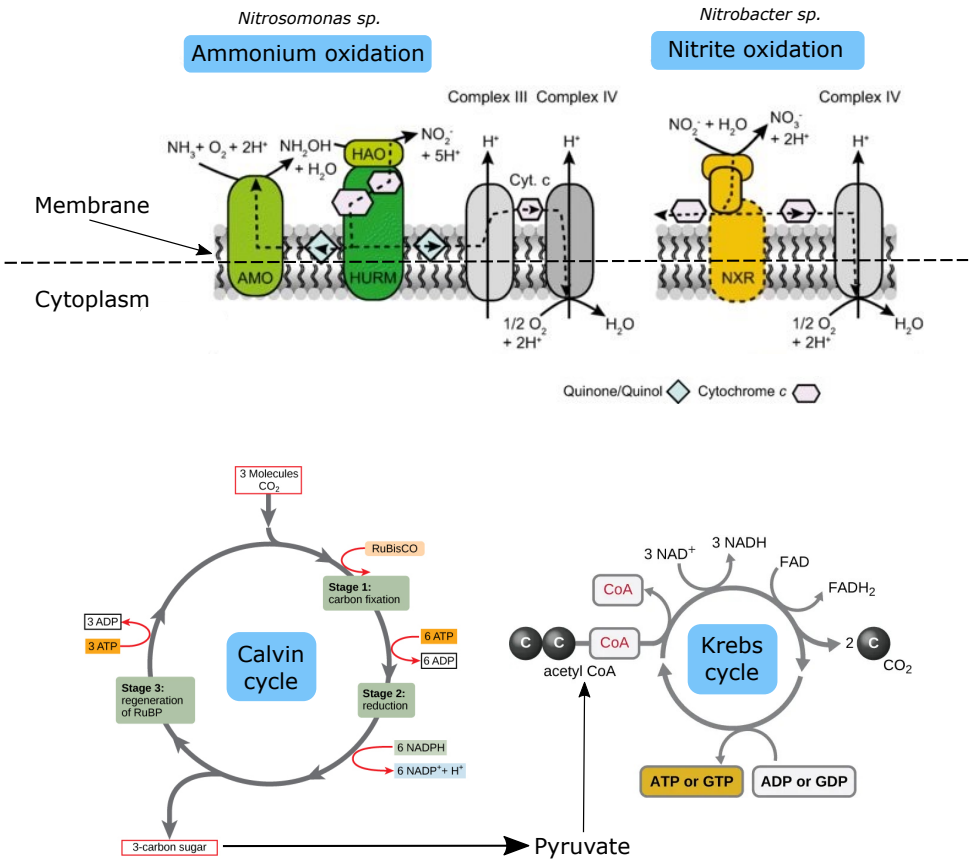

Figure 1.25 – Ammonium and nitrite oxidation and CO_2 fixation in nitrifying bacteria (modified from Koch et al. (2019), Molnar and Gair (2015) and Parker et al. (2016)). AMO, ammonia monooxygenase; HAO, hydroxylamine dehydrogenase; HURM, hydroxylamine-ubiquinone reaction module; NXR, nitrite oxidoreductase; Cyt. c, cytochrome c.

ter sp. is more sensitive to visible light than *Nitrosomonas sp.*, with high intensities potentially causing cell death through cytochromes photooxidation. As a result, *Nitrosomonas sp.* is more prevalent than *Nitrobacter sp.*, with a ratio of approximately 7/3 (*Nitrosomonas sp.* to *Nitrobacter sp.*) (Cébron 2004). These findings are consistent with research indicating that NO_2^- tends to accumulate in microalgae-sludge consortia due to the sensitivity of *Nitrobacter sp.* to high light conditions, resulting in a longer latency period for its development. Accordingly, nitrification rates were higher in darkness compared to light, suggesting that if nitrifier inoculation were to be performed in the pond, it would be ideally conducted during the nighttime (Fan et al. 2022).

Nitrifiers, despite being aerobic bacteria, can adapt to survive for extended periods in anaer-

obic conditions by reducing their metabolism to very low rates. However this adaptation comes at the cost of energy loss and can result in fluctuations in bacteria concentrations depending on presence or absence of oxygen (Diab et al. 1993). Additionally, Cébron (2004) found that nitrifying bacteria such as *Nitrosomonas sp.* and *Nitrobacter sp.* demonstrated the ability to grow in mixotrophic conditions using fructose as an organic carbon source. However, the ability for mixotrophy varied among strains in this study. Furthermore, *Nitrosomonas sp.* may also have the capability to utilize urea as a source of ammonium ions (NH_4^+).

1.4.2.4 Other bacteria

Denitryfying bacteria, including well-known representatives like *Pseudomonas aeruginosa*, are versatile organisms capable of both aerobic and anaerobic metabolism. During denitrification, these bacteria reduce nitrites or nitrates, typically found in their membranes, to form dinitrogen (N_2) or nitrogen oxides (Martens 2005).

Sulfur-oxidising bacteria are also expected to be present in HRAP systems, deriving energy from the oxidation of reduced sulfur compounds to form sulphates (Berben et al. 2019).

Phosphorus-Accumulating Bacteria are another group found in wastewater environments. These bacteria thrive in environments with alternating oxic and anoxic conditions, making them likely candidates for HRAP systems where such conditions are favoured by the alternating light and dark cycles (Bankston et al. 2020).

1.4.3 Interactions between microalgae and bacteria in HRAP systems

1.4.3.1 Symbiosis/competition in presence of organic carbon

Algae and bacteria are involved in complex trophic relationships, spanning from symbiosis and commensalism to competition. During the daytime, as depicted in Figure 1.26, microalgae produce O_2 that is consumed by heterotrophic bacteria. In turn, heterotrophic bacteria oxidize organic molecules, producing CO_2 that is consumed by microalgae. Autotrophic bacteria such as nitrifiers also consume O_2 and CO_2 produced by microalgae and heterotrophic bacteria, respectively. Exopolysaccharides produced by bacteria facilitate their attachment to microalgae,

enhancing these exchanges (Unnithan et al. 2014). It has been reported that the presence of algae significantly improves the development of aerobic taxa such as heterotrophic, nitrifying and phosphorus-accumulating bacteria (Bankston et al. 2020).

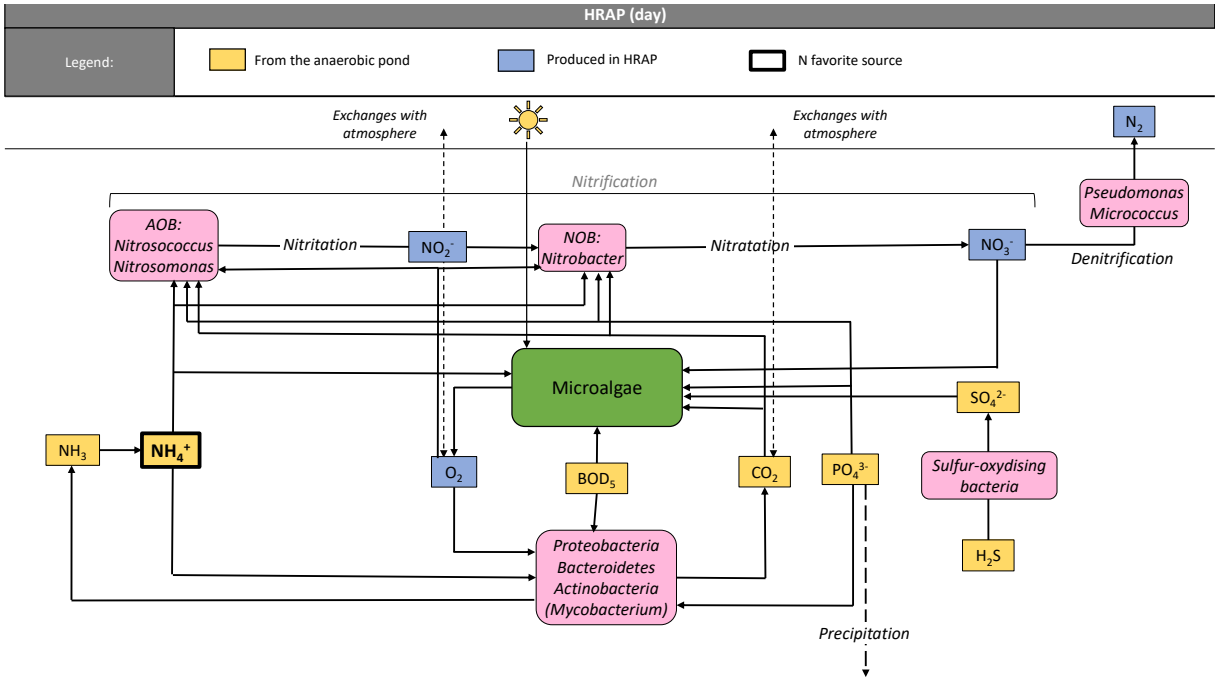

Figure 1.26 – Main chemical and biological processus occurring in HRAP during the day (Fallowfield and Garrett 1985, Cébron 2004, Canziani 2010)

At night, microalgae cease photosynthesis and switch to respiration to sustain cellular maintenance, initiating a competition for oxygen with autotrophic and heterotrophic bacteria (Figure 1.27). In this competition, if we consider microalgae as autotrophic organisms, bacteria are expected to have an advantage because, as part of the respiration process, they oxidise organic molecules present in the medium, whereas microalgae use their own carbohydrates, leading a loss in algal biomass. However, during both day and night periods, microalgae can utilize external organic carbon sources through photoheterotrophy during the day or chemoheterotrophy in darkness, enabling them to avoid biomass loss due to cellular respiration. In this scenario, microalgae and bacteria compete for organic carbon and dissolved oxygen (Abiusi et al. 2020). The synergy between carbon sources and light in microalgae cultures is further considered in

Chapter 4, while the literature review below focuses on the effects of algae-bacteria associations on algal growth, pollutant removal, and the availability of O_2 and CO_2 in wastewater. A compilation of the main results is presented in Table 1.7.

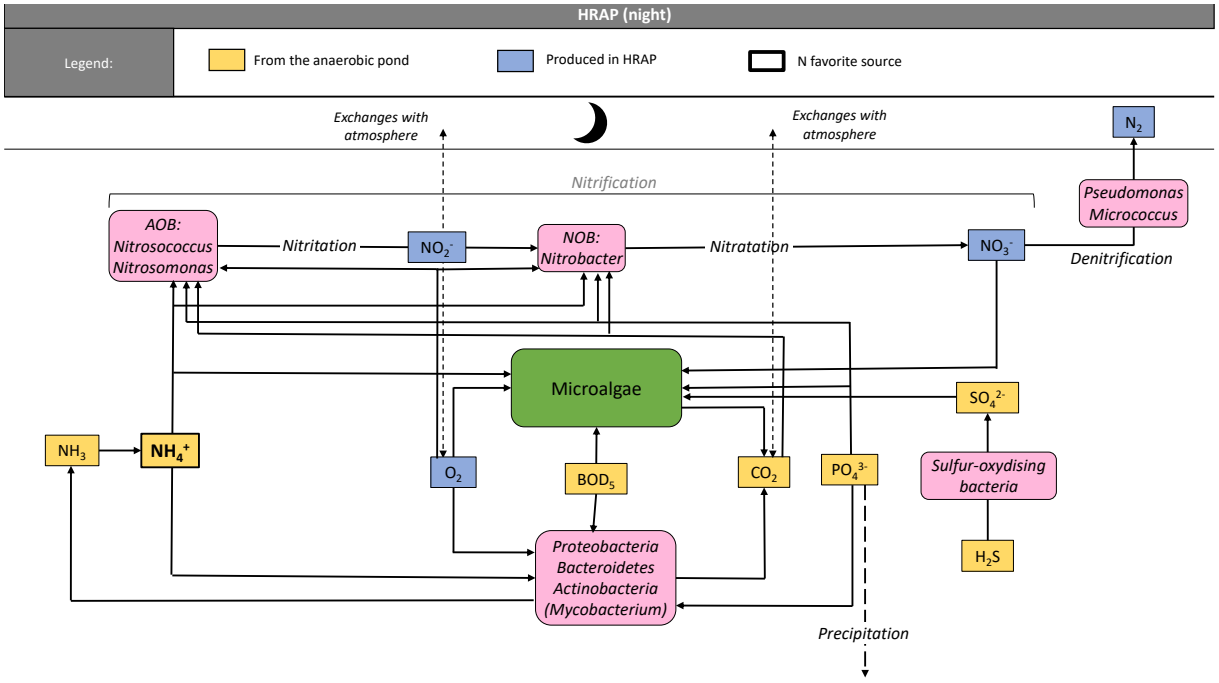

Figure 1.27 – Main chemical and biological processus occurring in HRAP during the night (Fallowfield and Garrett 1985, Cébron 2004, Canziani 2010)

For some authors, the association between microalgae and bacteria from wastewater in a day-night cycle resulted in symbiosis, leading to improvements in biomass growth and pollutant removal compared to the performance of microorganisms cultivated alone. For example, Marcilhac (2014) reported that the presence of bacteria *Azospirillium sp.* was linked to growth increase of the microalgae *C. vulgaris*. Similarly, Bankston et al. (2020) observed that in digested effluent naturally containing nitrifiers, heterotrophs, and phosphorus-accumulating bacteria with a day-night cycle of 14:10 h light:dark (1400 μmol.m^{-2}.s^{-1} during the light phase), adding microalgae *C. sorokiniana* resulted in an 53 % improvement in N removal, 21 % in P removal, and 57 % in COD removal. Complete nitrification was achieved in the presence of microalgae but not in the sole effluent. Similarly, in synthetic wastewater under 12:12 h light:dark conditions

(222 μmol.m^{-2}.s^{-1} during the light phase), a consortium of *Acinetobacter pittii*/*Scenedesmus obliquus* showed significantly higher N, P, and COD removal compared to organisms alone (Russel et al. 2020). Chlorophyll *a* concentration in coculture was twice as high as when microalgae were cultivated alone, indicating higher algal biomass. Enhanced performance in coculture compared to microalgae and bacteria cultures alone was attributed to efficient O_2 and CO_2 exchanges. Dissolved oxygen and CO_2 remained sufficient in the coculture in both light and dark phases (above 5 mgO_2.L^{-1} and 130 mgC.L^{-1}, respectively), while O_2 dropped with bacteria alone and CO_2 dropped with microalgae alone. However, it's worth noting that dissolved CO_2 concentrations were 5 to 10 times higher in these experiments (conducted in half-filled conical flasks) than in HRAP. While liquid-gas exchange may be lower in flasks compared to an open raceway like HRAP, potentially limiting CO_2 loss through the gas phase, inorganic carbon in the liquid phase remains much higher than theoretically expected considering the concentration of organic carbon supplied. This discrepancy questions the validity of the CO_2 concentrations presented in this study. Nonetheless, regardless of the exact values, CO_2 concentration significantly increased in coculture, indicating that bacterial production compensated widely for microalgae consumption. Similarly, in this study, algae provided more O_2 during the day than bacterial heterotrophic needs without requiring external aeration (Russel et al. 2020).

While those studies highlighted mutualistic relationships between microalgae and bacteria from wastewater, conflicting results have also been reported. Since microalgae are mixotrophic, they can consume not only CO_2 as a carbon source but also organic carbon. This dual capability introduces complexities into their interactions with bacteria.

Similarly to the studies cited above by Russel et al. (2020) and Bankston et al. (2020) cited above, Sforza et al. (2018) reported a higher N and P removal with a consortium of microalgae *C. protothecoides*/bacteria from activated sludge compared to bacteria alone. However, COD removal was lower in the consortium than in bacteria and microalgae alone. Contrary to the results reported by Russel et al. (2020), the growth of the consortium resulted in a negative oxygen production rate, with the oxygen consumption rate by bacteria being much faster than microalgal production even at the highest algae-to-bacteria biomass ratio of 10:1. Also, even with

bacteria present, microalgae were limited in CO_2 compared to a non-limited culture supplied with external CO_2. Experiments conducted by Russel et al. (2020) with a similar algae-to-bacteria ratio and synthetic medium yielded opposite results. In their study, O_2 and CO_2 were always in excess in the consortium due to symbiosis and gas exchanges between algae and bacteria. The main difference between these two studies is the incident irradiance applied, which was much lower in the study by Sforza et al. 2018, where the main interaction was competition for dissolved oxygen and organic carbon (45 μmol.m^{-2}.s^{-1}), compared to the study by Russel et al. 2020, where symbiotic interaction was reported (222 μmol.m^{-2}.s^{-1}). The lower oxygen production by photosynthesis induced by the lower incident light in the study by Sforza et al. (2018) could probably not compensate for the respiration rate by both microalgae and bacteria. Competition between microalgae and nitrifying bacteria for CO_2 was also reported by Zhang et al. (2020). Applying 100 ml.min^{-1} of aeration in 500 ml glass bottles containing synthetic wastewater resulted in lower inorganic carbon in the liquid phase and competition between algae *S. obliquus* and autotrophic bacteria from sludge.

In the study by Sforza et al. (2018), the focus was on the effect of algal mixotrophy of axenical *C. protothecoides* on the O_2 balance. The addition of organic carbon sources as acetate, peptone, and meat extract to a BG11 medium significantly increased microalgae growth rate but also reduced net O_2 production by 78 % compared to autotrophic culture with bicarbonate as the sole carbon source. Specifically, a lower oxygen production rate was observed with acetate compared to peptone and meat extract, indicating a better affinity of *C. protothecoides* with acetate than with the other carbon sources. In real wastewater (without bacteria), the oxygen production rate was also reduced by 70 % compared to autotrophic conditions. These results suggest a significant contribution of microalgae to the overall heterotrophic activity in wastewater, including during the day. Flores-Salgado et al. (2021) investigated the specific contributions of microalgae and heterotrophic bacteria to the production and consumption of oxygen during the night and day. The natural consortium contained *Desmodesmus sp.* and *Chlorella sp.*, and the incident irradiance for the day experiment was 300 μmol.m^{-2}.s^{-1}. Acetate was used as the organic carbon source. Microalgae consumed 14.73 mgO_2.gVSS^{-1}.h^{-1} in darkness and produced

13.76 $mgO_2.gVSS^{-1}.h^{-1}$ in light. Heterotrophic bacteria consumed 2.37 $mgO_2.gVSS^{-1}.h^{-1}$ both in light and dark experiments. While photosynthetically produced O_2 was sufficient to cover heterotrophic needs during the day, 86 % of respiration at night was due to microalgae. Althrough the ratio algae to bacteria was not specified in this study, both this study and the study by Sforza et al. (2018) suggest a significant contribution of microalgae to respiration over the day-night cycle and a notable competition with bacteria.

The consensus among most studies is that both algal and bacterial biomass can utilize nutrients such as N-NH_4^+ and P-PO_4^{3-} present in wastewater for their growth (Figure 1.26). Additionally, it has been observed that the levels of N and P in real or synthetic wastewater are typically sufficient to support the growth of both microalgae and bacteria. Furthermore, Sforza et al. (2018) demonstrated that in cases of competition for organic carbon with bacteria and/or depletion of CO_2, microalgae were capable of utilizing organic N to compensate for the lake of carbon, thereby improving overall N removal.

Based on the results reported in the cited studies, several factors influencing the symbiosis/competition between microalgae and bacteria in wastewater in laboratory-scale experiments can be identified:

• **The organic carbon source:** The type and degradability of organic carbon source present in wastewater can influence the competition between microalgae and heterotrophic bacteria for carbon and may impact the overall oxygen production by microalgae (Sforza et al. 2018).

• **Algae/bacteria ratio:** The optimal ratio of microalgae to bacteria may vary depending on the specific conditions of the experiment, including the type of microorganisms used, the composition of the wastewater, and the incident irradiance. Studies have reported varying optimal ratios ranging from 1:2 to 2:1 (Fan et al. 2022, Russel et al. 2020, Fallowfield and Garrett 1985). Theoretically, according to stoichiometric equations of microalgal growth in autotrophy, heterotrophic bacteria and nitrifying bacteria, an equilibrium is reached between O_2 and CO_2 consumed and produced with 61% of heterotrophic bacteria, 38% of microalgae and 1% of nitrifying bacteria in biomass (calculated from stoechiometric equations in Abiusi et al. (2020),

Reference	**Bankston et al. (2020)**	**Sforza et al. (2018)**	**Russel et al. (2020)**	**Fan et al. (2022)**	**Flores-Salgado et al. (2021)**
Medium	Digestate	BG11 + acetate + peptone + meat extract	SWW (glucose, beef extract, peptone)	Sludge + aeration	BG11 + acetate
Light	14:10h, 1400 μmol/m^2/s	15:15min, 45 μmol/m^2/s	12:12h 222 μmol/m^2/s	56 μmol/m^2/s + dark	300 μmol/m^2/s + dark
Microorganisms	*C. sorokiniana*, ANOB, HB, PAO	*C. prototheecoides*:bacteria from AS (1:1 to 10:1)	*S. obliquus*:*A. pittii* (HB) (2:1)	*C. sorokiniana*:sludge (2:1)	*Desmodesmus sp.* and *Chlorella sp.* + HB
Effect of adding algae on pollutants removal	N removal: +53%, P removal: +21%, COD removal: +57%	N removal +, COD removal -	N removal +, P removal +, COD removal +	N removal +, P removal +, COD removal -	
Growth	Algal growth +29%	Organic carbon improved algal growth. No effect of bacteria on algal growth	Algal growth improved x2		
O_2		No net O_2 production	Enough O_2 (dropping when microorganisms cultivated alone)		O_2 uptake at night > O_2 production day
CO_2		Algae limited by CO_2	Enough CO_2 (dropping when microorganisms cultivated alone)		

Table 1.7 – Synthesis of previous studies on algae-bacteria interactions in effluent treatment (ANOB=Ammonium and Nitrite Oxidising Bacteria, HB=Heterotrophic Bacteria, PAO=Phosphorus Accumulating Organisms, AS=Activated Sludge, SWW=Synthetic Wastewater)

Guardia and Calvo (2001) and Poughon et al. (1999)).

• **Light:** The incident photosynthetic photon flux density applied to the cocultures significantly influences the interactions between microalgae and bacteria. High PFD levels have been associated with improved nutrient removal and oxygen availability in coculture, while low PFD levels may lead to competition for carbon and oxygen between algae and bacteria (Sforza et

al. 2018, Bankston et al. 2020, Flores-Salgado et al. 2021, Russel et al. 2020, Fan et al. 2022). Results appear to be light-dependent, highlighting the importance of considering the diurnal variations in irradiance when studying microalgae-bacteria interactions.

These factors demonstrate the complex and dynamic nature of the interactions between microalgae and bacteria in wastewater systems, which can vary depending on environmental conditions and experimental parameters. Further research is needed to better understand these interactions and optimize their utilization in wastewater treatment processes.

1.4.3.2 Nitrogen cycle and interactions microalgae-nitrifiers

The dynamics of nitrogen species in wastewater and their utilization by microalgae and nitrifying bacteria play a crucial role in wastewater treatment processes. While nitrogen is primarily present as NH_4^+ in wastewater, a significant portion is converted into NO_3^- by nitrifying bacteria (Vargas et al. 2016, Evans et al. 2005). Studies such as Vargas et al. (2016) have estimated that approximately 60 % of N-NH_4^+ is nitrified, with 40 % being assimilated by microalgae. In this study, nitrifiers were found to have a higher NH_4^+ uptake rate compared to microalgae, which could potentially impact algal growth negatively. Generally, microalgae uses NH_4^+ before NO_3^- because it consumes 13% less energy during metabolic conversion. As nitrifiers consume a significant amount of NH_4^+ to convert it into a less easily assimilable molecule, nitrifiers could be considered as having a negative impact on algal growth (Ebeling et al. 2006, Lachmann et al. 2019). Additionally, studies on cyanobacteria like *Synechococcus* have shown that the use of NH_4^+ instead of NO_3^- can increase biomass production, especially in light-limited conditions (Ruan and Giordano 2017).

Overall, the relationship between microalgae and nitrifying bacteria regarding nitrogen utilization is complex and influenced by various environmental and culture conditions. Understanding these dynamics is essential for optimizing wastewater treatment processes and enhancing the efficiency of nutrient removal by microalgae. Further research is needed to elucidate the specific mechanisms underlying these interactions and their implications for wastewater treatment.

The relationship between nitrifiers and microalgae in wastewater treatment systems like

HRAPs is indeed complex and multifaceted. While nitrifiers can influence microalgal growth, an excessive proportion of algae has been shown to reduce the population of nitrifying bacteria in consortia (Fallahi et al. 2021). This suggests that there is a dynamic interplay between these microorganisms, where changes in one population can affect the other.

However, from a practical perspective, storing nitrogen in algal biomass may be more beneficial than releasing it into the atmosphere through nitrification-denitrification processes (Sforza et al. 2018) and volatilization. This is because algal biomass can potentially be valorized for various applications, such as biofuel production, animal feed, or fertilizer. By incorporating nitrogen into algal biomass, it can be effectively removed from wastewater and utilized in valuable downstream processes, contributing to the overall sustainability and efficiency of wastewater treatment systems.

Understanding and optimizing the interactions between nitrifiers and microalgae in HRAPs is essential for maximizing nutrient removal efficiency while also harnessing the potential benefits of algal biomass production. Further research into the dynamics of these microbial communities and their responses to different environmental conditions will be crucial for improving the performance of wastewater treatment systems and advancing the utilization of microalgae in biotechnology applications.

1.4.3.3 Other interactions microalgae-bacteria

Interactions between microalgae and bacteria can take lots of different forms, from beneficial to deleterious or even lethal. Bacteria can increase turbidity and reduce light availability for microalgae. Microalgae and bacteria tend also to form flocs by attachement of bacteria on microalgae cell surface. Generally, all sorts of organic aggregates can form in wastewater, combining algae, bacteria and organic molecules: it results in anoxic conditions inside the aggregate where anaerobic processes are willing to occur. However, aggregated bacteria are also able to resuspend (Fuentes et al. 2016). Some bacteria can also lyse algal cell to use intracellular compounds as nutrients (Fuentes et al. 2016). Lethal effects of algae-bacteria interactions also include the production of algicidal or bactericidal compounds (Oviedo et al. 2022). However, this kind of lethal

interactions are not occuring in every consortium. For example, Sforza et al. (2018) reported no inhibition effect of microalgal growth in real wastewater compared to sterilised wastewater. Bacteria can also bring vitamins, antibiotics, growth promoters beneficial for microalgal growth. Bacteria can produce siderophores like vibrioferrin that makes Fe(III) available for algae which uses Fe(III) for inorganic carbon fixation (Fuentes et al. 2016). Substances produced by bacteria can influence biofilm and antibiotic production by microalgae, but also enhance heterotrophic bacteria growth (Unnithan et al. 2014).

Indeed, the interactions between microalgae and bacteria in wastewater-like media can vary from mutualistic to competitive, depending on various factors including experimental conditions and the composition of the microbial community. In real systems like HRAP, these interactions are likely to be dynamic and influenced by factors such as light availability, nutrient concentrations, and the metabolic activities of both microalgae and bacteria. Understanding the dynamics of carbon fluxes, oxygen dynamics, and the interactions between microalgae and bacteria is essential for accurately modeling and predicting the behavior of HRAP systems. This knowledge can help optimize system performance, determine the need for external CO_2 supplementation, and ultimately improve the efficiency of wastewater treatment and resource recovery processes. Further research in this area is crucial for advancing our understanding of complex microbial communities and their roles in engineered ecosystems like HRAP.

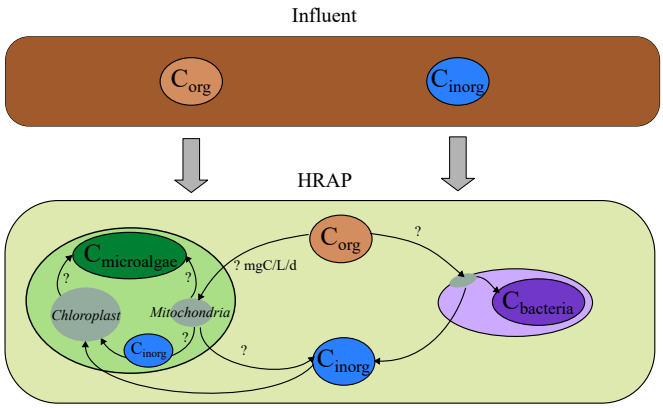

Figure 1.28 – Potential carbon fluxes in microalgae-bacteria consortium in presence of organic carbon (Fallowfield and Garrett 1985)

Microalgae are also expected to have complex interactions with pathogen microorganisms targeted in wastewater treatment due to their major impact on physicochemical conditions in the pond.

1.5 Disinfection processes in HRAP and the role of microalgae

1.5.1 Generalities on viruses

1.5.1.1 Viruses in wastewater

In wastewater, viruses come from human fecal matter, food production, animal husbandry, seasonal surface runoff, wind blown soil, waterfowl or atmospheric deposition (Corsi et al. 2014). Enteric viruses like adenovirus, rotavirus, hepatitis A virus, noroviruses, coxsackievirus, echovirus, reovirus and astrovirus are the principal human pathogenic viruses in wastewater, responsible for various symptoms like nausea, vomiting, fever, diarrhea but also respiratory diseases such as bronchiolitis (Corpuz et al. 2020). More than a hundred of enteric viral strains have been identified as aquatic contaminants (Farkas et al. 2020).

An infected person releases from 10^5 to 10^{12} of enteric viruses per gram of fecal material (Gerba 2000). Viruses are then present in significant quantities in wastewater and have very low infectious doses (one single viral particle can cause an infection in a susceptible person), meaning they are likely to infect a significant part of the population when released in the natural environment. Efficient disinfection is then necessary to eliminate the risk of epidemics (Zhong et al. 2016).

1.5.1.2 Viruses composition and life cycle

Viruses are obligate intracellular parasites because they cannot replicate independently and must infect other organisms to multiply. Unlike cells, viruses lack a genome replication system and are therefore not classified as cells or living organisms (Louten 2016). Average size of viruses is 100 nm. Their genetic material can be composed of either DNA or RNA, but not both, and this genome is encapsulated within a protective protein shell called a capside. The capside can

be of helical, icosahedral, or more complex structure (Figure 1.29). Icosahedral structure is more common. In enveloped viruses, such as the coronavirus responsible for COVID-19, the capside is surrounded by a lipid membrane (Louten 2016). Those enveloped viruses are more susceptible to inactivation in wastewater due to the sensitivity of their lipid membrane to environmental factors. This is not the case for enteric viruses, very abundant in wastewater, that are non enveloped (Corpuz et al. 2020). As a result, they may be more resilient in wastewater and more resistant to certain disinfection methods compared to enveloped viruses. Understanding the structure and characteristics of different viruses is crucial for developing effective strategies to control their transmission and ensure public health safety.

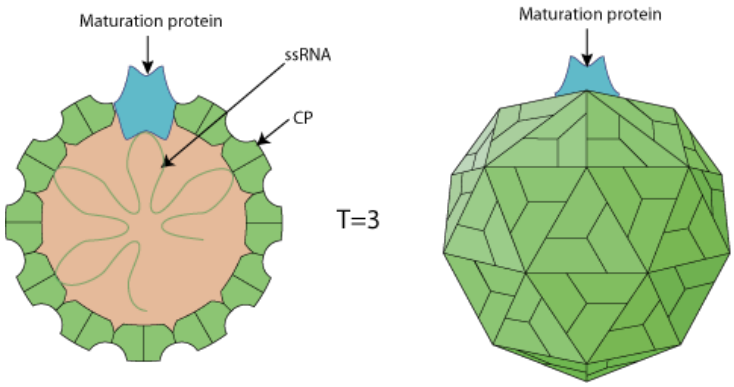

Figure 1.29 – MS2 virus structure. Source: https://viralzone.expasy.org (Golmohammadi et al. 1993)

Viruses first attach to a host cell and enter it. After entering the host cell, the virus disassembles to release its genome, which is then replicated using the host's cellular machinery. The replicated genome is then encapsulated again to form progeny viruses that are finally released into the host cell environment (Ryu 2017). Figure 1.30 shows *E. coli* infection by the coliphage MS2. In the case of MS2, the A-protein allows host recognition and attachment (Majiya et al. 2018).

1.5.2 Disinfection processes

In HRAP systems, sunlight, which includes UVB (280-315 nm), UVA (315-400 nm) and visible light (Vis, 400-800 nm), are the main factor responsible for microorganisms and viruses

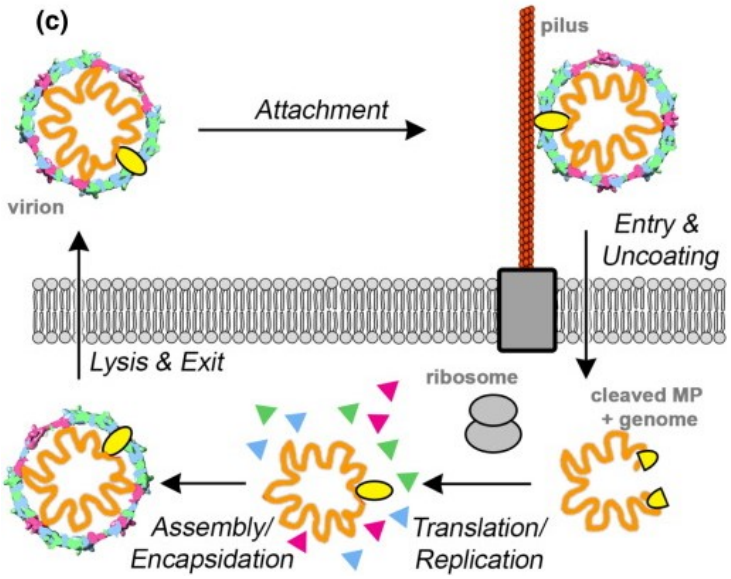

Figure 1.30 – Infection of *E. coli* by MS2 virus (Rolfsson et al. 2016)

inactivation. Seasons, time of the day, geographical location, air pollution, ozone thickness, and cloud cover can influence this inactivation process (Bolton et al. 2011), but biological and physicochemical characteristics of the pond like biomass concentration, turbidity, presence of organic molecules, pH or oxygen levels also play significant roles.

1.5.2.1 Direct UV inactivation

Among sunlight radiations, UVB is the most energetic radiation, followed by UVA and visible light. Due to its high energy, UVB radiation can cause direct damage to the RNA and DNA of microorganisms and viruses. In fact, inactivation by UVB has been reported to be two orders of magnitude faster than by UVA or visible light for microorganisms and viruses such as *Escherichia coli*, *Enterococcus faecium*, MS2, and ΦX174 viruses (Bolton et al. 2011). Additionally, significant removal rates (denoted as K) under UVB treatment have been reported for MS2 virus ($K = 3.7\ h^{-1}$) and *E. coli* ($K = 37\ h^{-1}$) (Lian et al. 2018). The inactivation by UV irradiation depends on factors such as irradiance, exposure time, and temperature. For instance, Lian et al. (2018) found the highest MS2 inactivation rate at 30 °C for a UVB dose of 6 $W.m^{-2}$, which was the highest temperature and UVB dose tested. While the UVB dose rate appeared

to saturate at 6 $W.m^{-2}$, there was a notable synergy between high temperature and UVB dose. High temperature can impact the folding of proteins in viruses and enhance the production of toxic compounds (Park et al. 2021). However, no significant effect of temperature (tested between 20 and 30 °C) was observed for *E. coli* inactivation. This lack of effect may be attributed to the increasing efficiency of the DNA repair system enzymes in *E. coli* at higher temperature (30°C), as lethal effects on *E. coli* have been reported only for temperatures exceeding 50 °C (Wegelin et al. 1994). Therefore, while lethal effects of high temperatures may be observed in HRAP systems for viruses (as temperature can exceed 30 °C in ponds during summer), they are less likely to affect bacteria.

While relevant efficiency of UVB on pathogens inactivation was proved by several studies, it is important to consider that 99 % of UVB radiation is absorbed within the first 2.5 cm of a Waste Stabilisation Pond (WSP), and attenuation is expected to be even higher in HRAP due to the higher concentration of algal biomass (Bolton et al. 2010). Yet, UVA and visible light exhibit greater penetration depths, reaching up to 13 and 43 cm respectively in wastewater pond (Table 1.8). The substantial attenuation of UVB in turbid mediums suggests that UVA and visible light may play a significant role in microorganisms and viruses inactivation in HRAP. UVA and visible light were not sufficient to inactivate MS2 virus in reverse osmosis water but were effective against *E. coli* (Bolton et al. 2011). In the case of viruses, UVA does not cause damage through direct effect of wavelength on DNA/RNA, but via ROS produced via photosensitisers. In the case of *E. coli*, those photosensitisers are endogeneous whereas viruses require exogenous photosensitisers. Despite high efficiency of solar UV radiations was reported in numerous studies, inactivation by UV can be followed by a significant regrowth, microorganisms and viruses being able to repair their genome using enzymes (Putois 2012). Lesions to virus genetic caused by UVB could also be repaired during dark period (at night) within host cells, further highlighting the potential limitations of UV-based disinfection methods (Park et al. 2021).

1.5.2.2 Factors implied in UV attenuation in HRAP

Wastewater turbidity significantly affects the penetration of UVB, UVA, and visible light. On average, UVB, UVA, and visible light penetrate approximately three times further in freshwater than in WSP, as illustrated in the Table 1.8. It is important to note that HRAPs are generally more turbid than WSPs due to higher algal biomass, which further attenuates all types of radiation.

Type of radiation	Depth of 1% penetration in WSP	Depth of 1% penetration in freshwater
UVB	8cm	23cm
UVA	13cm	45cm
Visible	43cm	124cm

Table 1.8 – Respective euphotic depth for UVB, UVA and visible light in Waste Stabilisation Pond and in freshwater, whicg is the depth at which 1% of the incident surface irradiance is recorded (Bolton et al. 2011)

Turbidity in HRAP is mainly attributable to suspended solids. In HRAP systems suspended solids are constituted of fibers, toilet paper, living or dead zooplankton, microalgae, bacteria or flocs, humic acid but also a small mineral part (10% of total suspended solids according to Azema et al. (2002)) like sand. According to Azema et al. (2002), particles can be soluble ($<$ 0.001 μm), colloidal (0.0011 μm), supracolloidal (1100 μm) or settleable ($>$100 μm). Suspended solids regroup particles of 1 μm or bigger, so mainly supracolloidal or settleable particles.

On average, one inhabitant produces 70 g of suspended solids per day, which corresponds to 0.54 gTSS.L^{-1} in municipal wastewater (Rosenwinkel et al. 2001). However, depending on pretreatment and influent nature, a wide range of TSS concentration can be found in influent wastewater: Foladori et al. (2020) reported TSS concentrations ranging from 0.2 to 3.9 g.L^{-1} in domestic wastewaters. In activated sludge processes, higher concentrations of solids are expected to increase the efficiency of organic matter removal by favouring floc formation (Foladori et al. 2020). It is not the case in HRAP systems, where light penetration in the pond is critical for microalgal growth and UV disinfection, and consequently for depollution efficiency. Yet, Incropera and Privoznik (1979) reported significant optical densities at 550 nm for wastewa-

ters, ranging from 0.055 and 0.132, underscoring the importance of understanding the optical properties of wastewater in HRAP systems.

Bolton et al. (2011) reported that in HRAP systems, turbidity, encompassing absorbance and scattering, is predominantly influenced by suspended materials rather than chlorophyll *a*, microalgae being less impactful. According to this study, turbidity accounts for 73 % of the variability in UVB attenuation, 72 % for UVA attenuation, and 45 % for visible light attenuation, suggesting a significant impact on HRAP performance in terms of sunlight-mediated bacterial inactivation. In contrast, divergent findings were reported for a 70 cm depth WSP, where absorbance, the dominant attenuation process, was primarily attributed to microalgae rather than wastewater itself (Curtis et al. 1994). Additionally, Incropera and Privoznik (1979) investigated absorbance, scattering and diffusion of a primary domestic effluent and a symbiotic culture of microalgae *Chlorella pyrenoidosa*. Particle size analysis of the wastewater revealed the absence of settleable particles, with solids ranging between 0.79 and 3 μm, and more than 50 % of particles between 0.79 and 1 μm, averaging 1.11 μm. In comparison, the average particle size of the symbiotic microalgae culture in wastewater was 1.85 μm, indicating that microalgae were the largest particles present. Interestingly, both pure wastewater and wastewater with microalgae exhibited extinction mainly due to scattering rather than absorption. However, a strong difference was observed in the extinction cross-sections for microalgae and wastewater: extinction cross-section for the coupled microalgae and wastewater was six times higher than for wastewater alone and two times higher than for pure microalgae. Consequently, the extinction was mainly due to microalgae, contrary to results from other studies such as Bolton et al. (2011) where turbidity, which is assumed to be assimilated to extinction, was mainly due to suspended solids rather than chlorophyll a. This difference must be due to the nature and the pretreatment of the wastewater, leading to significant differences in particle size distribution and their contributions to radiations extinction. In Incropera and Privoznik (1979), turbidity and particle size seem to be very low (3 μm maximum) compared to values reported for other wastewater analysis: for example, Azema et al. (2002) measured particles sizes up to 1000 μm, with a peak around 30 μm.

Previous studies showed that maximum particle size in wastewater could vary by a factor of 1000 depending on the origin and pretreatment of wastewater. Nevertheless, because of chlorophyll a, b and carotenoids contributing to absorbance cross sections of microalgae always seems to be higher than wastewater. However, as reported in Incropera and Privoznik (1979), suspended solids cause non-negligible scattering and should therefore be included in models simulating radiative transfer in HRAP systems. Moreover, absorbance cross section of wastewater seems to be higher for the lowest wavelengths: UV should therefore be more impacted than visible light by suspended solids, which could be determinant in solar disinfection.

Brahmi et al. (2010) studied *Pseudomonas aeruginosa* UV inactivation in secondary treated wastewater taking into account TSS concentration. Results allowed to identify three stages in microorganisms removal process:

• **First stage:** This stage is characterized by a high disinfection efficiency, during which the most vulnerable microorganisms, those not associated with suspended solids, are rapidly inactivated by UV radiation.

• **Second stage:** As the number of free-floating microorganisms decreases, the removal rate slows down. This is attributed to the shielding effect of suspended solids, which absorb and dissipate UV radiation, thereby reducing its effectiveness in inactivating microorganisms associated with these solids.

• During the **third stage**, the number of microorganisms is stable: indeed, all the individual organisms are already inactivated and the rest forms flocs with suspended solids. This phenomena explains why, even with strong UV dose, it is impossible to exceed a certain level of removal: a fraction of microorganisms will be invulnerable protected by suspended solids.

To conclude, due to both organic detritus and microalgae, only a small fraction of a 30cm-depth pond is expected to be irradiated by disinfecting solar radiations, even during the daytime. During the night time, inactivation was reported to be 10 times slower than in sunlight (Park et al. 2021). In contradiction with the results obtained by Brahmi et al. (2010) where suspended solids inhibited inactivation, in darkness, inactivation was lower in the absence of suspended solids, suggesting particles and flocs could play a role in dark disinfection (Park et al. 2021).

Considering low inactivation in darkness and strong occurrence of dark zones in HRAP, other parameters than UV like Reactive Oxygen Species, pH and DO should be relevant in HRAP disinfection process.

1.5.2.3 Oxidative stress by ROS

High energy from UV are also able to break chemical bonds that constitute organic molecules, leading to division of the parent compound in free radicals able to damage microorganisms and viruses (Putois 2012). Those organic molecules are called photosensitisers, light absorbing compounds located inside the cells (endogenous) or outside the cells (exogenous) that transfer their energy to other chemical species, like oxygen. This way, sensitisation of those compounds by light implies the formation of ROS that immediately damages membrane by oxidation, then attack intracellular compounds and finally inhibits respiration by attacking enzymes of the respiratory chain, leading to microorganism or virus lyse (Bolton et al. 2011, Putois 2012).

1.5.2.3.1 Endogenous photosensitisers

Endogenous photosensitisers are organic compounds present in low concentrations inside the cell or on the cell membrane and include flavins and porphyrin derivatives, cytochromes, NAD^+ (Nicotinamide adenine dinucleotide), NADH (reduced form of NAD), quinones, and various chromophores (Bolton 2012). It is worth noting that viruses, unlike bacteria, are not affected by sensitisation of endogenous photosensitizers. This is because viruses lack a bound chromophore within their protein structures that could act as an endogenous photosensitiser (Davies 2003). In a general way, viruses are more resistant to disinfectants than bacteria (Zhong et al. 2016)

1.5.2.3.2 Exogenous photosensitisers

Exogenous photosensitisers are organic compounds that are found outside microbial cells, and include, in the case of wastewater, humic substances, photosynthetic pigments and dissolved organic matter (Bolton 2012). It was reported that nitrites and nitrates could also act like photosensitisers and produce ROS (Dong and Rosario-Ortiz 2012). Bolton et al. (2011) reported higher UVA inactivation rates of MS2 virus compared to reverse osmosis water, which lacks such

organic components. Moreover, components found in wastewater allowed to inactivate microorganisms and viruses even in the dark. On the contrary, UVB was less efficient in wastewater because penetration of those radiations is very weak in turbid water.

1.5.2.4 pH and DO

Microalgal growth in HRAP often leads to significant increases in pH and dissolved oxygen levels. During summer, oxygen concentrations can reach 30 $mgO_2.L^{-1}$ in the upper layers, while pH values frequently exceed 10 at midday (Sutherland et al. 2021).

Research by Chambonniere et al. (2020) reported that peaks of *E. coli* removal was correlated with peaks in light, temperature, pH and DO. In the same way, *E. coli* removal efficiency was the highest in the late afternoon on sunny summer days and dropped during heavy rainfall months. High pH can decrease the stability of microbial cells and high DO increases the formation of toxic Reactive Oxygen Species, however high pH and dissolved oxygen were only significant for disinfection when coupled with UVA and visible light (in opposition to UVB) despite conflicting results due to different microorganisms and viruses (Bolton 2012). High pH and DO, by inducing conformational changes in bacterial cells and viral capside structures, allow the creation of sites suitable for photo-oxidative attack by UVA and visible light, enhancing photo-oxidation and improving solar inactivation efficiency. pH and DO did not have any effect while coupled with UVB because, by itself, this very energetic radiation predominates in disinfection process (when ignoring attenuation through the water column).

High pH and DO while not coupled to photosensitisers nor solar radiations did not significantly affect MS2 virus inactivation (Bolton et al. 2011). Another study supports this statement and reported similar survival rates for MS2 virus at pH levels of 4, 7, and 10 (Lin et al. 2020). However, it's important to note that the DO concentration used in Bolton et al. (2011) study was relatively low (8.5 $mg.L^{-1}$) compared to the concentrations typically reached in HRAP. Therefore, the potential impact of higher DO concentrations on MS2 virus inactivation in HRAP warrants further investigation.

1.5.3 Conclusion on potential microalgae impact on pathogens solar inactivation

Microalgae turned out to be closely associated with many factors that significantly impact solar inactivation in HRAP, including UV penetration, pH, DO, and potentially photosensitisers. Research has shown that high pH and DO levels resulting from microalgal growth can synergize with UVA, visible light, and photosensitisers to enhance the inactivation of microorganisms and viruses. While different microorganisms and viruses exhibit varying sensitivities to inactivation factors (Bolton 2012), presence of photosensitisers was always reported to enhance inactivation. Photosensitisers originated from wastewater, however microalgae could also potentially release exogenous photosensitisers or play the role of an endogenous photosensitiser to enhance microorganisms and viruses inactivation. This raises the question of the relevance of those photosensitisers of algal origin compared to wastewater photosensitisers. However, due to relatively high algal biomass, microalgae are expected to be the main contributor to solar radiations attenuation in HRAP and consequently to inhibit pathogens solar inactivation. As illustrated in the Figure 1.31, the balance between positive and negative effect of microalgae on pathogens inactivation in HRAP is still not clear in the literature. While Curtis et al. (1994) suggested removing algae to improve UV penetration and the removal of faecal coliforms in a tertiary treatment downstream of HRAP, other studies reported that *E. coli* could be removed within 4 days in an outdoor raceway inoculated with *S. obliquus* while *E. coli* was still present after 10 days in the non-inoculated pond (Sebastian and Nair 1984). Knowing the contribution of UV attenuation and ROS production by both microalgae and wastewater to inactivation in HRAP would be valuable in designing potential tertiary treatments downstream of HRAP aimed at improving pathogen removal.

1.6 Conclusion

In conclusion, HRAP systems constitute promising technologies with a significant margin of progression. Indeed, interaction mechanisms occurring in those ponds between microalgae,

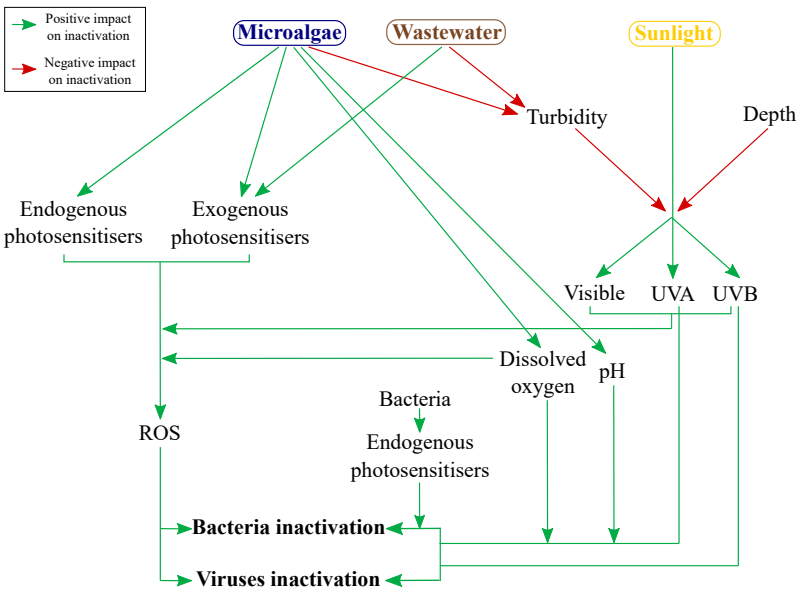

Figure 1.31 – Links between parameters involved in microorganisms and viruses inactivation in HRAP (red arrows corresponds to negative effects on inactivation and green arrows corresponds to positive effects on inactivation) (Bolton 2012)

bacteria and viruses and their impact on pollutants and pathogens removal is still unclear, especially at large scale and along the day-night cycle in solar conditions. Further research should go toward an integrative approach of HRAP behaviour in the aim of improving pollutants removal and disinfection.

Identified gaps of knowledge

- Large-scale systems mixing and characterisation
- Carbon fate and gas exchanges between microalgae and bacteria in dynamic solar conditions
- Impact of microalgae in pathogens solar inactivation
- Relevance of using lab photobioreactors to simulate large-scale system

Chapter 2

Studied systems and analytical methods

2.1 Peterborough HRAP: study on the large-scale pilot

2.1.1 Objective of the study

Peterborough HRAP was constructed in 2018 in South Australia with the aim of implementing wastewater treatment using microalgae on a large scale (Figure 2.1). The HRAP comprises a meandering 1-km length, 4-m width and 30-cm depth channel mixed with a paddlewheel. As the mixing is expected to be heterogeneous in a pond of this size, the purpose of this study is to investigate the diversity of physicochemical conditions inside the pond by establishing 3D flow velocity, dissolved oxygen, carbon, phosphates and nitrogen profiles (see Chapter 3).

2.1.2 Study site and data collection in the pond

2.1.2.1 Study site

Peterborough HRAP (S32°58′24.143″ E138°48′5.958″) is operated in the mid-North of South Australia. The HRAP consists of six butyl rubber lined channels (Figure 2.2) with a combined length of 1 km. The HRAP receives abattoir and domestic wastewater pre-treated in an anaerobic pond with a HRT of 3 days. The pond operates at a wastewater depth of 300 mm and a hydraulic retention time of 10 days, employing a paddlewheel for mixing. The calculated volume of wastewater within the HRAP was 1284 m^3.

Figure 2.1 – Peterborough HRAP (Photo: Rajina K C)

2.1.2.2 In situ wastewater measurements

The first campaign of in situ measurements and wastewater sampling of the HRAP was carried out between 28th and 30th November 2022.

In situ measurement and sampling was conducted at 26 cross sections (CS, Figure 2.2) distributed along the length of the channel from the paddlewheel. Each bend had one CS before and after it, and the remaining CS were approximately 55 m apart from each other.

A gantry (Figure 2.3) was designed to facilitate simultaneous measurements at three horizontal locations and three depths within the pond channel. By convention, the left and right banks were defined looking downstream in the direction of the flow. The gantry consisted of a horizontal bar spanning the channel width with three vertical graduated bars fixed at the centre, left and right sides of the channel. The left and right vertical bars were positioned 1350 mm from the central vertical bar. Consequently, the left and right bank measurements were recorded relative to the centre of the channel. Note that this method was adopted because the channel width varied between channel cross sections. The gantry, once centred in the channel, was low-

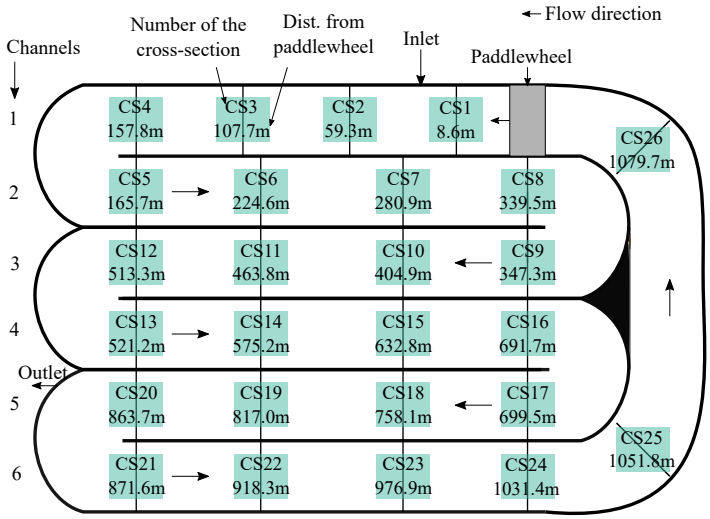

Figure 2.2 – Localisation of the cross sections in the pond and their distance from the paddlewheel

ered until the three vertical bars stood on the pond bottom. The nominal wastewater depth was 300 mm, but due to the earthen construction, the depth ranged from 250 to 400 mm. The operational depth at each cross section was recorded from the graduations on the vertical bars. Sensors were attached 30 mm from the bottom of the vertical bars, and the first measurements were recorded at each of the three channel widths. The gantry was then sequentially raised to record measurements at mid-pond depth (150 mm) and 50 mm below the surface of the pond. In this manner, nine measurements were recorded at each pond cross section. Simultaneously, wastewater samples (250 mL) were collected from the nine locations at each cross section using hoses attached 30 mm from the bottom of each vertical bar and a pump head attached to a cordless drill. The samples were transported on ice, subsequently stored in a coldroom (3°C) and analysed within 24 hours of collection.

A second gantry was constructed to enable the measurement of the fluid flow velocity at the nine locations and 26 cross sections, employing the methodology described earlier (Figure 2.4).

A multiparameter pH/DO/conductivity/temperature sensor was affixed to each vertical bar of the gantry. Specifically, a HANNA HI 98194 was attached on the centre bar and a YSI 556 MPS was attached to each of the left and right vertical bars. To ensure consistency, sensors

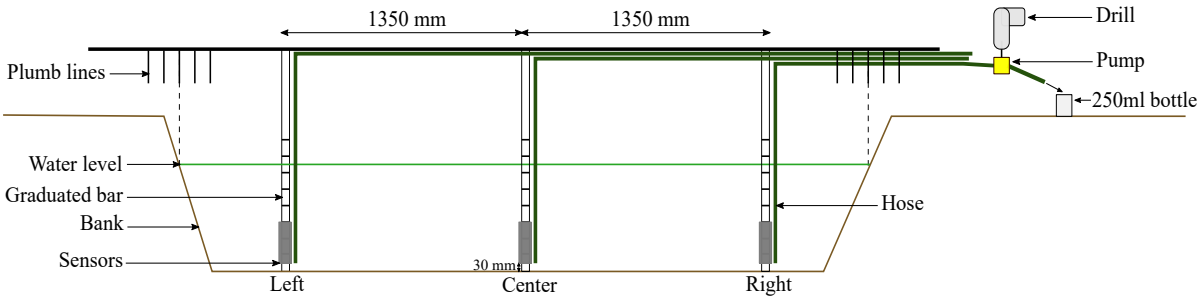

Figure 2.3 – Gantry equipped with multiparameter sensors and wastewater sampling hoses

were normalised with respect to each other, accounting for differences in calibration in standard solutions (pH) and in air (dissolved oxygen). Additionally, flowmeters (Marsh McBirney Model 2000 Flo-Mate) were fixed 30 mm from the bottom of the vertical bars on the second gantry.

Incident photosynthetically active radiation (PAR, 370-650 nm) was continuously measured using a MQ-200X quantum meter 2π from Apogee Instruments on November 29th.

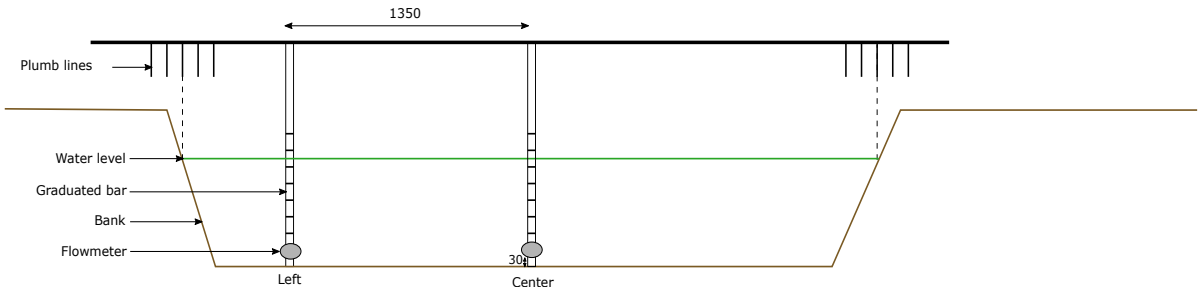

Figure 2.4 – Gantry equipped with flowmeters

2.1.2.3 PAR attenuation by wastewater in the HRAP

Photosynthetically active radiation (PAR, 370-650 nm) through pond depth was measured using an MQ-200X 2π quantum sensor (Apogee Instruments). The sensor, attached to a gradu-

ated bar, was submerged in the centre of the pond successively at depths 350, 250, 150, 100, 50 and 5 mm from the surface. The measurements were conducted near CS 3 to ensure paddlewheel mixing while minimizing wave action that could confound the measurements.

2.1.3 Analysis of wastewater composition

2.1.3.1 Suspended solids

Total suspended solids were determined using Test 2540 D described in Standard Methods for the Examination of Water and Wastewater (APHA 1981). V_S = 50 mL of wastewater were filtered through a pre-dried (105°C/24h) and weighed GFC filter (Whatman, 1.6 μm). The filter was then dried (105°C/24h), weighed again and the suspended solids concentration C_{SS} (mg.L^{-1}) were determined by difference (Eq. 2.1):

$$C_{SS} = \frac{m_f - m_{dry}}{V_S} \tag{2.1}$$

with m_f the weight of the dry filter (in g) and m_{dry} the weight of the filter + the dried biomass (in g).

2.1.3.2 Measurement of floc size

5 mL of wastewater samples were fixed with 2 drops of Lugol solution. Subsequently, 10 μL of the fixed sample were transferred to a Malassez cell and the longest dimension of each organic floc was measured microscopically at a magnification x400 using an Olympus BX43 microscope. This operation was repeated three times for each sample.

2.1.3.3 Determination of chlorophyll a

Chlorophyll a (μg.L^{-1}) was determined using Test 10200 (Chlorophyll trichromatic method) in Standard Methods for the Examination of Water and Wastewater (APHA 1981). Wastewater (25 mL) was filtered through a GFC filter, chlorophyll a was then extracted (4°C/24h) into 90% aqueous acetone. After centrifugation (5 min at 12,000 rpm), the absorbance of the supernatant

was measured at 664, 647 and 630 nm using a Shimadzu UV-1800 spectrophotometer against aqueous acetone blank. The chlorophyll a concentration was determined using a trichromatic equation (Equations 2.2 and 2.3):

$$Abs_{Chla} = 11.85Abs_{664} - 1.54Abs_{647} - 0.08Abs_{630} \tag{2.2}$$

$$Chl_a = \frac{Abs_{Chla} \cdot V_{acetone}}{V_{sample}} \tag{2.3}$$

2.1.3.4 Determination of N-NH_4^+, N-NO_3^-, N-NO_2^-, P-PO_4^{3-}, total carbon (TC), TOC and TIC concentrations

The concentration of N-NH_4^+, N-NO_3^-, N-NO_2^- and P-PO_4^{3-} was determined in filtered wastewater samples (0.45 μm) using Skalar SANplus Systems Nutrients analyser. Total carbon, total organic carbon and inorganic carbon concentrations were determined in GFC (Whatman) filtered wastewater using Shimadzu TOC-L carbon analyser.

2.1.3.5 Alkalinity measurement

OH^-, CO_3^{2-} and HCO_3^- concentrations were determined by titration following Standard Operating Procedure Lakes for pH and alkalinity (MassWWP 2001).

H_2SO_4 at a concentration C_{acid}=0.05 M was added progressively to a V_{sample}= 20 mL sample filtered at 1.6 μm until reaching a pH of 8.3. OH^- and CO_3^{2-} ions concentrations in mol.L^{-1} is deduced as below (Equation 2.4), $V_{acid_{pH8.3}}$ being the volume of acid added to reach pH 8.3. If the pH of the sample is lower than 8.3, there is no OH^- and CO_3^{2-} ions.

$$[OH^-] + [CO_3^{2-}] = \frac{C_{acid} \cdot V_{acid_{pH8.3}}}{V_{sample}} \tag{2.4}$$

Total alkalinity TA (OH^-, CO_3^{2-} and HCO_3^- concentrations) was obtained from the equation 2.5 below, where $V_{acid_{pH5}}$ is the volume of acid added to reach pH 5.

$$TA = \frac{C_{acid} \cdot V_{acid_{pH5}}}{V_{sample}} \tag{2.5}$$

Bicarbonates concentration was deduced according to Equation 2.6:

$$[HCO_3^-] = TA - ([OH^-] + [CO_3^{2-}]) \tag{2.6}$$

2.1.3.6 Biochemical Oxygen demand (BOD5)

Biological Oxygen Demand was determined by measuring oxygen consumption of samples over 5 days using WTW OxiTop OC100 system.

2.1.4 Statistics and data visualisation

Statistical analyses were conducted using SPSS software. Normal distribution of the data was verified using Kolmogorov normality test. For mean comparisons, Friedman test was used when normal distribution was not verified (non-parametric test) and T-test for related samples when normal distribution was verified (parametric test). Spearman test was used for correlations. Statistical significance was accepted when P $\leq$0.05. Figures were drawn using MATLAB2022b.

2.2 Torus photobioreactor: experiments at laboratory scale

2.2.1 Objective of the study

In the Chapter 3 investigating the heterogeneity of Peterborough HRAP, heterotrophic activity was attributed solely to bacteria. However, wastewater contains a wide range of organic molecules including compounds potentially consumable by microalgae, in photoheterotrophy or chemoheterotrophy. Moreover, specific interactions between microalgae and bacteria are still unclear and such a large scale study does not permit to investigate this issue. The purpose of the study at laboratory scale is then to cultivate microalgae and bacteria in controlled conditions in order to investigate in a first time the relative contributions of photoautotrophy and photoheterotrophy to mixotrophic growth of the microalgae *Scenedesmus obliquus* in synthetic

wastewater (Chapter 5), and in a second time the fate and role of carbon sources in microalgae-bacteria interactions in synthetic wastewater under simulated solar conditions (Chapter 6).

2.2.2 Torus PBR

A sterilisable and well-mixed photobioreactor was used to cultivate microorganisms in a controlled environment, so as to discriminate the contributions of microalgae and bacteria in a HRAP. The inox torus PBR presents the advantage of being steam-sterilisable and perfectly homogeneous due to its circular shape and the helix mixing the culture (Figure 2.5).

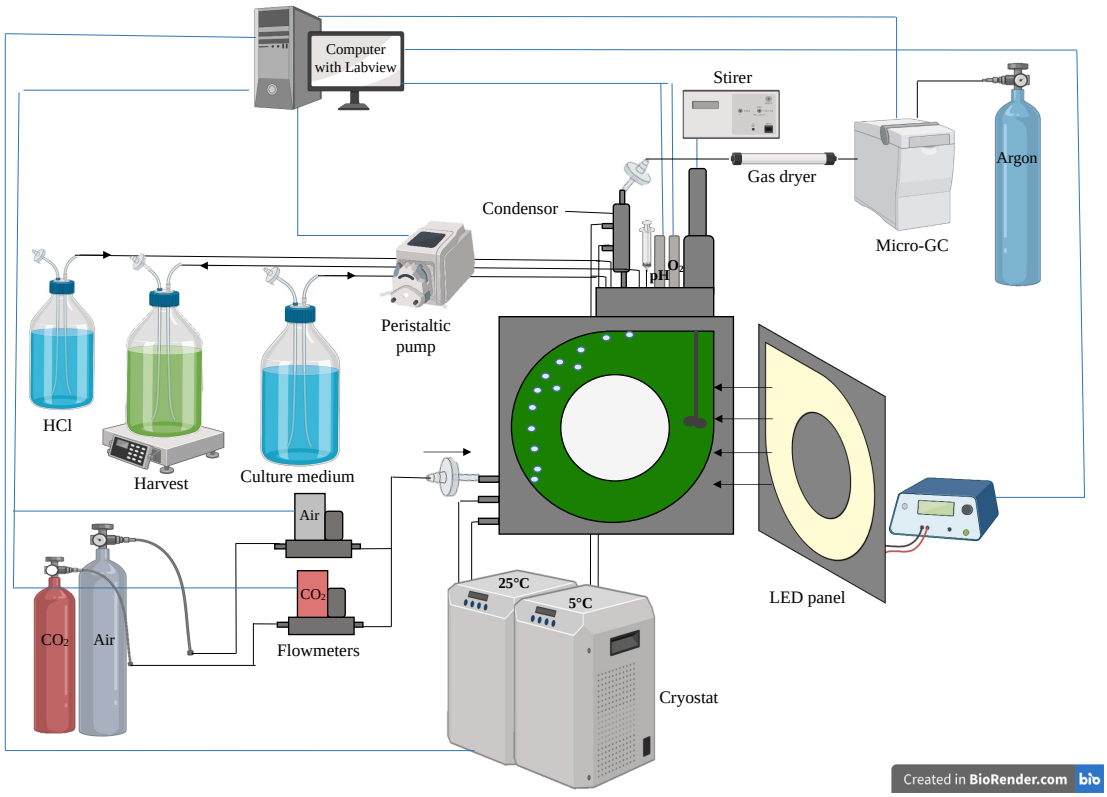

Figure 2.5 – Torus PBR equipment and instrumentation

Yet, the torus PBR is only 4 cm-depth with a working volume of 1.4 L. The culture depth is then much lower in the torus PBR than in a real-scale HRAP, consequently light availability is expected to be higher in the torus PBR than in a HRAP. However, considering that microalgae in a HRAP are limited by light, they should also be limited by light in the torus so the labora-

tory experiments are as representative as possible of the real system. Yet, due to self shading, light availability and algal biomass concentration are interdependent variables. In a shallower reactor, light availability is higher and biomass growth higher. As microalgae grow, turbidity increases and light availability decreases. A radiative model coupled to a kinetic model constitutes a useful tool to estimate light availability inside a microalgae culture by considering the interactions between incident irradiance, depth and algal biomass concentration. An existing radiative model coupled with a kinetic model (Pierre Albrand 2022, personal communication) was used to simulate algal growth and light attenuation in a 4 cm depth and in a 30 cm depth reactor. Figure 2.6 shows that, in a light-limited regime, the average light G_{mean} in a 4 cm depth reactor is equal to the average light in a 30 cm depth reactor due to the higher algal biomass concentration in the 4 cm depth reactor. In this case, light limitation occurring in the torus PBR is representative of light limitation in the HRAP.

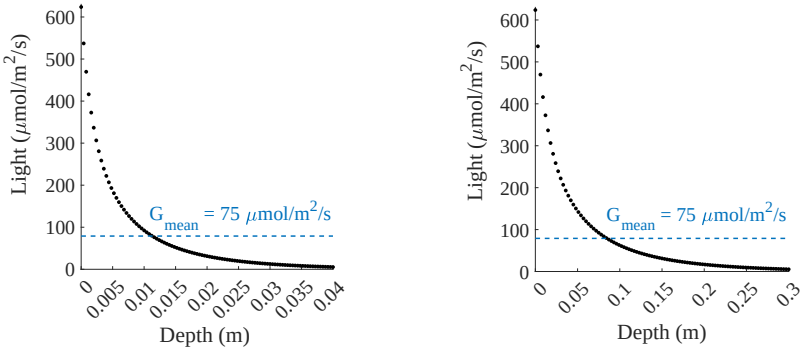

Figure 2.6 – Light attenuation profile in (a) 4 cm depth torus PBR (b) 30 cm depth HRAP

Microorganisms were then cultivated in inox 1.4 L torus photobioreactor illuminated by a LED panel. The culture medium, a synthetic wastewater described in Appendix A, was injected at a continuous flowrate with a peristaltic pump and the culture was simultaneously harvested at the same flowrate. An air flowmeter regulated the air or dinitrogen N_2 flowrate injected in the PBR. pH was regulated at 7.5 with a Proportional Integral Derived (PID) control, either by CO_2 (flowmeter) or chlorohydric acid HCl (peristaltic pump) injections. Temperature was regulated at 23°C with a thermostat. pH, temperature and flowrates were visualised and controlled through

a Labview interface (Figure 2.5). Before inoculation, the PBR, canulas and tubes were sterilized with steam for 2 hours. Culture medium, HCl, filters for air entry and exit, tubes, inoculum and harvesting bottles were sterilized for 20 min at 121°C. After inoculation, the microalgae culture was kept in batch for a few days in order to increase microalgae concentration. Then, the pump for feeding the PBR with fresh medium and harvesting the culture was actioned: the culture was operated in continuous.

The nutrient (N, P and S) concentration in classical anaerobically pretreated wastewater had sometimes to be adjusted in order to compensate for the higher algal growth rate in the torus PBR compared to the HRAP and avoid nutrient limitation in the torus PBR. In light-limited regime (nutrients supplied in excess) presented in Figure 2.6, the average light in the 4 cm depth reactor is the same as in the 30 cm depth. However, when classical anaerobically pretreated wastewater concentrations in C, N, P and S are supplied to 4 and 30 cm depth cultures, higher growth rate in the 4 cm depth reactor implies faster nutrients consumption. The 4 cm depth culture is limited by nutrients while the 30 cm depth one is limited by light (Figure 2.7). In order to obtain similar limitation conditions in the real-scale HRAP and in the torus PBR, the nutrient concentration in the synthetic wastewater was increased in some cases to avoid any mineral limitation.

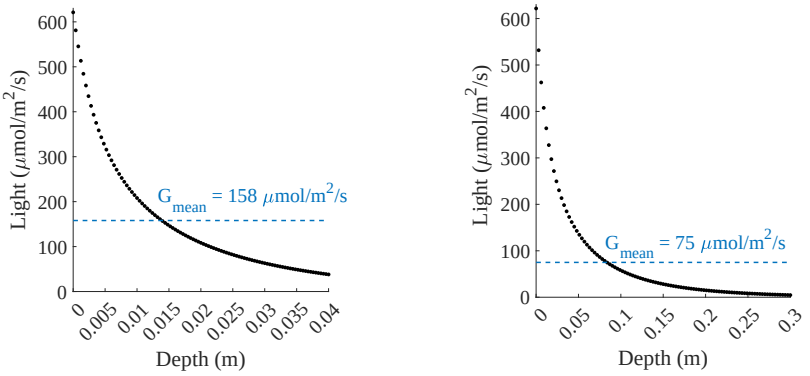

Figure 2.7 – Light attenuation profile in microalgae culture with nutrient supply equal to anaerobically pretreated wastewater composition in: (a) 4 cm depth torus PBR (b) 30 cm depth HRAP

2.2.3 Simulation of day-night cycles

The incident PFD q_0 in μmol.m^{-2}.s^{-1} as a function of time t (in number of seconds since midnight), follows a sinusoidal function as follows:

- When $t < t_{SR}$ or $t > t_{SS}$, with t_{SR} the time of sunrise and t_{SS} the time of sunset:

$$q_0 = 0 \tag{2.7}$$

- When $t_{SR} < t < t_{SS}$:

$$q_0 = q_{0_{max}} \cdot sin(\pi \cdot \frac{t - t_{SR}}{t_{SS} - t_{SR}}) \tag{2.8}$$

with $q_{0_{max}}$ the PFD intensity at the zenith in μmol.m^{-2}.s^{-1}. This value was set at 700, typical of an average spring day in Nantes (France).

2.2.4 Inoculum

2.2.4.1 *Scenedesmus obliquus*

As a means to simplify microalgae-bacteria consortium system, a single strain of microalgae was chosen for studying microalgae-bacteria interactions. Capable of adapting to various environmental conditions due to their phenotypic plasticity (Lürling 2003), the specie *Scenedesmus obliquus* is widely found in HRAPs (Fallowfield and Garrett 1985, Ruas et al. 2020, Plouviez et al. 2019) and easy to grow. For these reasons, *Scenedesmus obliquus* was selected as a microalgae model. The strain used in the experiments was isolated from a natural consortium and genetically identified in 2018. It was kept in nitrate Bold Basal Medium (BBM) (Appendix A) in sterile 250 ml erlenmeyer flasks stirred with magnet bar.

2.2.4.2 *Escherichia coli*

Similarly, a single heterotrophic bacteria strain was chosen. *Escherichia coli* is frequently found in wastewater and is a well-known and easy to grow microorganism. *E. coli* strains ATCC

700728 was purchased in the form of swabs from Humeau laboratory and kept at 4°C. Approximately one week before cultivation, bacteria was spread on Tryptone Soy Agar (TSA) plates and incubated for a few days at 30°C. At D-2, colonies were sampled from agar plate to inoculate Lysogeny Broth (LB) liquid medium in 100 ml erlenmeyer flask, then incubated at 30°C. After 24h, 10 ml were taken from LB broth *E. coli* culture to inoculate a 250 ml erlenmeyer flask containing M9 minimal medium (Appendix A) added with acetate or glucose depending on the carbon source used in the experiment. The flask was then incubated at 30°C 24h before inoculating the reactor.

2.2.5 Culture monitoring

2.2.5.1 Online measurements

pH and temperature in the liquid phase were measured using a Mettler Toledo InPro 3203i-120 pH sensor, while dissolved oxygen was monitored with Mettler Toledo InPro 6860i O_2 sensor.

Molar fractions of N_2, O_2 and CO_2 at the exit of the PBR in the gas phase were determined using an Agilent micro gas chromatography 490 (Figure 2.8). The gas exit was cooled at 5 °C using a condenser, and drierite columns were installed before the micro-GC to prevent moisture from affecting the micro-GC columns. The carrier gas used was Argon 2 from Alphagaz.

The micro gas chromatograph consists of a pump that draws in the sample, which is then carried through the micro-GC columns by the carrier gas. N_2, O_2 and H_2 gases are separated based on their retention time on the column A, while CO_2, being heavier, is separated on the column B. Each gas measured corresponds to a peak with a specific retention time and an area proportional to its concentration. A backflush time is determined to protect column A from heavy compounds that could damage it. The backflush time must be sufficiently long to prevent loss of information on the target gas, but if it is too long, there is a higher risk of letting heavy compounds reaching the column A.

The software Soprane calculates the molar fractions ys_{N_2}, ys_{O_2} and ys_{CO_2} from the peak areas using a calibration curve derived from four standard gas bottles. These calculated fractions are then synchronised with simultaneous Labview records (including sensors in the liquid phase and

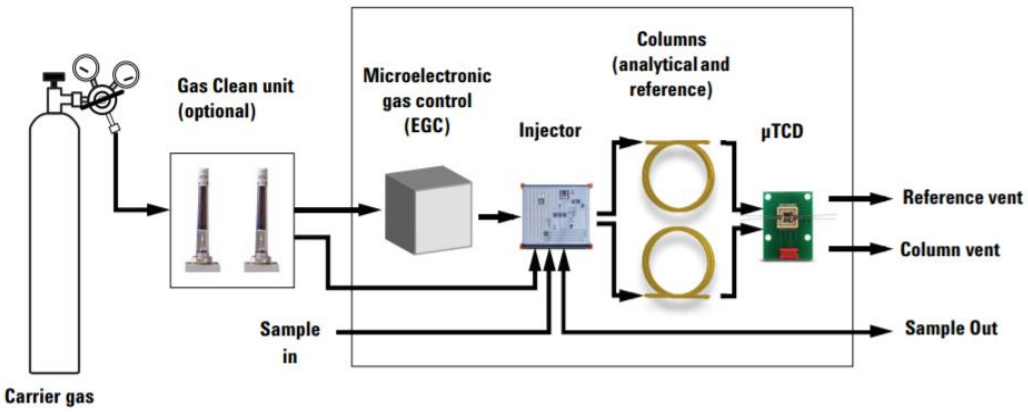

Figure 2.8 – Functioning of micro gas chromatograph 490 (Bonnanfant 2020)

flowmeters for gas entry) using a MATLAB routine. The signal of the CO_2 flowrate can exhibit significant noise due to pH variations and is therefore filtered using the MATLAB filter function.

The net volumetric production of O_2 and CO_2 in the culture is subsequently calculated using the molar gas fractions exiting the PBR, the concentrations of dissolved gases in the liquid phase, the incoming gas flowrate, pH, and temperature, as detailed below. Tables 2.1 summarizes the constant values used in these equations.

Constant	Value	Units
R (perfect gases constant)	8.3144	$m^3.Pa.K^{-1}.mol^{-1}$
P (atmospheric pressure)	101300	Pa
V_R (reactor volume)	$1.4 \cdot 10^{-3}$	m^3

Table 2.1 – Values and units for constants used for the calculation of net volumetric production of O_2 and CO_2

The sum Qe_{tot} of Qe_{airN_2} and Qe_{CO_2}, the volumetric flowrates of air or N_2 and CO_2 entering the PBR respectively, were then converted into the incoming molar flowrate G_{in} ($mol.h^{-1}$). This conversion uses the ideal gas law, where R is the universal gas constant, P is the pressure in the

PBR, and T is the temperature in the PBR:

$$G_{in} = \frac{Qe_{tot} \cdot 10^{-6} \cdot 60}{V_{mol}}$$
$$V_{mol} = \frac{R \cdot T}{P} \tag{2.9}$$

In the case of cultures sparged with air without injections of CO_2, the molar fractions of CO_2, N_2 and O_2 entering the PBR, respectively ye_{CO_2}, ye_{N_2} and ye_{O_2} were determined by analyzing the injected air composition with the micro-GC. In the case of cultures sparged with a mixture of N_2 and CO_2, ye_{CO_2}, ye_{N_2}, and ye_{O_2} are calculated as follows:

$$ye_{CO_2} = \frac{Qe_{CO_2}}{Qe_{N_2} + Qe_{CO_2}}$$
$$ye_{N_2} = 1 - ye_{CO_2} \tag{2.10}$$
$$ye_{O_2} = 0$$

The molar flowrate outgoing the PBR G_{out} is then deduced as shown below, with ys_{N_2} measured by the micro-GC:

$$G_{out} = \frac{G_{in} \cdot ye_{N_2}}{ys_{N_2}} \tag{2.11}$$

The transfer rates N_{O_2} and N_{CO_2} ($mol.h^{-1}$) can then be calculated from the difference between the molar flowrates of O_2 or CO_2 entering and exiting the PBR, with ys_{O_2} and ys_{CO_2} measured by the micro-GC:

$$N_{O_2} = G_{in} \cdot ye_{O_2} - G_{out} \cdot ys_{O_2}$$
$$N_{CO_2} = G_{in} \cdot ye_{CO_2} - G_{out} \cdot ys_{CO_2} \tag{2.12}$$

If the molar O_2 or CO_2 flowrate exiting the PBR is higher than the incoming flowrate, the gas is produced and N is negative. If it is lower, the gas is globally consumed and N is positive. The transfer terms of the volumetric production rates of O_2 and CO_2, respectively $r_{O2_{tr}}$ and $r_{CO2_{tr}}$, were then calculated as the opposite of N over the volume of the PBR V_R:

$$r_{O_{2_{tr}}} = -\frac{N_{O_2}}{V_R}$$
$$r_{CO_{2_{tr}}} = -\frac{N_{CO_2}}{V_R} \tag{2.13}$$

The accumulation terms for O_2 and CO_2 in the liquid phase were also considered for calculating the volumetric O_2 and CO_2 production rates. The signal of dissolved oxygen concentration in the PBR was derived over time to determine the oxygen accumulation term $r_{O_{2_{acc}}}$:

$$r_{O_{2_{acc}}} = \frac{dC_{O_2}}{dt} \tag{2.14}$$

As TIC was measured offline, inorganic carbon data was first interpolated to determine $r_{CO_{2_{acc}}}$. Moreover, the inorganic carbon analysis (method detailed in the offline analysis paragraph) provides the total inorganic carbon concentration; however, the dissolved CO_2 concentration is needed for the calculation of volumetric CO_2 production rate. Dissolved CO_2 in the PBR, C_{CO_2}, was deduced from TIC in the PBR, C_{TIC}, pH, and temperature T as follows:

$$\begin{aligned}
[H^+] &= 10^{-pH} \\
K_1 &= e^{\frac{-1.209 \cdot 10^4}{T} - 3.678 \cdot 10 \cdot log(T) + 2.355 \cdot 100} \\
K_2 &= e^{\frac{-1.243 \cdot 10^4}{T} - 3.548 \cdot 10 \cdot log(T) + 2.2 \cdot 100} \\
K &= 1 + \frac{K_1}{[H^+]} + \frac{K_1 \cdot K_2}{[H^+]^2} \\
C_{CO_2} &= \frac{C_{TIC}}{K}
\end{aligned} \tag{2.15}$$

Interpolated C_{CO_2} was then derived over time to determine the CO_2 accumulation term $r_{CO_{2_{acc}}}$:

$$r_{CO_{2_{acc}}} = \frac{dC_{CO_2}}{dt} \tag{2.16}$$

In the same way, dissolved CO_2 in the culture medium Ce_{CO_2} was given by the formula below, where Ce_{TIC} is the concentration of total inorganic carbon in the culture medium:

$$Ce_{CO_2} = \frac{Ce_{TIC}}{K} \tag{2.17}$$

The dilution terms $r_{O_{2_{dil}}}$ and $r_{CO_{2_{dil}}}$ account for the O_2 and CO_2 supplied by the culture medium in the final production rates:

$$\begin{aligned} r_{O_{2_{dil}}} &= -D \cdot (Ce_{O_2} - C_{O_2}) \\ r_{CO_{2_{dil}}} &= -D \cdot (Ce_{CO_2} - C_{CO_2}) \end{aligned} \tag{2.18}$$

Finally, the transfer, accumulation, and dilution terms are compiled to calculate the total volumetric molar rate of O_2 and CO_2, respectively r_{O_2} and r_{CO_2}, in mol.m^{-3}.h^{-1}:

$$\begin{aligned} r_{O_2} &= r_{O_{2_{tr}}} + r_{O_{2_{acc}}} + r_{O_{2_{dil}}} \\ r_{CO_2} &= r_{CO_{2_{tr}}} + r_{CO_{2_{acc}}} + r_{CO_{2_{dil}}} \end{aligned} \tag{2.19}$$

2.2.5.2 Offline measurements

2.2.5.2.1 Microalgal productivity

2.2.5.2.1.1 Dry weight

A known volume of culture V_S around 6 mL is determined with a precision scale considering that the density of the culture is similar to the density of water. The sample is filtered through a microfiber glass filter 0.7 μm porosity previously weighed (m_f in g) then dried at 105°C for 24h and weight after drying (m_{dry} in g). The total biomass concentration in the PBR C_X in g.L^{-1} is calculated as follows:

$$C_X = \frac{m_{dry} - m_f}{V_S} \tag{2.20}$$

The volumetric productivity P_X in gC_X.L^{-1}.d^{-1}, so the quantity of biomass produced per unit of time and culture volume, is given by the equation 2.21 where C_X is the biomass concentration in the culture and D the dilution rate in days^{-1}:

$$P_X = C_X \cdot D \tag{2.21}$$

Areal productivity S_X (in $gC_X.m^{-2}.d^{-1}$) represents the quantity of biomass produced per unit of time and illuminated surface and is given by the Equation 2.22:

$$S_X = \frac{P_X \cdot 1000}{a_{light}} \tag{2.22}$$

where a_{light} (in m^{-1}) is the inverse of the culture depth e (in m):

$$a_{light} = \frac{1}{e} \tag{2.23}$$

2.2.5.2.1.2 Turbidity

Algal growth can also be measured by turbidity. Approximately 1.5 mL sample was transferred into a plastic spectrophotometer cuvettes and the absorbance at 750 nm was measured with spectrophotometer JASCO V-630. This method provides an instantaneous order of magnitude of algal concentration in the PBR and is used in complementarity with dry weight measurement.

2.2.5.2.2 Pigments

Pigments contained in microalgal cells (chlorophyll *a*, chlorophyll *b* and carotenoids) were extracted from the biomass with methanol. In a first time, a volume V_1 between 0.2 and 2 mL of microalgae culture (the higher the algal biomass, the lower the sample volume) was taken from the culture sample and put in Ependorf tubes. Those tubes were then centrifugated in MiniSpin centrifuge at 13400g for 10 min in order to separate the biomass from the culture medium. The supernatant was removed with caution and a volume $V_2 = 1.5$ mL of methanol was added to the biomass recovered in the pellet. The tubes were then transferred into an ultrasonic bath for 1 min for homogenisation, then incubated at 45°C for 1 hour. Then, tubes were centrifuged again at 13400g for 10 min in order to separate the biomass from the pigments extracted and dissolved in the methanol phase. The biomass remaining at the bottom of the tube after centrifugation

should be white: if it still contains green pigmentation, pigment extraction was incomplete. Finally, absorbance at 750, 665, 652 and 480 nm were measured on the supernatant previously recovered with caution from the centrifuged tube using spectrophotometer JASCO V-630.

Pigments concentration in μg/ml were deduced as below:

$$C_{chla} = \frac{V_2}{V_1}(-8.0962 \cdot A_{652} + 16.5169 \cdot A_{665}) \tag{2.24}$$

$$C_{chlb} = \frac{V_2}{V_1}(27.4405 \cdot A_{652} + 12.1688 \cdot A_{665}) \tag{2.25}$$

$$C_{carotenoids} = \frac{V_2}{V_1}(4 \cdot A_{480}) \tag{2.26}$$

Then, pigment content x_{pig} in the biomass was given by the following equation:

$$x_{pig} = \frac{C_{pig}}{C_{X_{alg}} \cdot 1000} \tag{2.27}$$

2.2.5.2.3 Radiative properties

A kinetic model coupled with a radiative model allows accurate prediction of light availability and algal biomass productivity in a PBR. A radiative model is a precise tool to determinate the amount of light absorbed over the reactor depth, considering depth, algal biomass, pigment content and specific microalgae characteristics called radiative properties. Yet, radiative properties of *Scenedesmus obliquus* were not reported in the literature. Due to the non-spherical shape of *Scenedesmus obliquus*, absorption and scattering cross-sections cannot be determined by theoretical formulas and require experimental measurements.

A simple method described by Kandilian et al. (2016) for measuring spectral microalgae absorption cross-section was used to determine the absorption cross section. Note that absorption is the dominant phenomena and that scattering and phase function are considered negligible. This method relies on normal-hemispherical transmittance and reflectance measurements for wavelengths between 350 and 800 nm on microalgae samples of different concentrations. As

explained in the diagram below (Figure 2.9), the fraction of incident light beam reflected by the sample is deduced from the amount of photons detected in the integration sphere located between the sample and the incident beam using a Agilent Cary 5000 spectrophotometer UV-Vis-NIR. Similarly, the fraction of incident light beam transmitted by the sample is deduced from the amount of photons detected in the integration sphere located behind the sample after the light source.

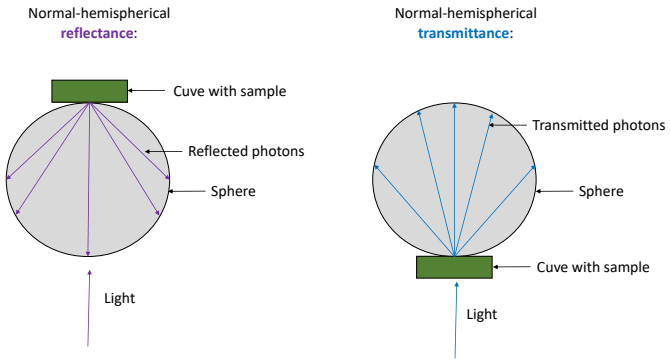

Figure 2.9 – Principle of radiative properties measurement

Absorbance cross sections Ea (in $m^{-2}.kg^{-1}$) for each wavelength were deduced from the fractions of photons reflected and transmitted for each wavelength and from the biomass concentration in the sample using an Excel algorithm based on inverse method. Knowing biomass concentration, the algorithm calculates the predicted transmittance and reflectance fractions. Then, the absorbance cross sections were estimated by minimising the error between measured and predicted transmittance and reflectance fractions.

In parallel, pigments concentration was measured in the culture on the same day. A data base for modeling radiative transfer in the culture was constituted with each absorbance cross section values Ea corresponding to a pigment content value.

2.2.5.2.4 Fluorescence

Photosynthetic microalgae efficiency, represented by the ratio F_v/F_m, was measured with a PAM fluorimeter. Before the measurement, the sample was diluted and kept in the dark for 15

min.

2.2.5.2.5 Bacterial productivity

Due to the very small size of bacteria and to low bacterial biomass, the dry weight method can raise a problem of sensitivity for estimating bacterial biomass in a culture. Moreover, in microalgae-bacteria cocultures, separating microalgae and bacteria by filtration in order to weigh separately the algae and the bacteria is unefficient due to the formation of microalgae-bacteria flocs. For this reason, dry weight, turbidity at 600 nm and Colonies Forming Units (CFU) were measured on a concentrated bacteria batch culture in order to establish correlations between those quantities. Using such correlations might permit the prediction of bacterial dry weight using more sensitive methods such as turbidity and CFU.

2.2.5.2.5.1 In bacteria culture

In the case of pure cultures of bacteria, bacterial growth was measured directly by turbidity at 600 nm (Figure 2.10).

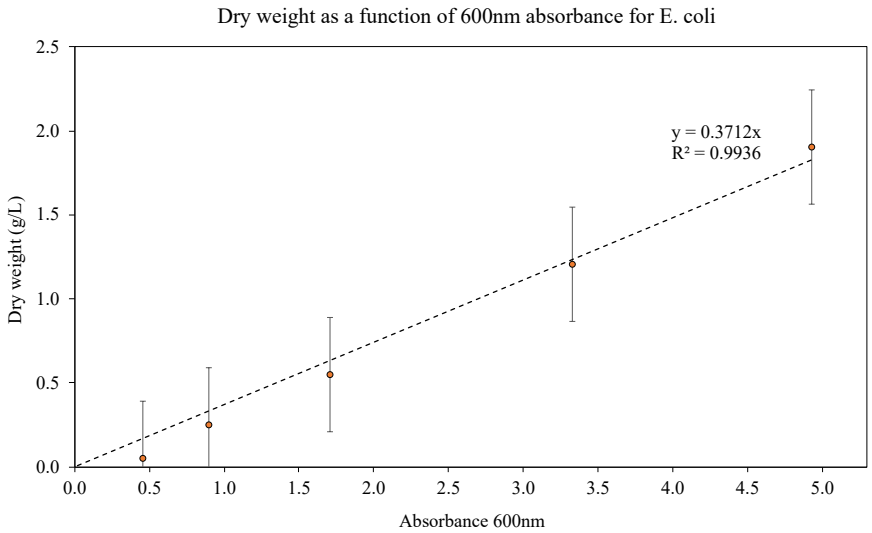

Figure 2.10 – Correlation curve between turbidity and dry weight for *E. coli*

Then, the equation of the correlation curve below allows to deduce bacterial biomass concentration $C_{X_{bact}}$ in g.L^{-1} from the turbidity measurement Abs600:

$$C_{X_{bact}} = 0.3712 \cdot Abs600 \tag{2.28}$$

2.2.5.2.5.2 In microalgae-bacteria co-culture

In microalgae-bacteria cocultures, determining bacterial growth by turbidity is not possible because microalgae contribute significantly to the absorbance. Separating bacteria from microalgae is possible by inoculating the mixture of microalgae and bacteria on a non-selective medium such as TSA plate kept in the dark, where bacteria will grow but not microalgae. The sample is diluted 10^4 to 10^8 times depending on bacterial concentration in the culture in order to observe between 15 and 300 individual colonies on the plate after incubation (Figure 2.11).

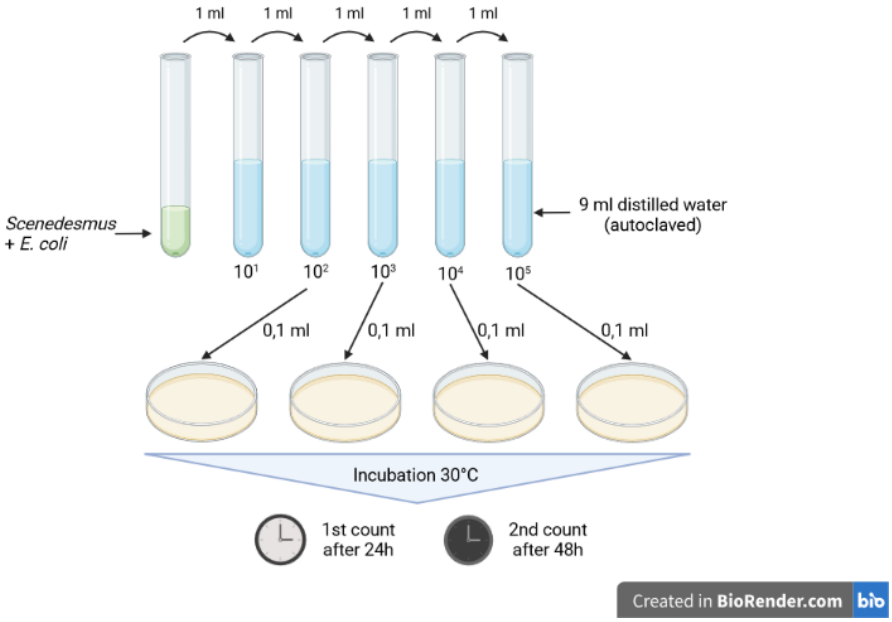

Figure 2.11 – Method for *E. coli* CFU determination

Serial dilutions of a 1 mL sample from the coculture were completed using sterile 9 mL NaCl solution tubes. 0.1 mL of the diluted sample was then transferred on a TSA agar plate and spread with a cell spreader. At least two different dilutions each in triplicates were inoculated. The plates were then incubated at 30°C for at least 2 days. A first count was done after 24 hours and a second one after 48 hours. Each time, every new colony was counted. The bacterial

concentration in the PBR is given by the formula below, where n is the number of colonies on the plate, DF the dilution factor and V the volume in mL inoculated on the plate:

$$CFU = \frac{n \cdot DF}{V} \tag{2.29}$$

Then, the equation of the correlation curve on Figure 2.12 previously established on an *E. coli* batch culture allows to deduce the bacterial concentration in g.L^{-1} :

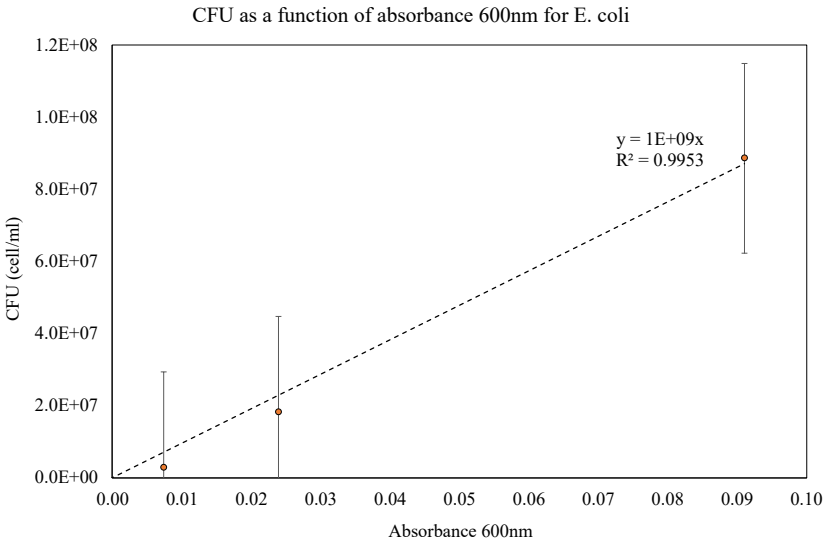

Figure 2.12 – Correlation curve between turbidity and CFU for *E. coli*

$$C_{X_{bact}} = \frac{0.3712 \cdot CFU}{10^9} \tag{2.30}$$

The total biomass C_X concentration (*S. obliquus* + *E. coli*) is determined from the total dry weight value described before. Microalgal biomass concentration in g.L^{-1} is deduced as below:

$$C_{X_{alg}} = C_X - C_{X_{bact}} \tag{2.31}$$

2.2.5.2.6 Organic and inorganic carbon

Organic and inorganic carbon concentrations (in $mgC.L^{-1}$) were measured using a Shimadzu TOC-L analyser. Previously, the sample was diluted at least 10 times and filtered with a 0.2 μm syringe filter.

2.2.5.2.7 Ionic elements

Anions (Cl^-, NO_2^-, NO_3^-, PO_4^2-, SO_4^2-) and cations (Na^+, NH_4^+, K^+, Mg^{2+}, Ca^{2+}) concentrations in $mg.L^{-1}$ were measured by ionic chromatography with a Dionex ICS-1100. Previously, the sample was diluted at least 10 times and filtered with a 0.2 μm syringe filter.

2.2.5.3 Stoichiometric analysis and data reconciliation

One of the aims of this laboratory- scale study was to quantify the carbon and oxygen fluxes in microalgae cultures and in microalgae-bacteria cocultures. The determination of fluxes relies on mass balance and stoichiometric analysis coupled with a method of data reconciliation. Due to the inherent uncertainties in each measurement, achieving a close mass balance is challenging. Data reconciliation aims to enhance the coherence of the mass balance by assigning greater weight to the more precise measurements and less weight to less precise ones in order to reach a coherence of the mass balance. This method uses the redundancy of information, such as biomass productivity, acetate consumption rate, and net CO_2 production rate, which can provide overlapping insights.

The vector $\boldsymbol{r_m}$ of the measured net rates of acetate, CO_2, NH_3, algal biomass ($x1$), bacterial biomass ($x2$), and O_2 is written as follows:

$$\boldsymbol{r_m} = \begin{bmatrix} r_{HAc} \\ r_{CO_2} \\ r_{NH_3} \\ r_{x1} \\ r_{x2} \\ r_{O_2} \end{bmatrix} \tag{2.32}$$

The vector $\boldsymbol{F}$ represents the estimated standard deviations for each rate r of the vector $\boldsymbol{r_m}$:

$$\boldsymbol{F} = \begin{bmatrix} SD_{HAc} \\ SD_{CO_2} \\ SD_{NH_3} \\ SD_{x1} \\ SD_{x2} \\ SD_{O_2} \end{bmatrix} \tag{2.33}$$

Algal photoautotrophic growth, algal photoheterotrophic growth, and bacterial chemoheterotrophic growth are the three reactions expected to occur during the light phase. During the night, algal and bacterial chemoheterotrophic growth are the two reactions considered. The stoichiometric equations for these reactions were deduced as follows from the elemental composition of *S. obliquus* determined by Garcia-Moscoso et al. (2015):

$$\begin{aligned} \mathrm{CO_2} + 0.16\,\mathrm{NH_3} + 0.6985\,\mathrm{H_2O} &\rightarrow \mathrm{CH_{1.877}N_{0.16}O_{0.478}} + 1.11\,\mathrm{O_2} \\ 0.5\,\mathrm{C_2H_4O_2} + 0.16\,\mathrm{NH_3} &\rightarrow \mathrm{CH_{1.877}N_{0.16}O_{0.478}} + 0.1103\,\mathrm{O_2} + 0.3015\,\mathrm{H_2O} \\ \mathrm{C_2H_4O_2} + 0.16\,\mathrm{NH_3} + 0.8895\,\mathrm{O_2} &\rightarrow \mathrm{CH_{1.877}N_{0.16}O_{0.478}} + 1.3\,\mathrm{H_2O} + \mathrm{CO_2} \end{aligned} \tag{2.34}$$

The stoichiometric equation for bacterial chemoheterotrophic growth was deduced from the elemental composition of *E. coli* determined by Folsom and Carlson (2015) and from the *E. coli* yield coefficient for acetate, determined by Guardia and Calvo (2001):

$$0.625\,\mathrm{C_2H_4O_2} + 0.368\,\mathrm{NH_3} + 0.324\,\mathrm{O_2} \rightarrow \mathrm{CH_{1.74}N_{0.23}O_{0.43}} + 1.16\,\mathrm{H_2O} + 0.4\,\mathrm{CO_2} \tag{2.35}$$

According to the mass conservation principle, in a microalgae-bacteria coculture fed with acetate, the carbon balance is defined by the following equation, where each rate r is weighted by the number of carbon atoms in acetate, CO_2, algal biomass $x1$, and bacterial biomass $x2$:

$$2r_{HAc} + r_{CO_2} + r_{x1} + r_{x2} = 0 \tag{2.36}$$

In the same way, the nitrogen balance is defined by the following equation:

$$r_{NH_3} + 0.16r_{x1} + 0.23r_{x2} = 0 \tag{2.37}$$

Balances on oxygen and hydrogen require the rate of water production r_w, which is challenging to measure experimentally. An redox balance resolves this issue. Mass balance on each element C, H, O, and N are expressed by multiplying each side of the equation by the oxidation number of each element and then summing them to formulate the redox balance.

C	$2r_{HAc} + r_{CO_2} + r_{x1} + r_{x2} = 0$	$\times 4$
H	$4r_{HAc} + 3r_{NH_3} + 1.877r_{x1} + 1.74r_{x2} + 2r_w = 0$	$\times 1$
O	$2r_{HAc} + 2r_{CO_2} + 0.478r_{x1} + 0.43r_{x2} + 2r_{O_2} + r_w = 0$	$\times$(-2)
N	$r_{NH_3} + 0.16r_{x1} + 0.23r_{x2} = 0$	$\times$(-3)

These four mass balance equations can be combined as follows:

$$r_{HAc}(8+4-4) + r_{CO_2}(4-4) + r_{NH_3}(3-3) + r_{x1}(4+1.877-2\times 0.478-3\times 0.16) + r_{x2}(4+1.74-2\times 0.43-3\times 0.23) + r_{O_2}(-4) + r_w(2-2) = 0 \tag{2.38}$$

The redox balance is then defined as follows:

$$8\,r_{HAc} + 4.44\,r_{x1} + 4.19\,r_{x2} - 4\,r_{O_2} = 0 \tag{2.39}$$

The stoichiometric coefficents of carbon, nitrogen, and redox balances are combined in the consistency matrix $\boldsymbol{C}$ as follows. The three rows correspond to C, N, and electron balances, while the six columns stand for acetate, CO_2, NH_3, algal biomass, bacterial biomass, and O_2:

$$\boldsymbol{C} = \begin{bmatrix} 2 & 1 & 0 & 1 & 1 & 0 \\ 0 & 0 & 1 & 0.16 & 0.23 & 0 \\ 8 & 0 & 0 & 4.44 & 4.19 & -4 \end{bmatrix} \tag{2.40}$$

The vector of measurement errors $\hat{\boldsymbol{\Delta}}$ is estimated as follows:

$$\begin{aligned} \hat{\boldsymbol{\Delta}} &= \boldsymbol{F} \cdot \boldsymbol{C}' \cdot \boldsymbol{P^{-1}} \cdot \boldsymbol{C} \cdot \boldsymbol{r_m} \\ \boldsymbol{P} &= \boldsymbol{C} \cdot \boldsymbol{F} \cdot \boldsymbol{C}' \end{aligned} \tag{2.41}$$

Next, the measured rates r_m are corrected using $\hat{\boldsymbol{\Delta}}$ to estimate the rates $\hat{\boldsymbol{r_m}}$:

$$\hat{\boldsymbol{r_m}} = \boldsymbol{r_m} - \hat{\boldsymbol{\Delta}} \tag{2.42}$$

The variance-covariance matrix for the estimated rates $\hat{\boldsymbol{F}}$ is deduced:

$$\hat{\boldsymbol{F}} = \boldsymbol{F} - \boldsymbol{F} \cdot \boldsymbol{C}' \cdot \boldsymbol{P^{-1}} \cdot \boldsymbol{C} \cdot \boldsymbol{F} \tag{2.43}$$

The vector of the absolute errors for $\hat{\boldsymbol{r_m}}$, $\boldsymbol{\Delta}\hat{\boldsymbol{r_m}}$, is then deduced:

$$\boldsymbol{\Delta}\hat{\boldsymbol{r_m}} = \sqrt{diag(\hat{\boldsymbol{F}})} \tag{2.44}$$

The weighting matrix $\boldsymbol{W}$ is calculated by taking the reciprocical of the variance as the weight:

$$\boldsymbol{W} = diag(diag(\frac{1}{\hat{\boldsymbol{F}}})) \tag{2.45}$$

The reactions equations for algal and bacterial growth allow the establishment a stoichiometric matrix $\boldsymbol{\nu}$, defined by its number of rows m and columns n. Each column corresponds to a reaction during the light phase (photoautotrophy by microalgae, photoheterotrophy by microalgae, and chemoheterotrophy by bacteria, denoted as $\boldsymbol{\nu_{light}}$) and during the night phase (chemoheterotrophy by microalgae and bacteria, denoted as $\boldsymbol{\nu_{dark}}$), while the six rows corre-

spond to acetate, CO_2, NH_3, algal biomass, bacterial biomass, and O_2. Here, the *E. coli* yield coefficient for acetate was determined from Guardia and Calvo (2001) ($Y_{SX} = 1.6$ mol $C_{X_{bact}}$/mol acetate).

$$\boldsymbol{\nu_{light}} = \begin{bmatrix} 0 & -0.5 & -1 \\ -1 & 0 & 0.4 \\ -0.16 & -0.16 & -0.368 \\ 1 & 1 & 0 \\ 0 & 0 & 1.6 \\ 1.11 & 0.1103 & -0.324 \end{bmatrix} \tag{2.46}$$

$$\boldsymbol{\nu_{dark}} = \begin{bmatrix} -1 & -1 \\ 1 & 0.4 \\ -0.16 & -0.368 \\ 1 & 0 \\ 0 & 1.6 \\ -0.8898 & -0.324 \end{bmatrix} \tag{2.47}$$

The vector of the reaction rates $\boldsymbol{J}$ is finaly deduced as follows:

$$\begin{aligned} \boldsymbol{J} &= \boldsymbol{V} \cdot \boldsymbol{\nu'} \cdot \boldsymbol{W} \cdot \hat{\boldsymbol{r_m}} \\ \boldsymbol{V} &= (\boldsymbol{\nu'} \cdot \boldsymbol{W} \cdot \boldsymbol{\nu})^{-1} \end{aligned} \tag{2.48}$$

$\boldsymbol{J}$ is the vector of the reaction rates $\boldsymbol{J_1}$, $\boldsymbol{J_2}$ and $\boldsymbol{J_3}$, respectively the reactions rates for photoautotrophic microalgal growth, photoheterotrophic microalgal growth and chemoheterotrophic bacterial growth for the daytime. For the nighttime, the vector $\boldsymbol{J}$ contains only two values: the reaction rate for chemoheterotrophic growth of microalgae and bacteria. Then, the rates of acetate, CO_2, O_2, NH_3, algal biomass and bacterial biomass attributed to each reaction can be deduced from the stoichiometric equations of each reaction.

The absolute error on the reaction rate $\boldsymbol{J}$, $\boldsymbol{\Delta J}$, is deduced from the covariance matrix for J $\boldsymbol{Covar_J}$ calculated from the quadratic deviation criterion $\boldsymbol{\phi}$:

$$\begin{aligned} \boldsymbol{\Delta J} &= \sqrt{\boldsymbol{Covar_J}} \\ \boldsymbol{Covar_J} &= diag(\frac{\boldsymbol{\phi}}{(m-n)\cdot \boldsymbol{V}}) \\ \boldsymbol{\phi} &= (\hat{\boldsymbol{r_m}} - \boldsymbol{\nu}\cdot\boldsymbol{J})' \cdot \boldsymbol{W}(\hat{\boldsymbol{r_m}} - \boldsymbol{\nu}\cdot\boldsymbol{J}) \end{aligned} \tag{2.49}$$

2.3 Modeling microalgae-bacteria interactions in the torus PBR

2.3.1 Principle

In parallel to the experiments conducted in the torus PBR, mechanisms of microalgae-bacteria interactions in HRAP were investigated using a theoretical modeling approach to simulate and analyze the consortium dynamics over day-night cycles. Here, the hypothesis of a synergy between microalgae and bacteria considering only exchanges of O_2 and CO_2 was tested. The model was then purposefully chosen as simple, with one strain of microalgae, one strain of bacteria and one organic carbon source. A radiative model coupled with a kinetic model of microalgal and bacterial growth were implemented in MATLAB 2022b. Figure 2.13 illustrates the block diagram of the kinetic model.

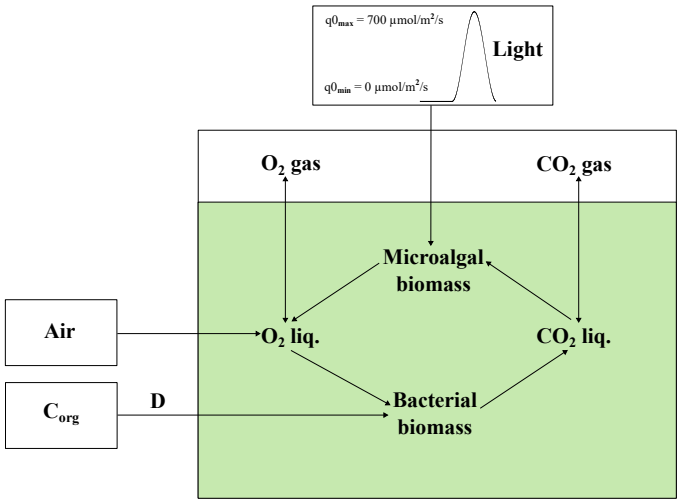

Figure 2.13 – Block diagram of the kinetic model aiming at simulating photoautotrophic growth of *S. obliquus*, chemoheterotrophic growth of *E. coli* and gas exchanges

2.3.2 Modelling of light transfer and light limitation

The PFD q_0 (in μmol.m^{-2}.s^{-1}) was calculated as a function of time t according to the Equations 2.7 and 2.8. Light extinction in the PBR was modelled considering algal biomass concentration $C_{X_{alg}}$, depth z and microalgae mass absorption coefficient Ea that is correlated to pigment content C_{pig}. According to the Beer-Lambert law, the local irradiance G_λ in μmol.m^{-2}.s^{-1} for a given wavelength is given by the Equation 2.50:

$$G_\lambda = q_\lambda \cdot \mathrm{e}^{-Ea \cdot C_{X_{alg}} \cdot z} \tag{2.50}$$

where q_λ is the PFD in μmol.m^{-2}.s^{-1} for each specific wavelength, Ea in m^{-2}.kg^{-1} is the mass absorption coefficient (determined experimentally as explained in the previous section). The specific rate of photon absorption $\mathcal{A}$ can be calculated from the local irradiance G_λ:

$$\mathcal{A} = \int_{PAR} Ea_\lambda \cdot G_\lambda \, d\lambda \tag{2.51}$$

The efficiency of photons conversion $G_{\gamma 1}$ is then derived as follows:

$$G_{\gamma 1} = \frac{1}{L} \cdot \int_0^z \frac{\mathcal{A}}{K + \mathcal{A}} \, dz \tag{2.52}$$

Here, K represents the half-saturation constant for photosynthesis. $G_{\gamma 2}$ denotes the degree of inhibition of maintenance processes by light:

$$G_{\gamma 2} = \frac{1}{L} \cdot \int_0^z \frac{K'}{K' + \mathcal{A}} \, dz \tag{2.53}$$

The specific photon uptake rate q_γ is calculated as follows:

$$q_\gamma = \rho_m \cdot K \cdot G_{\gamma 1} \tag{2.54}$$

The specific growth rate of microalgae q_{XT} can be determined as follows:

$$q_{XT} = \phi_{XT} \cdot (q_\gamma - \frac{J_m}{\phi_m \cdot G_{\gamma_2}})$$

$$\phi_{XT} = \frac{1}{((1 - \hat{x_{pig}}) \cdot \frac{1}{\phi_X} + \hat{x_{pig}} \cdot \frac{1}{\phi_{pig}})} \tag{2.55}$$

$$\hat{x_{pig}} = \omega_{pig} \cdot (1 - G_{\gamma 1})$$

The specific rate of pigment formation q_{pig} can also be calculated as follows:

$$q_{pig} = x^*_{pig} \cdot (1 - G_{\gamma 1}) \cdot q_{XT} \tag{2.56}$$

Additionally, the molar fraction of pigments in the total biomass x_{pig} can be calculated as:

$$x_{pig} = \frac{C_{pig}}{C_{X_{alg}}} \cdot \frac{M_X}{1 - \frac{C_{pig}}{C_{X_{alg}}} \cdot M_{pig} + \frac{C_{pig}}{C_{X_{alg}} \cdot M_X}} \tag{2.57}$$

When the light is insufficient to promote algal growth ($q_0 \leq 20$ μmol.m^{-2}.s^{-1}), the biomass specific growth rate in darkness $q_{XT_{dark}}$ is defined as follows:

$$q_{XT_{dark}} = \frac{k_d}{M_{XT}} \tag{2.58}$$

with the biomass decay rate k_d at 20 °C (Le Borgne and Pruvost 2013) defined as:

$$k_d = -5.6 \cdot 10^8 \cdot \exp\left(\frac{-62.69 \cdot 10^3}{8.3143 \cdot 293.15}\right) \simeq -0.0038 \tag{2.59}$$

and the C-molar mass for algal biomass M_{XT} defined as:

$$M_{XT} = x_{pig} \cdot M_{pig} + (1 - x_{pig}) \cdot M_X \tag{2.60}$$

Finally, when $q_0 \leq 20$ μmol.m^{-2}.s^{-1}, the specific rate of pigment formation q_{pig} is equal to 0.

The parameters used in the equations above are presented in the Table 2.2. The maximum specific rate for maintenance J_m, half-saturation constants for photosynthesis K and for maintenance inhibition at light K', and maximal pigment molar fraction x^*_{pig} were determined by fitting the modeled biomass, and pigment concentration with experimental data obtained from *S. obliquus* batch cultures. These cultures were grown in photoautotrophy in the torus PBR using BBM medium with nutrients in excess, and pH was controlled by CO_2 injections. To simulate a range of irradiances experienced by the microalgae under simulated solar conditions, one batch culture was exposed to 100 μmol.m^{-2}.s^{-1}, while another was exposed to 800 μmol.m^{-2}.s^{-1}.

Constant	Symbol	Value	Units
Reactor depth	L	0.04	m
Reflected fraction of light at the rear of the reactor	R_S	0	
Half-saturation constant for photosynthesis	K	57.72	μmol.m^{-2}.s^{-1}
	K'	1	μmol.m^{-2}.s^{-1}
Maximal primary quantum yield of photosynthesis	ρ_m	0.8	
Maximal pigment molar fraction	x^*_{pig}	0.1486	
Molar quantum yield for the formation of one C-mole of biomass	ϕ_X	0.0976	C-mol.mol^{-1}
Molar quantum yield for the formation of one C-mole of pigment	ϕ_{pig}	0.0841	C-mol.mol^{-1}
Molar quantum yield for the hydrolysis of one mole of ATP (maintenance)	ϕ_m	0.9011	C-mol.mol^{-1}
Maximum specific rate for maintenance	J_m	0	
C-molar mass for biomass	M_X	$23.3 \cdot 10^{-3}$	kg.C-mol^{-1}
C-molar mass for pigments	M_{pig}	$15.9 \cdot 10^{-3}$	kg.C-mol^{-1}

Table 2.2 – Values and units for constants used in light transfer modelling equations (Urbain 2017)

2.3.3 Modeling of gas-liquid transfer

2.3.3.1 Solubility of O_2 and CO_2

The concentration of dissolved gases in the liquid phase depends, among other factors, on their solubility in water. The solubility of O_2 depends on salinity and temperature, whereas the solubility of CO_2 depends on pH and temperature. The Henry coefficient is the parameter that

describes the solubility of gases in liquid. It was determined for O_2 and CO_2 under conditions of constant pH (pH = 7.5), temperature (T = 296.15°K or 23 °C), and the salinity specific to the synthetic wastewater used.

- **O_2**

First, the Bunsen coefficient α_0 for solubility is corrected for salinity:

$$\alpha_{sal} = \alpha_0 \cdot 10^{-\sum H_i \cdot I_i} \tag{2.61}$$

with the Schumpe coefficients H_i for each ion i presented in Appendix B, and the contribution of each ion i to ionic force I_i given by the following equation:

$$I_i = 0.5 \cdot c_i \cdot z_i^2 \tag{2.62}$$

with c_i representing the molar concentrations of each ion in the culture medium and z_i indicating the charges corresponding to each ion.

Henry's coefficient for O_2 is calculated as follows:

$$H_{O2} = \frac{101325 \cdot 0.022395}{\alpha_{sal}} \tag{2.63}$$

- **CO_2**

Henry coefficient for CO_2 depending on temperature T is calculated as follows:

$$H_{CO2} = \mathrm{e}^{-6789.04/T - 11.4519 \cdot log(T) - 0.010454 \cdot T + 94.4914} \cdot 101325 \cdot 10^{-3} \tag{2.64}$$

2.3.3.2 Modelling of the dynamic gas phase

The gas phase of torus PBR exhibits a plug-flow behaviour, as shown by Urbain (2017). Consequently, the concentrations of O_2 and CO_2 in the gas phase of the PBR cannot be assumed to be equal to those in the atmosphere. The gas phase must be considered dynamic, with concentrations of O_2 and CO_2 in the liquid phase calculated interdependently.

The parameters Δ_{O2} and Δ_{CO2} describe the gradients of O_2 and CO_2 concentrations between the gas and liquid phases, which drive mass transfer:

$$\begin{aligned}\Delta_{O2} &= \frac{(p \cdot ye_{O2}/H_{O2} - C_{O2}) - (p \cdot ys_{O2}/H_{O2} - C_{O2})}{log((p \cdot ye_{O2}/H_{O2} - C_{O2})/(p \cdot ys_{O2}/H_{O2} - C_{O2}))} \\ \Delta_{CO2} &= \frac{(p \cdot ye_{CO2}/H_{CO2} - C_{CO2}/K_{eq}) - (p \cdot ys_{CO2}/H_{CO2} - C_{CO2}/K_{eq})}{log((p \cdot ye_{CO2}/H_{CO2} - C_{CO2}/K_{eq})/(p \cdot ys_{CO2}/H_{CO2} - C_{CO2}/K_{eq}}\end{aligned} \tag{2.65}$$

with p representing the pressure in the reactor (assumed to be atmospheric pressure), ye denoting the molar fraction of gases in the gas phase at the inlet of the reactor, ys representing the molar fraction of gases in the gas phase at the outlet of the reactor, C indicating the concentration of gases in the liquid phase, and K representing the parameter that determines the solubility of CO_2 in water based on pH and temperature. The parameters Δ_{O2} and Δ_{CO2} are utilized hereafter in the calculation of dissolved gas concentrations in the liquid phase and their fractional distribution in the gas phase.

The volumetric molar gas transfer rates N_{O_2} and N_{CO_2} in units of mol.m^{-3}.h^{-1} are calculated as follows:

$$\begin{aligned}N_{O_2} &= \frac{-G_s \cdot ys_{O2}}{V_R} \\ N_{CO_2} &= \frac{-G_s \cdot ys_{CO2}}{V_R}\end{aligned} \tag{2.66}$$

with G_s representing the molar gas flow rate at the exit of the PBR and V_R denoting the volume of the PBR.

The constants used in the equations above are presented in the Table 2.3.

2.3.4 Modelling of algal growth, bacterial growth and gas exchanges

In this kinetic model, it is assumed that organic carbon is exclusively consumed by bacteria and that neither microalgae nor bacteria are limited by N, P and S.

During the daytime, microalgal growth depends on light and inorganic carbon availability.

Constant	Symbol	Value	Units
pH	pH	7.5	No unit
Temperature	T	296.15	°K
Bunsen coefficient in pure water	α_0	0.0294	No unit
Coefficient K_1 at T=23°C	K_1	$4.2628 \cdot 10^{-7}$	No unit
Coefficient K_2 at T=23°C	K_2	$4.4593 \cdot 10^{-11}$	No unit
Constant of equilibrium of CO_2 at pH=7.5 and T=23°C	K_{eq}	14.4993	No unit
Volume of the reactor	V_R	$1.4 \cdot 10^{-3}$	m^3

Table 2.3 – Values and units for constants used in gas-liquid transfer modelling equations (Urbain 2017)

Microalgal growth rate μ_{alg} when $q_0 \geq 20$ $\mu mol.m^{-2}.s^{-1}$ is expressed as follows. Here, q_{XT} incorporates the light limitation (see section above), and the limitation by inorganic carbon is expressed by a Monod equation:

$$\mu_{alg_{light}} = q_{XT} \cdot \frac{C_{CO2}}{C_{CO2} + K_{CO2_{alg}}} \cdot C_{X_{alg}} \tag{2.67}$$

During the night time, microalgae cannot utilize light for cell maintenance and the main maintenance process becomes respiration, implying a potential limitation by oxygen expressed using a Monod equation in the microalgal growth rate defined below:

$$\mu_{alg_{dark}} = q_{XT_{dark}} \cdot \frac{C_{O2}}{C_{O2} + K_{O2_{alg}}} \cdot C_{X_{alg}} \tag{2.68}$$

where C_{O2} the dissolved oxygen in $mol.m^{-3}$.

Bacterial growth is limited by organic carbon and dissolved oxygen. Similarly to microalgal growth rate, bacteria growth rate μ_{bact} is expressed as follows:

$$\mu_{bact} = \mu_{max_{bact}} \cdot \frac{C_{O2}}{C_{O2} + K_{O2_{bact}}} \cdot \frac{C_S}{C_S + K_{S_{bact}}} \cdot C_{X_{bact}} \tag{2.69}$$

where C_S is the concentration of organic carbon in the culture and $C_{X_{bact}}$ is the bacterial biomass concentration. The volumetric production rates of O_2 and CO_2 for bacteria can then be deduced as:

$$\begin{aligned} r_{O2_{bact}} &= Y_{O2_{bact}} \cdot \mu_{bact} \cdot C_{X_{bact}} \\ r_{CO2_{bact}} &= Y_{CO2_{bact}} \cdot \mu_{bact} \cdot C_{X_{bact}} \end{aligned} \tag{2.70}$$

In light conditions, the volumetric production rates of O_2 and CO_2 for microalgae are expressed as:

$$\begin{aligned} r_{O2_{alg}} &= Y_{O2_{alg_{light}}} \cdot \mu_{alg_{light}} \cdot C_{X_{alg}} \\ r_{CO2_{alg}} &= Y_{CO2_{alg_{light}}} \cdot \mu_{alg_{light}} \cdot C_{X_{alg}} \end{aligned} \tag{2.71}$$

In darkness conditions, the volumetric production rates of O_2 and CO_2 for microalgae are expressed as:

$$\begin{aligned} r_{O2_{alg}} &= Y_{O2_{alg_{dark}}} \cdot \mu_{alg_{dark}} \cdot C_{X_{alg}} \\ r_{CO2_{alg}} &= Y_{CO2_{alg_{dark}}} \cdot \mu_{alg_{dark}} \cdot C_{X_{alg}} \end{aligned} \tag{2.72}$$

The constants used in the equations above are presented in Table 2.4.

Constant	**Symbol**	**Value**	**Units**
E. coli specific growth rate (Andersen and Von Meyenburg 1980)	$\mu_{max_{bact}}$	0.3	h^{-1}
Half saturation constant for CO_2 for microalgae (Casagli et al. 2021)	$K_{CO2_{alg}}$	$3.33 \cdot 10^{-6}$	$mol.m^3$
Half saturation constant for O_2 for bacteria (Casagli et al. 2021)	$K_{O2_{bact}}$	$6.25 \cdot 10^{-5}$	$mol.m^3$
Half saturation constant for organic carbon for bacteria (Casagli et al. 2021)	$K_{S_{bact}}$	$1.6 \cdot 10^{-3}$	$kgC.m^3$
Yield for CO_2 for microalgae (light) (Garcia-Moscoso et al. 2015)	$Y_{CO2_{alg_{light}}}$	42.08	$mol/kgC_{X_{alg}}$
Yield for O_2 for microalgae (light) (Garcia-Moscoso et al. 2015)	$Y_{O2_{alg_{light}}}$	46.72	$mol/kgC_{X_{alg}}$
Yield for CO_2 for microalgae (dark) (Garcia-Moscoso et al. 2015)	$Y_{CO2_{alg_{dark}}}$	42.08	$mol/kgC_{X_{alg}}$
Yield for O_2 for microalgae (dark) (Garcia-Moscoso et al. 2015)	$Y_{O2_{alg_{dark}}}$	51.77	$mol/kgC_{X_{alg}}$
Yield for organic carbon for bacteria (Guardia and Calvo 2001)	$Y_{S_{bact}}$	1.6	$kgC_{X_{bact}}/kgC_{org}$
Yield for CO_2 for bacteria (Folsom and Carlson 2015)	$Y_{CO2_{bact}}$	10.49	$mol/kgC_{X_{bact}}$
Yield for O_2 for bacteria (Folsom and Carlson 2015)	$Y_{O2_{bact}}$	8.49	$mol/kgC_{X_{bact}}$

Table 2.4 – Values and units for constants used in gas-liquid transfer modelling equations

2.3.5 State variables

Finally, the state variables of algal biomass, bacterial biomass, dissolved O_2, dissolved CO_2, fractions of O_2 and CO_2 in the gas phase, organic carbon concentration, pigment concentration, and the molar gas flowrate outgoing the PBR, G_s, evolve over time as shown below. The state variables were described by solving an algebro-differential system.

$$\frac{dC_{X_{alg}}}{dt} = (\mu_{alg} - k_d - D) \cdot C_{X_{alg}}$$

$$\frac{dC_{X_{bact}}}{dt} = \mu_{bact} \cdot C_{X_{bact}} - D \cdot C_{X_{bact}}$$

$$\frac{dCO_2}{dt} = D \cdot (C_{CO_{2_{in}}} - C_{CO_2}) + r_{CO_{2_{alg}}} + r_{CO_{2_{bact}}} + K_L a_{CO_2} \cdot \Delta_{CO_2}$$

$$\frac{dO_2}{dt} = D \cdot (C_{O2_{in}} - C_{O_2}) + r_{O_{2_{alg}}} + r_{O_{2_{bact}}} + K_L a_{O_2} \cdot \Delta_{O_2}$$

$$0 = \frac{p \cdot Q_e}{R \cdot T} \cdot V_R \cdot (ye_{CO_2} - ys_{CO_2}) - K_L a_{CO_2} \cdot \Delta_{CO_2} \tag{2.73}$$

$$0 = \frac{p \cdot Q_e}{R \cdot T} \cdot V_R \cdot (ye_{O_2} - ys_{O_2}) - K_L a_{O_2} \cdot \Delta_{O_2}$$

$$\frac{dC_S}{dt} = -\frac{\mu_{bact}}{Y_{S_{bact}}} \cdot C_{X_{bact}} + D \cdot (C_{S_{in}} - C_S)$$

$$\frac{dC_{pig}}{dt} = q_{pig} \cdot M_{pig} \cdot C_{X_{alg}} - D \cdot C_{pig}$$

$$0 = G_e \cdot (1 - ye_{O2} - ye_{CO2}) - G_s \cdot (1 - ys_{O2} - ys_{CO2})$$

The constants utilized in the equations above are listed in Table 2.5.

Constant	Symbol	Value	Units
Dilution rate of the culture	D	0.008	h^{-1}
Concentration of organic carbon in the inlet	$C_{S_{in}}$	0.260	kgC_{org}/m^3
Concentration of O_2 in the inlet	$C_{O2_{in}}$	0	mol/m^3
Concentration of CO_2 in the inlet	$C_{CO2_{in}}$	0	mol/m^3
O_2 fraction in the air injected	ye_{O_2}	0.21	
CO_2 fraction in the air injected	ye_{CO_2}	0.0004	
Air flowrate	Q_e	0.0018	m^3/h
Mass transfer coefficient for O_2	$K_La_{O_2}$	1.32	h^{-1}
Mass transfer coefficient for CO_2	$K_La_{CO_2}$	1.12	h^{-1}
Pressure	p	$1.013 \cdot 10^5$	Pa
Perfect gases constant	R	8.3143	J/mol/K

Table 2.5 – Values and units for constants used in the calculation of the derivatives of the state variables (Urbain 2017)

2.4 Characterisation of microalgae impact on virus inactivation

2.4.1 Objective of the study

While microalgae impact bacterial activity and pollutants removal, it is also expected to influence significantly solar inactivation of pathogens. Microalgae are expected to contribute significantly to turbidity and attenuation of solar radiations in HRAP, however, they are also responsible for high oxygen concentration, high pH and production of ROS favouring disinfection, questioning the relative impact of microalgae on pathogen inactivation. The purpose of this study (Chapter 7) is to estimate the impact of microalgae on indicator viruses inactivation, in terms of UV attenuation (inhibition of inactivation) and production of ROS (enhancement of inactivation), using a laboratory UV cabinet.

2.4.2 UVA cabinet

MS2 inactivation experiments were conducted using solely UVA to simulate sun radiations. Indeed, MS2 inactivation rate with visible radiations was not significantly different from inactivation rate in the dark (Bolton et al. 2011). In addition, UVB is very rapidly attenuated in HRAPs (Craggs et al. 2004) and could not be detected at all in Peterborough HRAP. The effect of UVB on pathogens inactivation is then expected to be negligible in such a turbid medium.

UVA LEDs (Bergquist) are fixed to a panel Reliance Laboratories suspended in a closed wood cabinet. Samples are placed under the panel in a shaking Ratek water bath chiller to maintain a constant temperature of 20°C, compensating the warming due to LEDs irradiation.

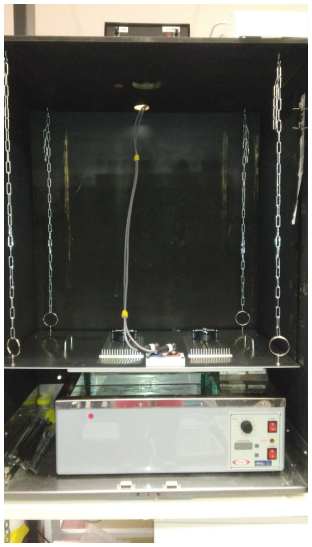

Figure 2.14 – UVA cabinet

The location of each bottle sample in the water bath chiller was determined to minimise the deviation of incident UVA irradiance between the samples (Appendix C). Each of the six samples was irradiated with 5 LEDs corresponding each to one range of wavelength in the UVA spectrum (365 nm, 370-375 nm, 380-385 nm, 385-390 nm, 395-400 nm). The operator can set the power of each range of wavelength via the interface RLED site controller. For calibration, a Solar Light UVA weatherproof detector PMA2110-WP connected to Solar Light PMA2100 meter recorded the UVA intensity at each of the six bottle sample locations beneath a quartz disc (that stands for the quartz cap used during samples incubation) for six different power. A polynomial correlation between the power applied and the UVA incident irradiance measured on average on the six sample locations was deduced (Figure 2.15).

2.4.3 Preparation of the culture mediums

In order to investigate the effects of UV attenuation and ROS on MS2 inactivation, MS2 was incubated in six different types of media: reverse osmosis (RO) water, BBM, wastewater,

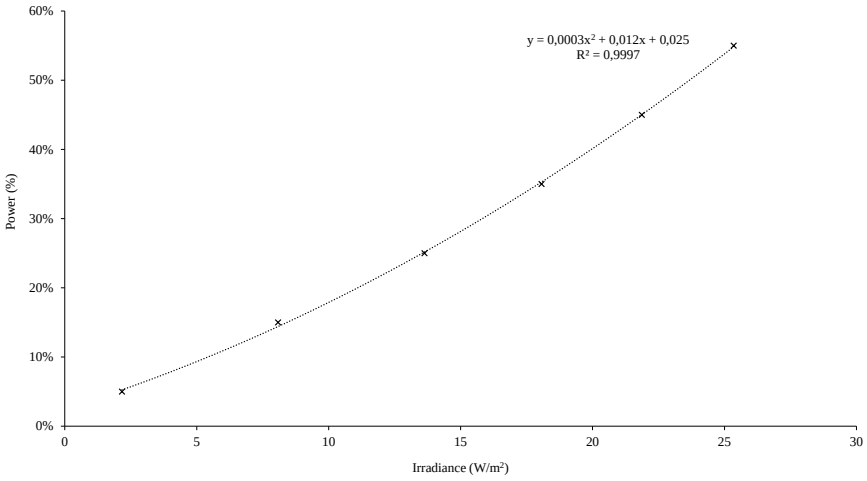

Figure 2.15 – Calibration curve predicting the power value to apply depending on the UVA incident irradiance

filtered wastewater, microalgae and microalgae extract. Their preparation and utilization are synthesized in Table 2.6.

Microalgae was isolated from Peterborough HRAP samples by successive spreading on BBM agar plates. Ten isolated algae colonies were first resuspended in 25 mL conical flasks containing BBM and grown under approximately 80 μmol.m^{-2}.s^{-1} PAR light. The microalgae culture was then transferred in larger volumes of BBM until reaching approximately 6 mg.L^{-1} of chlorophyll *a*, as measured in Peterborough HRAP (Figure 2.16).

Different methods were tested in order to obtain an extract of organic molecules from the microalgal cells. Figure 2.17 present the total dissolved organic carbon concentration in a microalgae culture before and after extraction using ultrasonic bath, three freezing-defreezing cycles and heating at 80°C for 30 min. The results clearly demonstrate that heating is the most efficient method for extracting organic molecules from microalgae. Part of the microalgal stock was then heated at 80°C for 30 min in order to extract organic molecules from the cells and filtered at 0.45 μm.

Anaerobically pre-treated wastewater was sampled at the surface of Peterborough anaerobic pond (Figure 2.18) and stored at 4°C. Part of the wastewater was filtered at 0.45 μm.

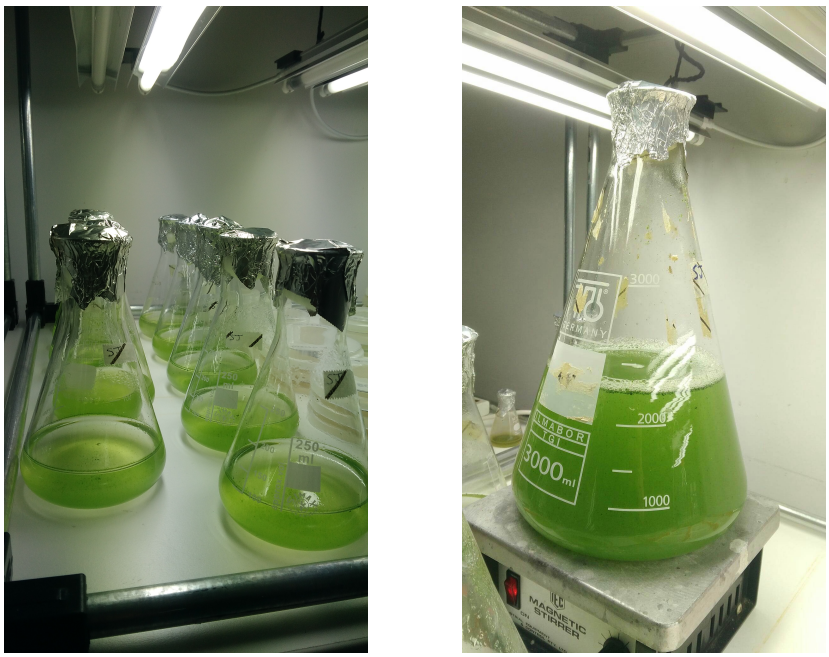

(a) (b)

Figure 2.16 – Cultures of microalgae isolated from Peterborough HRAP (a) Isolated species (b) Final mixture

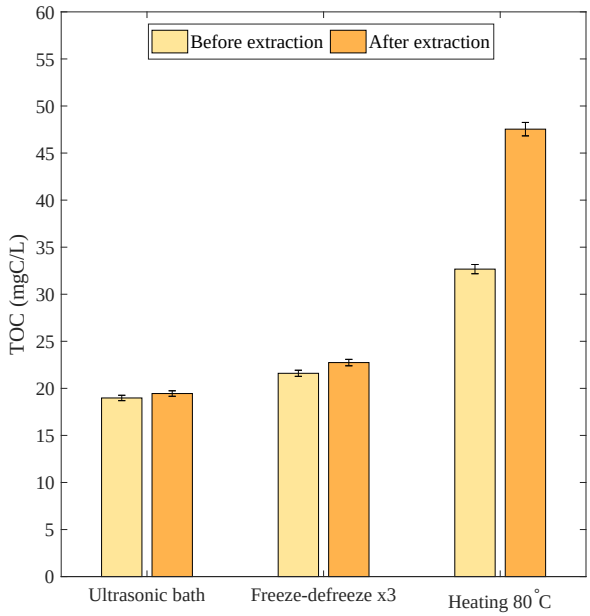

Figure 2.17 – Dissolved organic carbon in microalgae culture before and after sonication, freezing-defreezing and heating

Figure 2.18 – Anaerobic pond upstream Peterborough HRAP

Purpose	Media	Preparation
Baseline	RO water	RO water sterilised for 20 min at 121°C
Effect of BBM components	BBM	BBM prepared as explained in Appendix A and sterilised for 20 min at 121°C
Effect of wastewater on UVA attenuation	Wastewater	Wastewater from the outlet of the anaerobic pond
Effect of exogenous photosensitisers from wastewater	Filtered wastewater	Anaerobically pretreated wastewater filtered at 1.6 μm then 0.45 μm
Effect of microalgae on UVA attenuation; Effect of photosensitisers from microalgal cells	Microalgae	Microalgae isolated from Peterborough HRAP then grown in BBM
Effect of photosensitisers from molecules contained inside microalgae	Microalgae extract	Microalgae isolated from Peterborough HRAP then grown in BBM, heated at 80°C, filtered at 1.6 μm then 0.45 μm

Table 2.6 – Purpose and preparation of each media

2.4.4 MS2 and *E. coli* stock and MS2 quantification

2.4.4.1 Stock

The F-RNA coliphage virus MS2 was used a non-pathogenic surrogate for the behaviour of human pathogenic viruses in the environment. MS2 is a coliphage virus that needs to infect coliform bacteria to multiply. *E. coli* ATCC 700891, resistant to streptomycin and ampicillin, was used as the host coliform and kept in a microtube at -20°C in 50% glycerol/50% tryptone

water. Ahead of the preparation of the MS2 stock, *E. coli* was spread on a TSA plate and incubated at 37°C for 24 hours. An isolated *E. coli* colony from the plate was then resuspended in 10 mL Tryptone Soya Broth (TSB) and incubated in a Stackable Incubator Shaker (Innova) 24 hours at 37°C at 100 rpm before being kept at 4°C until use. For preparing a new *E. coli* stock, the tube containing TSB + *E. coli* was centrifuged at 3000 rpm for 15 min, then the supernatant was removed and 1 mL of 50% glycerol/50% tryptone water was transferred into the tube to resuspend the *E. coli* biomass. This new *E. coli* stock was then transferred in 1 mL cryotubes and frozen a -20°C.

The MS2 stock was prepared 24 hours before inoculation of the samples. 5 mL of TSA containing antibiotics streptomycin and ampicillin were transferred into 10 ml sterile tubes and kept between 50 and 60°C to keep the agar liquid. Then, 500 μL of TSB broth containing *E. coli* were transferred into the tube. This top layer agar was poured over a bottom layer of prepoured TSA agar plates. Two drops of MS2 15597-B1 stock solution were poured in the middle of the plate. The plate was incubated overnight at 37°C. If MS2 effectively infected *E. coli*, a stain appeared on the centre of the plate after a few hours. Subsequently, 9 mL of reverse osmosed water were poured onto the plate. The plate was then placed in the incubator at 37°C for 45 min and swirled every 10 min. The water was then transferred on to a new plate where MS2 effectively infected *E. coli*. Again, the plate was placed in the incubator for 45 min and swirled every 10 min. This step was repeated for 4 successive MS2 plates. The liquid recovered on the last plate was then syringe filtered at 0.45 μm into 100 mL reverse osmosis water to remove *E. coli* particles. This new MS2 stock, at a concentration of 10^6-10^8 PFU/mL was then split into several 10 mL tubes and kept at 4°C. The samples destined to be incubated in the UV cabinet were incubated with 1 mL of this stock on the following day.

2.4.4.2 Quantification of MS2 virus

The double layer agar method was used to quantify MS2 in the samples after incubation in the UV cabinet (Noble et al. 2004). Serial dilutions of MS2 samples were done according to the initial concentration of the stock in order to count between 15 and 300 MS2 colonies

on the plate. 5 mL of TSA containing antibiotics streptomycin and ampicillin were poured in 10 mL sterile tubes and kept between 50 and 60°C to keep the agar liquid. Then, 500 μL of TSB broth containing *E. coli* and 200 μL of diluted MS2 sample were transferred into the agar tube. This top layer agar was poured over a bottom layer of prepoured TSA agar plates. This plating step was repeated for another dilution of the MS2 sample, each in triplicates. The 6 plates obtained were incubated for 24 hours at 37°C. The following day, MS2 was quantified from the number of plaques on the plate, corresponding to locations where *E. coli* was infected by MS2 and was unable to grow (Figure 2.19). All the plates with a MS2 count between 15 and 300 were considered for the calculation of MS2 concentration. The Plaque Forming Unit (PFU) concentration (in PFU.mL^{-1}) was deduced from the equation below, where n is the number of plaques counted on the plate, DF is the dilution factor and 5 is the conversion factor to PFU.mL^{-1}:

$$PFU = n \cdot DF \cdot 5 \tag{2.74}$$

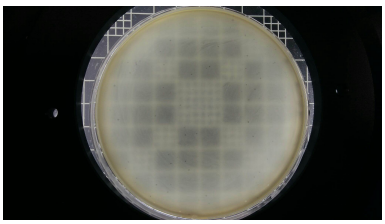

Figure 2.19 – MS2 plate count

The MS2 inactivation rate K in h^{-1} was calculated according to the equation below, where t is the time in h from the beginning of the incubation, n_t is the number of viable viruses remaining at time t and n_0 the number of viable MS2 at the beginning of the incubation:

$$K = \frac{-log10\frac{n_t}{n_0}}{t} \tag{2.75}$$

The experimental plan is further detailed in the Chapter 7.

Chapter 3

Overview of microorganisms' activity in HRAP by Peterborough HRAP 3D characterisation

---

This Chapter has been published in Algal Research in vol. 80 (2024).

Co-authors contributions: Solène Jahan: Original draft, Visualization, Methodology, Investigation, Formal analysis, Conceptualization (80%). Rajina K C: Review & editing, Conceptualization (1%). Felipe Sabatté: Review & editing, Methodology, Investigation (5%). Sam Butterworth: Review & editing, Methodology, Investigation (5%). Jérémy Pruvost: Review & editing, Supervision (1%). Guillaume Cogne: Review & editing, Supervision (1%). Mariana Titica: Review & editing, Supervision (1%). Howard Fallowfield: Review & editing, Supervision, Methodology, Investigation, Conceptualization (7%).

3.1 Introduction

Peterborough HRAP, currently the largest HRAP treating wastewater in Australia, was constructed in 2018 in South Australia with the aim of implementing this promising technology on a large scale (Figure 3.1). The site comprising two anaerobic ponds for wastewater pretreatment, two HRAPs each covering an area of 5000 m^2 and two storage ponds is designed to treat 470 m^3 of wastewater daily from an abattoir and 1700 inhabitants each day.

Previous studies at Kingston on Murray, South Australia, have demonstrated that the per-

Figure 3.1 – Global view of Peterborough HRAP (Photo: Howard Fallowfield)

formance of HRAP met the national reuse guidelines for wastewater intended for the irrigation of non-food crops (NRMMC 2006, Fallowfield et al. 2018). The single loop HRAP, sharing similar geographical climate with Peterborough HRAP and fed from a septic tank effluent achieved an average removal efficiency of 92 % for BOD_5, 65 % for N-NH_4^+, 18 % for P-PO_4^{3-} and a 1 $\log_{10}$ reduction of F-RNA coliphage (Buchanan et al. 2018a). Peterborough HRAP has so far been approached as a black box, focusing primarily on characterizing the inlet and the outlet. While this approach was essential for evaluating the overall performance of the system, it raised questions about the diversity of physicochemical conditions within the pond. The Peterborough HRAP consists of a one-kilometre channel meandering in six sub-channels and mixed by a paddlewheel. A significant loss of load and associated heterogeneous mixing might be expected in a reactor of this size, considering in addition that the HRAP is nominally 30 cm deep. However, large scale HRAPs are relatively understudied. The general principle of mass conservation in fluids dynamic implies that wastewater flow velocity must be conserved along the channel (Acheson 2009). Also, while CFD modelling of a large scale single loop HRAP predicted the occurrence of dead zones in the bends (Inostroza et al. 2021), to our knowledge there has been no experimental 3D characterisation of flow velocity and physicochemical parameters in large-scale HRAP such as at Peterborough. Understanding the heterogeneity of large-scale ponds is crucial since lower algal productivities and nutrient removals were reported in large ponds (1 ha) than in smaller

ponds (5 and 330 m^2) even though bigger paddlewheels were utilized for the large ponds than for the smaller ones, raising questions about the mixing efficiency in large scale HRAPs (Sutherland et al. 2020). Mixing mainly influences concentration fields of chemicals, including organic matter, nutrients and dissolved oxygen. Efficient mixing also increases the likelihood of microorganisms encountering pollutants they are intended to remove from the wastewater (Grobbelaar 1994). Microalgal growth is also reliant on light availability in the pond, itself dependant on efficient mixing circulating microalgae from the bottom of the pond to the surface where the irradiance is higher and supports photosynthesis (Demory et al. 2018). Pathogen inactivation within the HRAP system largely depends on high pH and dissolved oxygen concentration and to the exposure to UV radiation which causes direct damage to pathogens RNA and DNA and are also able to break chemical bonds that constitute organic molecules, leading to division of the parent compound in free radicals able to damage microorganisms (Bolton 2012, Park et al. 2021). Mixing has then a profound impact on the treated water quality by exposing microbial pathogens to higher UV irradiation at the pond surface (Park et al. 2021). The purpose of this unique study was to determine experimentally the 3-dimensional flow velocity profile of Peterborough HRAP and the influence on the heterogeneity of the physicochemical parameters that serve as indicators of biological activity, namely dissolved oxygen, pH, suspended solids, chlorophyll *a*, organic and inorganic carbon, ammonium, nitrite, nitrate and orthophosphate. To achieve this goal, a gantry equipped for *in situ* measurements and wastewater sampling was deployed across the channel, enabling data collection along the length, depth and width of Peterborough HRAP. This comprehensive approach aims to assess the distribution of photosynthetic, heterotrophic and nitrifying activities at different locations within the HRAP.

3.2 Material and methods

3.2.1 *In situ* measurements

A gantry equipped with sensors and hoses was deployed in the pond for measurement of pH, DO, conductivity, temperature, flow velocity and for sampling at 3 different depth, 3 different

positions across the channel and 26 cross-sections (CS) along the 1km-length channel. Samples were analysed for suspended solids, nutrients, organic and inorganic carbon, chlorophyll *a*, flocs size, alkalinity and BOD_5 as detailed in Chapter 2.

The composition of the anaerobically pre-treated wastewater is presented in Table 3.1.

Element	**Concentration ($mg.L^{-1}$)**
$N\text{-}NH_4^+$	94.6 ± 25.6
$N\text{-}NO_2^-$	0.43 ± 1.6
$N\text{-}NO_3^-$	0.07 ± 1.7
$P\text{-}PO_4^{3-}$	10.8 ± 3.0
BOD_5	96.1 ± 55.0

Table 3.1 – Characterisation of anaerobically pre-treated wastewater (inlet).

3.2.2 Normalisation between sensors

Even if calibrated the same way, the three multiparameter sensors used to simultaneously measure pH and DO on the left side, centre and right side of the channel did not display the same pH and DO values while immersed in a standard solution. For comparison of the results obtained along the width of the channel, pH deviation between the three sensors was estimated by immerging the 3 sensors in the same pH 7 standard solution. Dissolved oxygen deviation was estimated by measuring simultaneously ambient air oxygen concentration with the three sensors. The sensor measuring the nearest value from the standard was chosen as the reference and the others were normalised according to this sensor. The HANNA HI 98194 n°2 sensor was here the reference for both pH and DO (Table 3.2). For DO, it appeared that deviation between the sensors increased when measured value increased so correction applied was expressed as a percentage of the raw value. This way, all pH and DO measurements were normalised depending on the sensor they were measured with.

3.2.3 Normalisation of diurnal changes in wastewater DO and pH

The measurements at the 26 cross sections, as described in the Chapter 2, were completed over a 10 hours period from 10 am to 7 pm. Diurnal variation in DO and pH values within

Sensor position	Model	Measured pH in a pH7 standard solution	Correction to apply on pH	Measured DO in ambient air (mg/L)	Correction to apply on DO
Right sensor	YSI 556 MPS n°3	7.42	-0.52	6.30	+36%
Centre sensor	HANNA HI 98194 n°2	6.90	0	8.54	0%
Left sensor	YSI 556 MPS n°4	6.85	+0.05	9.15	-7%

Table 3.2 – Variability of pH and DO measurements between left, center and right sensors and resulting corrections to apply

HRAPs treating wastewater is a known phenomenon (Sutherland et al. 2021). The primary objective of this study was to spatially compare the DO and pH values within the 1 km long channel, independently of their respective diurnal variations. As DO and pH were measured along the channel, width, and depth, DO and pH were simultaneously recorded at a fixed point in Channel 2 to measure their diurnal variation (Figure 3.2). The variations in DO within the HRAP throughout the day were successfully modelled by a polynomial regression (p-value $<$ 0.001; Eq. 3.1),

$$DO_{pred_t} = -268.01t^2 + 349.08t - 89.137 \tag{3.1}$$

with DO_{pred_t} in mgDO.L^{-1} at time t (in days) when measurements of DO at the respective cross section was obtained.

DO measurements commenced at t=0.44 at 10:30am. The DO measurements collected throughout the day at the respective cross sections were normalised to the fitted commencing DO (t=0.44; Eq. 3.1) using Equation 3.2.

$$DO_{norm_t} = DO_{meas_t} - (DO_{pred_t} - DO_{ref_{10h30}}) \tag{3.2}$$

where:

DO_{norm_t} = the normalised DO (mg.L^{-1}) value at the respective cross section at time t (days) corrected for the diurnal influence;

DO_{meas_t} = DO measured at the respective cross section at time t (days);

$DO_{ref_{10h30}}$ = the fitted DO (mg.L^{-1}, Eq. 3.1), at 10:30am (t = 0.44 days).

The pH measured at the fixed point showed no significant change over the course of the day and attempts to model it with either linear or polynomial regression did not yield statistically significant results (p-values=0.321 and 0.566 respectively).

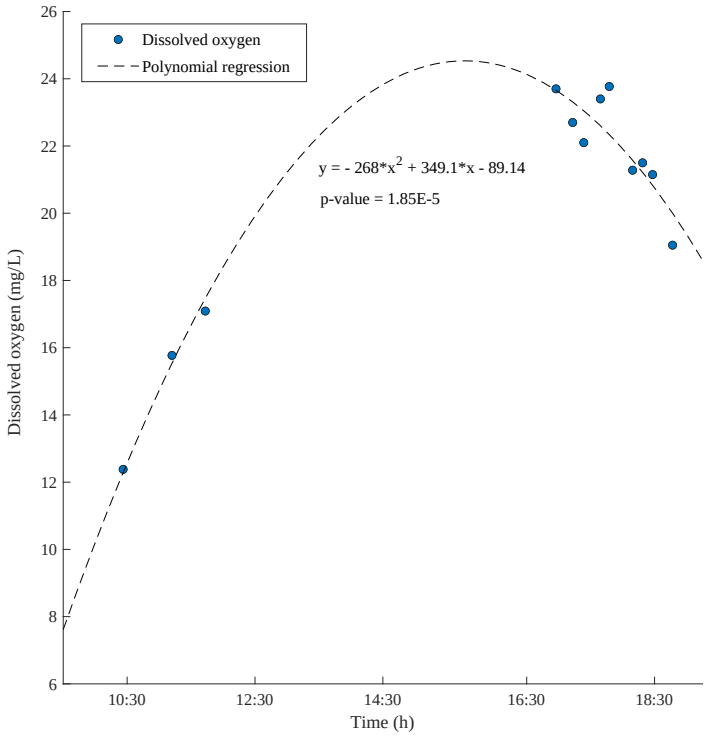

Figure 3.2 – DO diurnal variation and resulting polynomial regression

3.2.3.1 In situ measurements and wastewater sampling June 2023

A second sampling and measurements campaign was completed on June 14th - 15th 2023 to complete the data set obtained during the first campaign conducted in November 2022 (see Chapter 2). Targeted, comparative dissolved oxygen measurements were carried out using HANNA HI 98194 and YSI 556 MPS sensors within 5 min to minimise potential diurnal variation. The measurements were conducted before and after the paddlewheel at CS 26, 1 and 2, as well as before and after the first bend at CS 4 and 5. Additionally, the same sensor was employed to

measure dissolved oxygen concentration across the width of the channel at CS 2, 6 and 10. In situ concentrations of N-NH_4^+ and N-NO_3^- were measured in the middle of each of the six channels within one hour using a YSI ProDSS nutrient sensor. Additionally, wastewater samples were collected at CS 1, 3, 6, 10, 14, 18 and 22 (see cross sections CS in Chapter 2) to determine floc size, partial and total alkalinity, BOD_5 and COD of the wastewater along the channel length.

3.3 Results

3.3.1 Environmental conditions

On November 29th 2022, during the in situ measurements of DO, pH, conductivity and temperature, the maximum irradiance reached 2000 μmol.m^{-2}.s^{-1} attained around 1 pm, while the air temperature was 20°C. The sky remained consistently clear, providing stable conditions favourable for the measurements. The wastewater temperature in the HRAP exhibited diurnal variation, ranging from 15 to 25°C. The conductivity was 1567 μS.cm^{-1} and the pH varied from 8 to 10. Microscopic observation revealed that the microalgal population in the HRAP was predominantly composed by *Actinastrum sp.*, *Scenedesmus sp.* and *Chlorella sp.*, with diatoms and cyanobacteria present to a lesser extent.

3.3.2 Flow velocity

The overall flow velocity in the HRAP remained relatively constant, averaging 0.2 m.s^{-1} in average, in agreement with the principle of mass conservation (Figure 3.3).

The only exception to this stability occurred near the exit of the 180° bends, where a notable contrast in flow velocities was observed. Lower flow velocities were measured along the internal bank, while the external bank exhibited higher flow velocities reaching 0.5 m.s^{-1} and surpassing velocities elsewhere in the pond. Flow velocities measured at the bottom of the HRAP were also significantly lower than values recorded at mid-depth and near the surface ($p < 0.001$). Coefficient of variation of the nine flow velocity values measured at each cross-section was 71 % for the cross-section located at the exit of the bends against 22 % for the other cross sections.

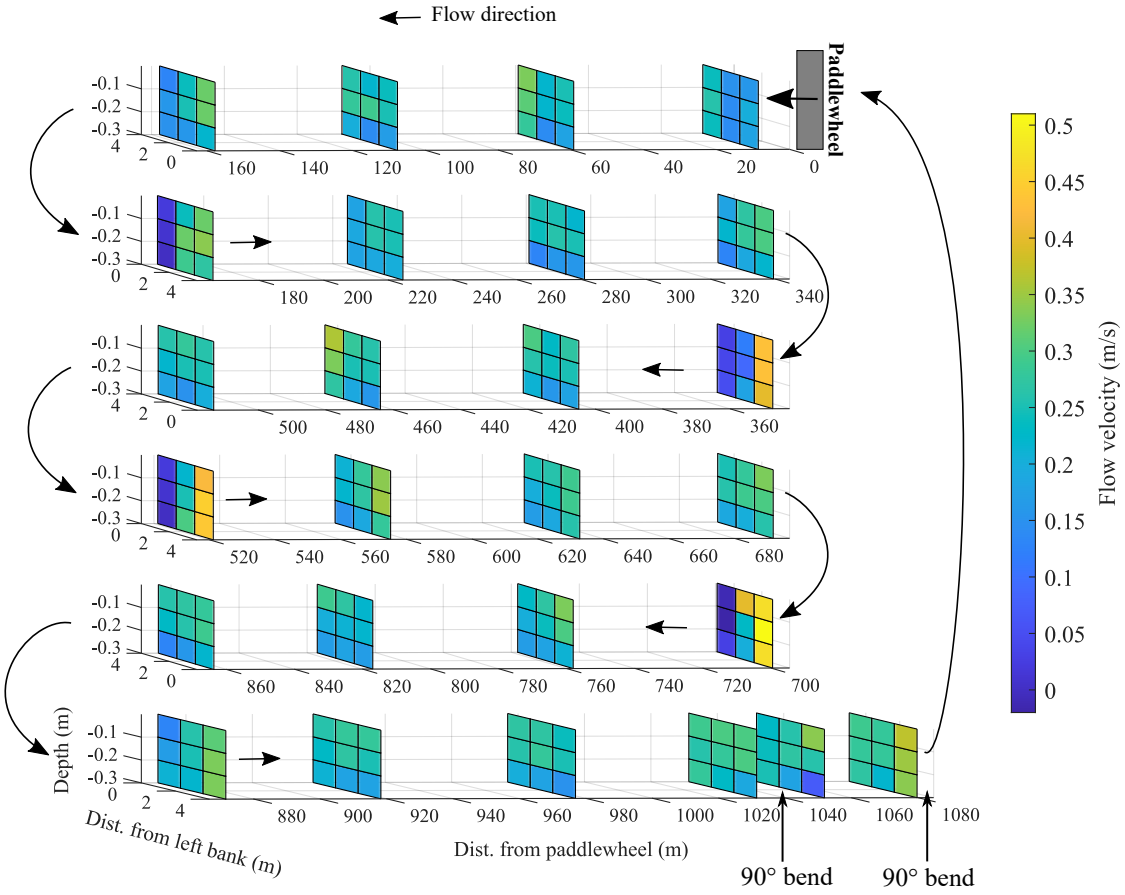

Figure 3.3 – Flow velocity (m.s^{-1}) in Peterborough HRAP throughout channel length, width and depth

The mean cross section flow velocity exhibits a slight increase at CS26 (0.29 m.s^{-1}), the last cross section before the paddlewheel, in comparison to CS1 (0.19 m.s^{-1}), the first cross section after the paddlewheel. Even while this observation has not been reported in other studies investigating flow velocity in HRAP, this variation can be attributed to the influence of the paddlewheels rotation which induces an aspiration effect on the water flowing towards the paddlewheel, thereby elevating the flow velocity at CS26. The paddlewheel introduces turbulence, leading to a local lower average flow velocity in the turbulent area immediately after the paddlewheel at CS1. Electrical energy consumption by the paddlewheel motor, calculated from the

continuously monitored current (2.05 amps) and voltage was 0.85 kWh, meaning the volumetric electric power consumption dedicated to pond mixing is 0.7 $W.m^{-3}$ considering the total HRAP volume is 1284 m^3.

3.3.3 Suspended solids

In the HRAP, the mean concentration of suspended solids, including particle larger than 1.6 μm encompass microalgae, bacteria, zooplankton and organic detritus, was 1 $g.L^{-1}$. Despite those settleable particles are sensitive to mixing efficiency, Figure 3.4 depicts a suspended solids distribution in the pond that aligns with the flow velocity profile. The suspended solids concentration remains consistent along the length of the channel. Regions characterised by dead zones, where flow velocity is close to zero, and the bottom of the HRAP exhibit significantly higher suspended solids concentrations ($p < 0.001$). In the dead zones, suspended solids concentration reaches 5-13 $g.L^{-1}$. Additionally, suspended solids concentration demonstrates a significant ($p < 0.001$) negative correlation with flow velocity, unaffected by distance from the paddlewheel.

3.3.4 Chlorophyll *a* and dissolved oxygen

One of the studys objectives was to assess the spatial impact on DO and microalgal chlorophyll a concentration, considering the relative distance from the paddlewheel, channel width and depth. Figure 3.5 shows the DO concentration in the HRAP corrected according to diurnal variations as explained in the Section 3.2.3. Considering that the estimation of the diurnal variation by setting up a fixed point was associated with imprecisions due to biofilm and plants accumulation around the sensor after a few hours, corrected DO diurnal variations were estimated in a 5 $mg.L^{-1}$ range. The measurements commenced in the morning at CS5 in Channel 2, when irradiance and DO were already high, and concluded at CS4 in Channel 1 in the evening when irradiance and DO were lower. Surprisingly, the normalised DO concentration at CS4 in Channel 1 was two-fold higher than those taken in the morning at CS5 in Channel 2. However, when dissolved oxygen measurements were repeated within a 5 min interval in June 2023 before (CS4) and after (CS5) the first bend, no significant difference in DO concentration was

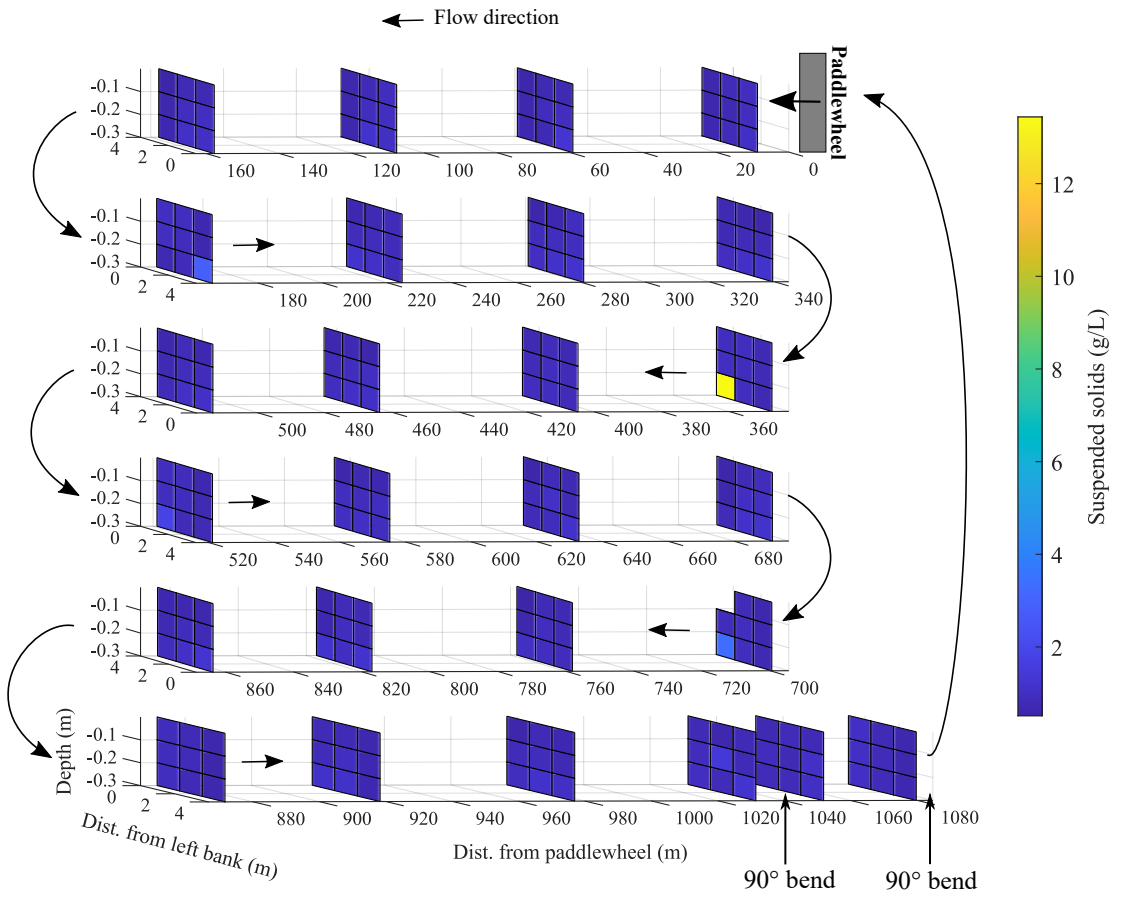

Figure 3.4 – Suspended solids (g.L^{-1}) in Peterborough HRAP throughout channel length, width and depth

observed between the two cross sections. Similarly, Figure 3.5 suggests a decrease in DO after the paddlewheel, indicating turbulence induced by the paddlewheel stripping DO from the wastewater. However, DO was not significantly different before (CS26) and after (CS1) the paddlewheel when measurements were performed within a 5 min interval in June 2023, implying DO stripping was not occurring. The discrepancies between measurements taken within 5 min of each other and those taken over longer time intervals (hours) suggest that normalization method may not adequately compensate for diurnal variation. Initial measurements suggested that wastewater near the left bank had higher DO concentrations than either the centre or the right bank. Repeat measurements in June 2023 using a single sensor for the three measuring

points, however, showed no difference between centre, left or right banks along the length of the channel, showing that the difference observed in November 2022 was an artifact due to the use of three different sensors for the left, center and right measurements. Besides, DO concentration was not significantly different between the surface and the bottom of the pond.

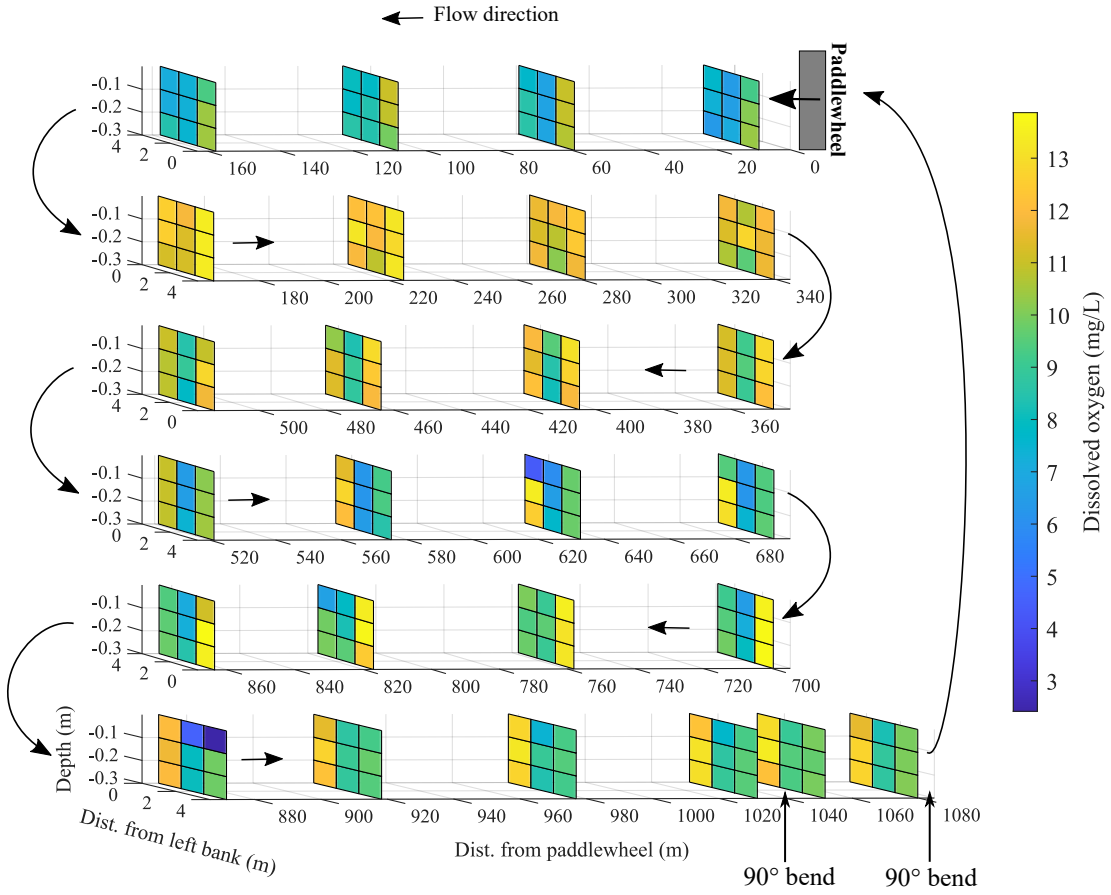

Figure 3.5 – Dissolved oxygen (mg.L^{-1}) in Peterborough HRAP throughout channel length, width and depth

Despite the confounding factor associated with the measurement of DO concentration along the channel length in November 2022, the mean chlorophyll *a* concentration was consistent in both the first and last channel, 6.4 and 6.7 mg.L^{-1} respectively (Figure 3.6). This indicates an homogeneous distribution of microalgae, implying similar photosynthetic activity throughout the entire 1 km channel length.

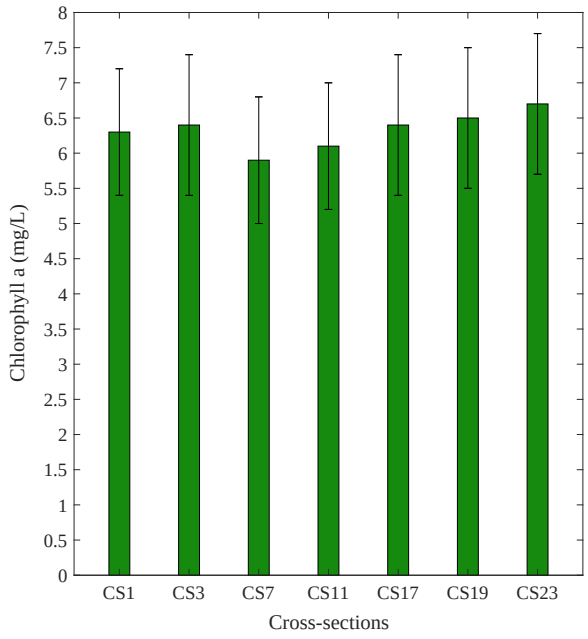

Figure 3.6 – Chlorophyll a concentration (mg.L^{-1}) at different cross-sections along the length of the channel

Estimation of microalgal biomass through suspended solids measurement in HRAP is challenging because microalgae are mixed with bacterial biomass and organic detritus. Chlorophyll a content in algal cells, assumed to be approximately 2 % (Cromar and Fallowfield 2003), was used as a conversion factor to estimate algal biomass in total suspended solids. In Peterborough HRAP, algal biomass was estimated at 30 % of suspended solids.

3.3.5 Total organic carbon (TOC)

The primary role of microalgae is to supply oxygen for chemoheterotrophic bacteria engaged in the degradation of organic carbon. The concentration of total organic carbon was consistent throughout depth, across the width and along the entire length of the channel (Figure 3.7). Interestingly, in the dead zones with high suspended solids concentration and the potential accumulation of organic matter, the organic carbon appeared to be degraded similarly to the other areas in the pond. The hypothesis is that anaerobic processes occur in dead zones to degrade organic carbon. Another possibility is that the organic carbon in the pond consists

mainly of recalcitrant carbon. The inlet wastewater to the HRAP from the anaerobic pond had a BOD_5 of 70 $mg.L^{-1}$. In June 2023, the mean BOD_5 within the HRAP was 18 $mg.L^{-1}$, indicating a BOD_5 removal of 74 %. Heterotrophic activity appears to be homogeneous and unaffected by the distance from the paddlewheel, depth or dead zones within the HRAP.

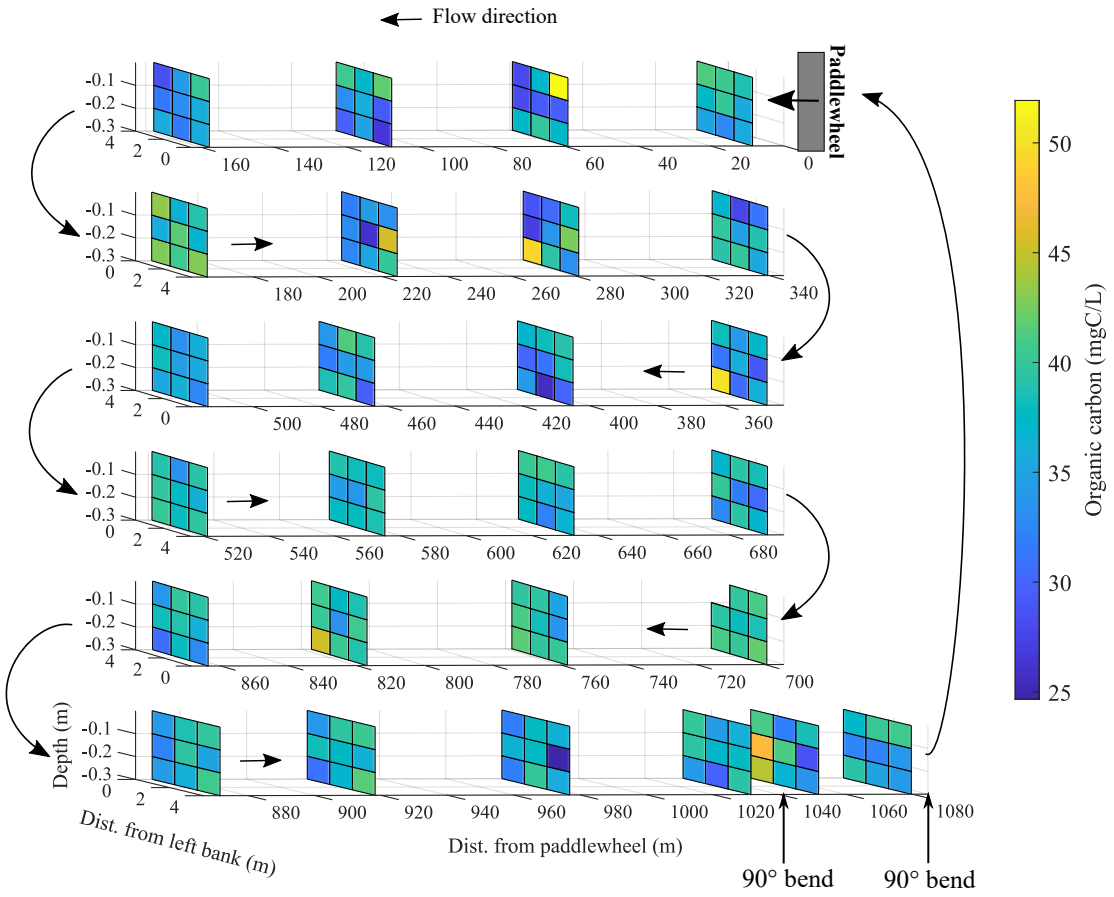

Figure 3.7 – Total organic carbon ($mgC.L^{-1}$) in Peterborough HRAP throughout channel length, width and depth

3.3.6 Nitrifying activity

Nitrification is the process in which ammonium oxidizing bacteria convert ammonium to nitrite which is subsequently oxidised to nitrate by nitrite oxidizing bacteria (Ward et al. 2011). Ammonia, especially in high pH conditions, can be toxic to microalgae (Collos and Harrison

2014), so its conversion to non-toxic nitrate is beneficial (Arauzo and Valladolid 2003). Furthermore, the biological oxidation of ammonia within the treatment plant is advantageous since oxidation in environments receiving the discharged wastewater is avoided, reducing the likelihood of DO depletion in these environments (Li et al. 2012). Spatial heterogeneity in inorganic nitrogen concentrations was observed within the HRAP. Within the dead zones where flow velocity was very low and the suspended solids concentration was very high, ammonium concentration was high and nitrite and nitrate concentrations were low. Moreover, ammonium concentration was significantly higher and nitrate and nitrite concentrations were lower at the bottom of the pond compared to the surface ($p < 0.001$). The observed stratification of nitrification in the HRAP was correlated with the stratification of suspended solids. The high concentration of suspended solids may contribute to the formation of micro-anaerobic zones within the organic flocs, reducing oxygen availability for nitrifying bacteria. The formation of those micro-anaerobic zones, not detectable using classical dissolved oxygen probes, may explain the depth stratification of nitrification and the inhibition of this process in the dead zones even while dissolved oxygen remains constant and above the limitation threshold. The ammonium concentration increased between the paddlewheel and the end of the channel (Figure 3.8) due to the mineralisation of organic nitrogen. The nitrite concentration remained constant (Figure 3.9), whereas nitrification, evidenced by the nitrate concentration, decreased with distance from the paddlewheel (Figure 3.10).

This relationship between nitrite and nitrate concentrations was consistent with incomplete nitrification. Several factors, including a potential imbalance between AOBs and NOBs within the wastewater, as well as substrate availability for nitrification, could contribute to incomplete nitrification. The availability of substrates required for nitrification is also a consideration. Despite the decrease in nitrification with distance from the paddlewheel, there was no evidence of DO limitation since DO remain high along the channel length. Flocs, comprising microalgae, bacteria and detritus, were present in the wastewater in November 2022 (Figure 3.11a). These flocs might create microenvironments and impact the diffusion of substrates such as $N\text{-}NH_4^+$, $N\text{-}NO_2^-$ and gases (O_2 and CO_2) essential for bacteria involved in nitrification. According to

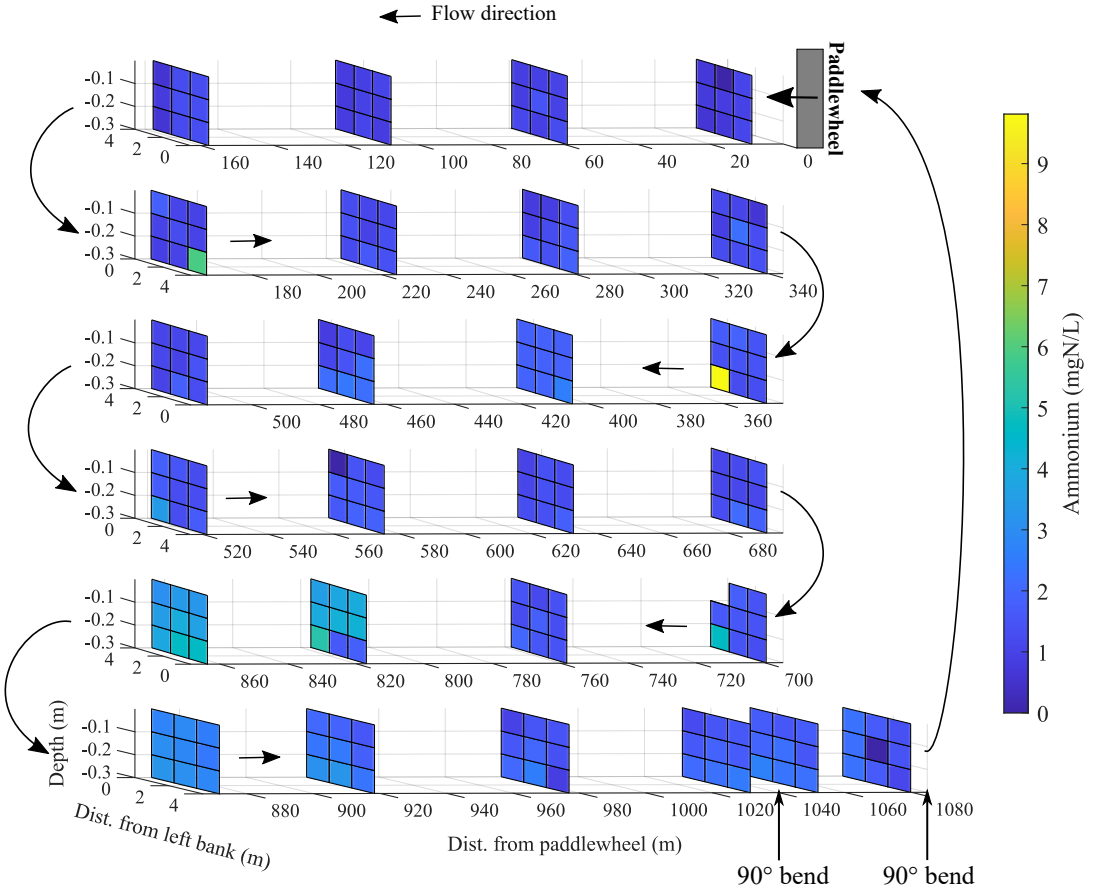

Figure 3.8 – Ammonium (mgN-NH_4^+.L^{-1}) in Peterborough HRAP throughout channel length, width and depth

Fan et al. (2017), smaller floc size can lead to higher oxygen diffusion property and higher NH_4^+ removal rates by nitrification. This study implies flocs size from 200 to 700 μm, comparable to the size of the flocs observed in Peterborough HRAP. According to this study, DO concentrations below 2 mg.L^{-1} could be observed within flocs of this size. Anaerobic conditions are then likely to be found inside the flocs found in Peterborough HRAP, even during the daytime. At night, DO in the water column drops and remains below 2 mg.L^{-1} for 7 h in Peterborough HRAP. During this period, anaerobic processes are likely to occur both in the water column and within the flocs. Furthermore, competition for these resources amongst bacteria within the flocs could also influence the nitrification. The observed decrease in nitrification along the channel

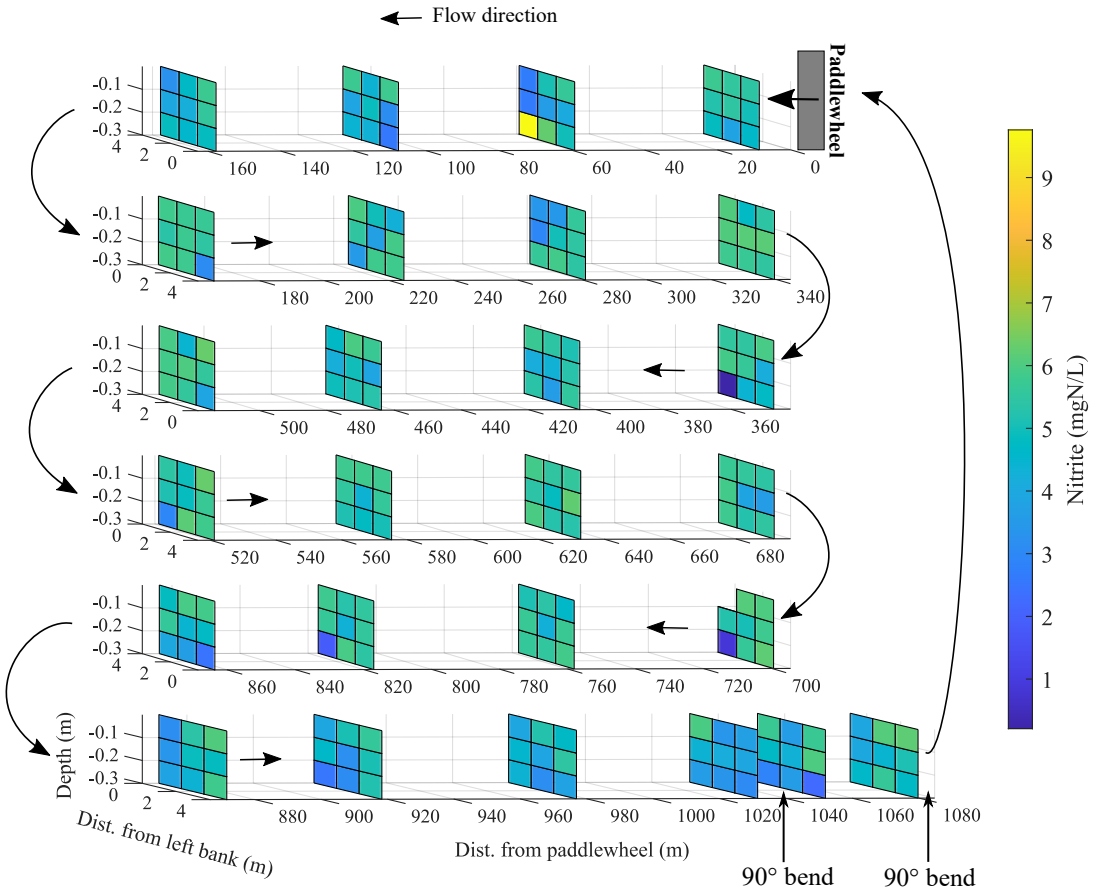

Figure 3.9 – Nitrites (mgN-NO_2^-.L^{-1}) in Peterborough HRAP throughout channel length, width and depth

length might be associated with the stability of the flocs (Fan et al. 2017). Flocs in Channel 1 may disaggregate after passing through the paddlewheel, providing better access to essential resources for nitrifying bacteria. Subsequently, the flocs may re-aggregate (Hargreaves 2013), re-establishing limitations on resources in subsequent channels where the flow velocity is similar to that in Channel 1 but with less turbulence. Measurements taken in June 2023 provide some support for this hypothesis. In contrast to those made in November 2022, nitrification increased with distance from the paddlewheel. Furthermore, the microalgae were planktonic and typically colonial in structure (Figure 3.11b). In the absence of complex flocs, the potential for microclimates within them to influence nitrification was also removed.

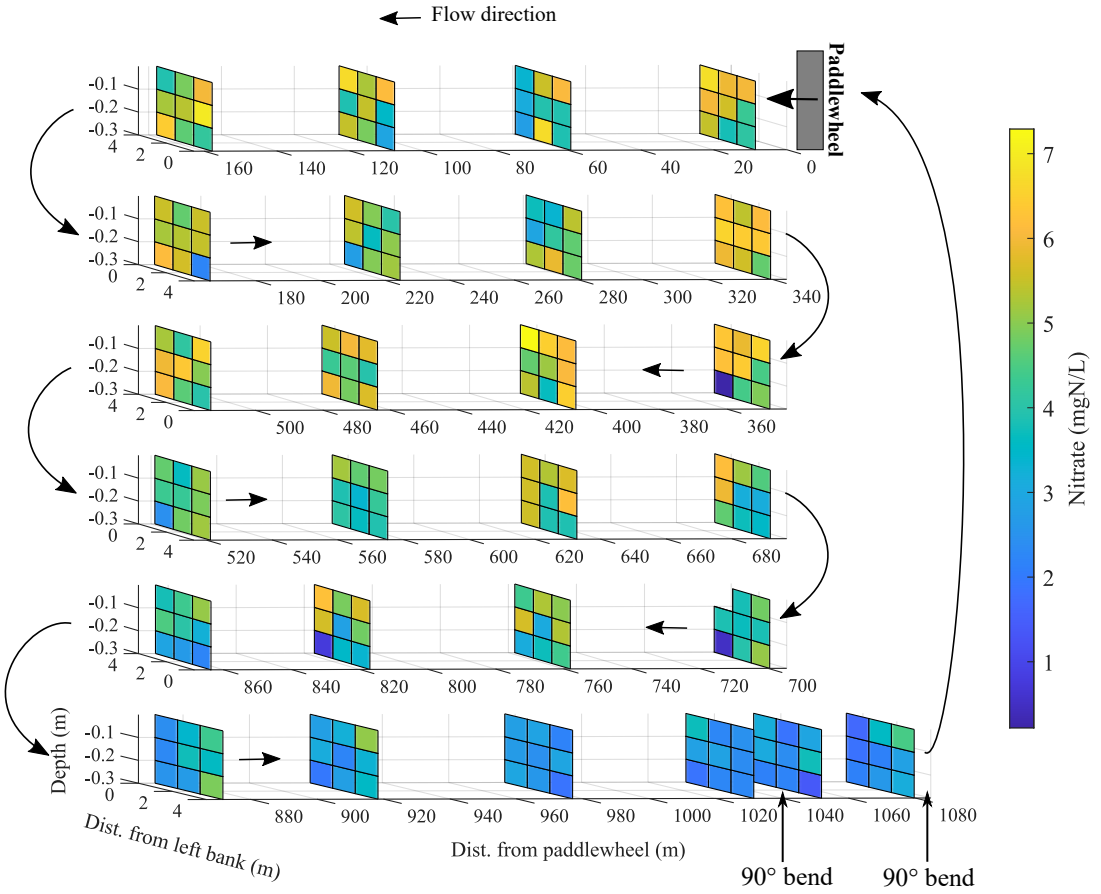

Figure 3.10 – Nitrates (mgN-NO_3^-.L^{-1}) in Peterborough HRAP throughout channel length, width and depth

Interrogation of the wastewater composition also provides a rationale for increased nitrification in Channel 1 in the November 2022 field campaign. Total inorganic carbon concentration (TIC) was lower in Channel 1 (17.4 mgC.L^{-1}) than in subsequent channels, where the mean concentration was 23.4 mgC.L^{-1} (Figure 3.12). High pH (8-10) of the HRAP wastewater influences the inorganic carbon equilibrium towards bicarbonate and carbonate ions and the absence of free CO_2. TIC stripping due to pH and paddlewheel turbulence is therefore an unlikely cause of the lower TIC concentration in Channel 1 compared with subsequent channels.

Similarly, the mean orthophosphates concentration was also lower in Channel 1 (5.6 mgP.L^{-1}) than in Channels 26, where the concentration was 7.0 mgP.L^{-1} (Figure 3.13). Given that pH

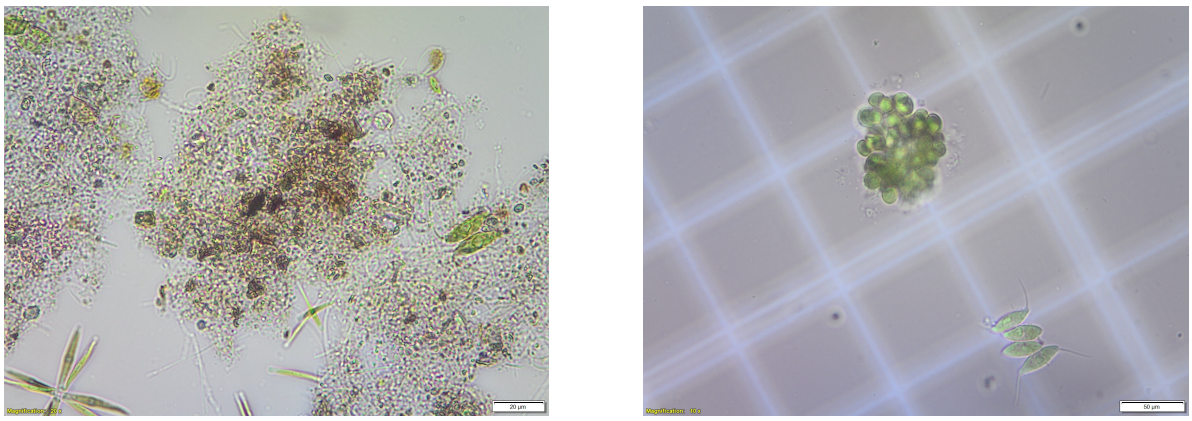

(a) (b)

Figure 3.11 – Microscopic observation of the HRAP wastewater during the first campaign in November 2022 (a) and during the second in June 2023 (b).

conditions were similar throughout the HRAP phosphate precipitation is unlikely the cause of the difference in Channel 1 compared with other channels. It is therefore likely that the lower orthophosphate and TIC concentrations in Channel 1 was due to higher consumption by microorganisms in the wastewater. Furthermore, the chlorophyll *a* concentration was constant throughout the HRAP; microalgae are unlikely responsible for the difference in orthophosphates and TIC consumption in Channel 1. Overall, the results indicate a higher nitrifying activity in Channel 1 likely due to higher nitrification in this channel.

3.3.7 Turbidity and attenuation of solar radiations

The absorbance at 750 nm of anaerobically treated wastewater and HRAP mixture were 0.6 and 2.0 respectively. Due to the high turbidity and depth of HRAP, the attenuation of Photosynthetically Active Radiations (PAR) was significant in the pond. Light was fully attenuated below 10 cm depth (Figure 3.14a), leaving two thirds of the ponds in the darkness. Besides, the Figure 3.14b shows that UVA radiations are fully attenuated below 1 cm depth. UVB radiations could not be measured inside the pond at all.

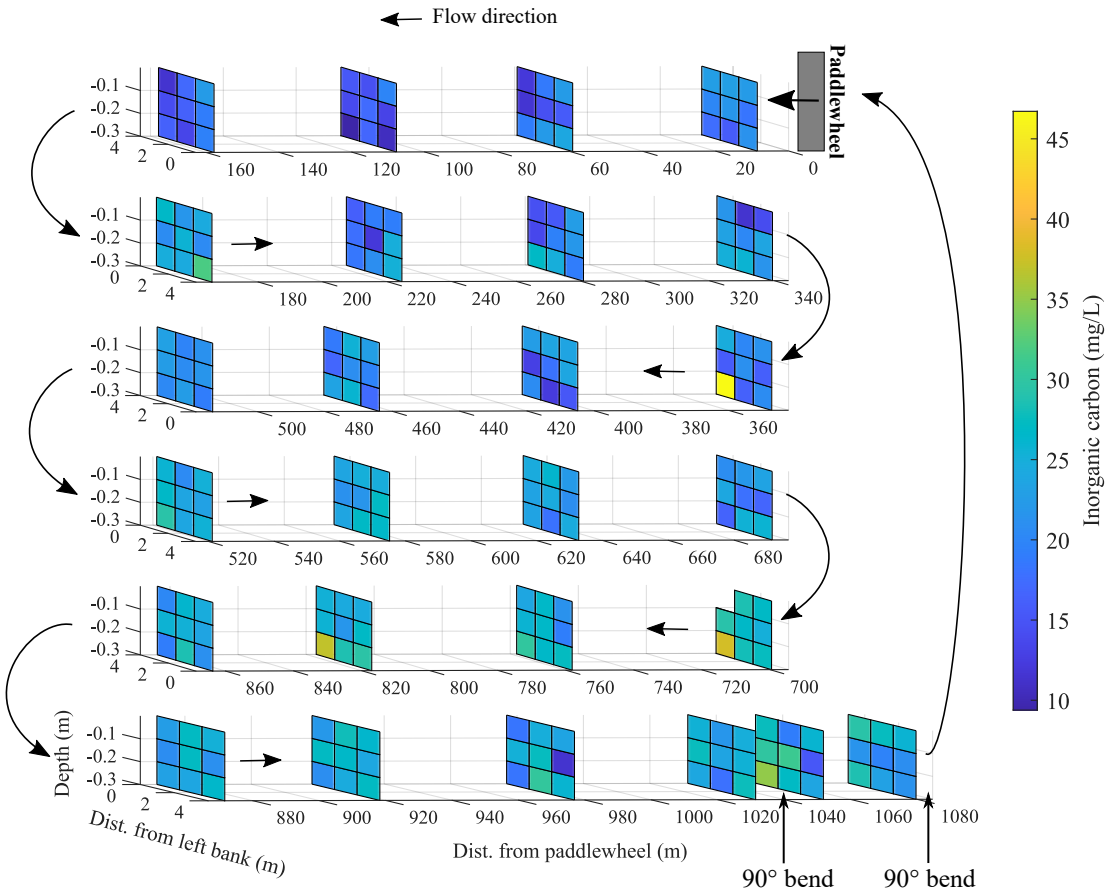

Figure 3.12 – Total inorganic carbon (mgC.L^{-1}) in Peterborough HRAP throughout channel length, width and depth

3.4 Discussion

3.4.1 Flow velocity

The mixing velocity of 0.2 m.s^{-1} has been widely adopted by HRAP practitioners (LGA 2020) since the work of Benemann et al. (1978) since it optimizes mixing, maintaining algal biomass in suspension while minimizing paddlewheel energy consumption. This value was attained and conserved along the 1 km channel of Peterborough HRAP. Yet, dead zones where flow velocity was very low or null were revealed at the exit of the bends. The mean cross sectional flow velocity was marginally higher at CS26 (0.29 m.s^{-1}), the last cross section before the paddlewheel,

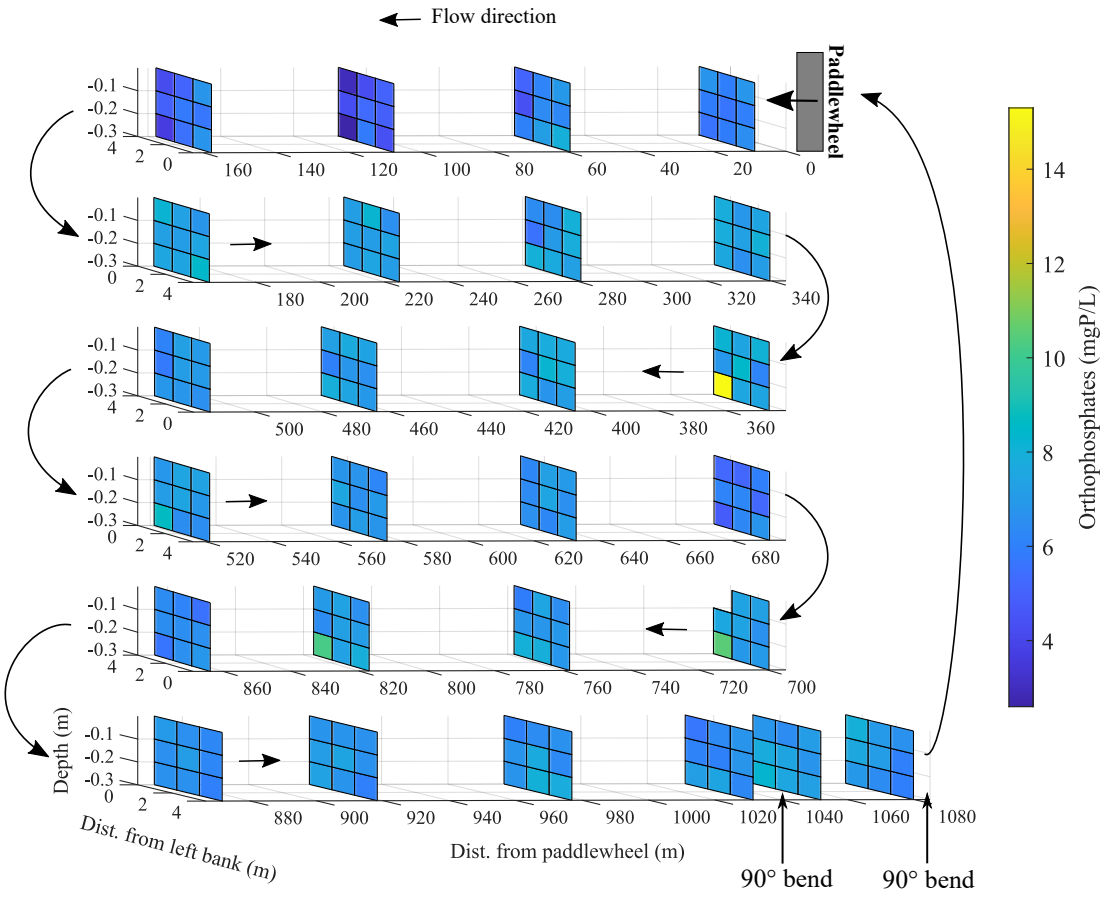

Figure 3.13 – Orthophosphates (mgP-PO_4^{3-}.L^{-1}) in Peterborough HRAP throughout channel length, width and depth

compared with CS1 (0.19 m.s^{-1}), the first cross section after the paddlewheel. In contrast, the mean cross sectional flow velocity must be conserved along the channel to satisfy the principle of mass conservation. This result suggests that increasing the number of measuring points per cross-section would improve determination of mean cross section flow velocity. However, is should be recognised that there are significant practical constraints when determining cross sectional flow velocities on a serpentine HRAP of this length.

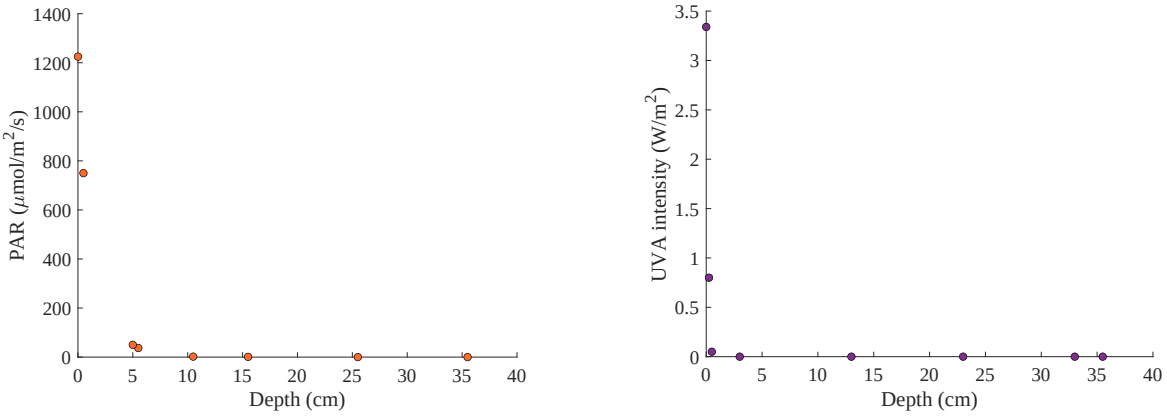

(a) (b)

Figure 3.14 – (a) PAR attenuation (μmol.m^{-2}.s^{-1}) and (b) UVA attenuation (W.m^{-2}) over the pond depth.

3.4.2 Suspended solids

CFD modelling of the trajectory of microalgal cells in raceways (Fernández del Olmo et al. 2021) predicted poor vertical mixing in raceway ponds mixed with a paddlewheel and suggested that populations of microalgal cells would be constantly deprived of light while others would be oversaturated. On the contrary, reconstruction of Lagrangian trajectories (Demory et al. 2018) in a pond of similar geometry demonstrated that cells change layers periodically due to paddlewheel mixing and that their position oscillate between top and bottom of the pond. In our study, similar to flow velocity, suspended solids concentration was conserved along the channel length, showing efficient suspension of biggest particles due to a sufficient flow velocity of 0.2 m.s^{-1} maintained along the channel length, with an exception in the dead zones where suspended solids tend to accumulate. Also, suspended solids concentration was significantly higher at the bottom of the pond compared to mid-depth and surface. However, samples pumped at 30 mm above the pond floor are likely to contain resuspended sediment not normally present within the water column.

3.4.3 Dissolved oxygen

No anaerobic zones were detected, even within the dead zones. The wastewater, in the large serpentine HRAP at Peterborough, was homogeneous regarding dissolved oxygen and chlorophyll *a* concentrations suggesting mixing supported uniform microalgal growth throughout the HRAP. Significantly, DO was homogeneous throughout the depth, showing paddlewheel mixing was sufficient to provide DO for heterotrophic aerobic degradation of organic molecules at all depths. In addition, measuring DO along a 1 km channel turned out to be challenging considering photosynthetically produced DO is dependent on irradiance and varies throughout the day. Estimation of the diurnal variation by setting up a fixed point was also associated with technical difficulties because of biofouling associated with prolonged deployment. For this reason, it is recommended to setup a wire mesh upstream the fixed sensor in order to prevent the plants to aggregate around the sensor and to form anaerobic zones around the sensor. The sensor should also be agitated regularly to dislodge any entrapped material fouling the sensor.

3.4.4 Nitrification

In the first sampling campaign in November, nitrification decreased with distance from the paddlewheel. Measurements repeated in June 2023, showed the opposite with a decrease in ammonium and an increase in nitrate with distance from the paddlewheel. This can be explained by the discharge of the influent rich in ammonium and lacking in nitrates just after the paddlewheel that leads to higher ammonium and lower nitrate in Channel 1 than in the next channels. Microscopic observation of the June samples showed very low numbers and size of organic flocs, whereas samples collected in November had much higher numbers of organic flocs. This suggests that organic flocs influence nitrification, potentially via incorporation of nitrifiers into flocs reducing access to substrates such as DO, CO_2, ammonium or nitrite. A previous study (Sutherland et al. 2020) demonstrated that nitrification was lower in larger ponds (1 ha) than in smaller ones (5 and 300 m^2). Considering that mixing is expected to be more heterogeneous in larger ponds, the hypothesis of a link between mixing/turbulence and nitrification was also considered in their study, supporting the hypothesis of the present study. Moreover,

microalgae turned out to represent only 30 % of total suspended solids in Peterborough HRAP, with the rest being flocs of organic detritus and bacteria from the anaerobic pond, and likely to form within micro-anaerobic zones unfavourable for nitrifiers. Nitrification may then be impacted by the quality of the anaerobic pond outlet. This hypothesis is supported by Foladori et al. (2020) that demonstrated that high total suspended solids was associated with a lower ammonium removal rate and nitrification due to lower global DO availability in the bulk water (no DO measurement was done within the flocs however). As both aerobic and anaerobic, denitrifying bacteria, are also expected to play a role in nitrogen removal (Evans et al. 2005) in Peterborough HRAP. Further investigations are needed to clarify associations amongst mixing, flocs size, nitrification and denitrification in micro anaerobic zones within flocs. Incomplete denitrification constitute a relevant object of study while considering the sustainability of the process as incomplete denitrification can significantly contribute to the production of the greenhouse gas N_2O (Shu et al. 2024). Nitrification and phosphorus removal could then be improved, however, enhanced competition between nitrifiers and microalgae for inorganic carbon might be expected. Microalgae could play a major role in nitrification by keeping a high dissolved oxygen concentration in the pond (Bankston et al. 2020). Nitrifiers could also be an interesting clue for phosphorus removal improvement. The area just after the paddlewheel, because of its higher turbulence, seems to be the most suitable area in the pond for nitrifiers development. However, even in this area, phosphorus concentration is still high compared to rejection standards (<2 $mgP.L^{-1}$, NRMMC 2006, ARMCANZ 1997), suggesting global biomass phosphorus uptake is in general too low compared to phosphorus inlet. Indeed, $P\text{-}PO_4^{-3}$ removal rate was only 13 %, while BOD_5 and NH_4^+ removal rates reached 73.7 % and 71.6 % respectively. Consequently, treated wastewater at the outlet of Peterborough HRAP could be used for irrigation of non-food crops but should not be discharged to surface water because of too high phosphorus concentration in the treated water.

3.4.5 Sun radiations

On a first hand, PAR measurements along the pond depth revealed that two thirds of the ponds were in the darkness, where respiration would be expected rather than photosynthesis. However, as demonstrated in the section 3.3.4, no stratification of dissolved oxygen was observed, confirming that mixing was efficient and supporting homogeneous DO throughout the HRAP.

On another hand, UV measurements revealed that UVA radiations were fully attenuated below 1 cm depth, while UVB could not even be detected inside the pond. The important attenuation of UV radiations in the pond is likely due to the very high turbidity, attributable to both microalgae and detritus from wastewater. Yet, pathogens inactivation, that constitutes a crucial step for reaching national requirements for treated water, relies on UV radiations that damages the DNA/RNA of viruses and microorganisms. This observation suggests that the very high turbidity in Peterborough HRAP could inhibit pathogens inactivation, questioning the global impact of microalgae on the efficiency of pathogens removal. The impact of turbidity induced by wastewater and microalgae on pathogens inactivation will be further investigated in Chapter 7.

3.4.6 Power consumption

Finally, conservation of flow velocity along the 1 km-channel with a low energy consuming paddlewheel demonstrates the potential of large scale HRAPs in improving energy efficiency: a power consumption of 2 $W.m^{-3}$ was needed for maintaining a flow velocity of 0.2 $m.s^{-1}$ in a 100 m^2 raceway (Mendoza et al. 2013), against only 0.7 $W.m^{-3}$ for Peterborough which is 50 times bigger in terms of area. Overall, the results demonstrate that a large-scale paddlewheel mixed HRAP maintains flow velocity and homogeneity throughout the pond, while economy of scale results in decreased power consumption per unit volume of treated wastewater when compared to smaller ponds.

3.5 Conclusion

The flow velocity and physicochemical 3D profile of a serpentine HRAP with 6 parallel channel sections was characterised for the first time. In situ cross-sectional measurements of flow velocity, dissolved oxygen, pH and contemporaneous wastewater sampling were conducted at 26 sites along the length (>1 km), depth (0.3 m) and width (4 m) of a 5000 m^2 HRAP. Peterborough HRAP turned out to be a surprisingly well-mixed pond allowing homogeneous photosynthetic and heterotrophic activity. Mean flow velocity of 0.2 $m.s^{-1}$ was conserved along the channel and wastewater was homogeneously over saturated with photosynthetically derived dissolved oxygen (DO >20 $mg.L^{-1}$) at midday. However, results suggest that nitrifiers could have been impacted by a lack of turbulence due to the distance from the paddlewheel, suggesting that the level of local mixing could be a more relevant parameter to evaluate HRAP mixing rather than flow velocity (Figure 3.15). Further investigations are needed to clarify associations amongst mixing, flocs size, nitrification and denitrification in micro anaerobic zones within flocs. Further research would be necessary to identify potential limiting parameters for biomass activity and improve the quality of the treated water, notably regarding microalgae-bacteria interactions. This Chapter provided an overview of the global availability of oxygen and carbon in a large-scale HRAP, however carbon and oxygen fate within the microalgae-bacteria consortium is still understudied. In the present study, organic carbon consumption was attributed exclusively to heterotrophic bacteria, however a fraction of the organic carbon present in wastewater is expected to be consumed by microalgae in mixotrophy, potentially impacting carbon and oxygen fate within the consortium. In order to provide a better understanding of microalgae-bacteria interactions, Chapter 4 will investigate the likelihood of organic carbon consumption by microalgae in HRAP and the interactions with light through a literature review, while Chapter 5 will experimentally determine the relative contributions of photoautotrophy and photoheterotrophy in mixotrophic algal growth in terms of carbon and oxygen fate, before determining the fate and role of carbon and oxygen in a microalgae-bacteria coculture in synthetic wastewater and simulated solar conditions in Chapter 6. The present chapter also revealed a very strong attenuation in HRAP of UV radiations from the sun involved in solar pathogens disinfection, raising an important issue regarding the impact

of microalgae on pathogens inactivation that will be further investigated in Chapter 7.

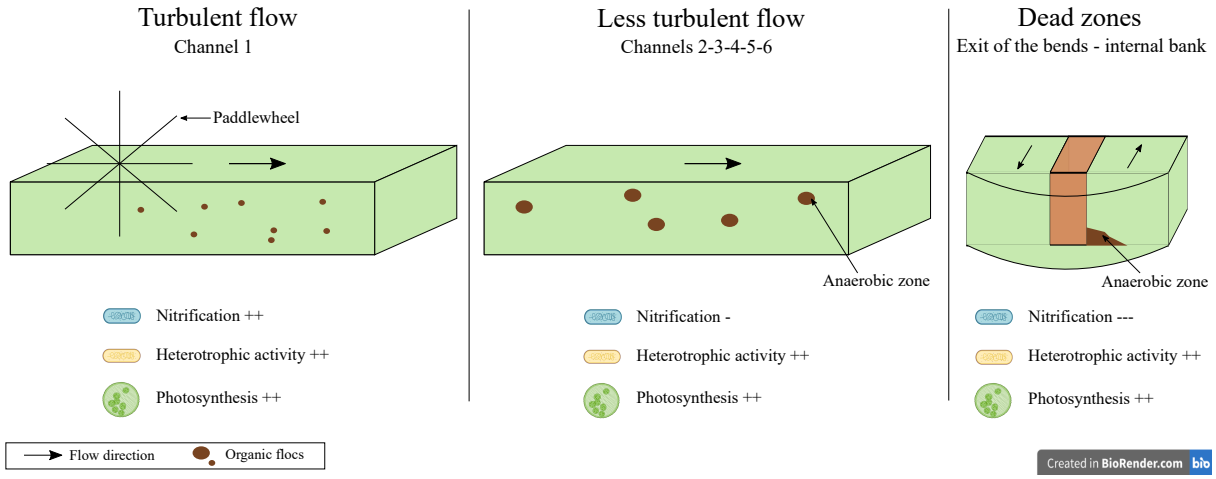

Figure 3.15 – Effect of the distance from the paddlewheel on different microorganmisms' populations in Peterborough HRAP

Highlights

- Serpentine 1 km length HRAP was well mixed.
- Homogeneous wastewater chemical and microbial composition was observed.
- Suspended solids influence nitrification.
- Penetration of solar radiations inside the pond was very low.

Chapter 4

Synergy between carbon source and light in microalgal culture from the perspective of wastewater treatment in high rate algal ponds

---

This Chapter has been published in Algal Research in the special issue Microalgae for wastewater bioremediation to fulfil new discharge limits of the Urban Wastewater Treatment Directive, vol. 79 (2024).

Co-authors contributions: Solène Jahan: Original draft (80%). Guillaume Cogne: Review & editing (10%). Jérémy Pruvost: Review & editing (2.5%). Mariana Titica: Review & editing (2.5%). Howard Fallowfield: Review & editing (5%).

4.1 Introduction

Using solar light as an energy source in microalgae-based wastewater treatment is crucial for maintaining sustainability. To maintain treatment efficiency, microalgae need to exhibit resilience, especially during periods of reduced sunlight. According to Young et al. (2019b), Suther-

land et al. (2014b), Buchanan et al. (2018b), Sutherland et al. (2020) and Paing et al. (2003), nutrient concentrations in the influent wastewater to HRAPs typically range from 1.2 to 6.3 mM NH_4^+ or NO_3^-, 0.2 to 0.4 mM PO_4^{3-}, and 0.6 mM SO_4^{2-}, after pretreatment either in anaerobic ponds, septic tanks, facultative ponds, or digesters. Mineral nutrients primarily arise from the degradation of organic molecules and are consequently naturally present in HRAP systems. It is then commonly assumed that nitrogen, phosphorus, and sulphur required for microalgal growth are present in excess in wastewater. As a result, light is often considered as the principal growth-limiting factor in HRAPs (Sutherland et al. 2015, Borowitzka and Moheimani 2013, Voltolina et al. 2005, Sutherland et al. 2021). However, the N/P ratio is not always optimal in wastewater from domestic settings. In certain cases, the supplementation of wastewater with nitrate has been shown to enhance microalgal growth rates compared to non-enriched wastewater (Mutanda et al. 2011). This indicates that while nutrient concentrations may generally be sufficient, the specific balance of nitrogen and phosphorus can influence microalgal growth in HRAPs.

In addition, the composition of the carbon source and its fate in biological processes can be variable in these systems. Carbon is the predominant element in algal biomass, representing nearly 50 % of the total biomass expressed as dry weight (Basu et al. 2013b). Typically, the primary carbon source for microalgae is CO_2, which, after dissolution in the liquid medium, is assimilated by photosynthesis (Pruvost et al. 2022). Autotrophic microalgal cultures without external CO_2 addition are usually limited by carbon (Le Gouic et al. 2021). However, when growing in wastewater, mineralization of organic matter by heterotrophic bacteria provides an additional source of CO_2 for algal autotrophic growth (Russel et al. 2020). In the context of algal wastewater treatment, organic matter may serve as a significant source of carbon not only for bacteria but also for microalgae (Nirmalakhandan et al. 2019). Although microalgae are mainly autotrophic (Li et al. 2023), many species can grow heterotrophically or mixotrophically. The question thus arises about the interaction and relative importance of organic and inorganic carbon sources for microalgal growth and their contribution to wastewater treatment. Some studies have explored the effect of sparging additional CO_2 on microalgal growth in wastewater-fed HRAPs identifying that while biomass productivity was not necessarily improved by CO_2 enrichment using CO_2

recovered from anaerobically produced biogas (Young et al. 2019b), a significant increase in both biomass productivity and nutrient removal was reported when sparging a mixture of 30% pure CO_2 and 70% N_2 into raceway ponds treating raw or anaerobically digested abattoir wastewater compared to non-enriched ponds (Ruas et al. 2020, Shayesteh et al. 2021). In these experiments CO_2 does not seem to interfere with organic carbon degradation; rather it is improved due to enhanced biomass concentration. The balance between autotrophic and photoheterotrophic growth in microalgae depends on the ratio of available energy from light and organic matter. This balance is considered to be influenced by algal acclimation to light changes during diurnal cycles (Nirmalakhandan et al. 2019). Microalgae have demonstrated the capacity to grow on certain organic molecules. However, the actual availability of organic molecules to microalgae in wastewater is not well understood due to dispersed and incomplete information about wastewater composition. While adaptation to changing light conditions in autotrophic environments has been partly investigated, the role of organic carbon uptake is still poorly understood.

Understanding how microalgae interact with and utilize organic carbon in wastewater can provide valuable insights into their growth dynamics and contribute to optimizing wastewater treatment processes in HRAPs. Further research is needed to elucidate the specific mechanisms and implications of organic carbon uptake by microalgae in wastewater treatment systems. This review aims to collate existing information on the varying composition of domestic wastewater and the affinity of microalgae for organic molecules, which may contribute to the growth of microalgae in wastewater HRAPs. This first section also addresses the availability of inorganic carbon in relation to HRAP physicochemical conditions. Subsequently, the review delves into possible synergies between organic and inorganic carbon consumption and the role of the carbon source in microalgal adaptation to light changes. Given the importance of using axenic cultures in any experiments investigating organic carbon consumption by microalgae, this review also takes into account research conducted using laboratory photobioreactors and defined media. Finally, the review considers the extrapolation of lab-based experimental results to the operation and performance of large scale HRAPs.

4.2 Relevance of microalgal consumption of organic and inorganic carbon in wastewater

4.2.1 Organic carbon

HRAP influent is typically subject to pretreatment leading to solids settlement and partial mineralization of organic molecules. After primary treatment in an anaerobic pond, the average organic load in wastewater is around 200 mgCOD.L^{-1} (chemical oxygen demand) (Assemany et al. 2015, El Hamouri et al. 2003, El Hamouri 2009). While a precise characterisation of organic molecules after pretreatment in a non-covered anaerobic pond is not easily ascertainable, the COD composition in raw domestic wastewater from the literature comprises 10-40 % lipid, 17-65 % proteins, and 12-67 % carbohydrate (Owusu-Agyeman et al. 2023, Lester 2001, Chipasa and Mdrzycka 2006, Xu et al. 2023, Huang et al. 2010, Ravndal et al. 2018). Huang et al. 2010 reported that volatile fatty acids and sugars represented 5.4 % and 11 %, respectively, of total COD in domestic wastewater. In swine wastewater, it was reported that acetate represented 70 % of total VFA (Wang et al. 2015). While large molecules like polysaccharides, cellulose, starch, or proteins can be degraded by heterotrophic bacteria, microalgae are limited to utilizing smaller molecules such as sugars, sugar alcohols, sugar phosphates, amino acids, and organic acids (Abeliovich and Weisman 1978, Abreu et al. 2022). Numerous species of microalgae can successfully grow on VFA as the sole carbon source (Huang et al. 2024, Patel et al. 2022, Su et al. 2021, Lacroux et al. 2020). *Scenedesmus obliquus*, for example, demonstrated an uptake of 98 % of butyrate, 97 % of propionate and 95 % of acetate (Lin et al. 2017). The affinity of this species for glucose is also clearly demonstrated (Abeliovich and Weisman 1978, Bouarab et al. 2004, Ye et al. 2023, Wang et al. 2022, Gao et al. 2021). Other species like *Selenastrum capricornutum*, *Chlamydomonas reinhardtii*, and *Chlorella vulgaris* are also capable of consuming organic nitrogen from wastewater (Sun and Simsek 2017). While research has shown that organic nitrogen is almost completely mineralised to ammonium during pretreatment in an anaerobic pond, resulting in low organic nitrogen concentrations in a HRAP (Zhao et al. 2018), some organic molecules are more readily available to microalgae; for example, a higher biomass of *Scenedesmus obliquus*

is reported in synthetic wastewater containing sucrose than in one containing humic acid (Zhao et al. 2023b) likely due to humus complex structure making it more resistant to microbial assimilation and degradation (Popa et al. 2022). Thus, microalgae are capable of utilizing VFA and sugars among the organic molecules found in wastewater. This utilization could account for 41 mgCOD.L^{-1} within a total COD of 249 mg.L^{-1} (Huang et al. 2010). However, VFAs are products of metabolic reactions such as fermentation that occur following anaerobic pretreatment upstream of the HRAP. Consequently, VFA concentrations are expected to be higher after anaerobic pretreatment than those reported for raw wastewater, thus demonstrating the importance of fully understanding the requirements of a pre-treatment schedule for effective HRAP operation.

4.2.2 Inorganic carbon

The CO_2 concentration in an aqueous solution in equilibrium with the atmosphere where the CO_2 concentration is 415 ppm (IPCC 2023), is $2.6{\cdot}10^{-6}$ mM at pH 7. The carbon uptake by microalgae typically far exceeds the atmospheric CO_2 diffusion rate (Sialve and Steyer 2013). The availability of inorganic carbon to microalgae in a wastewater-fed HRAP, without an external CO_2 supply, mainly relies on CO_2 produced by respiration. The total inorganic carbon concentration usually ranges between 1 and 3 mM in HRAP (Sutherland et al. 2021, El Ouarghi et al. 2003). Overall, biomass production is enhanced by a higher dissolved inorganic carbon (DIC) concentration up to a certain value where it can be considered non-limiting. This concentration is estimated at 1 mM DIC for *Chlorella vulgaris* (Le Gouic et al. 2021). However, the pH in HRAP often fluctuates between 8 and 11 (Sutherland et al. 2021). At those pH values, DIC is mainly in the form of HCO_3^- and CO_3^{2-}. Experiments suggesting that CO_3^{2-} cannot be used as an inorganic carbon source by microalgae were conducted at uncontrolled pH. Consequently, it is not possible to differentiate between the effect of CO_3^{2-} availability and the inhibition of cell mechanisms by high pH on algal growth (Gao et al. 2021).

4.2.3 Synergy between organic and inorganic carbon consumption

Despite the lack of information on the availability of inorganic carbon in wastewater for microalgae, there is general agreement in the literature that 1.3 mM organic carbon, which may be higher after pretreatment due to VFA production, and 1-3 mM TIC are potentially available to microalgae in wastewater (Figure 4.1). The presence of organic carbon in wastewater is often reported to result in an energetic gain for metabolism and enhanced algal growth (Nirmalakhandan et al. 2019, Abreu et al. 2022, Bouarab et al. 2004, Cecchin et al. 2018). The capacity of microalgal species to utilize inorganic or organic carbon sources is influenced by external environmental conditions such as pH and by the specific ability of the microalgal strain to use either sources (Gao et al. 2021, Pobernik et al. 2008, Duan et al. 2020, Alkhamis and Qin 2013, Nair and Chakraborty 2020). An intermediate metabolism response during simultaneous photoheterotrophic and photoautotrophic activity has been investigated for a broad range of microalgal species (Shoener et al. 2019b).

Gao et al. considered the impact of the ratio of total inorganic carbon (TIC) as CO_3^{2-} and HCO_3^- to total organic carbon (TOC) as acetate and glucose on biomass production by *Chlorella vulgaris* (Gao et al. 2021). When using glucose as the organic carbon source, the TIC:TOC ratio that achieves the highest biomass is 2:1, whereas it is 3:1 when using acetate. They demonstrated an influence of the TIC:TOC ratio on RuBisCO and citrate synthase activity, with the highest RuBisCO activity measured when the carbon source is only inorganic. In contrast, the highest citrate synthase activity is when the carbon source is only organic. As the TIC:TOC ratio decreases, RuBisCO activity also decreases from 1594 $U.g^{-1}$ when TIC is the sole carbon source to 500 $U.g^{-1}$ when TOC is the only source. In comparison, citrate synthase activity increases from approximately 300 $U.g^{-1}$ when the carbon source is solely TIC to 5542 $U.g^{-1}$ when only TOC is the source. This relationship is maintained regardless of the carbon composition of the TIC (carbonate or bicarbonate) or TOC (acetate or glucose) source used, even while those compounds have a reverse impact on pH. It is important to note that in wastewater, TOC is predominant compared to TIC, with a TIC:TOC ratio close to 1:2. However, this ratio considering the actual availability of TOC for microalgae is probably closer to 1:1. The

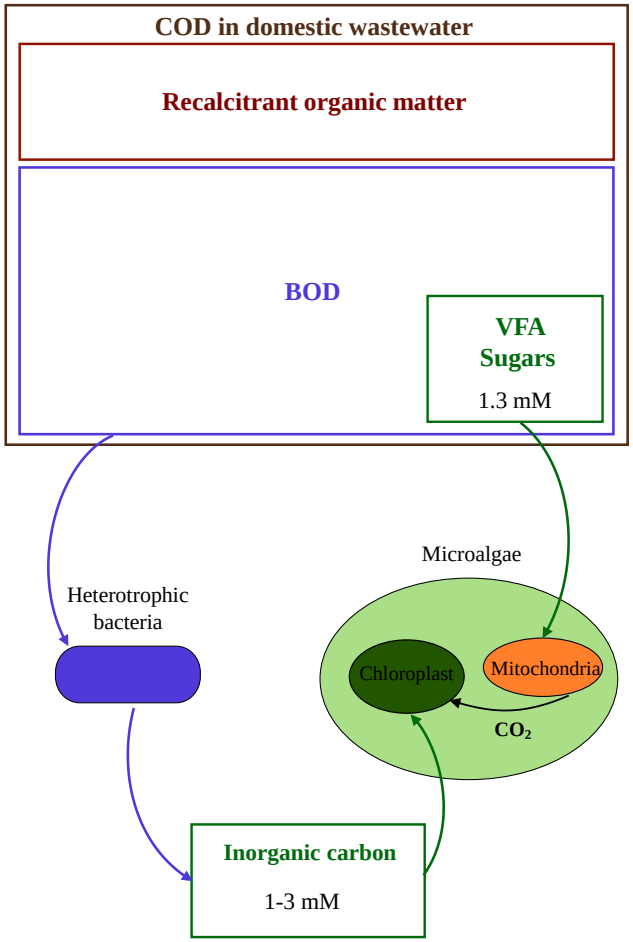

Figure 4.1 – Overview of carbon sources assimilable by microalgae in domestic wastewater

mechanisms regulating photosynthesis were compared in cultures of *Chlorella sorokiniana* in autotrophy (sparged with 1 % CO_2) and mixotrophy (33.3 mM of glucose in the culture medium and sparged with 1 % CO_2) at an irradiance of 100 μmol.m^{-2}.s^{-1} by measuring the efficiency of the photosynthetic system located in the thylakoid membrane (Li et al. 2016). In contrast to previous results (Gao et al. 2021), photosynthetic activity increases in the cultures with glucose compared to the autotrophic cultures sparged with CO_2. However, the autotrophic cultures may be limited for carbon, and the higher photosynthetic efficiency in mixotrophic cultures may be due to the availability of additional CO_2 produced by glucose oxidation. Another study

(Cecchin et al. 2018) claims that, in mixotrophic cultures with acetate, the microalgae *Chlorella sorokiniana* is recovering CO_2 produced by acetate oxidation, suggesting the hypothesis of an alternative carbon fixation pathway in parallel to the Calvin cycle, which utilizes inorganic carbon produced in mitochondria. Additionally, there are indications of possible exchanges between the mitochondria and the chloroplast through the cytosol, facilitated by the ADP/ATP exchange carrier on the chloroplast and mitochondria membranes of *Chlorella zofingiensis*. This enables coordination between photosynthesis and respiration (Zhang et al. 2017), offering a potential explanation for the observed phenomenon where biomass production in mixotrophy exceeds the sum of autotrophy and heterotrophy. In this study (Cecchin et al. 2018) as in others (Gao et al. 2021), RuBisCO and citrate synthase activity are both reduced in mixotrophy compared to autotrophy and heterotrophy, respectively. The higher growth observed in mixotrophy requires more energy, supporting the hypothesis of coordination between photoautotrophy and photoheterotrophy in mixotrophy for *Chlorella vulgaris*. Since glucose is available outside the cell, the necessity for the microalgae to produce organic carbon by photosynthesis may be reduced, explaining down-regulation of the Calvin cycle. Consequently, only a fraction of the ATP produced in the thylakoid membrane during the light phase serves in the Calvin cycle for carbon fixation, with the remainder being transported in the cytosol for cell metabolism (Zhang et al. 2017). In contrast, other studies with *Chlorella sorokiniana* (Abiusi et al. 2020) and *Micractinium pusillum* (Bouarab et al. 2004) report that autotrophic and heterotrophic growth are independent processes and that the sum of biomass production by these two growth modes is equal to biomass production in mixotrophy.

4.3 Impact of light on microalgae in HRAP under autotrophic, heterotrophic and mixotrophic conditions

4.3.1 Light availability in HRAP

In open systems exposed to sunlight, incident light on the culture system varies depending on day-night cycles, sun trajectory, cloud cover, and culture system configuration (Chiu et al. 2016).

Light attenuation also occurs due to wastewater turbidity and self-shading of microalgae cells. At an incident photon flux density of 100 μmol.m^{-2}.s^{-1}, full attenuation was achieved in the first 30 cm of a 40 cm deep HRAP containing 0.27 g.L^{-1} of microalgae and 2.5 mg.L^{-1} of chlorophyll *a* (Kim et al. 2018); the bottom 10 cm were a dark zone in the HRAP. Biomass concentration in the pond and microalgae pigmentation emerge as key factors (Bonnanfant 2020). Dark volumes negatively impact biomass productivity, dependent on the residence time of microalgae in the dark zone (Pruvost et al. 2015, Demory et al. 2018). In an intentionally mixed HRAP, microalgae experience a dynamic interplay between both dark and photoinhibiting conditions, and a constantly changing fluence rate dependent on mixing and light attenuation throughout the HRAP.

4.3.2 Impact of day-night cycles on biomass growth

Adaptation mechanisms within the microalgal cell optimize light utilization efficiency and prevent cell damage in the diurnal conditions of HRAP operation (Bonnanfant et al. 2021). These adaptative processes can manifest in a matter of minutes to a few days from the onset of light perturbation. Additionally, more extended processes related to strain selection occur over the course of the season in open ponds (Assemany et al. 2015), although these will not be discussed further here. The impact of low and high light on autotrophic microalgae cell is relatively well known and is synthetized in Table 4.1.

Different behaviours are observed in presence of organic carbon. There is no biomass loss at night when fed-batch cultures of *Chlorella sorokiniana* receives a 100 % increase in acetate concentration, from an initial supply rate of 0.11 ml of acetic acid per day (Nair and Chakraborty 2020). Although mixotrophic microalgae should theoretically be able to use external organic carbon as an energy source for growth in the dark, several studies report that no growth occurs in the dark in the presence of glycerol, glucose or acetate, suggesting that adding organic carbon to the culture medium may only limit biomass losses by providing energy without allowing biomass production (Alkhamis and Qin 2013, Gao et al. 2022). The highest growth rate of *Micractinium pusillum* is measured at an irradiance of 182 μmol.m^{-2}.s^{-1} in autotrophic conditions (growth

	Low light (predominance of respiratory activity)	High light (saturating irradiance conditions)
Conditions in HRAP	Irradiance below 110 μmol.m^{-2}.s^{-1} (Legrand et al. 2016)	Can reach 2000 μmol.m^{-2}.s^{-1} in summer (Artu 2016)
Impact on algal biomass	• Loss of 1 % of biomass per hour (Bonnanfant et al. 2021) • 6-20 % of biomass loss over a 10 h-night (Artu 2016, Hindersin et al. 2014) • Reduction of carbon fixation efficiency (Ye et al. 2023) • Regulation of carbohydrates consumption at night (Baroukh et al. 2016) • Low temperature at night slows down the decrease in biomass (Hindersin et al. 2014, Edmundson and Huesemann 2015, Le Borgne and Pruvost 2013)	Stagnation or decrease of algal growth (Breuer et al. 2013, Gris et al. 2014)
Impact on light stress		• Acceleration of electron transport away from PSII (Bonnanfant et al. 2019) • Photoinhibition ($F_v/F_m < 0.7$) after a step from 75 to 765 μmol.m^{-2}.s^{-1} (Bonnanfant et al. 2021) • Drop in oxygen production, F_v/F_m and growth rate (Vonshak et al. 2000)
Impact on pigments	40 % less pigments in darkness than in light conditions (Abeliovich and Weisman 1978)	• 80 % loss in chlorophyll after a step from 700 to 1500 μmol.m^{-2}.s^{-1} (Krimech et al. 2022) • Takes several hours to occur (Legrand et al. 2016)
Impact on cell composition	Less carbohydrates than in light conditions because of respiration (Gao et al. 2022)	Increase in lipids and carbohydrates accumulation (Deng et al. 2019, Gao et al. 2022, Agarwal et al. 2019)
Impact on enzymes	Increase of citrate synthase activity (Gao et al. 2022)	Increase of RuBisCO activity (Gao et al. 2022)

Table 4.1 – Impact of low irradiance and high irradiance on algal cell in autotrophy

rate of 0.58 d^{-1}) compared with an irradiance of 150 μmol.m^{-2}.s^{-1} in mixotrophic conditions (0.82 d^{-1}) (Bouarab et al. 2004), showing that adding organic carbon not only increases the growth rate but also reduces the irradiance required to achieve the maximum rate. This hypothesis is confirmed by a study (Agarwal et al. 2019) showing that the biomass obtained after 8 days in a mixotrophic batch culture using 2.7 mM glucose as an organic carbon source irradiated at 100 μmol.m^{-2}.s^{-1} is similar to that obtained by autotrophic cultures irradiated at 900

μmol.m^{-2}.s^{-1}. Additionally, a review (Abreu et al. 2022) also reports that microalgae need less energy from light in the presence of organic carbon. In contrast, it is reported (Li et al. 2020) that increasing irradiance in the absence of organic carbon could lead to greater biomass production than in the presence of organic carbon, further suggesting that this is a consequence of the degradation of photosynthetic pigments induced by the presence of organic molecules. Other studies (Zhang et al. 2017, Li et al. 2014) claim the contrary, implying that the presence of organic carbon contributes to photoprotection mechanisms (see below). A culture of *Chlorella protothecoides* at 25 °C on a 16:8 h day:night cycle at 150 μmol.m^{-2}.s^{-1} in the presence of glucose produces twice the biomass compared to simple autotrophic growth, whereas the same biomass production is determined for autotrophic and mixotrophic conditions under continuous light, highlighting the role of organic carbon in adaptation to day-night cycles (Patel et al. 2019). Significant interactions between trophic conditions and photoperiod are also shown for *Isochrysis galbana* grown on acetate, glucose, and glycerol at 50 μmol.m^{-2}.s^{-1} (Alkhamis and Qin 2013). Autotrophic cultures yielded lower biomass than mixotrophic cultures and are not affected by photoperiod. However, photoperiod affects the biomass yield of mixotrophic cultures: when the light period is 4 h biomass decreases and increases when light period is increased to 12 h. This difference suggests that microalgae in autotrophic conditions are limited by carbon (no inorganic carbon supply is noted in the study) and not by light, which would not be the case for the mixotrophic culture as they were supplied with additional organic carbon. In comparison, the effect of light period on microalgae has been investigated for *Aphanothece microscopica Nageli* grown in autotrophy in non-limiting inorganic carbon conditions (Jacob-Lopes et al. 2009). Biomass production is positively correlated with the duration of the light period. Consumption of CO_2 is also positively correlated with biomass productivity and the light period. The reported responses to light may be species-related since the organisms used in the studies reviewed above were *Chlorella protothecoides* (chlorophyte), *Isochrysis galbana*(haptophyte), and *Aphanothece microscopica Nageli* (cyanobacteria).

4.3.3 Effect on light stress

Hydrodynamic modelling of cell trajectory in a single-loop HRAP suggests that cells could experience abrupt light changes from limiting to inhibiting irradiances in a short time scale (12 s) (Demory et al. 2018). Photoinhibition, measured through non-photochemical quenching NPQ and F_v/F_m, occurs at lower irradiances in autotrophic cultures than in mixotrophic cultures (Abreu et al. 2022), indicating potential photoprotection linked to organic carbon uptake, as observed in *Spirulina sp.* cultivated on glucose. Additionally, it has been reported that the growth rate and F_v/F_m of autotrophic cultures of *Spirulina platensis* are more sensitive to irradiance changes than those growing mixotrophically (Vonshak et al. 2000). The growth rate in autotrophic cultures starts to decrease at an irradiance of 150 μmol.m^{-2}.s^{-1}, while mixotrophic cultures maintain the same growth rate at 75 to 150 μmol.m^{-2}.s^{-1}. Furthermore, at high irradiance (3000 μmol.m^{-2}.s^{-1}), a decrease in oxygen and the maximum efficiency of PSII is more pronounced in autotrophic than mixotrophic cultures. High light stress could be energetically costly for the cell, and cells cultivated in mixotrophy seem to recover faster from high light stress, potentially resulting in energy savings. However, it is also reported that as the irradiance increases to above the light saturation irradiance for photosynthesis, the difference in growth rate between autotrophic and mixotrophic cultures decreases, suggesting a similar inhibitory effect at high irradiances occurs in the presence or absence of organic carbon (Bouarab et al. 2004). Finally, in *Spirulina platensis*, the maximum photosynthetic rate, light saturation point, light compensation point, and dark respiration are reported to be higher in mixotrophic than autotrophic cultures (Vonshak et al. 2000). Nevertheless, some studies cited in a mixotrophic review (Abreu et al. 2022) often report disruptions of the photosynthetic apparatus in the presence of organic carbon sources.

4.3.4 Effect on pigments

Several studies cited in a mixotrophic review (Abreu et al. 2022) report lower pigment contents in microalgal biomass (chlorophyll *a*, chlorophyll *b* and carotenoids) in microalgal cells when cultivated with organic carbon compared to autotrophic algal cells. For instance, at 900

μmol.m^{-2}.s^{-1}, chlorophyll a cell content decreases by 45 % between autotrophic and mixotrophic cultures (Agarwal et al. 2019). Those findings are consistent with other studies indicating that mixotrophic cells are less dependent on light, making pigments less crucial for cell energy production. The reduction in pigment content may serve to mitigate the risk of photoinhibition, and the increased respiration in mitochondria, observed in mixotrophic cells, could also interfere with pigments synthesis (Abreu et al. 2022). Another study (Agarwal et al. 2019) suggests that mitochondrial electron flow could affect chlorophyll content. However, it is important to note that a better correlation exists between irradiance and pigments than between carbon source and pigments (Vonshak et al. 2000). Additionally, when comparing and interpreting pigment content data (g pigment.g biomass^{-1}), the varying algal biomass between autotrophic and heterotrophic cultures should also be considered, as microalgae tend to produce more pigments when biomass increases to compensate for the adverse effect of self-shading (Abreu et al. 2022).

4.3.5 Effect on cell composition

High irradiance can induce oxidative stress in microalgal cells, and lipids within the cell can act as receptors for excess electrons, playing a protective role. Interestingly, mixotrophic cells do not increase their lipid content for protection against high irradiance (Agarwal et al. 2019). While the lipid content of mixotrophic cells is higher than that of autotrophic cells, this is not a response to irradiance but a consequence of utilizing external carbon source for lipid synthesis. In contrast, autotrophic cells rely on their internal carbon stocks. Another study (Shishlyannikov et al. 2014) supports this findings and emphasizes the role of acetate in enhancing fatty acid synthesis. Although high irradiance does not significantly impact the lipid content of mixotrophic cells, dark conditions can have an effect (Zhang et al. 2017). Dark incubated, heterotrophic cultures of *Chlorella zofingiensi* exhibit higher carbon and fatty acid contents compared to irradiated mixotrophic cultures. Typically, an increase in fatty acid and starch content leads to a decrease in the percentage of proteins. Changes in irradiance and carbon source availability can also result in a transfer of carbon atoms from proteins to lipids (Agarwal et al. 2019). In the study, the response to irradiance in terms of metabolite production was investigated, and high irradiances

led to accumulation of sugars, which act as osmo-protectants for the cell membrane. The level of the antioxidant trehalose was found to be 9 times higher under high irradiance conditions (900 μmol.m^{-2}.s^{-1}) compared to incubation at 100 μmol.m^{-2}.s^{-1}. Additionally, more trehalose is found in cells grown in the presence of organic carbon, leading to an alteration of photosynthetic activity. The study suggests that carbohydrate and lipid synthesis may be favoured in the presence of organic carbon in the culture medium, especially under stressful irradiance conditions. In conclusion, the cellular composition of mixotrophic algae plays a significant role in enhancing photoprotection at high irradiance. These cells demonstrate the ability to modulate pathways such as internal organic molecule stocks, pigments, and carbon utilization depending on the available carbon source and the level of irradiance to which they are exposed.

4.3.6 Effect on RuBisCO and citrate synthase activities

The effect of irradiance on microalgal enzymes when grown in presence of both organic and inorganic carbon has been studied by measuring RuBisCO and citrate synthase activities for irradiances from 0 to 222 μmol.m^{-2}.s^{-1}, at TIC:TOC ratios of 1:1 and 3:1 (Gao et al. 2022). The applied organic carbon supply of 16.7 mM is comparable to the total organic load in wastewater but may not align precisely with the organic load available for microalgae. RuBisCO activity was reported to increase with TIC:TOC ratios while the opposite was observed for citrate synthase activity. Nevertheless, RuBisCO activity increases with increasing irradiance regardless of the TIC:TOC ratio. The maximal RuBisCO activity (approximately 2000 U.g^{-1}) is observed at 150 μmol.m^{-2}.s^{-1}. In contrast, citrate synthase activity increases as irradiance decreases, reaching its maximum value in darkness (approximately 3400 U.g^{-1}). Despite this higher citrate synthase activity and the consumption of external organic carbon in darkness, productivity in the dark is zero. This suggests that the external organic carbon only compensates for ATP demand to prevent biomass losses, and light is necessary to observe net growth. Similar results are reported (Zhang et al. 2017), highlighting a decrease in citrate synthase activity in the presence of light compared to incubation in the dark, both in the presence of organic carbon.

4.3.7 Effect on carbon uptake

Light is directly correlated with the growth rate and should consequently have an impact on carbon consumption. It is reported (Deng et al. 2019) that the duration of the light period (from 0 to 24 h) in a day-night cycle has no effect on glucose uptake by *Chlorella kessleri*. This finding is not supported by another study (Mitra et al. 2012), where a longer dark period is found to increase the storage of carbohydrates in *Chlorella vulgaris* from glucose present in large quantities in the culture medium. It is reported that at 25 °C, *Chlorella vulgaris* grown in mixotrophic conditions (with glucose and bicarbonate supply) and at an irradiance of 93 μmol.m^{-2}.s^{-1} removes 81 % of the supplied organic carbon after 9 days of batch culture, compared to 88 % at 222 μmol.m^{-2}.s^{-1} (Gao et al. 2022). In contrast, the optimal irradiance for the growth of *Chlorella kessleri* is measured at 90 μmol.m^{-2}.s^{-1} (Deng et al. 2019). However, glucose uptake is favoured by lower irradiances between 30 and 90 μmol.m^{-2}.s^{-1}. These results align with previous findings (Patel et al. 2019), demonstrating that under non-limiting light conditions (150 μmol.m^{-2}.s^{-1}), glucose does not enhance microalgal growth. It is also emphasized that under optimal irradiance conditions, where microalgal growth is not limited by energy supply, organic substrate is not assimilated (Bouarab et al. 2004). On the contrary, when irradiance is too low, cytochromes linked to respiration process are synthesized. It is reported that, to compensate for the absence of light, the maximal rate of acetate consumption is 1.6 times higher in the dark than in the light, and the affinity for the substrate is 1.3 times higher. Moreover, when respiration is artificially inhibited, a reduction of acetate incorporation of only 17.8 % is observed in irradiated conditions compared to 49.8 % in dark-incubated cultures, highlighting a metabolic adaptation to irradiance in terms of carbon uptake. In conclusion, microalgal mechanisms are constantly transitioning in day-night cycles. In solar conditions, the transition from 765 to 75 μmol.m^{-2}.s^{-1} can occur in only a few hours, especially in sunny conditions at the end of the day and even quicker in cloudy conditions. A theoretical investigation of microalgae culture in light-changing conditions reports that optimal light conversion is impossible in solar conditions due to the rapid kinetics of radiation conditions compared to those associated with photosynthetic growth. This often results in high photon flux densities combined with low biomass concentrations and an

increased risk of an oversaturating light climate (Pruvost et al. 2015). The global influence of organic carbon on adaptation to darkness and excessive light is summarized in Figure 4.2.

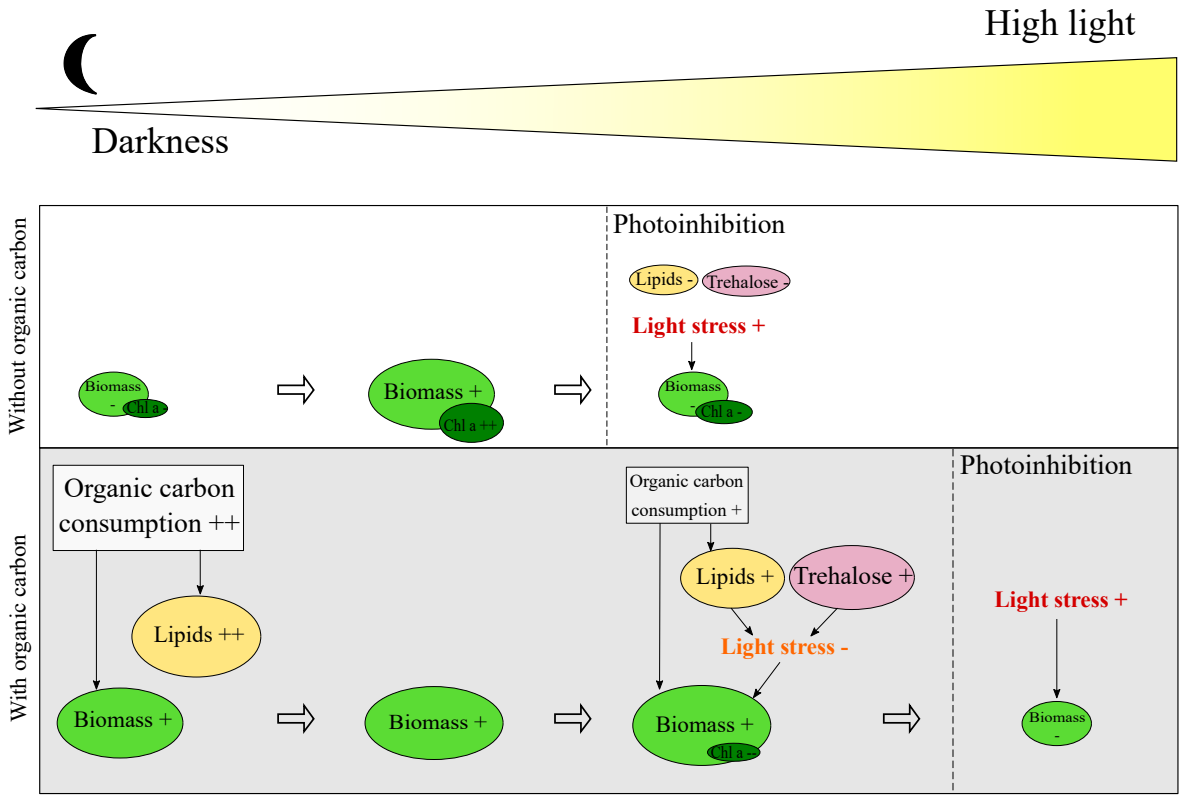

Figure 4.2 – Impact of irradiance on microalgae in presence and absence of assimilable organic carbon

4.4 Lab-scale experiments representativity of HRAP actual conditions

Most of the laboratory studies cited in this review concur that assimilating organic carbon enhances microalgae productivity, energy efficiency, and the synergy between heterotrophy and autotrophy. Some studies indicate that algal light requirements decrease in the presence of organic carbon, and low irradiance is associated with increased organic carbon consumption. Additionally, organic carbon uptake leads to higher fatty acid content, contributing to improve

photoprotection under high irradiance conditions. Research also suggests that supplying organic carbon can mitigate biomass loss in dark conditions. At the enzymatic level, RuBisCO and citrate synthase activity are strongly related to the TIC:TOC ratio and irradiance, indicating the cells ability to adjust photosynthesis and respiration based on the provided carbon source and light intensity (Figure 4.3). To evaluate the relative significance of these phenomena in HRAP systems, it is crucial to compare the conditions under which these laboratory findings are derived with those expected to occur in a HRAP. The concentration of organic carbon utilized in the laboratory studies mentioned above range from 16.7 to 200 mM and the supplied molecules (acetate, glucose, glycerol) are consistently well assimilated by microalgae (Gao et al. 2021, Deng et al. 2019, Lin and Wu 2015, Li et al. 2016, Gao et al. 2022, Agarwal et al. 2019). In contrast, the organic carbon concentration in anaerobically pre-treated wastewater is lower, typically varying between 8.3 and 16.7 mM (Assemany et al. 2015, El Hamouri et al. 2003, El Hamouri et al. 1995, El Hamouri 2009). The concentration of organic carbon potentially consumable by microalgae could be roughly estimated at around 1.3 mM by cross-referencing wastewater composition data with studies investigating microalgaes affinity for different organic carbon sources (Huang et al. 2010, Abeliovich and Weisman 1978, Huang et al. 2024, Patel et al. 2022, Su et al. 2021, Lacroux et al. 2020, Bouarab et al. 2004, Ye et al. 2023, Wang et al. 2022, Gao et al. 2021). In conclusion, while organic carbon consumable by microalgae in wastewater can constitute a non-negligible part of the total organic carbon present, both the concentration and the affinity by algal species are often much lower than in the studies cited above. Consequently, heterotrophy is likely to be less relevant in HRAP systems than in laboratory-scale studies included in this review.

While light is a crucial parameter for investigating the contribution of photosynthetic growth of microalgae, relying solely on lab-scale experiments to represent real outdoor conditions poses challenges. For example, the incident photons flux density applied in all the laboratory studies cited in this review is typically lower than the average values obtained in solar conditions in an HRAP, especially in summer (>1000 μmol.m^{-2}.s^{-1}). Additionally, the condition of light attenuation, which provides more insight into photon availability for the culture as it is related to the

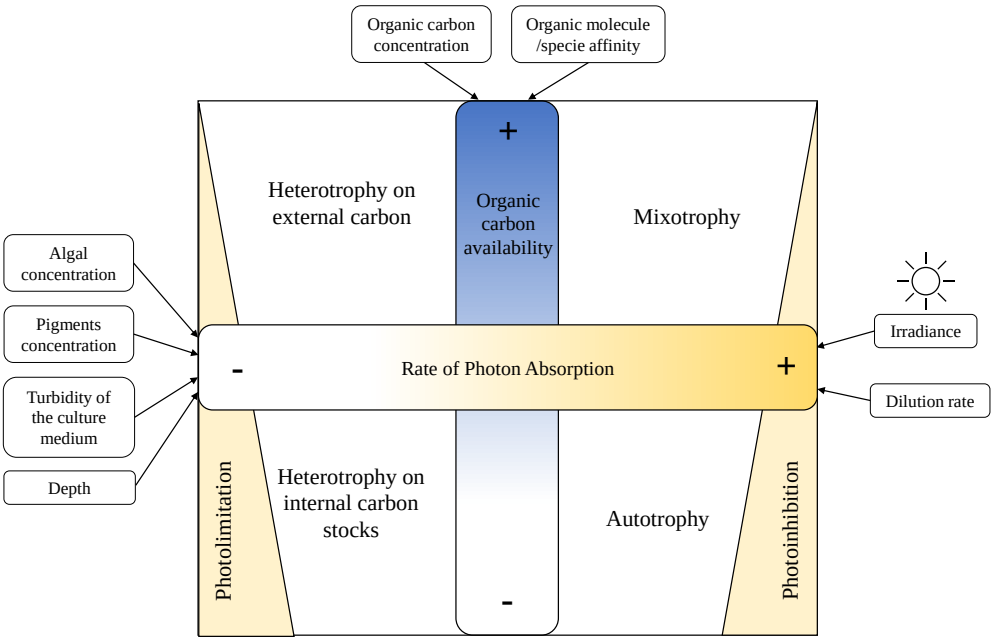

Figure 4.3 – Overview of factors influencing light and organic carbon availability for microalgae and the different trophies occurring depending on variations in those conditions

light effectively received by microalgae cells, depends on a complex set of interdependent parameters such as biomass concentration, pigment content, and reactor depth. Therefore, comparing results from different reactors (e.g., flasks, bubble columns, flat photobioreactors, raceways) cultivating different species at various concentrations can hardly lead to a reliable comparison of the results. Although it has been proposed to use more representative quantities such as the rate of photon absorption (Bonnanfant et al. 2021, Legrand et al. 2016), light is typically characterized only by the irradiance value, which is insufficient. For example, according to the Beer-Lambert law, a conical flask of 250 ml with 100 ml of working volume (culture depth = 2.5 cm), containing 2.5 g.L^{-1} of algal biomass irradiated with 150 μmol.m^{-2}.s^{-1} (a typical configuration of laboratory experiments cited above) presents a transmitted light intensity five times higher than a classical HRAP operated at a depth of 30 cm, containing 0.3 g.L^{-1} of algal biomass and irradiated with 2000 μmol.m^{-2}.s^{-1}. Light attenuation is then significantly higher in an HRAP than in a conical flask. Even the lowest incident irradiance applied (35 μmol.m^{-2}.s^{-1}) (Patel et al. 2019) does not match the very low irradiance transmitted by an HRAP due to increased

depth. This suggests that photoinhibition is less likely to occur in an HRAP than reported in laboratory experiments (and photolimitation more likely to occur). Furthermore, in the same series of laboratory experiments, cell adaptation to light (lipid content, pigment content, enzymatic activity) would differ between two cultures of different biomass concentrations due to the difference in light attenuation, and consequently light received per cell (as represented by the rate of photon absorption). Conclusions could then be a consequence of biomass concentration and not necessarily directly related to changes in carbon source supply. Similarly, the production of inorganic carbon through the oxidation of organic molecules and gas-liquid mass transfer influenced by reactor geometry and bubbling should also be considered, as it directly impacts carbon growth limitation. Indeed, an important consideration in the context of HRAPs is the dynamic nature of light exposure, which varies throughout the day due to factors such as solar angle, cloud cover, and shading from surrounding structures. Most of the laboratory experiments cited in this review utilize constant light conditions, providing limited insight into how microalgae adapt to fluctuating light intensities, as would occur in outdoor environments. Understanding the ability of microalgae to adapt to dynamic light conditions is crucial for optimizing HRAP performance. This includes studying how microalgae adjust their pigment composition and enzymatic activity in response to changes in light intensity over time. Additionally, investigating the overall effect of day-night alternation on the growth process is essential, considering factors such as the fluctuation of carbon and oxygen concentrations and their influence on microalgal growth rates. To address these questions, future research should focus on conducting experiments that more accurately mimic the dynamic light conditions experienced in outdoor HRAPs. This may involve using controlled lighting systems capable of simulating diurnal light cycles or conducting experiments outdoors under natural light conditions. By better understanding how microalgae respond to dynamic light environments, we can improve the design and operation of HRAPs for enhanced microalgal biomass production. Considering the lower organic carbon availability in wastewater compared to the synthetic medium used in laboratory studies, HRAP conditions are likely to be excluded from the top-right part of the diagram in Figure 4.3. This region corresponds to conditions with very high photon and organic carbon availability, under which

photoheterotrophy and mixotrophy (using external organic carbon) are expected to be the main processes. The current understanding of the type of organic molecules found in wastewater, their availability to microalgae, and their interactions with light represent major bottlenecks in developing a meaningful model for predicting HRAP behaviour. Existing models aiming to simulate HRAP often overlook microalgae heterotrophic growth (Casagli et al. 2021, Solimeno et al. 2017, Nordio et al. 2024). Although another model offers new insights into microalgal heterotrophy in modelling algal growth in wastewater (Murwanashyaka et al. 2020), it is validated using a high concentration of glucose (2000 $mg.L^{-1}$) as a carbon source, which is not representative of wastewaters organic load or availability. In conjunction with laboratory experiments, modelling should be regarded as a valuable tool for predicting the dynamic behaviour of microalgal growth under the influence of various interacting physical, biological, and chemical factors. A model can be used to predict, control, monitor, and enhance our understanding of the system by addressing its complex interactions. Similar to laboratory experiments, models must strike a balance between fidelity to the studied system and simplicity. A review (Shoener et al. 2019a) analyses 300 published phytoplankton models, offering insights into the components that should be considered when modelling microalgae cultures based on reactor geometry, environmental, physicochemical, and limitations conditions. According to this work, considerations such as bacterial growth, algal mixotrophy, light attenuation, and medium turbidity, photoacclimation, microorganisms growth on internal quotas rather than on medium substrates, pH and its effect on inorganic carbon form, temperature regarding inhibitory values, as well as carbon storage due to fluctuating light should all be taken into account for accurately representing HRAP conditions. This work not only provides a useful tool for developing HRAP-representative models but also offers insights into experimental conditions that should be particularly considered in laboratory studies simulating HRAP conditions. Modelling, laboratory, and outdoor experiments must be combined to advance our understanding of microalgae behaviour in wastewater. However, particular attention should be paid to the selection of experiments to ensure complementarity and representativeness.

4.5 Conclusion

Organic carbon supply plays a crucial role in influencing the modulation of pigments, cell composition, and metabolites in response to varying light received. The positive impact of organic carbon supply on algal growth is particularly significant in day-night cycle, emphasizing its relevance in adapting to light changes. While a correlation appears to exist between organic carbon supply and photoprotection, as well as biomass maintenance in darkness, the underlying mechanisms remain unclear. Many studies focus on biomass, pigments, and cell composition under constant light, but exploring metabolites and enzymes in realistic simulated solar conditions could offer new insights into cell adaptation mechanisms and their dynamic along the day-night cycle. In addition, carbon and oxygen fate in mixotrophic microalgae culture and the impact on microalgae-bacteria interactions in the perspective of wastewater treatment are still missing in the literature. This question will be further investigated in the Chapter 5. Further qualitative and quantitative investigation of pretreated influent composition may also shed light on carbon availability for microalgae in HRAP systems and refine our understanding of microalgae behaviour within the complex consortium they form with bacteria in HRAP.

Highlights

- Organic carbon helps modulate cell functions for adaptation to solar conditions.
- Further characterisation of wastewater organic carbon after pretreatment is needed.
- Light attenuation factors and affinity with organic molecules must be considered.
- Modelling, lab and large-scale studies should be combined for further research.

Chapter 5

Relative contributions of photoautotrophy and photoheterotrophy to mixotrophic growth of *Scenedesmus obliquus* in synthetic wastewater

5.1 Introduction

Biological secondary wastewater treatment systems relies on the ability of chemoheterotrophic bacteria to degrade complex compounds present in wastewater, breaking them down into simpler compounds such as CO_2 or other organic molecules. When microalgae are integrated into wastewater treatment systems, both bacteria and microalgae could contribute to heterotrophic activity. While microalgae have demonstrated ability to utilize certain simple organic molecules for their growth, as demonstrated in Chapter 4, the complexity of organic compounds in wastewater suggests that bacterial degradation is the primary mechanism for breaking down organic matter. During the wastewater treatment process, easily biodegradable molecules are quickly consumed in the initial stages, leading to a decrease in their availability over time. However, complex substances can also undergo degradation into smaller and more assimilable molecules,

notably during pretreatment in anaerobic ponds. This process not only aids in organic matter breakdown but also increases the fraction of organic carbon available for both bacteria and microalgae in subsequent treatment stages.

As demonstrated in Chapter 4, microalgae exhibit versatile metabolic capabilities, allowing them to adapt their growth strategies based on environmental conditions (Figure 5.1). The balance between photoautotrophic, photoheterotrophic and mixotrophic growth modes depends on the ratio of available energy from light and from organic matter (Nirmalakhandan et al. 2019). Factors such as light intensity, organic carbon concentration, affinity with the organic molecule, and environmental conditions influence the metabolic flexibility of microalgae, allowing them to optimize their growth strategies for survival and proliferation in various habitats.

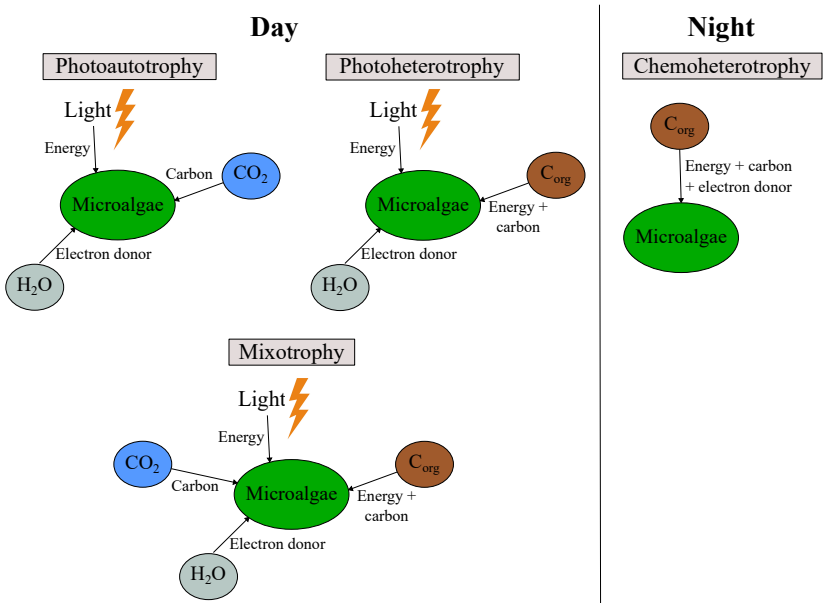

Figure 5.1 – Energy source, carbon source and electron donor for microalgae in photoautotrophy, photoheterotrophy, mixotrophy and chemotrophy. C_{org}: organic carbon; C_{inorg}: inorganic carbon

In the daytime within HRAP, microalgae are likely experiencing mixotrophic conditions due to the presence of light, inorganic carbon produced by bacteria, and organic carbon from wastewater. Various studies have explored the contributions of photoautotrophic and photoheterotrophic growth to mixotrophic growth, examining factors such as biomass productivity, pigment content, cell composition and enzyme activity. However, outcomes vary depending on

incident irradiance levels, the source of organic carbon, and carbon concentrations in the culture. Moreover, understanding carbon fluxes between inorganic and organic carbon in the liquid phase, CO_2 in the gas phase, and carbon stored in the biomass remains unclear. Often, information about inorganic carbon concentrations in both liquid and gas phases is missing, hindering the establishment of a comprehensive carbon balance and impeding investigations into carbon fate in mixotrophic microalgae cultures. While the contribution of photoautotrophic and chemoheterotrophic growth to oxygen balance in mixotrophy has been studied (Abiusi et al. 2020), experiments in photoheterotrophy were not conducted as part of this study. Oxygen transfer in the gas phase was also not considered. Furthermore, studies investigating mixotrophy often overlook available nitrogen, phosphorus, and sulfur, potentially underestimating biomass productivity due to nutrient limitations.

The present study investigates the contribution of photoautotrophy and photoheterotrophy to the mixotrophic growth of the axenical microalgae specie *Scenedesmus obliquus* under light conditions, with a focus on the role and fate of organic carbon, inorganic carbon, and oxygen in microalgal growth. Experiments conducted in sterile conditions within a photobioreactor aim to quantify the fractions of organic and inorganic carbon consumed by microalgae when both sources are available, as well as to determine the extent to which inorganic carbon derived from the oxidation of organic carbon can be reused for autotrophic growth. As it is not possible to represent the complexity of organic molecules present in wastewater, a molecule easily assimilable by microalgae was chosen to simulate the organic load in wastewater in order to investigate competition between microalgae and bacteria. Acetate was then selected based on its high affinity with microalgae as discussed in Chapter 4.

5.2 Materials and methods

- **Experimental setup and culture conditions**

As detailed in Chapter 2, an axenical strain of the microalga *Scenedesmus obliquus* was cultivated under photoautotrophic, photoheterotrophic, and mixotrophic conditions in a sterile 1.4 L torus photobioreactor operated at a dilution rate of 0.024 h^{-1}. The temperature within

the PBR was maintained at 23 °C, and an incident light intensity of 200 μmol.m^{-2}.s^{-1} was supplied by a LED panel. The PBR was continuously fed with synthetic culture medium and sparged with either N_2 or air to ensure a non-inhibitory dissolved oxygen concentration. pH was controlled at 7.5, with CO_2 injections utilized for pH regulation in the photoautotrophic culture where the carbon source was inorganic. Additionally, the synthetic medium was supplemented with 0.84 g.L^{-1} of sodium bicarbonate (equivalent to 120 mgC.L^{-1}) to ensure a non-limiting concentration of inorganic carbon for the microalgae. In the photoheterotrophic culture, organic carbon was the sole carbon source, and pH was adjusted using 0.5 M HCl injections. The culture medium was supplemented with 0.44 g.L^{-1} of sodium acetate (equivalent to 130 mgC.L^{-1}). In the mixotrophic culture, where both inorganic and organic carbon sources were present, pH regulation was achieved through CO_2 injections, and the culture medium was supplemented with 0.84 g.L^{-1} of sodium bicarbonate and 0.44 g.L^{-1} of sodium acetate.

The culture conditions selected for the experiments in autotrophy, photoheterotrophy and mixotrophy are synthesised in Table 5.1. A dilution rate of 0.024 h^{-1} was chosen to mitigate the formation of dark zones that would occur more prominently with the lower dilution rates typically used in HRAP systems.

Synthetic wastewater was prepared using the following components and concentrations in g.L^{-1}: NH_4Cl 0.3; $MgSO_4$,7H_2O 0.2; $CaCl_2$,2H_2O 0.074; $NaCH_3COOH$ 0.44; Na_2EDTA, 2H_2O 0.05; $FeSO_4$, 7H_2O 0.014; KH_2PO_4 0.063 (see Appendix A). Trace elements solutions containing Zn, Co, Cu, Mn, B, and Mo were also added to the medium. The experiment in mixotrophy was first conducted using this classical synthetic wastewater, but the high productivity obtained led to a limitation in NH_4^+ and PO_4^{3-}. Consequently, the experiment was repeated using concentrated synthetic wastewater to ensure that algal productivity and associated gas productions were not influenced by mineral limitation. Sodium acetate $NaCH_3COOH$ was used as the organic carbon source in photoheterotrophy and mixotrophy at a concentration of 130 mgC$_{org}$.L^{-1}, which is representative of the concentration of organic carbon in anaerobically pretreated wastewater.

	Autotrophy	**Photo-heterotrophy**	**Mixotrophy limited in nutrients**	**Mixotrophy non-limited in nutrients**
Carbon sources	$NaHCO_3$ 120mgC.L^{-1} + CO_2 injections	$NaCH_3COOH$ 130mgC.L^{-1}	$NaHCO_3$ 120mgC.L^{-1} + CO_2 injections + $NaCH_3COOH$ 130mgC.L^{-1}	$NaHCO_3$ 120mgC.L^{-1} + CO_2 injections + $NaCH_3COOH$ 130mgC.L^{-1}
pH regulation	pH 7.5 with CO_2 injections	pH 7.5 with HCl injections	pH 7.5 with CO_2 injections	pH 7.5 with CO_2 injections
Culture medium	Synthetic wastewater concentrated x2	Synthetic wastewater	Synthetic wastewater	Synthetic wastewater concentrated x2
Gas injection	N_2 (30 ml.min^{-1})	Air (150 ml.min^{-1})	Air (150 ml.min^{-1})	N_2 (30 ml.min^{-1})
Microorganisms	*S. obliquus*	*S. obliquus*	*S. obliquus*	*S. obliquus*
Incident irradiance	200 μmol.m^{-2}.s^{-1}	200 μmol.m^{-2}.s^{-1}	200 μmol.m^{-2}.s^{-1}	200 μmol.m^{-2}.s^{-1}
Dilution rate	0.024 h^{-1}	0.024 h^{-1}	0.024 h^{-1}	0.024 h^{-1}
Temperature	25°C	25°C	25°C	25°C

Table 5.1 – Culture conditions for autotrophic, photoheterotrophic, mixotrophic limited and non limited experiments

- **Data collection**

O_2 and CO_2 molar fractions in the gas phase were measured using online gas chromatography, while dissolved oxygen in the liquid phase was monitored online using a probe. Biomass concentration, turbidity, pigments, inorganic and organic carbon, NH_4^+, PO_4^{3-}, and SO_4^{2-} were measured offline daily on a 30 mL culture sample. Subsequently, biomass productivity, oxygen and carbon dioxide production, and consumption were deduced from these measurements. As explained in the Chapter 2, a stoichiometric analysis coupled with data reconciliation was used to estimate carbon, oxygen and nitrogen fluxes in different trophic conditions.

5.3 Results

5.3.1 Contribution of photoautotrophy and photoheterotrophy to biomass productivity in mixotrophy

S. obliquus achieved a productivity of 12.2 g.m^{-2}.d^{-1} in photoautotrophy (Figure 5.2) and a biomass concentration of 0.53 g.L^{-1}. Carbon and nutrient analyses revealed an excess of

inorganic carbon, NH_4^+, PO_4^{3-}, and SO_4^{2-}, with concentrations of 81 mgC.L^{-1}, 65 mgN.L^{-1}, 21 mgP.L^{-1}, and 15 mgS.L^{-1}, respectively.

In photoheterotrophy, *S. obliquus* reached a productivity of 4.3 g.m^{-2}.d^{-1} (Figure 5.2) and a biomass concentration of 0.21 g.L^{-1}. Similar to the experiment in photoautotrophy, NH_4^+, PO_4^{3-}, and SO_4^{2-} were found in excess (at concentrations of 56 mgN.L^{-1}, 15 mgP.L^{-1}, and 36 mgS.L^{-1}, respectively). However, acetate was quickly consumed during the first days of the culture, indicating a high affinity of *S. obliquus* for this molecule. Limited consumable organic carbon remained, confirming that the low productivity of *S. obliquus* in photoheterotrophic conditions was due to organic carbon limitation.

S. obliquus reached a productivity of 16.5 g.m^{-2}.d^{-1} in mixotrophy (Figure 5.2) with a biomass concentration of 0.74 g.L^{-1}. Notably, NH_4^+ and PO_4^{3-} concentrations dropped to zero due to higher biomass productivity and nutrient consumption, unlike in the autotrophic and photoheterotrophic cultures. Consequently, productivity in this mixotrophy experiment, limited in N and P, was suspected to be underestimated. To address this, the experiment was repeated with an increase in mineral nutrient concentrations in the culture medium to evaluate microalgal productivity in mixotrophy under non-limited nutrient conditions. In this second trial, N, P, and S were present in non-limiting concentrations in the culture (at concentrations of 64 mgN.L^{-1}, 16 mgP.L^{-1}, and 51 mgS.L^{-1}, respectively). As shown on Figure 5.2, surface productivities in mixotrophy, limited and non-limited in nutrients, were not significantly different, indicating that nutrient limitation did not significantly impact productivity.

Interestingly, the surface productivity obtained in mixotrophy (16.5 g.m^{-2}.d^{-1}) equals the sum of surface productivities in autotrophy (12.2 g.m^{-2}.d^{-1}) and photoheterotrophy (4.3 g.m^{-2}.d^{-1}). Organic carbon supply led to a 35 % increase in biomass productivity in mixotrophy compared to photoautotrophy. Since the photoautotrophic culture was not carbon limited, the productivity increase upon adding acetate is likely due to the additional energy provided by acetate oxidation. Overall, these results suggest that photoautotrophy contributes up to 74 % to mixotrophic growth, while photoheterotrophy contributes up to 26 %.

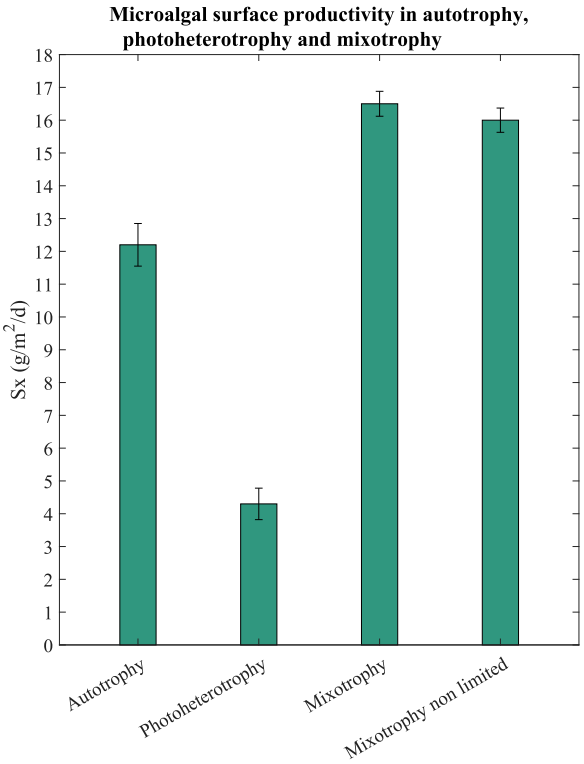

Figure 5.2 – Surface microalgal productivities in autotrophy, photoheterotrophy and mixotrophy limited and non-limited in N and P

5.3.2 Organic carbon, inorganic carbon and oxygen fate and their contribution to algal growth

With the aim of understanding the contribution of different trophic modes to carbon fluxes in mixotrophy, a carbon balance between the carbon supplied to the culture (inlet) and the carbon measured in the culture (outlet) was established. The distribution of carbon into the biomass, the gas phase, and the liquid phase in the inlet and the outlet is presented in Table 5.2 and Figure 5.3. In this analysis, elemental compositions of *S. obliquus* was given by Garcia-Moscoso et al. (2015).

Total carbon fluxes in the inlet and the outlet of the PBR should be equal in steady state in a continuous culture. Errors of 9.6 %, 5.5 %, and 0.5 % were found when comparing carbon fluxes in the inlet and in the outlet of photoautotrophic, photoheterotrophic, and mixotrophic cultures,

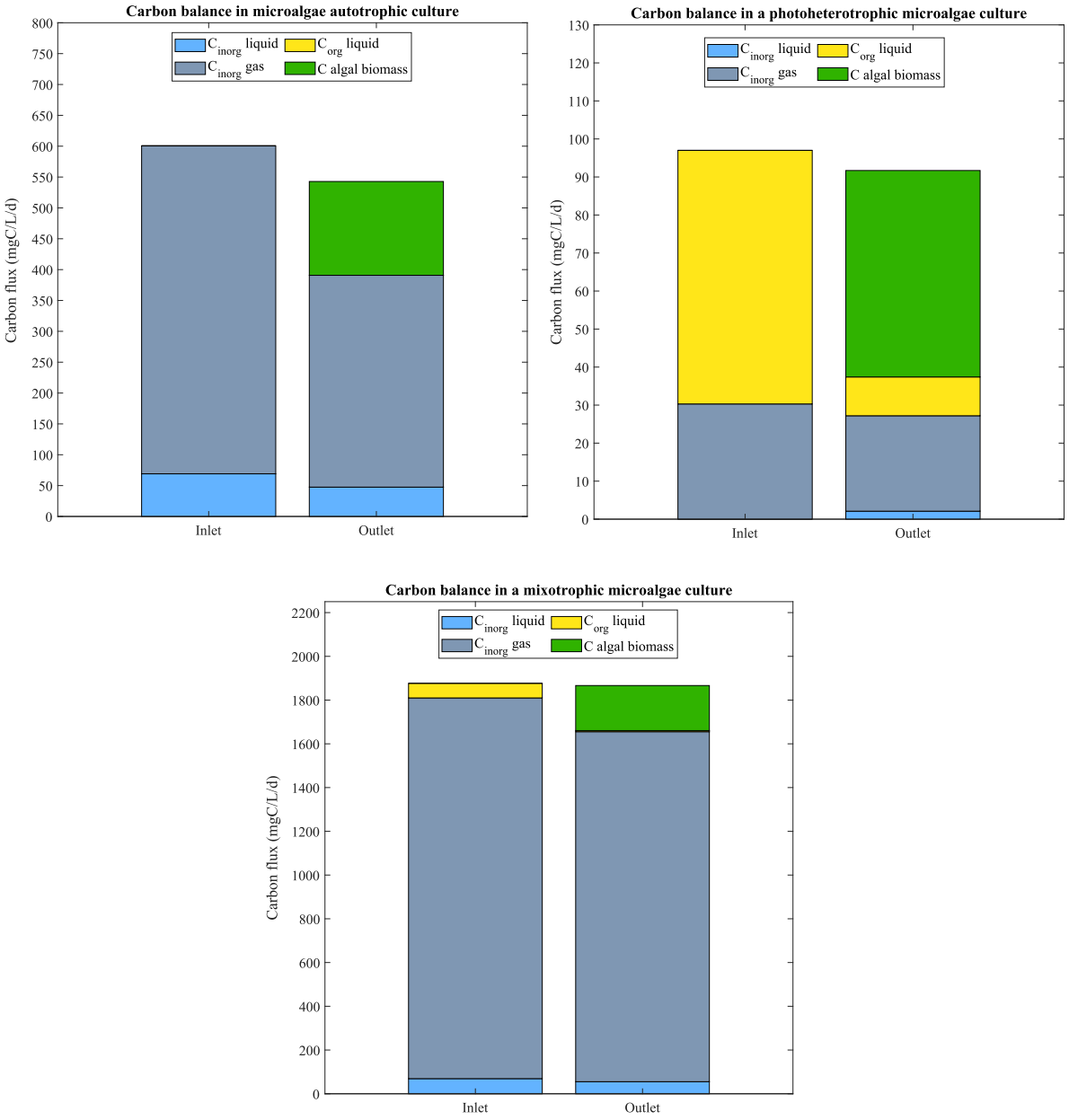

Figure 5.3 – Carbon balance deduced from carbon flux in the inlet and the outlet of autotrophic, photoheterotrophic and mixotrophic *S. obliquus* cultures

respectively. This was considered acceptable for further analysis. A stoichiometric analysis coupled to data reconciliation was performed in order to estimate carbon, oxygen and nitrogen fluxes in the culture. The results are presented in the Figure 5.4. For the stoichiometric analysis, the

	Photoautotrophy		**Photoheterotrophy**		**Mixotrophy**	
	Inlet PBR (mgC/L/d)	Outlet PBR (mgC/L/d)	Inlet PBR (mgC/L/d)	Outlet PBR (mgC/L/d)	Inlet PBR (mgC/L/d)	Outlet PBR (mgC/L/d)
C biomass	0	152	0	54.3	0	206
C_{org} (liquid phase)	0	0	66.7	10.2	66.7	5.3
C_{inorg} (liquid phase)	69.1	47.5	0	2.1	69.1	55.2
C_{inorg} (gas phase)	531.5	343.3	30.3	25.1	1740.8	1600
Total	600.6	542.8	97	91.7	1876.6	1866.4
Error	**9.6%**		**5.5%**		**0.5%**	

Table 5.2 – Carbon balance showing the repartition of carbon supplied between biomass, liquid phase and gas phases for photoautotrophic, photoheterotrophic and mixotrophic cultures

reactions occurring in the reactor are assumed to be the following, established from elemental analysis of *S. obliquus* from Garcia-Moscoso et al. (2015).

Algal photoautotrophy:

$$CO_2 + 0.16\,NH_3 + 0.6985\,H_2O \rightarrow CH_{1.877}N_{0.16}O_{0.478} + 1.11\,O_2 \tag{5.1}$$

Algal photoheterotrophy:

$$0.5\,C_2H_4O_2 + 0.16\,NH_3 \rightarrow CH_{1.877}N_{0.16}O_{0.478} + 0.1103\,O_2 + 0.3015\,H_2O \tag{5.2}$$

• **Photoautotrophy**

In the photoautotrophic culture, 2.1 mol.m^{-3}.h^{-1} of inorganic carbon as sodium bicarbonate and CO_2 was supplied to the culture. Of this input, 0.544 mol.m^{-3}.h^{-1} were incorporated into the algal biomass (Figure 5.4). While a large portion of the carbon supplied to the culture left the PBR through the gas phase as CO_2 (1.2 mol.m^{-3}.h^{-1}), around 8 mM of inorganic carbon remained in the liquid phase. Le Gouic et al. (2021) stated that carbon limitation occured below a TIC concentration of 1 mM, confirming that the photoautotrophic culture was not limited by

carbon. Overall, *S. obliquus* grown in photoautotrophy consumed 1.4 mmol.gC_x^{-1}.h^{-1} of CO_2 (Figure 5.5).

Measured O_2 production rate in photoautotrophy was coherent with the stoichiometry, 0.6038 mol.m^{-3}.h^{-1}.

• **Photoheterotrophy**

In the photoheterotrophic culture, 0.13 mol.m^{-3}.h^{-1} of organic carbon as acetate was supplied to the culture. The inorganic carbon flux in the inlet (0.11 mol.m^{-3}.h^{-1}) was due to the 0.04 % CO_2 present in the air injected in the PBR. This flux value was retrieved in the inorganic carbon in the outlet gas phase; CO_2 from air is then not considered as a carbon source for the culture, which is still considered in photoheterotrophy. Additionally, the TIC remains very low in the culture (0.4 mM). Around 67 % of the carbon from acetate supplied to the culture (0.087 mol.m^{-3}.h^{-1}) was incorporated into the biomass (Figure 5.4). According to a stoichiometric equation of microalgal heterotrophic growth, 50 % of the organic carbon consumed was stored as biomass and 50 % rejected as CO_2 (Abiusi et al. 2020). However, the photoheterotrophic culture exhibits a net CO_2 production rate close to zero (-0.042 mmol.gC_x^{-1}.h^{-1}, Figure 5.5). These results suggest that the CO_2 produced from organic carbon oxidation is fully reused for algal photoautotrophic growth.

Net measured volumetric O_2 production rate (-0.0092 mol.m^{-3}.h^{-1}) was found negative, which contradicts the stoichiometric equation that predicts that oxygen should be produced in photoheterotrophy. Here, the high air injection rate combined with the low microalgal growth and oxygen production associated probably affected the precision of the measurement of O_2 in the gas phase.

• **Mixotrophy**

In the mixotrophic culture, 0.13 mol.m^{-3}.h^{-1} of organic carbon as acetate and 6.3 mol.m^{-3}.h^{-1} of inorganic carbon as sodium bicarbonate and CO_2 were supplied to the culture. The significant CO_2 supply in the mixotrophic culture is due to the high algal productivity, which induced a strong increase in pH, subsequently increasing CO_2 injections for pH regulation. In mixotrophy, 80 % of the carbon from acetate supplied to the culture (0.104 mol.m^{-3}.h^{-1}) was incorporated

into the biomass (photoheterotrophic mode, Figure 5.4). Microalgae also fixed 0.562 mol.m^{-3}.h^{-1} of inorganic carbon (photoautotrophic mode). Although 73 % of the carbon consumed by the microalgae was originally supplied as inorganic, half of the carbon consumed from acetate was expected to be converted into CO_2 in the mitochondria (Abiusi et al. 2020). The produced CO_2 would then be fixed in photoautotrophy in the chloroplast. The actual contribution of the photoautotrophic process to carbon-equivalent biomass would then be 86 %, instead of the 74 % suggested by the photoautotrophic, photoheterotrophic, and mixotrophic productivities. Overall, *S. obliquus* grown in mixotrophy consumed 0.66 mmol.gC_x^{-1}.h^{-1} of CO_2 (Figure 5.5), which is 53 % less than in photoautotrophy.

The net CO_2 consumption rate relative to biomass was lower in mixotrophy than in photoautotrophy and was close to zero in photoheterotrophy, suggesting that no inorganic carbon was released in the gas phase after acetate oxidation, and that inorganic carbon produced from acetate oxidation was directly reused for photoautotrophic growth in photoheterotrophy and mixotrophy. However, the lower productivity obtained in photoheterotrophy compared to mixotrophy demonstrates that sole acetate, including CO_2 from acetate oxidation, was not sufficient to cover carbon needs in photoheterotrophy. Besides, CO_2 injections significantly improved biomass productivity in mixotrophy compared to photoheterotrophy.

Even though TIC was available in sufficient quantities in the mixotrophic culture (around 10 mM) to meet the carbon needs of microalgal cells, acetate consumption was significant (0.104 mol.m^{-3}.h^{-1}), and even higher than in photoheterotrophic culture (0.087 mol.m^{-3}.h^{-1}). Moreover, 27 % of the carbon in the mixotrophycally grown biomass originated from the organic carbon source. This result suggests that CO_2 is not necessarily the favored carbon source and confirms the high affinity of *S. obliquus* for acetate. Even though organic carbon likely plays a significant role in algal growth, organic molecules from wastewater are probably available in insufficient quantities to meet microalgal carbon needs. Microalgae would be limited by carbon and would then rely on bacterial oxidation of complex organic molecules for CO_2 supply. In terms of oxygen fate in mixotrophy, the oxygen was produced at 96% by photoautotrophy, the net oxygen production rate in photoheterotrophy being close to zero.

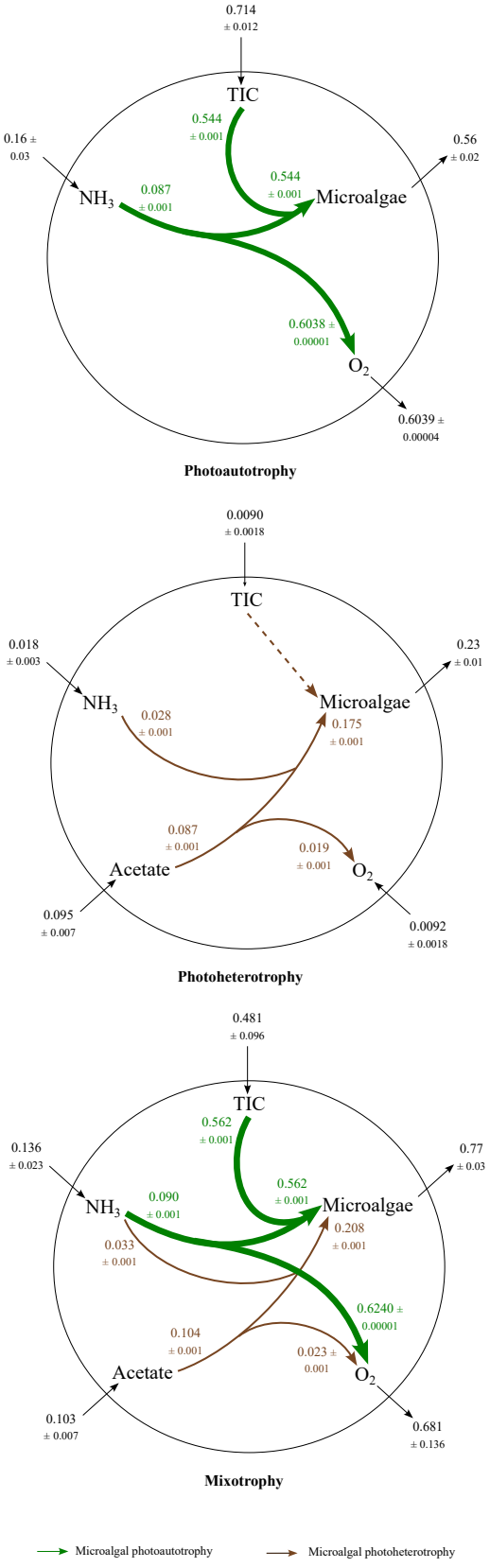

Figure 5.4 – Carbon, oxygen and nitrogen fluxes in mol/m^3/h in photoautotrophic, photoheterotrophic and mixotrophic *S. obliquus* culture

5.3.3 Oxygen balance

Oxygen concentration was maintained between 8 and 28 $mgO_2.L^{-1}$ using either N_2 in photoautotrophy or air in mixotrophy and photoheterotrophy. Oxygen consumption associated with acetate oxidation implied a lower oxygen production rate in mixotrophy (0.94 $mmolO_2.gC_x^{-1}.h^{-1}$) compared to photoautotrophy (1.14 $mmolO_2.gC_x^{-1}.h^{-1}$). In photoheterotrophy, net oxygen production is close to zero (-0.043 $mmolO_2.gC_x^{-1}.h^{-1}$) (Figure 5.5). In photoheterotrophy, oxygen production due to constant exposition to light does not compensate for oxygen consumption during acetate oxidation. In contrast, in mixotrophy, inorganic carbon supply enhances photoautotrophy, which becomes the main process and maintains a positive net oxygen production. However, net oxygen produced by microalgae is still significantly reduced in the presence of acetate in mixotrophy compared to photoautotrophy. It can then be confirmed that organic carbon significantly impacts the oxygen balance in microalgae culture.

5.3.4 Pigments

Modifications in pigment content are often reported in the literature for cells grown under different trophic conditions (Abreu et al. 2022, Agarwal et al. 2019). However, a better correlation is observed between light and pigments than between carbon source and pigments (Vonshak et al. 2000). Generally, pigment content in microalgal cells decreases as the MRPA increases (Artu 2016). In the photoheterotrophic culture, the MRPA was relatively high (23.8 $\mu mol.gC_x^{-1}.s^{-1}$) due to the low biomass concentration. Consequently, the chlorophyll *a* content in the cell was low (2.7 %). Le Gouic et al. (2021) also demonstrated that pigment content was strongly affected by carbon limitation and tended to decrease as carbon limitation increased, suggesting that microalgae regulate their metabolism through light absorption capacity in cases of carbon limitation. This hypothesis is plausible in photoheterotrophic culture, which is clearly carbon limited.

In contrast, the MRPA in the photoautotrophic culture was 9.4 $\mu mol.gC_x^{-1}.s^{-1}$ for a chlorophyll *a* content of 4.0 %. On one hand, the mixotrophic culture limited in nutrients exhibits a lower MRPA than the autotrophic one (6.9 $\mu mol.gC_x^{-1}.s^{-1}$) and a lower chlorophyll *a* content

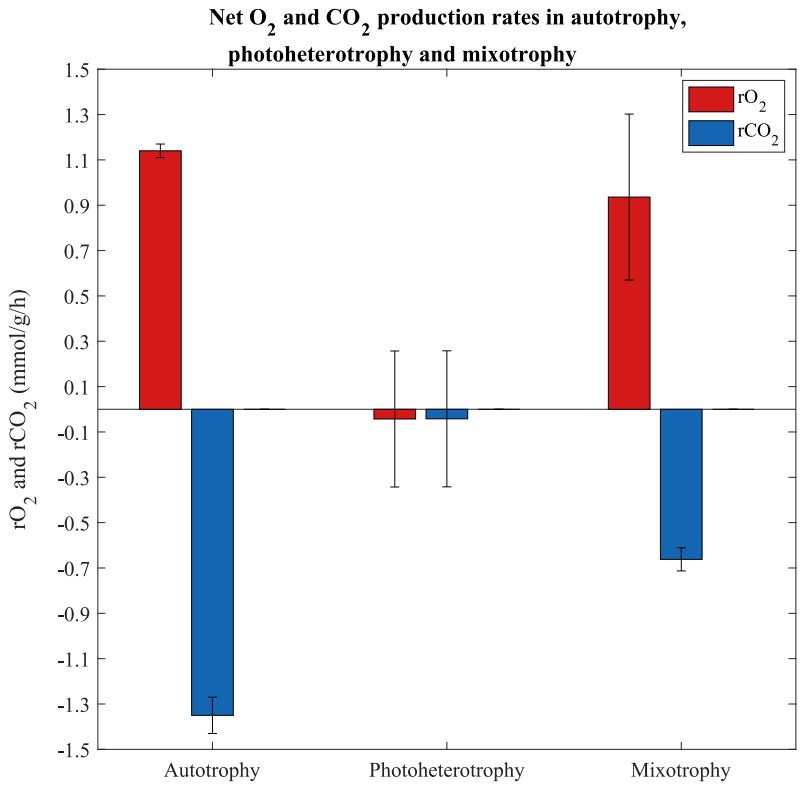

Figure 5.5 – Net productions rates of O_2 and CO_2 in autotrophy, photoheterotrophy and mixotrophy (normalised by the biomass concentration)

(3.3 %), contrary to the expected higher chlorophyll *a* content due to lower light availability. On the other hand, the experiment in mixotrophy without nutrient limitation showed expected results, with an MRPA of 6.9 μmol.gC_x^{-1}.s^{-1} and a chlorophyll *a* content close to 4.5 %, suggesting that lower chlorophyll *a* content in the culture with nutrient limitation was due to nitrogen depletion. In non-limiting nutrient conditions, chlorophyll *a* content increases as MRPA decreases regardless of the carbon source (Figure 5.6). In contrast, chlorophyll *b* and carotenoids, usually implicated in photoprotection mechanisms, did not show significant changes between different trophic modes.

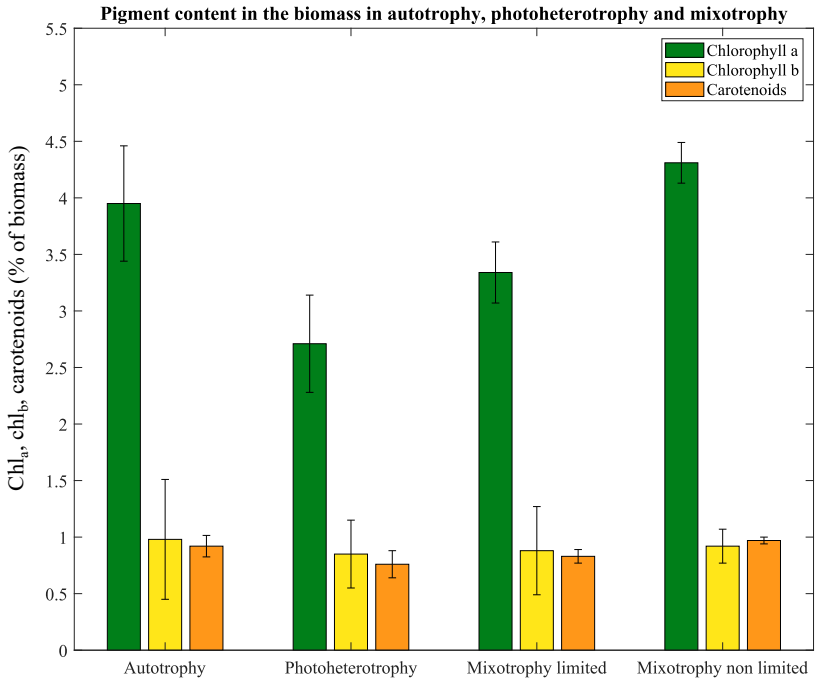

Figure 5.6 – Chlorophyll a, chlorophyll b and carotenoids content in the biomass in autotrophy, photoheterotrophy, mixotrophy limited and non-limited in nutrients

5.4 Discussion

The productivity in mixotrophy did not exceed the sum of productivities in photoautotrophy and photoheterotrophy, consequently no synergy was highlighted between the autotrophic and photoheterotrophic mode. This suggests that the simultaneous use of organic and inorganic carbon occurs independently. This observation is consistent with previous results obtained in autotrophic, heterotrophic, and mixotrophic cultures of green microalgae using acetate as the organic carbon source, where the sum of productivities in autotrophy and heterotrophy was also equal to the productivity in mixotrophy (Abiusi et al. 2020, Bouarab et al. 2004, Sim et al. 2019). Similar findings were reported by Andruleviciute et al. (2014) and Song and Pei (2018) where *Scenedesmus sp.* was grown on glycerin and xylose, respectively. However, another study based on carbon and energy metabolic mechanisms in mixotrophy through C13 labeled metabolite analysis reported in contrast a coordination or synergy between autotrophic and heterotrophic

modes (Zhang et al. 2021). Yet, it is important to note that biomass productivity in mixotrophy is always found to be higher than in photoautotrophy or in photoheterotrophy, implying a higher biomass concentration in the mixotrophic culture and a lower penetration of light through the culture. Limitation by light due to self-shading in mixotrophic cultures is then a key factor that might lead to underestimating algal productivities in mixotrophy. In other words, if synergy were occurring between autotrophic and heterotrophic modes, the productivity in mixotrophy would possibly not exceed the sum of photoautotrophic and photoheterotrophic productivities anyway because of limitation by light.

In photoautotrophy and mixotrophy, the MRPA was 9.5 and 6.9 μmol.gC_x^{-1}.s^{-1} respectively. However, an optimum MRPA was determined for green microalgae *Chlorella vulgaris* to be around 13-15 μmol.gC_x^{-1}.s^{-1} (Artu 2016). Below this value, the presence of a dark zone is likely to impact algal productivity. Thus, both photoautotrophic and mixotrophic cultures were probably limited by light. Biomass productivities might stagnate regardless of the carbon source consumed. Self-shading turns out to be a relevant confounding factor when investigating the contributions of different trophic modes. For further research, incident PFD should be adjusted throughout the culture to compensate for self-shading and to reach similar MRPA in every experiment.

This chapter also highlighted the capacity of *S. obliquus* to optimise the organic carbon supply by reutilizing CO_2 from acetate oxidation, as well as to reuse oxygen produced by photosynthesis for acetate oxidation, possibly through direct exchanges of oxygen and CO_2 inside the cell between the chloroplast and the mitochondria because of the low net O_2 and CO_2 production rates (Figure 5.7). This phenomenon was also observed by Smith et al. (2015), Grama et al. (2016), and Li et al. (2022), where O_2 and CO_2 exchanges occurred inside the cell. Another study based on molecular approach also suggested the potential recovery of inorganic carbon from acetate oxidation for *Chlorella sorokiniana* (Cecchin et al. 2018).

In this study, we retained acetate to simulate the organic carbon load in wastewater. As explained in the Chapter 4, wastewater is composed of a complex matrix of organic compounds that, for the majority, are less easily assimilable by microalgae than acetate. The contribution

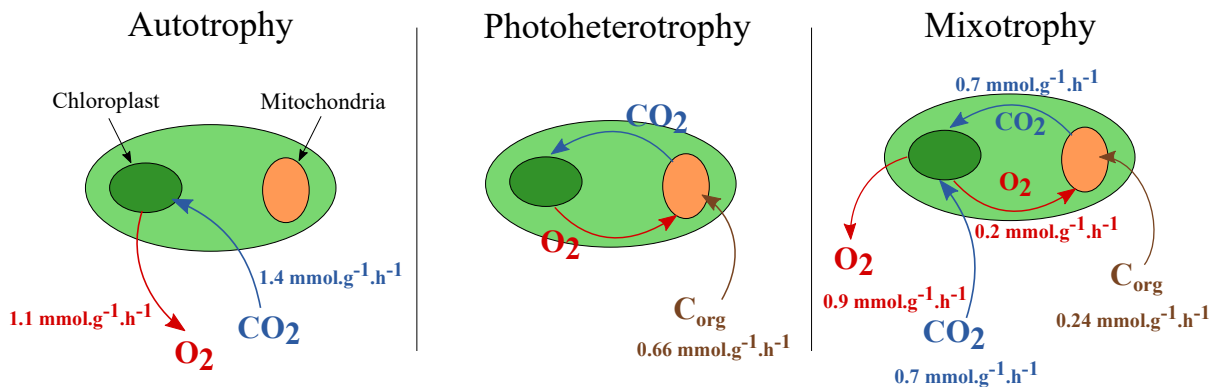

Figure 5.7 – Overview of O_2 and CO_2 dynamics in autotrophy, photoheterotrophy and mixotrophy

of photoheterotrophy in *S. obliquus* mixotrophic growth could then be overestimated in the present study compared to HRAP. However, the CO_2 supply in this study was also higher than the expected CO_2 bacterial production rate in wastewater, suggesting that photoautotrophic growth could also be overestimated compared to HRAP.

5.5 Conclusion

While productivity in mixotrophy was equal to the sum of productivities in photoautotrophy and photoheterotrophy, those two growth modes were not supposed to occur totally independently. Microalgae were able to optimize carbon sources by fully reutilizing inorganic carbon from acetate oxidation for photoautotrophic growth and oxygen from photosynthesis for photoheterotrophic growth. This possibly occurred through direct exchanges of oxygen and CO_2 inside the cell between the chloroplast and the mitochondria. While *S. obliquus* confirmed its high affinity with acetate, microalgae are likely limited by assimilable organic carbon in wastewater and would benefit from inorganic carbon supply. In the same way, the oxygen production rate was also dependent on CO_2 availability, which enhanced the contribution of photoautotrophic growth. In the context of wastewater treatment, the production of CO_2 by bacteria should improve algal growth, even if microalgae are able to use certain organic molecules as a carbon source. Besides, contrary to microalgae, bacteria are not able to recover CO_2 from organic carbon

oxidation, which might benefit microalgae in case of competition for organic carbon. Symbiotic-competitive interactions between microalgae and bacteria in HRAP are then expected. This chapter constitutes a foundation for further investigations into the interaction of *S. obliquus* with heterotrophic bacteria, notably regarding the role of bacteria in CO_2 supply to *S. obliquus*, as well as the role of microalgae in providing O_2 for bacterial growth in the presence of organic carbon assimilable by microalgae.

Highlights

- Mixotrophy was found to give better biomass productivities when compared to photoautotrophy and photoheterotrophy.
- Relative contribution of photoheterotrophy to mixotrophic growth of *S. obliquus* was 26%.
- Organic carbon is not sufficient to cover microalgal needs in wastewater and intrinsic source of CO_2 from bacterial respiration is needed.
- Oxygen production by microalgae relies on CO_2 supply.
- Microalgae-bacteria interactions in wastewater are expected to involve a mix of symbiosis and competition.

Chapter 6

Fate and role of carbon sources in microalgae-bacteria interactions in synthetic wastewater under simulated solar conditions

6.1 Introduction

The previous chapters provided insight into various issues related to microalgae-bacteria consortia behaviour in HRAP. Chapter 3 showed that, in a large-scale HRAP such as Peterborough HRAP, dissolved oxygen, organic and inorganic carbon − key indicators of microalgal and bacterial activity − were homogeneously distributed. This uniform distribution ensures that these components are potentially available for both microalgal and bacterial growth. The oxygen required for the bacterial degradation of organic carbon is produced photosynthetically and efficiently homogenized in the pond by the paddlewheel.

However, data available in the literature suggest that microalgae could utilize certain organic molecules present in wastewater as a carbon source, simultaneously with inorganic carbon produced by the oxidation of organic matter resulting from both microalgal and bacterial activities. Nevertheless, because bacterial growth kinetics are faster than those of microalgae and bacteria can consume a wider range of organic compounds, it is currently assumed that het-

erotrophic bacteria are the primary consumers of organic carbon in HRAP systems. However, previous studies have demonstrated that microalgae have a strong affinity with certain organic molecules frequently found in wastewater such as volatile fatty acids or simple sugars, which can influence their response to diurnal variations of light (see Chapter 4). Moreover, Chapter 5, which investigated the relative contributions of photoautotrophy and photoheterotrophy to the mixotrophic growth of *Scenedesmus obliquus* in synthetic wastewater, confirmed that the presence of an organic carbon source consumable by microalgae had a significant impact on O_2 and CO_2 balances. It also showed that *S. obliquus* growth is effectively limited by organic carbon in wastewater and benefits from an external CO_2 supply.

In HRAP, CO_2 is naturally supplied by bacteria. Considering that microalgae could potentially consume part of the organic carbon available in wastewater, interactions between microalgae and bacteria are expected to be a combination of competition and symbiosis. Synergistic relationships between microalgae and heterotrophic bacteria have already been observed (Russel et al. 2020, Su et al. 2012). However, given the complexity of trophic interactions within the microalgae-bacteria consortium, the fate of the carbon consumed, both organic and inorganic, between microalgal and bacterial biomass is still understudied. Moreover, as illustrated by the dissolved oxygen concentration measured in Peterborough HRAP over 24 hours (Figure 6.16), the photosynthetic response of microalgae is subject to light fluctuations along the day-night cycle. Therefore, it is essential to understand the consumption and/or production dynamics of O_2 and CO_2 over a 24-hour period to better comprehend the functioning of interactions between microalgae and bacteria in a HRAP.

Open systems like HRAP are subject to external biological contaminations. Consequently, they host natural consortiums formed of a diversity of bacterial and microalgal species. In addition, wastewater is a complex mixture containing carbohydrates, lipids, proteins, volatile fatty acids, minerals, metals, potential toxic compounds and suspended solids. Studying microalgae-bacteria interactions in such a complex system while overcoming inter-competition between different microalgal species or bacterial species, potential toxicity of wastewater molecules or specific affinity of organic molecules with given microorganisms can then be highly challenging.

Considering the complexity of the consortium of microorganisms present in a HRAP, it was decided to conduct a study at laboratory scale in a controlled photobioreactor, coupled to modelling work, in order to study the role and fate of the carbon source during microalgae-bacteria interactions in simulated solar conditions, approaching then the conditions encountered in HRAP systems. A preliminary theoretical approach based on modelling of a microalgae-bacteria coculture system under simulated solar conditions was then established. This model combined a radiative transfer model, which predicts light availability within the PBR, with a kinetic growth model for microalgae and bacteria, organic carbon being consumed exclusively by bacteria. The goal was to evaluate the behaviour of the coculture when microalgae are strictly photoautotrophic. This was completed by experiments where axenical microalgae (*Scenedesmus obliquus*) and chemoheterotrophic bacteria (*Escherichia coli*) were co-cultivated in a torus PBR, simulating a solar cycle and using synthetic wastewater. A stoichiometric analysis combined with data reconciliation was used to quantify carbon, nitrogen and oxygen fluxes within the microalgae-bacteria system. Finally, the relevance of using laboratory-scale photobioreactors to simulate microalgae-bacteria interactions in HRAP is discussed by comparing the conditions obtained in the PBR experiments with those in the large-scale HRAP in Peterborough.

6.2 Material and methods

- **Modelling**

A radiative model coupled to a kinetic model was implemented in Matlab 2022b, as described in Chapter 2. The dilution rate was set to 0.008 h^{-1} and organic carbon in the inlet to 260 $mgC.L^{-1}$. Light was supplied to simulate a day-night cycle (Figure 6.1).

- **Experimental setup and culture conditions**

As detailed in Chapter 2, axenical strains of the microalga *Scenedesmus obliquus* and the bacterium *E. coli* were cocultivated continuously in a sterile 1.4 L torus photobioreactor (PBR) on synthetic wastewater under simulated solar conditions. The culture conditions are summarized in Table 6.1. In the first experiment, acetate was used to simulate the organic load in

wastewater and supplied at a concentration of 130 mgC.L^{-1} (SWW acetate ×1). In the second experiment, the acetate supply was doubled to 260 mgC.L^{-1} (SWW acetate ×2) to prevent any effects of organic carbon limitation on the symbiosis. In the third experiment, glucose was used as the organic carbon source at a concentration of 130 mgC.L^{-1} to investigate the impact of the nature of the organic molecule on the symbiosis (SWW glucose ×1). Synthetic wastewater was prepared according to Appendix A. In each experiment, pH was regulated at 7.5 by hydrochloric acid (HCl) injections. Sterile air was continuously injected into the PBR at a flow rate of 30 ml.min^{-1}, both to mimic the mass transfer rate observed in real-scale HRAP and for the needs of gas analysis at the outlet. The dilution rate was set at 0.008 h^{-1}, within the range of dilution rates applied in real-scale HRAP.

	SWW x1 - Acetate	**SWW x2 - Acetate**	**SWW x1 - Glucose**
Carbon sources	Sodium acetate 130mgC.L^{-1}	Sodium acetate 260mgC.L^{-1}	Glucose 130mgC.L^{-1}
pH regulation	pH 7.5 with HCl injections	pH 7.5 with HCl injections	pH 7.5 with HCl injections
Culture medium	Synthetic wastewater	Synthetic wastewater concentrated x2	Synthetic wastewater concentrated x2
Gas injection	Air (30 ml.min^{-1})	Air (30 ml.min^{-1})	Air (30 ml.min^{-1})
Microorganisms	*S. obliquus* + *E. coli*	*S. obliquus* + *E. coli*	*S. obliquus* + *E. coli*
Incident irradiance	Day-night cycle	Day-night cycle	Day-night cycle
Dilution rate	0.0083 h^{-1}	0.0083 h^{-1}	0.0083 h^{-1}
Temperature	23°C	23°C	23°C

Table 6.1 – Culture conditions for experiments imitating HRAP conditions

Figure 6.1 presents the light intensity applied to the culture over 24 hours, simulating solar conditions.

- **Data collection**

O_2 and CO_2 molar fractions in the gas phase were measured using online gas chromatography, while dissolved oxygen in the liquid phase was monitored online using a probe. Biomass concentration, *E. coli* count, turbidity, pigments, inorganic and organic carbon, NH_4^+, PO_4^{3-}, and SO_4^{2-} are measured offline daily on a 30 mL culture sample. Subsequently, algal and bacte-

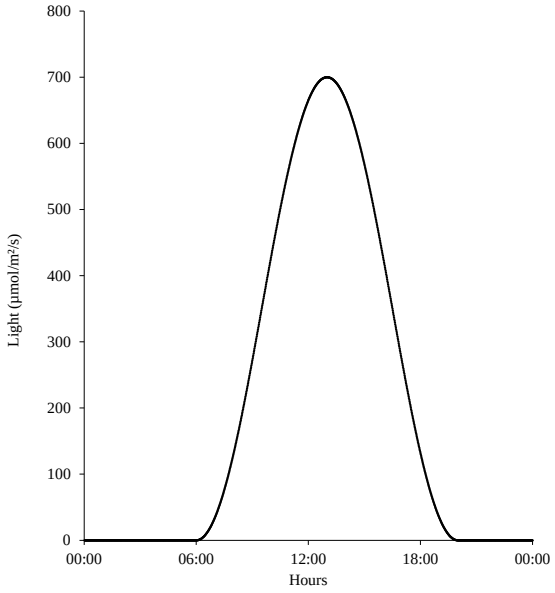

Figure 6.1 – Diurnal variation of the incident PFD

rial productivities, oxygen and carbon dioxide production and consumption were deduced from these measurements. As explained in Chapter 2, a stoichiometric analysis coupled with data reconciliation established based on carbon, nitrogen and redox balances was used to estimate the fate of carbon, oxygen and nitrogen within the consortium.

6.3 Results

6.3.1 Theoretical approach of microalgae-bacteria interactions

6.3.1.1 Calibration of the kinetic model for *S. obliquus*

As presented in Chapter 2, the model used to predict microalgae-bacteria interactions in a torus PBR fed with acetate allows to simulate both the abiotic phase (light and gas-liquid mass transfers) and the biotic phase (microalgal and bacterial kinetic growth). While the parameters used for modeling the abiotic phase are usually well-known, the growth parameters associated with the biotic phase, notably *S. obliquus* maximum specific rate for maintenance J_m, half-saturation constant for photon trapping by photosynthesis and maintenance inhibition by light

K and K', and maximal pigment molar fraction x^*_{pig}, were determined experimentally.

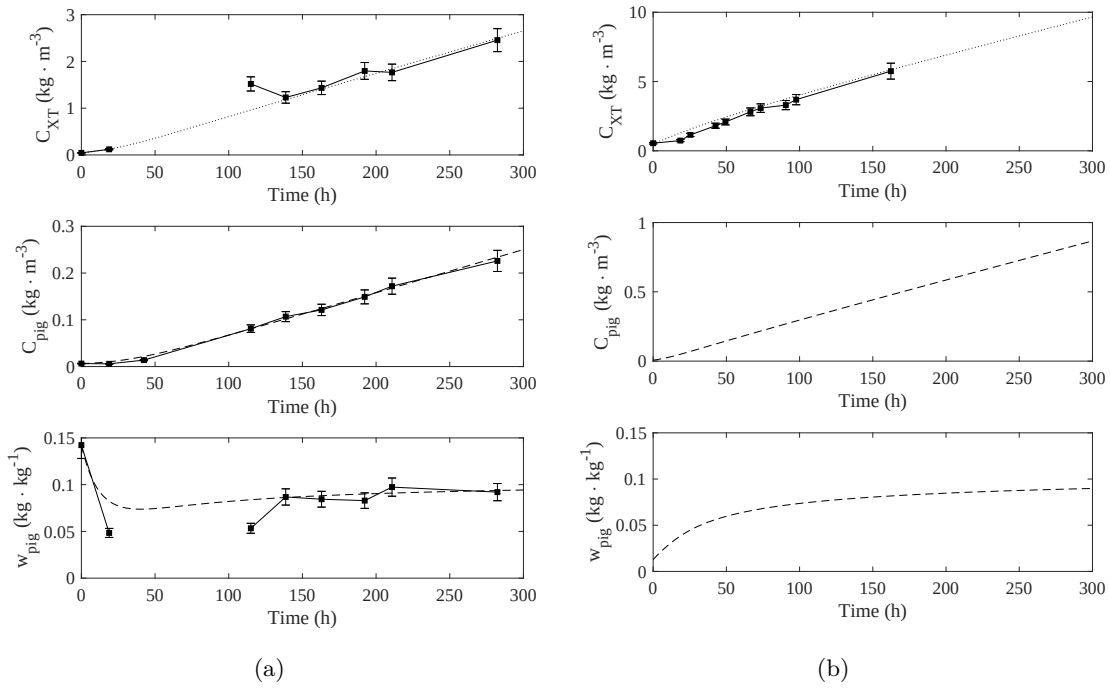

Figure 6.2 – Experimental (black dots) and modeled (dotted line) biomass concentration C_{XT}, pigment concentration C_{pig} and pigment content w_{pig} for 2 batch cultures of *S. obliquus* (a) at 100 μmol.m^{-2}.s^{-1} (b) at 800 μmol.m^{-2}.s^{-1}

The parameters J_m, K, K', and x^*_{pig} were identified by fitting the modeled biomass and pigment concentration with the experimental data obtained from two batches of *S. obliquus*, which were irradiated with light intensities of 100 and 800 μmol.m^{-2}.s^{-1}. The experimental and modeled results are presented in Figure 6.2, demonstrating a good fit between the model and experimental data. The optimized parameter values obtained from this fitting process were: $J_m = 0$, $K = 57.719$ μmol.m^{-2}.s^{-1}, $K' = 1$ μmol.m^{-2}.s^{-1} and $x^*_{\text{pig}} = 0.1486$. Note that J_m value was set to 0 as the experimental batch of *S. obliquus* demonstrated that this strain could reach high biomass concentrations (2 g.L^{-1}) under low light (100 μmol.m^{-2}.s^{-1}) without reaching a plateau, suggesting that this strain was not sensitive to dark zones. As $J_m = 0$, K' becomes then a non-sensitive parameter. Maximal pigment content x^*_{pig} was very high (14 %), which might be a consequence of the very low MRPA in the batch culture when biomass concentration reaches 2 g.L^{-1} at an incident irradiance of 100 μmol.m^{-2}.s^{-1}.

The *S. obliquus* kinetic model using these values was then validated. Model parameters for *E. coli* growth were taken from the literature (references are indicated in the Chapter 2) as *E. coli* is a well-known microorganism.

6.3.1.2 Modeling of a *S. obliquus*-*E. coli* coculture

The model was used to simulate algal and bacterial growth in coculture over a day-night cycle, applying a dilution rate D=0.008 h^{-1} and a organic carbon concentration in the inlet of 260 $mgC_{org}.L^{-1}$. As illustrated in Figure 6.3a, bacterial biomass dominated the consortium. Algal biomass fluctuated between 0.09 $g.L^{-1}$ at the end of the night to 0.12 $g.L^{-1}$ at midday, while bacterial biomass remained constant at a concentration of 0.42 $g.L^{-1}$. Figure 6.3b illustrates that bacteria reached the same biomass concentration when grown alone and in coculture. Note that in these simulations, organic carbon was the limiting parameter for bacterial growth, with a very low value of 0.11 $mgC_{org}.L^{-1}$ reached at stabilized state. As O_2 was not the limiting parameter, bacteria did not rely on microalgae for O_2 production. In contrast, microalgae reached lower biomass (0.04 $g.L^{-1}$) when grown alone compared to coculture with bacteria. This is due to the fact that during the daytime, microalgae were limited by TIC which is solely supplied by bacteria. Because microalgae depended on bacteria for TIC but bacteria did not rely on microalgae for O_2, synergy between the organisms was not observed numerically. This hypothesis will be justified further.

Besides, the question of the impact of the dilution rate on the ratio of algal and bacterial biomass was raised. At a dilution rate of 0.008 h^{-1}, algal biomass account for 22 % of the total biomass and reached a maximum of 25 % at a dilution rate of 0.004 h^{-1}. The ratio between algal and bacterial biomass is thus only slightly sensitive to dilution rate. This limited sensitivity can be explained by the dependence of microalgal growth on bacteria for TIC production. A dilution rate that disadvantages the bacteria, i.e. low dilution rates (0.004 h^{-1} in this example), reduces bacterial productivity, which directly decreases CO_2 production and consequently, microalgal growth. As a result, microalgal growth decreases simultaneously with bacterial growth, maintaining the relative ratio of the populations.

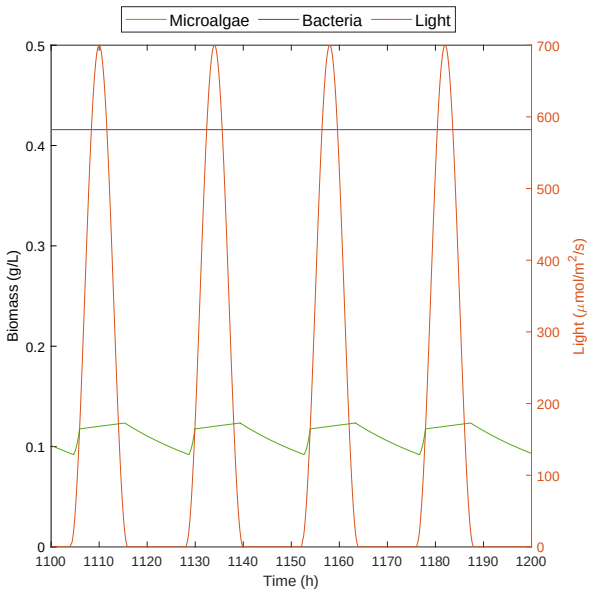

(a)

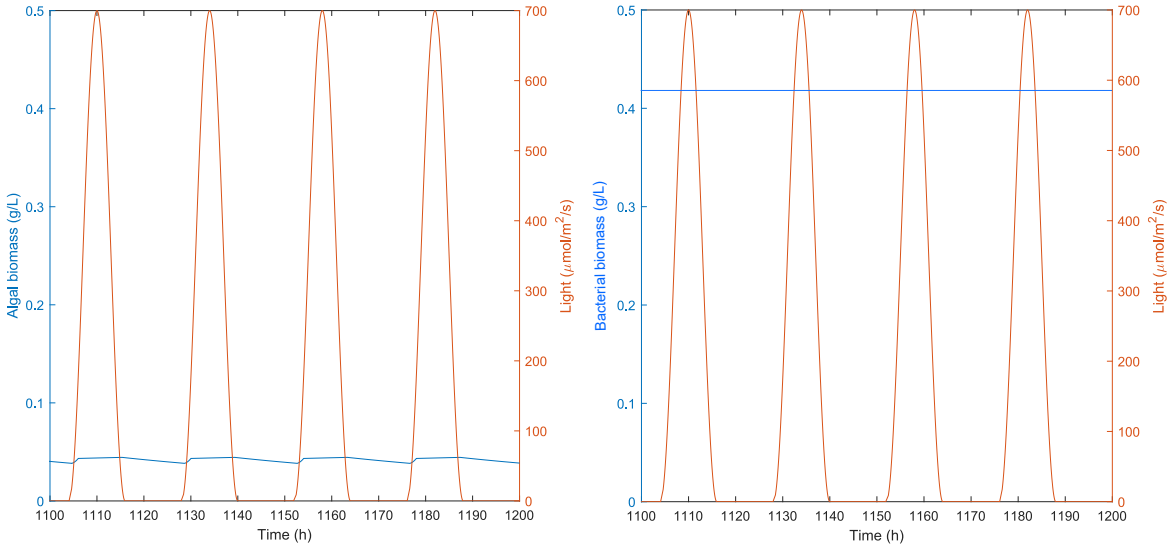

(b)

Figure 6.3 – (a) Modeled microalgal and bacterial biomass in coculture in day-night cycle, D=0.008 h^{-1}, C_{org}=260 mgC.L^{-1} (b) Modeled biomass in day-night cycle, D=0.008 h^{-1}, C_{org}=260 mgC.L^{-1} when microalgae were grown alone (left) and when bacteria were grown alone (right)

The Figure 6.4 represents the dynamics of DO, TIC, microalgal growth rate μ_{alg}, microalgal volumetric O_2 production rate $r_{O2_{alg}}$ and microalgal volumetric CO_2 production rate $r_{CO2_{alg}}$

simulated over a 24-hour cycle. The time is expressed in hours with sunrise occurring at $t = 0$. These simulations illustrate the interplay between light availability and the metabolic activities of microalgae, as well as the dependence of microalgae on bacteria for inorganic carbon, particularly CO_2, which is critical for their growth. The simulated data provide insights into the diurnal variations in the microalgal-bacterial consortium, highlighting the complexity of their interactions in a controlled environment.

After sunrise, microalgal growth rate μ_{alg} increased sharply up to 0.3 h^{-1} due to the rise of light intensity. Simultaneously, microalgal volumetric O_2 production rate $r_{O2_{alg}}$ increased to 1.67 $mol.m^{-3}.h^{-1}$ while microalgal volumetric CO_2 production rate $r_{CO2_{alg}}$ dropped to -1.50 $mol.m^{-3}.h^{-1}$. Within 2 hours after sunrise, DO reached 30 $mg.L^{-1}$ (a similar concentration was reached in Peterborough HRAP, Figure 6.16) and TIC dropped to zero. After TIC dropped to zero, microalgae were strongly limited in carbon. The growth rate then dropped to 0.01 h^{-1}, inducing a drop in $r_{O2_{alg}}$ to 0.052 $mol.m^{-3}.h^{-1}$ and a decrease in DO to 9.5 $mg.L^{-1}$ from 2 hours after sunrise to midday. Microalgal growth rate was then dependent on TIC, which remained close to zero until sunset. Algal growth rate remained then stable until sunset. Just before sunset, light decreased below 20 $\mu mol.m^{-2}.s^{-1}$, the threshold fixed for the start of algal decay in darkness. The growth rate then dropped to -0.02 h^{-1} for the nighttime. Algal decay in darkness involves respiration and thus relies on O_2. However, O_2 dropped to 5 $mg.L^{-1}$ at night, which slowed down the decay from the middle of the night until sunrise due to O_2 limitation. This explains the slight decrease in O_2 uptake and the rise in DO at the end of the night. TIC was continuously produced during the night, reaching 12.5 $mg.L^{-1}$ before sunrise. Microalgae consumed the TIC accumulated during the night and the CO_2 produced by bacteria during the first 2 hours after sunrise. During the daytime, because microalgal carbon needs were higher than the bacterial production of CO_2 ($r_{CO2_{bact}} = 0.035$ $mol.m^{-3}.h^{-1}$), no TIC was accumulated in the liquid phase during the day. On the contrary, oxygen production by microalgae broadly covered bacterial needs ($r_{O2_{bact}} = -0.028$ $mol.m^{-3}.h^{-1}$).

In the end, DO was directly influenced by $r_{O2_{alg}}$ which depended on the growth rate μ_{alg}. Those parameters presented then a similar trends. Without TIC limitation, the DO curve would

be expected to follow a bell-shaped curve similar to light intensity. Instead, it shows a short peak early in the morning, followed by a stabilization phase and a drop after sunset. Thus, the model demonstrated that DO was affected by TIC variations and that, in this case, CO_2 production by bacteria was insufficient to meet the carbon needs of the microalgae.

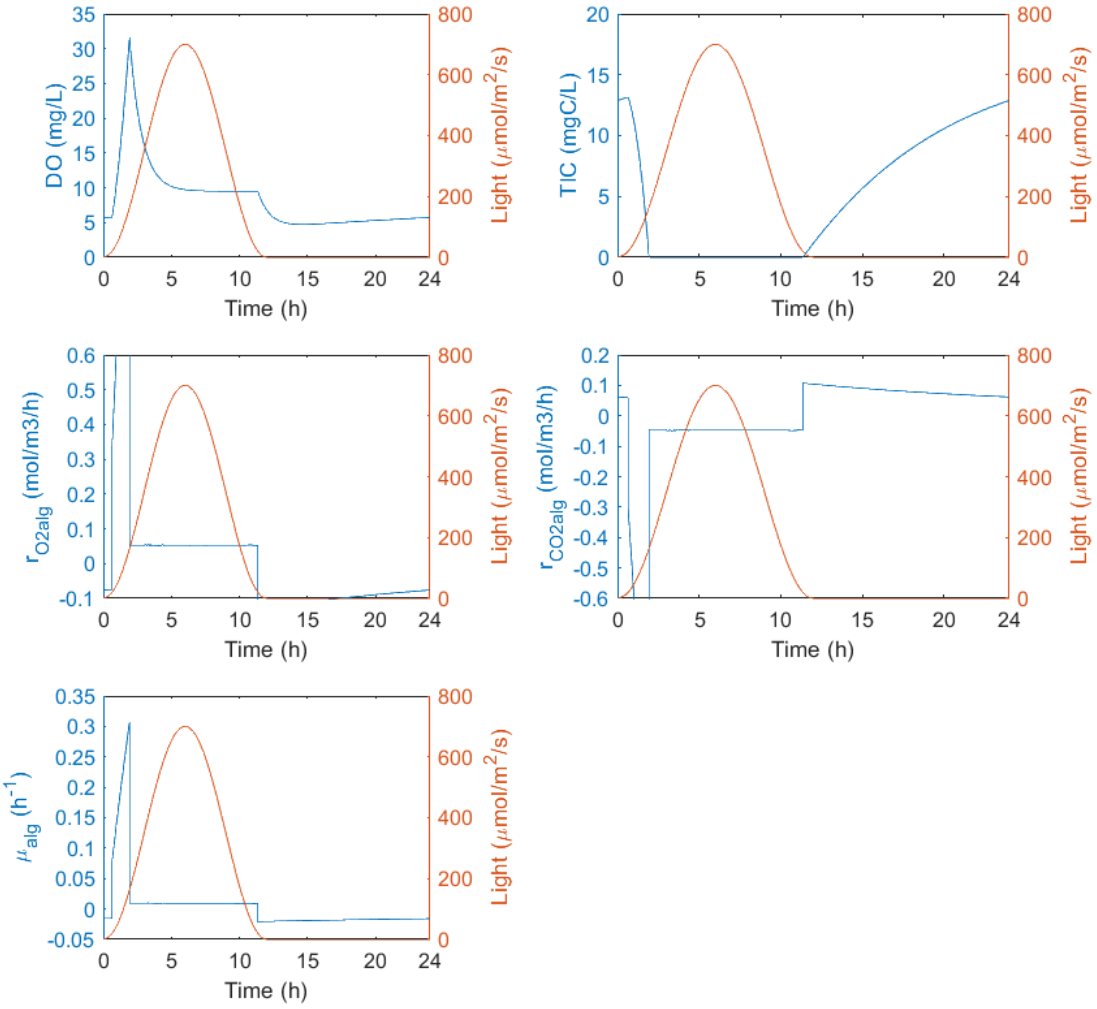

Figure 6.4 – First column: modeled DO, microalgal O_2 production rate $r_{O2_{alg}}$ and microalgal growth rate μ_{alg}; second column: TIC and microalgal CO_2 production rate $r_{CO2_{alg}}$

The model also allowed to calculate O_2 and CO_2 transfer rates through liquid and gas phases. The mass transfer coefficients $K_La_{O2} = 1.32\ h^{-1}$ and $K_La_{CO2} = 1.12\ h^{-1}$, chosen for their representativeness of HRAP (Bello et al. 2017, Le Gouic 2013), are significant and indicate

that gas-liquid transfer could influence the accumulation of O_2 and CO_2 in the liquid phase. Figure 6.5 shows the transfer rates of O_2 and CO_2 in mol.h^{-1}, respectively N_{O2} and N_{CO2}. A negative value of N_{O2} or N_{CO2} indicates that the gas is primarily transferred from the liquid to the gas phase, while a positive value indicates transfer from the gas to the liquid phase. Figure 6.5 illustrates that N_{O2} and N_{CO2} were negative throughout the day-night cycle, meaning that O_2 and CO_2 produced by microalgae and bacteria tended to be lost in the gas phase. However, this phenomenon is unlikely to impact TIC limitation for microalgae as the CO_2 transfer rate from the liquid to the gas phase N_{CO2} (-0.008 mol.m^{-3}.h^{-1}) is 6.3 times lower than the CO_2 consumption rate of microalgae (-0.05 mol.m^{-3}.h^{-1}) during periods when microalgal growth was limited by TIC.

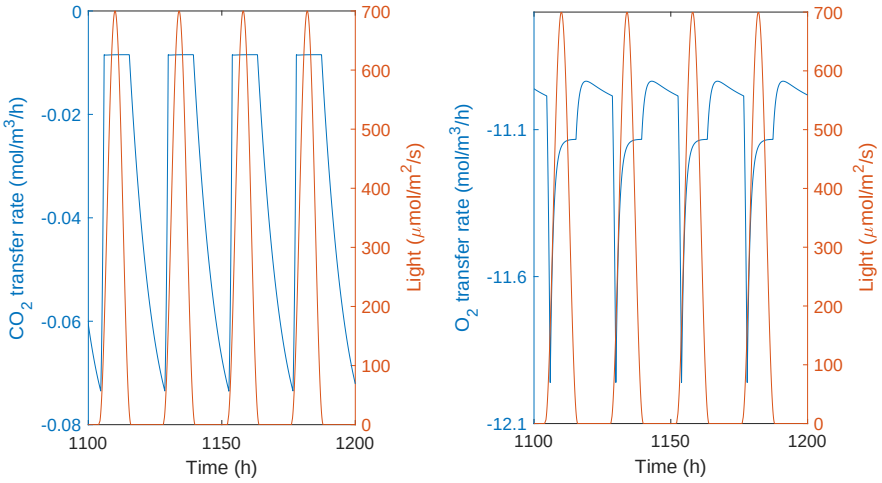

Figure 6.5 – Modeled O_2 and CO_2 volumetric transfer rates NO_2 and NCO_2

In the end, no complete synergy was observed in the model simulating the coculture of *S. obliquus* and *E. coli* when considering an organic carbon source utilized exclusively by bacteria. Algal growth was lower than expected in comparison to the usual biomass ratio in an HRAP, and bacteria did not rely on microalgae since they were limited by organic carbon and not by oxygen. The gas-liquid oxygen transfer was sufficient to meet bacterial oxygen needs, which is unlikely to occur in an HRAP. The following experimental investigation in the torus PBR is expected to provide insights that will confirm the behaviour observed with the model and identify the

missing elements necessary to accurately simulate microalgae-bacteria interactions in HRAP.

6.3.2 Experimental investigation of microalgae-bacteria interactions

6.3.2.1 Biomass productivities

Experimentally, total biomass achieved a productivity of 2.1 $g.m^{-2}.d^{-1}$ in the coculture supplied with acetate at a concentration of 130 $mgC.L^{-1}$, 4.5 $g.m^{-2}.d^{-1}$ in the coculture supplied with acetate at a concentration of 260 $mgC.L^{-1}$, and 1.1 $g.m^{-2}.d^{-1}$ in the coculture supplied with glucose at a concentration of 130 $mgC.L^{-1}$. These productivities are below the expected values based on Peterborough HRAP performances, which are estimated to be around 9.1 $g.m^{-2}.d^{-1}$ (0.3 $g.L^{-1}$ of microalgal suspension estimated from suspended solids and chlorophyll *a* measurements, at a HRT of 10 days and a depth of 30 cm) (Figure 6.6). NH_4^+, PO_4^{3-}, and SO_4^{2-} were present in excess in each of the three cocultures.

Biomass achieved an organic carbon consumption of 19.8 $mgC_{org}.L^{-1}.d^{-1}$, 40.1 $mgC_{org}.L^{-1}.d^{-1}$, and 14.2 $mgC_{org}.L^{-1}.d^{-1}$ in the coculture supplied with 130 $mgC.L^{-1}$ of acetate, 260 $mgC.L^{-1}$ of acetate, and 130 $mgC.L^{-1}$ of glucose, respectively (Figure 6.7). Doubling acetate supply doubled the acetate consumption and the biomass productivity.

Microalgae and bacteria represented respectively 71 % and 29 % of the biomass in the coculture supplied with 130 $mgC.L^{-1}$ acetate, compared with 73 % and 27 % in the coculture supplied with 260 $mgC.L^{-1}$ acetate (Figure 6.8). *S. obliquus* already demonstrated a strong affinity for acetate in Chapter 5 and clearly dominated the consortium here, suggesting that microalgae and bacteria were competing for acetate but with an advantage for microalgae.

In contrast, in the coculture using glucose as the carbon source, global biomass productivity was very low (1.1 $g.m^{-2}.d^{-1}$). Bacteria dominated the consortium, and microalgae could not grow. Low microalgal growth was likely due to a limitation by TIC and induced low oxygen production, low dissolved oxygen in the culture and limitation of bacterial growth by oxygen. Thus, bacteria reached low biomass concentration of 0.1 $g.L^{-1}$, producing low CO_2 thus enhancing the limitation of microalgal growth by TIC. In the model presented in Section 6.3.1.2, where organic carbon was consumed only by bacteria, microalgae were also in minority (22 %) while bacteria

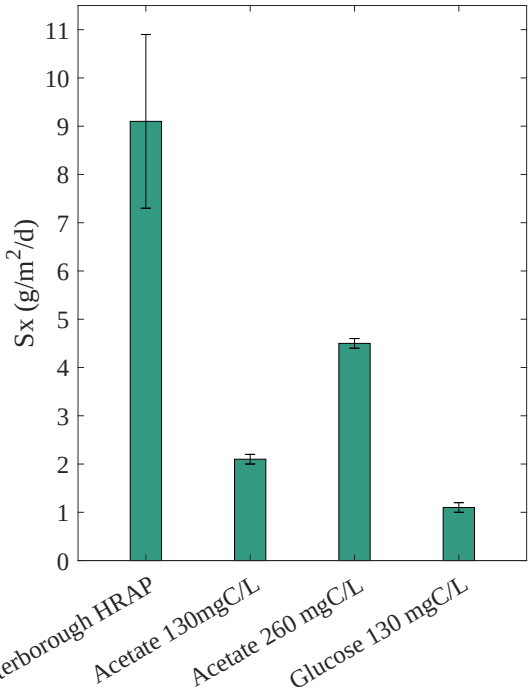

Figure 6.6 – Surface biomass productivities in Peterborough HRAP and in torus PBR supplied with synthetic wastewater with 130 mgC.L^{-1} of acetate, 260 mgC.L^{-1} of acetate and 130 mgC.L^{-1} of glucose

dominated the consortium (78 %) (Figure 6.3).

The Figure 6.9 represents algal and bacterial biomass along the day-night cycle in the coculture supplied with acetate at 260 mgC.L^{-1}. At night, a biomass loss of approximately 0.025 g.L^{-1} was observed, corresponding to 5 % of the biomass. Bacterial biomass remains relatively stable throughout the day-night cycle. The loss of biomass at night is then attributable to a decrease in microalgal growth rate due to the predominance of the respiration process (Le Borgne and Pruvost 2013).

6.3.2.2 O_2 and CO_2 dynamics in day-night cycle

Investigations into oxygen and carbon dynamics along the day-night cycle were conducted on the coculture supplied with 260 mgC.L^{-1} of acetate, where the limitation by organic carbon was unlikely.

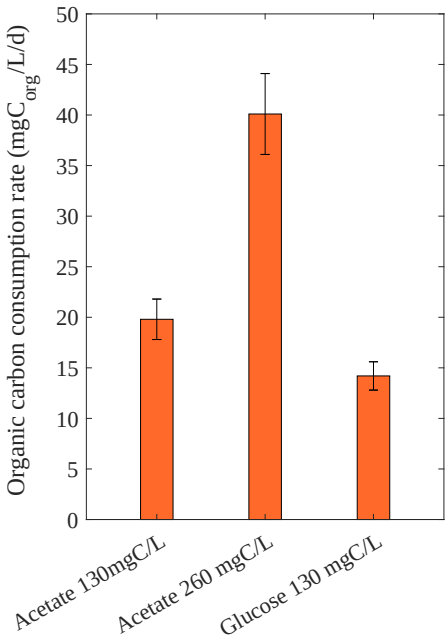

Figure 6.7 – Organic carbon consumption rate in the torus PBR supplied with synthetic wastewater with 130 mgC.L^{-1} of acetate, 260 mgC.L^{-1} of acetate and 130 mgC.L^{-1} of glucose

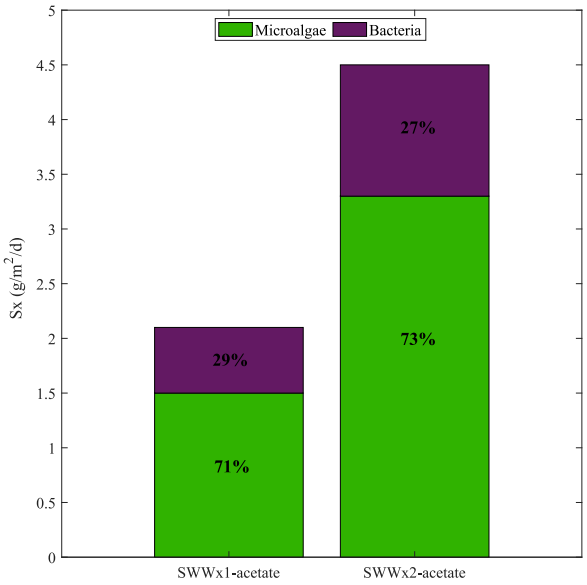

Figure 6.8 – Microalgal and bacterial productivities in synthetic wastewater supplied with 130 mgC.L^{-1} of acetate, 260 mgC.L^{-1} of acetate and 130 mgC.L^{-1} of glucose

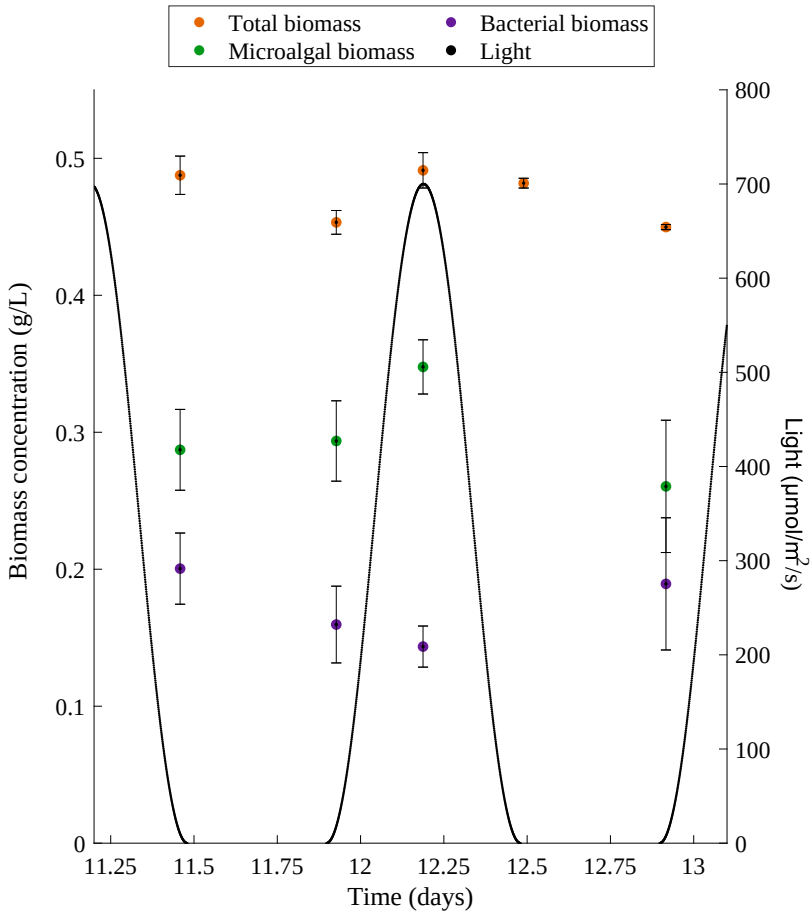

Figure 6.9 – Diurnal variations of total, microalgal and bacterial biomass in synthetic wastewater supplied with 260 mgC.L^{-1} of acetate. Black line is the irradiance, orange dots the total biomass, green dots microalgal biomass and purple dots the bacterial biomass

6.3.2.2.1 Dissolved oxygen

As illustrated on the Figure 6.10, dissolved oxygen levels dropped to 1.5 mg.L^{-1} during the night due to algal and bacterial respiration, reaching their peak value of 5.8 mg.L^{-1} approximately 3 hours after sunrise. Then, dissolved oxygen declined until midday before stabilizing around 2.7 mg.L^{-1}. This observation is consistent with the rapid increase in algal biomass following sunrise. Following sunset, dissolved oxygen levels decreased again and stabilized around 1.5 mg.L^{-1} for the period of the night. Moreover, the experimental DO curve closely resembles the DO curve generated by the model presented in Section 6.3.1.2 (Figure 6.4). The model re-

vealed that the decrease in DO immediately after the morning peak was caused by a decline in algal growth rate due to inorganic carbon limitation, which was quickly consumed after sunrise. As predicted by the model, DO remained stable in the afternoon as algal growth was limited by inorganic carbon, and then drops close to sunset when light became the limiting factor.

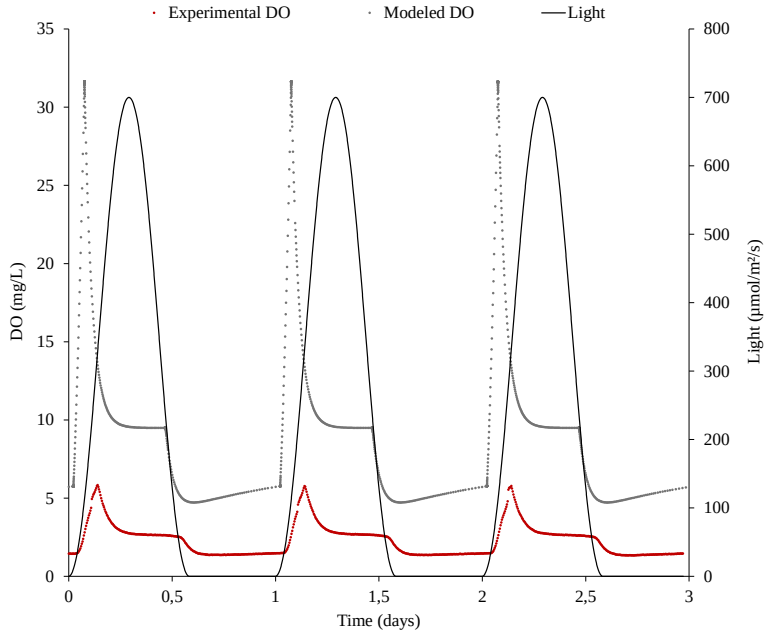

Figure 6.10 – Diurnal variations of dissolved oxygen in a coculture supplied with synthetic wastewater with 260 mgC.L^{-1} of acetate (in red) compared to the model (in grey)

Photosynthetically produced dissolved oxygen is found to be influenced by diurnal variations of light and reached low values (below 2 mg.L^{-1}) for a period of 10 hours at night, potentially leading to oxygen limitation for both microalgae and bacteria at night. Note that dissolved oxygen does not drop to 0 mg.L^{-1} due to aeration, which mimics mass transfer observed in raceways and to permit gas analysis. To assess the impact of aeration on dissolved oxygen availability, aeration was stopped at the end of the culture. Without aeration, DO concentrations exhibited higher amplitude, rising to 9 mg.L^{-1} during the day and dropping to 0 mg.$^{-1}$ at night. While stopping aeration did not affect bacterial biomass, microalgal biomass decreased from 0.42 g.L^{-1} to 0.29 g.L^{-1}, potentially due to oxidative stress during the day and oxygen limitation at night.

6.3.2.2.2 Dissolved organic and inorganic carbon

As illustrated on the Figure 6.11, total inorganic carbon concentration in the coculture reached 25.7 mgC.L^{-1} at the end of the nighttime due to algal and bacterial respiration, before dropping and stabilizing at 18.2 mgC.L^{-1} during the first 3 hours after sunrise due to the fixation of CO_2 by photosynthesis. This result is consistent with the rise in algal biomass observed just after sunrise. The variations of TIC throughout the day-night cycle are very similar to the TIC variations observed in the model. Modeled TIC increases during the night up to 12 mgC.L^{-1}, then drops quickly within 2 hours after sunrise before stabilising at a low value (Figure 6.4). This suggests that, in the experiment, microalgae were also limited in TIC from a few hours after sunrise.

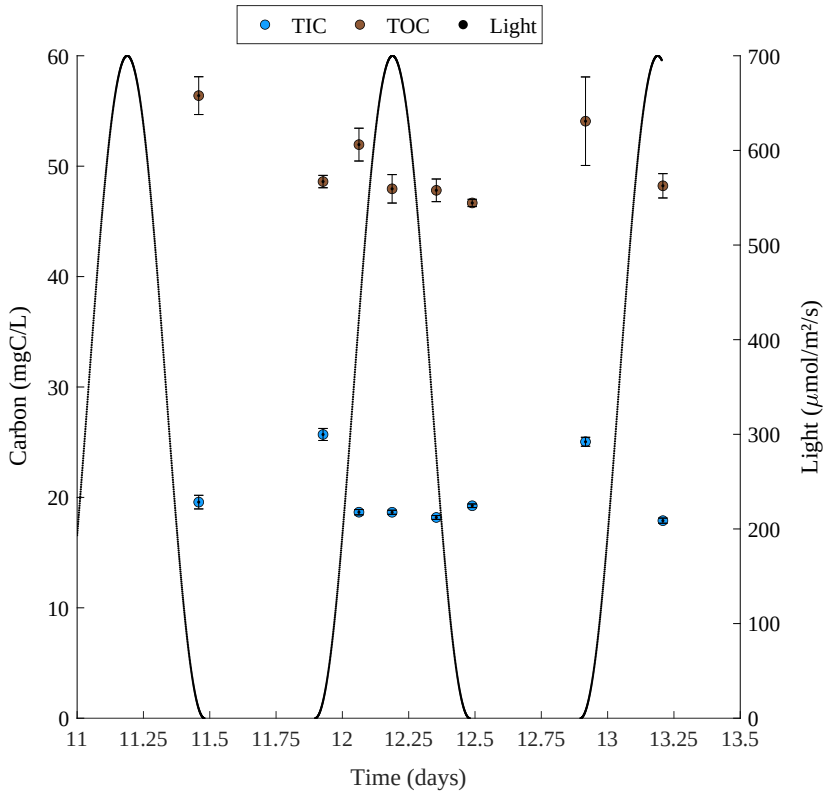

Figure 6.11 – Diurnal variations of total inorganic carbon (TIC) and total organic carbon (TOC) in a coculture supplied with synthetic wastewater with 260 mgC.L^{-1} of acetate

The model allowed to state that CO_2 transfer from the liquid to the gas phase due to air

injection did not significantly impact TIC limitation for microalgae, the transfer rate being much lower than microalgal CO_2 consumption rate. Yet, in the experiment, TIC concentration was not impacted by stopping the aeration at the end of the experiment, demonstrating experimentally that TIC variations throughout the day-night cycle were not artificially buffered by the aeration.

In contrast, variations of organic carbon observed along the day-night cycle are not consistent across several cycles and consequently do not seem to be correlated with light. While an increase in chemoheterotrophic activity by microalgae would be expected at night to compensate for the absence of light as an energy source, Figure 6.10 shows very low dissolved oxygen concentration at night, potentially limitating heterotrophic activity and acetate consumption at night for both microalgae and bacteria, explaining the absence of significant variations in organic carbon concentration in the coculture throughout the day-night cycle. In the model where organic carbon was consumed only by bacteria, organic carbon also remained constant throughout the day-night cycle due to bacteria limited by organic carbon.

6.3.2.2.3 Net volumetric O_2 and CO_2 production rates

While the measurements of dissolved oxygen and total inorganic and organic carbon concentrations is crucial for estimating the availability of oxygen and carbon for microorganisms in the culture, net O_2 and CO_2 production rates can be deduced by considering the O_2 and CO_2 concentrations measured in the gas phase. These measurements provide valuable insights into the metabolic activities of microorganisms and help in understanding the dynamics of oxygen and carbon exchange between the liquid and gas phases.

The Figure 6.12 illustrates how the net volumetric O_2 production rate, rO_2, changes throughout the day-night cycle. After sunset, rO_2 drops and stabilizes around -0.064 $mol.m^{-3}.h^{-1}$, indicating a net consumption of oxygen at night. After sunrise, rO_2 rises quickly and becomes positive when light exceeds 150 $\mu mol.m^{-2}.s^{-1}$. It reaches its peak value (0.15 $mol.m^{-3}.h^{-1}$) in the morning when light reaches approximately 400 $\mu mol.m^{-2}.s^{-1}$. However, as light intensity continues to increase up to 700 $\mu mol.m^{-2}.s^{-1}$, rO_2 starts to drop and stabilizes around 0.04 $mol.m^{-3}.h^{-1}$ in the afternoon. As light decreases below 225 $\mu mol.m^{-2}.s^{-1}$, rO_2 starts dropping again and

becomes negative when light falls below 150 μmol.m^{-2}.s^{-1}. At this point, dissolved oxygen in the culture becomes limiting and rO_2 stabilizes around -0.064 mol.m^{-3}.h^{-1}. Note that the rO_2 obtained experimentally present a shape similar to modeled $r_{O2_{alg}}$, with a peak early in the morning followed by a stabilised phase until sunset. This behaviour is attributed to TIC limitation after the rapid consumption of available TIC in the early hours after sunrise, as indicated by the drop in TIC observed in the early morning (Figure 6.11). Additionally, both before sunrise and after sunset, rO_2 becomes negative when light levels drop below 150 μmol.m^{-2}.s^{-1}, corresponding to a Mean Rate of Photons Absorption of 6.4 μmol.g^{-1}.s^{-1}, which reflects light availability in the culture. Overall, photosynthetic activity compensates for algal and bacterial respiration when the MRPA exceeds 6.4 μmol.g^{-1}.s^{-1}, which is the case for most of the day.

Dynamics of the net volumetric CO_2 production rate rCO_2 are also influenced by diurnal variations of light. Throughout the nighttime, rCO_2 progressively increases from -0.0053 to 0.03 mol.m^{-3}.h^{-1} due to algal respiration. Note that bacterial respiration is expected constant throughout the day-night cycle as bacteria were limited by organic carbon and not oxygen. Then, rCO_2 progressively decreases to -0.0053 mol.m^{-3}.h^{-1} from sunrise to sunset due to CO_2 fixation by photosynthesis. In the model where organic carbon is consumed only by bacteria, rCO_2 shows similar behaviour as rO_2, with a sharp drop early in the morning. However, in the experimental data, variations in CO_2 production show less amplitude, potentially due to microalgae reusing the CO_2 they produced while consuming acetate. Despite microalgae fixing CO_2 through photosynthesis during the day, rCO_2 predominantly takes positive values, even during daylight hours. This continuous positive value of rCO_2 can be attributed to the ongoing conversion of acetate into CO_2 by both microalgae and bacteria throughout the day-night cycle.

6.3.2.3 Carbon mass balance

Establishing a carbon mass balance between the carbon supplied to the culture (inlet) and the carbon measured in the culture (outlet) is crucial for understanding the contribution of microalgae and bacteria to carbon fluxes in the coculture. The distribution of carbon into the biomass, the gas phase, and the liquid phase in both the inlet and the outlet is summarized in

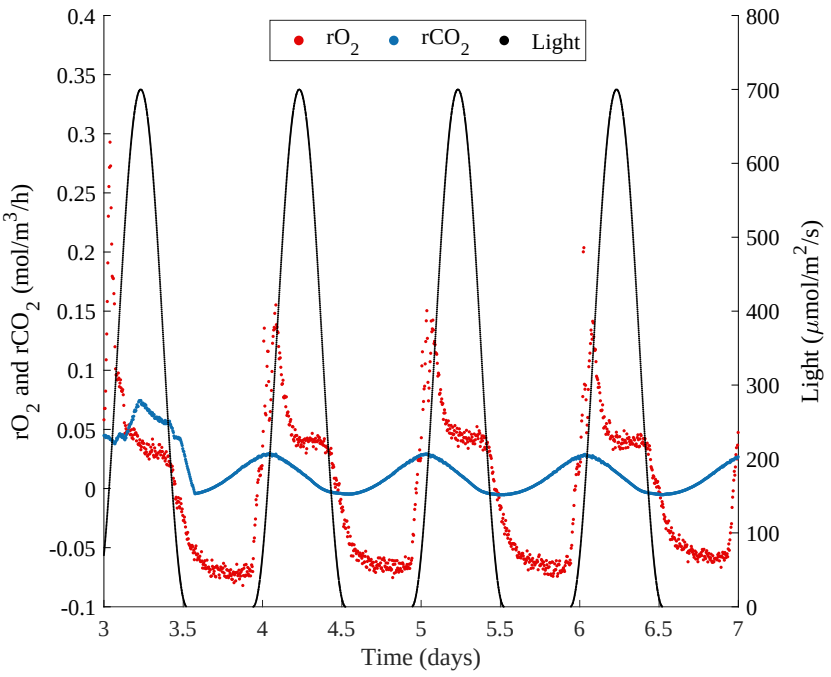

Figure 6.12 – Net O_2 and CO_2 volumetric production rates along the diurnal cycle in a coculture supplied with synthetic wastewater with 260 mgC.L^{-1} of acetate

Table 6.2 and Figure 6.13. In this analysis, elemental compositions of *S. obliquus* and *E. coli* were given by Garcia-Moscoso et al. (2015) and Folsom and Carlson (2015) respectively.

The error on the carbon balance, reflecting the disparity between the carbon fluxes in the inlet and in the outlet, was 33.5 % for the coculture supplied with 130 mgC.L^{-1} of acetate and 6.5 % for the coculture supplied with 260 mgC.L^{-1} of acetate. The error in the first case (33.5%) raises concerns about the reliability of the measurements. Data reconciliation would be necessary to facilitate the interpretation of carbon distribution in this coculture.

Nevertheless, the carbon balance in the second coculture display a low error between the carbon supplied to the culture and the carbon recovered in the outlet (6.5 %), allowing a first interpretation and estimation of the carbon fate within the consortium. As illustrated in Figure 6.13, the main source of carbon in the inlet is acetate, corresponding to a carbon flux of 68.3 mgC.L^{-1}.d^{-1}. The 6.1 mgC.L^{-1}.d^{-1} of inorganic carbon in the inlet is attributable to the 0.04 % of CO_2 present in the air injected into the PBR. Within the PBR (outlet), 83 % of the organic

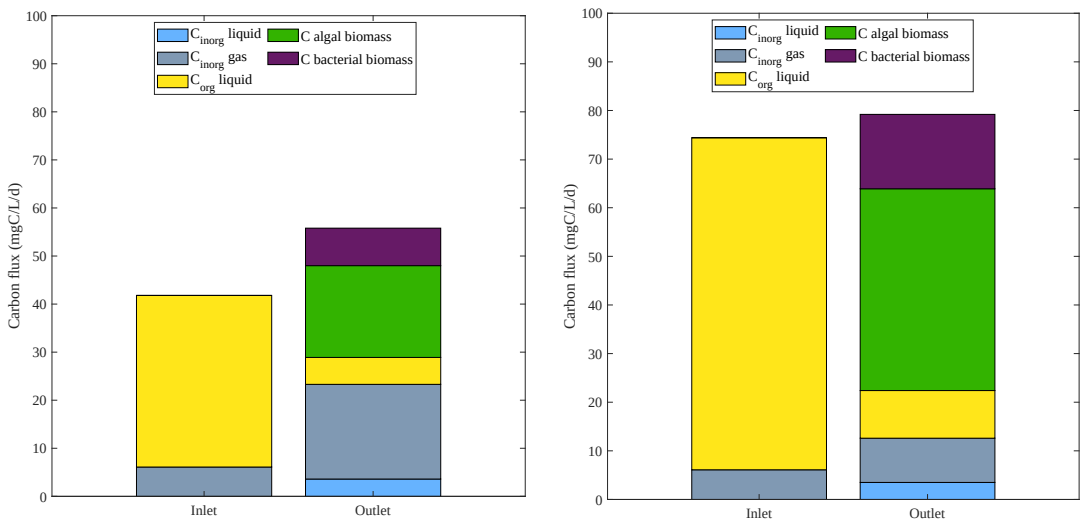

Figure 6.13 – Carbon balance showing the repartition of carbon supplied between the biomass, the liquid phase and the gas phase in the coculture supplied with (a) SWWx1 (130 mgC.L^{-1} of acetate) (b) SWWx2 (260 mgC.L^{-1} of acetate)

carbon supplied as acetate is consumed by microalgae and bacteria (comprising 61 % and 22 %, respectively). The inorganic carbon flux in the gas phase increases by 49 % compared to the inlet due to CO_2 release after acetate oxidation for biomass growth. The produced inorganic carbon is also found to be dissolved in the liquid phase (3.5 mgC.L^{-1}.d^{-1}).

	SWWx2 Acetate = 260 mgC/L		**SWWx1 Acetate = 130 mgC/L**	
	Inlet (mgC/L/d)	**Outlet (mgC/L/d)**	**Inlet (mgC/L/d)**	**Outlet (mgC/L/d)**
Carbon in the total biomass	0	56.8	0	26.9
Carbon in the algal biomass	*0*	*41.5*	*0*	*19.1*
Carbon in the bacterial biomass	*0*	*15.3*	*0*	*7.8*
C_{org} (liquid phase)	68.3	9.8	35.7	5.6
C_{inorg} (liquid phase)	0	3.5	0	3.6
C_{inorg} (gas phase)	6.1	9.1	6.1	19.7
Total	74.4	79.2	41.8	55.8
Error	**6.5%**		**33.5%**	

Table 6.2 – Carbon balance showing the repartition of carbon supplied between the biomass, the liquid phase and the gas phase in the coculture supplied with 130 and 260 mgC.L^{-1} of acetate

6.3.2.4 Data reconciliation-based stoichiometric analysis

Establishing the reactions occurring in the reactor is crucial for discriminating between microalgae and bacteria contributions to organic carbon consumption and inorganic carbon consumption and production. Moreover, each measurement carries an uncertainty, leading to non-closed mass balances. In order to improve the analysis of the experimental fluxes, a stoichiometric analysis was added. The reactions assumed to occur in the reactor are as follows, based on elemental analysis of *S. obliquus* and *E. coli* from studies by Garcia-Moscoso et al. (2015) and Folsom and Carlson (2015) respectively.

Algal photoautotrophy (during the daytime):

$$CO_2 + 0.16\,NH_3 + 0.6985\,H_2O \rightarrow CH_{1.877}N_{0.16}O_{0.478} + 1.11\,O_2 \tag{6.1}$$

Algal photoheterotrophy (during the daytime):

$$0.5\,C_2H_4O_2 + 0.16\,NH_3 \rightarrow CH_{1.877}N_{0.16}O_{0.478} + 0.1103\,O_2 + 0.3015\,H_2O \tag{6.2}$$

Algal chemoheterotrophy (during the nighttime):

$$C_2H_4O_2 + 0.16\,NH_3 + 0.8895\,O_2 \rightarrow CH_{1.877}N_{0.16}O_{0.478} + 1.3\,H_2O + CO_2 \tag{6.3}$$

Bacterial chemoheterotrophy (during the daytime and nighttime):

$$0.625\,C_2H_4O_2 + 0.368\,NH_3 + 0.324\,O_2 \rightarrow CH_{1.74}N_{0.23}O_{0.43} + 1.16\,H_2O + 0.4\,CO_2 \tag{6.4}$$

Data reconciliation allows for corrections to be applied to the measured rates of acetate, CO_2, NH_3, O_2, algal and bacterial biomass, while considering constraints imposed by the known stoichiometric relationships for *S. obliquus* photoautotrophic and photoheterotrophic growth and *E. coli* chemoheterotrophic growth, as well as their respective yield coefficients for acetate, found in the literature. This process, based on a pseudo steady-state assumption, enables the

assessment of carbon fluxes between algal biomass, bacterial biomass, dissolved organic carbon, and dissolved inorganic carbon.

This analysis focuses on two distinct stable phases along the day-night cycle, the first at the end of the afternoon and the second at the end of the night. The Figure 6.14 illustrates the reaction rates in the coculture supplied with 130 mgC.L^{-1} of acetate and the Figure 6.15 in the coculture supplied with 260 mgC.L^{-1} of acetate, during the daytime and the nighttime. Each reaction is represented by a different color: photoautotrophic algal growth in green, photoheterotrophic algal growth in brown, and chemoheterotrophic bacterial growth in purple. The reactants are placed at the beginning of the arrows, while the products are at the end. This diagram provides insight into the carbon fluxes within the system during both daytime and nighttime phases.

• **During the day**

In both experiments with 130 mgC.L^{-1} (SWWx1) or 260 mgC.L^{-1} (SWWx2) of acetate, *S. obliquus* and *E. coli* are clearly in competition for organic carbon. During the daytime, acetate is consumed at 69% and 67% by microalgae and at 31% and 33% by bacteria, in SWWx1 and SWWx2 respectively. This distribution remains consistent regardless of the acetate supply. Besides, NH_3 is predominantly consumed by microalgae, representing 69 % in both SWWx1 and SWWx2. This aligns with previous observations indicating a similar microalgae-to-bacteria ratio in SWWx1 and in SWWx2 (Figure 6.8). The stoichiometric analysis confirms that the higher microalgal productivity compared to bacterial productivity observed previously (Figure 6.8) is attributed to higher acetate consumption by microalgae.

The contribution of photoautotrophy to microalgal growth was 8 % in SWWx1 and 21 % in SWWx2, while photoheterotrophy accounts for 92 % and 79 %, respectively. This is supposedly due to the higher bacterial biomass production in SWWx2 (from 0.023 to 0.049 mol.m^{-3}.h^{-1}) enhanced by a higher acetate supply and producing more inorganic carbon (from 0.0053 to 0.0121 mol.m^{-3}.h^{-1}), which is then fixed by microalgae through photosynthesis at a rate of 0.032 mol.m^{-3}.h^{-1}.

The increase in supplied acetate enhances both photoheterotrophic and photoautotrophic mi-

croalgal growth (represented by the brown arrows on the Figure 6.15) but also photoautotrophic microalgal growth (represented by the green arrows). This finding is consistent with dissolved oxygen measurements. Despite doubling the biological oxygen demand in SWWx2, the average dissolved oxygen concentration remained similar to that in SWWx1. This suggests an increased contribution of photoautotrophic growth to compensate for the increased oxygen demand due to higher acetate supply.

For a same amount of biomass produced, photoautotrophic growth produces ten times more oxygen than photoheterotrophic growth. However, according to the stoichiometric analysis, in SWWx1 oxygen is produced at 46% by photoautotrophy and at 54% by photoheterotrophy. This is due to the very high contribution of photoheterotrophy to global algal growth (92%). On the contrary, in SWWx2 where the contribution of photoautotrophy to algal growth is higher, oxygen is produced at 73% by photoautotrophy and at 27% by photoheterotrophy. Only 34% and 20% of the oxygen thus produced by microalgae is consumed by bacteria in chemoheterotrophy in SWWx1 and SWWx2 respectively, leading to positive net oxygen production of the coculture during the daytime. Microalgal production of oxygen is then confirmed to be sufficient to cover bacterial needs, even while photoautotrophy is not the dominant growth mode. This explains why stopping aeration in the PBR at the end of the experiment did not affect bacterial growth. The oxygen production by microalgae was indeed sufficient to cover bacterial needs. Note that the same observation aligns with the results from the model, where bacteria exclusively consumed organic carbon. This suggests that microalgal oxygen production in the presence of light is sufficient, regardless of whether organic carbon is available for microalgae or not.

In the end, microalgae and bacteria exhibit a strong competition for acetate during the daytime. The competition for acetate , by inhibiting bacterial growth, seems to limit the production of CO_2, the CO_2 fixation by microalgae and the photoautotrophic growth. This hypothesis is supported by the higher contribution of photoautotrophic growth in SWWx2 when acetate supply and acetate concentration available in the culture are higher and competition for this carbon source supposedly lower.

In the model where organic carbon was exclusively consumed by bacteria, total biomass

was equivalent to biomass measured in the torus PBR where acetate was predominantly consumed by microalgae. This indicates that while competition for acetate affects the distribution of carbon between algal and bacterial biomass, it does not significantly impact the total biomass production.

- **At night**

In the absence of light, microalgal growth relies on chemoheterotrophic reaction. The organic carbon source utilized by the microalgae can either be external to the cell (acetate in this case) or the internal carbon stock of the cell. Measured acetate consumption rate is not significantly different at night and during the day, suggesting that acetate consumption by microalgae is maintained during the nighttime and that acetate was the organic carbon source utilized in chemoheterotrophy by microalgae. As chemoheterotrophy is the only mechanism supporting algal growth at night, competition for acetate is intensified compared to the daytime. At night, acetate is consumed at 81% and 64% by microalgae in SWWx1 and SWWx2 respectively. As microalgae does not produce oxygen at night, microalgae and bacteria compete for oxygen. Microalgae still dominate the consortium at night, and oxygen uptake at night is attributable at 92% and 83% to microalgae in SWWx1 and SWWx2 respectively.

While the experimental discrimination of algal and bacterial biomass based on total dry weight and bacterial plate count did not permit to observe slight variations of the biomass composition along the day-night cycle, the stoichiometric analysis reveals that sole chemoheterotrophic microalgal growth on acetate at night does not permit to maintain the microalgal productivity reached during the day. The experiment does not permit to state if the carbon source utilized by microalgae at night was only acetate or if the microalgae was also consuming its internal carbon stocks. The hypothesis of internal carbon stock consumption for microalgal cell maintenance at night could be supported by the slight decrease in biomass concentration at the end of the night (5%, Figure 6.9). In the model where organic carbon is not consumed by microalgae, a low total biomass loss of 5.6 % was observed as well, suggesting that acetate availability does not necessarily prevent algal decay in darkness conditions by inducing heterotrophic growth and that microalgae consume its internal carbohydrates stocks.

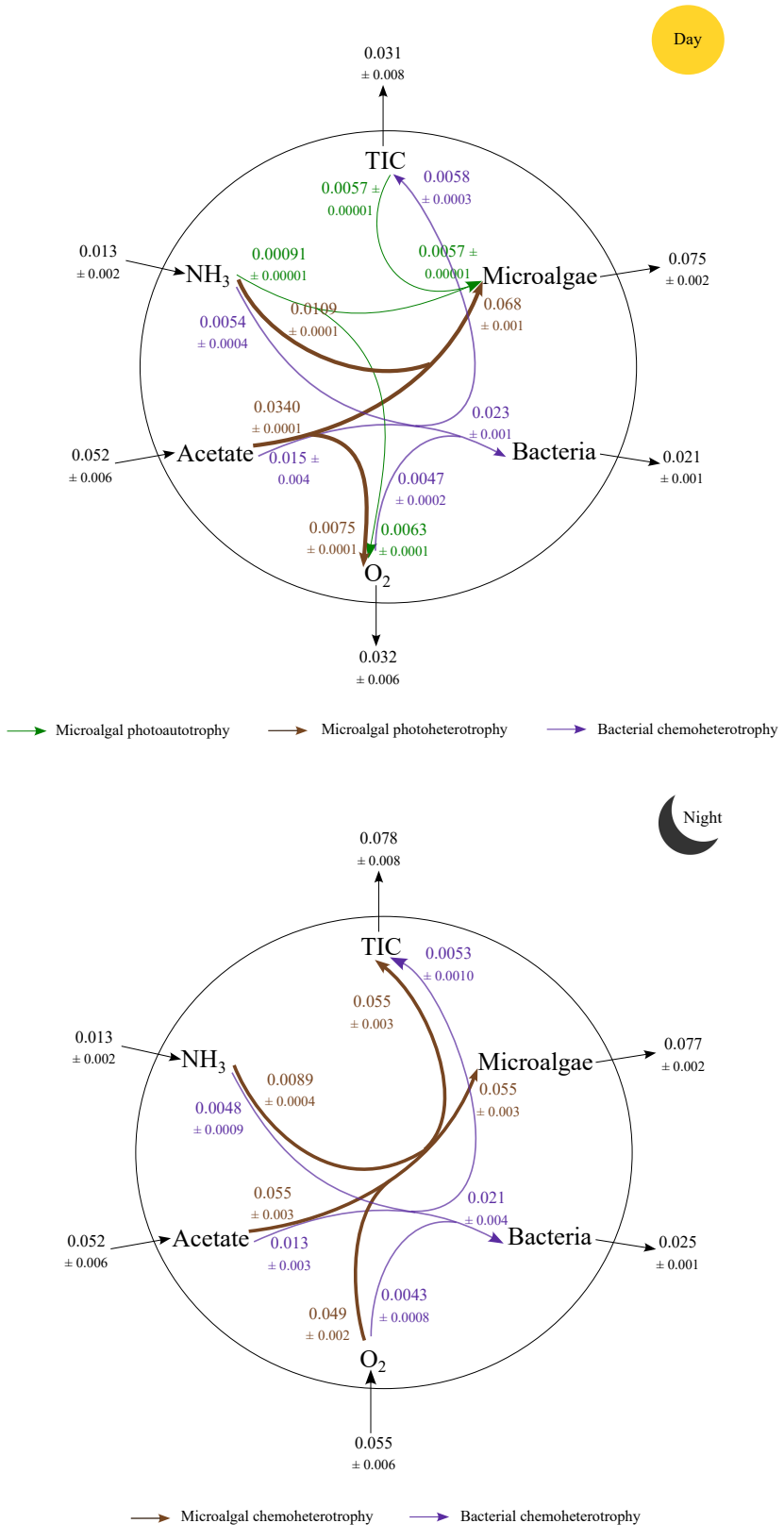

Figure 6.14 – Acetate, TIC, O_2 and NH_3 fluxes (in $mol.m^{-3}.h^{-1}$) in *S. obliquus-E. coli* coculture with 130 $mgC.L^{-1}$ of acetate supply during the daytime and the nighttime

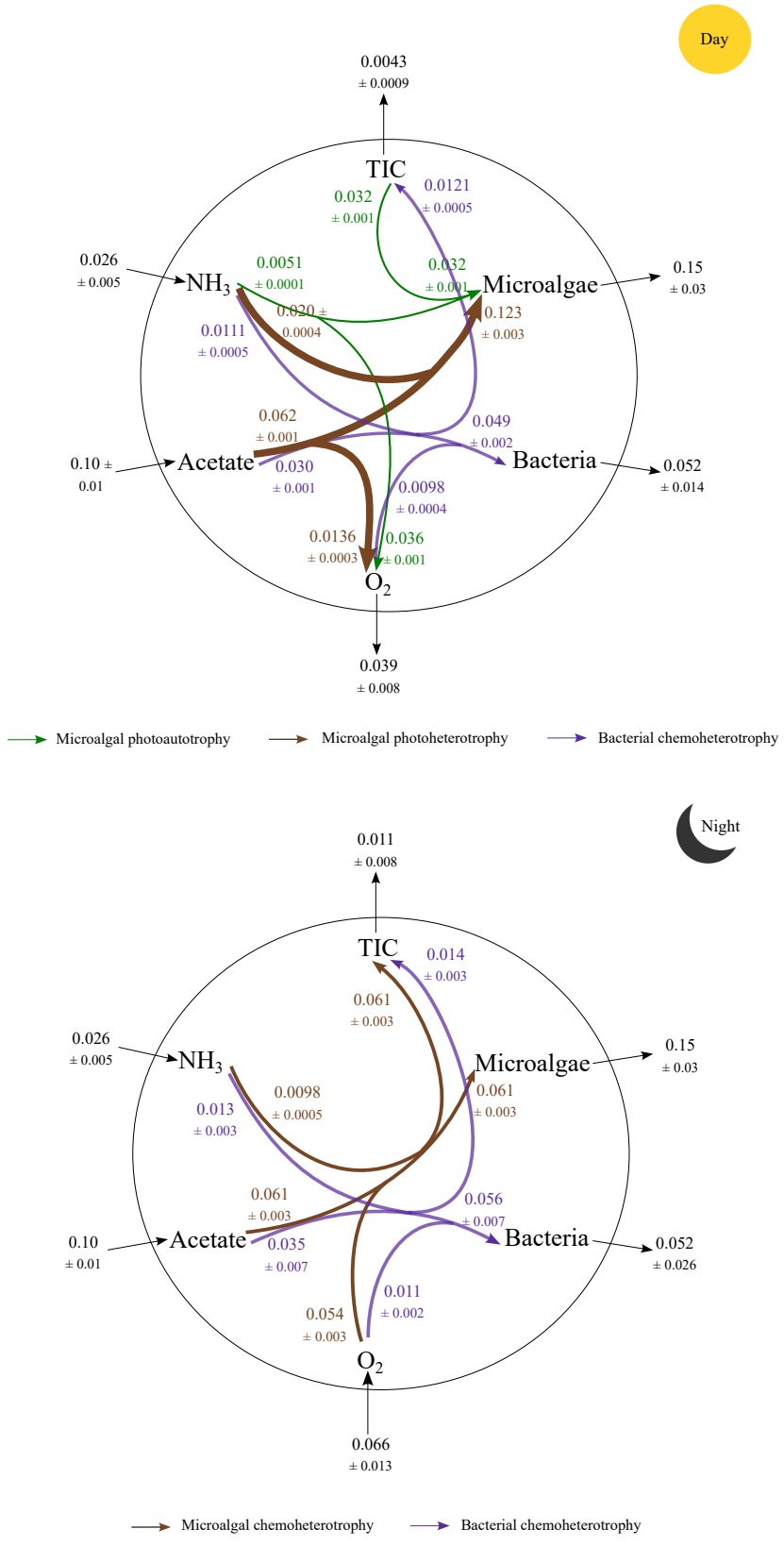

Figure 6.15 – Acetate, TIC, O_2 and NH_3 fluxes (in $mol.m^{-3}.h^{-1}$) in *S. obliquus-E. coli* coculture with 260 $mgC.L^{-1}$ of acetate supply during the daytime and the nighttime

6.3.2.5 Comparison with oxygen and carbon measured in Peterborough HRAP

The experimental setup used in this study to investigate the fate and role of carbon sources in microalgae-bacteria interactions aimed to mimic the conditions of light and carbon availability in a real-scale HRAP by using a laboratory-scale torus PBR. However, to simplify the system for better understanding microalgae-bacteria interactions mechanisms, synthetic wastewater with a single source of organic carbon, acetate, was used. Estimating to what extent the cocultures in the torus PBR were representative of the conditions observed in a real-scale HRAP is essential to inform on the relevance of using laboratory PBR to study large-scale systems from the perspective of wastewater treatment.

Table 6.3 compares the maximal concentrations of dissolved oxygen and average TIC and TOC concentrations measured during the daytime in Peterborough HRAP with the values measured in the torus PBR.

	Peterborough HRAP	**Torus - Acetate 130 mgC.L^{-1}**	**Torus - Acetate 260 mgC.L^{-1}**	**Torus - Glucose 130 mgC.L^{-1}**
Maximal value of dissolved oxygen (mg.L^{-1})	23	5	6	1
TIC (measured during the day) (mgC.L^{-1})	23	18	18	6
TOC (measured during the day) (mgC.L^{-1})	37	27	51	56

Table 6.3 – Dissolved oxygen, total inorganic and organic carbon measured during the day in Peterborough HRAP and cocultures in the torus PBR

Very high concentrations of dissolved oxygen were reached in the Peterborough HRAP (23 mg.L^{-1}), while dissolved oxygen only reached 5 to 6 mg.L^{-1} in the cocultures using acetate in the torus PBR. This difference is likely due to the significant consumption of acetate by microalgae in the torus PBR, reducing the net oxygen production in the culture, as demonstrated in Chapter 5. This is confirmed by the stoichiometric analysis and suggests that, in HRAP, microalgal growth is mainly autotrophic. In an HRAP fed with real wastewater, acetate and other molecules easily assimilable by microalgae would contribute only approximately for

10-15 % of the total organic load of raw wastewater, as explained in Chapter 4. However, this figure might be much higher after anaerobic pretreatment that favours VFA production. The contribution of microalgae to heterotrophic activity would be lower and oxygen production rate would be higher in the HRAP fed with real wastewater than in the torus PBR fed with synthetic wastewater using acetate. Moreover, the dissolved oxygen curve in Peterborough HRAP (Figure 6.16) is a bell-shaped curve that follows diurnal variations of light along the day, while the dissolved oxygen curve in the torus PBR presents a peak in the morning followed by a stabilization phase and a drop after sunset, due to an exisiting limitation in TIC for microalgae occurring shortly after sunrise. This suggests that microalgae are not limited by TIC in the Peterborough HRAP, confirming that CO_2 production by bacteria in the Peterborough HRAP is sufficient to meet algal needs, unlike in the torus PBR experiments. Besides, the concentration of inorganic carbon in the torus PBR was slightly lower (18 $mgC_{inorg}.L^{-1}$) than in Peterborough HRAP (23 $mgC_{inorg}.L^{-1}$). This confirms that the experiments in the torus PBR did not permit reproduction of the synergy expected.

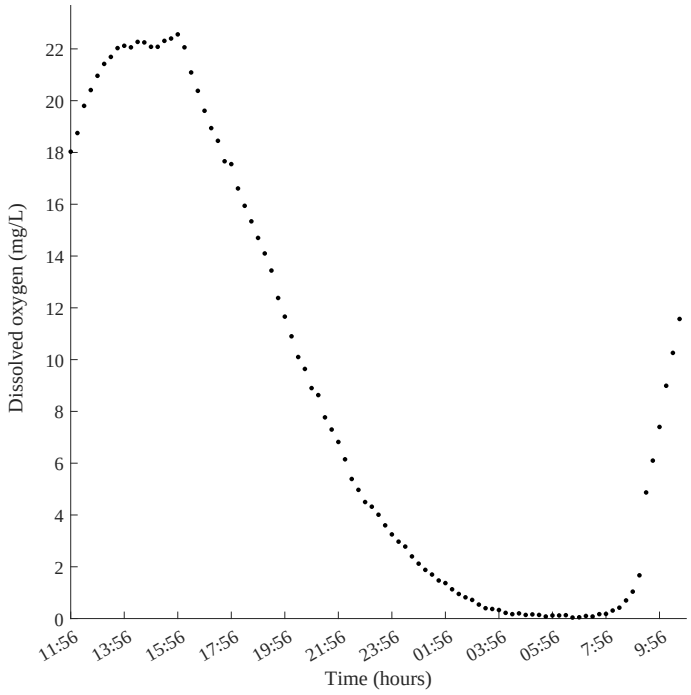

Figure 6.16 – Dissolved oxygen concentration in Peterborough HRAP over 24h

The concentrations of organic carbon in the coculture on synthetic wastewater in the torus PBR (27 and 51 $mgC_{org}.L^{-1}$) were comparable to organic carbon measurements in Peterborough HRAP (37 $mgC_{org}.L^{-1}$). However, the organic carbon measured in Peterborough HRAP is expected to be non-biodegradable carbon, given that the Biological Oxygen Demand, which corresponds to the fraction of the organic load degradable by microorganisms, was low (18 $mgO_2.L^{-1}$).

6.4 Discussion

6.4.1 Investigation of carbon and oxygen fate in a coculture in day-night cycle

- **Microalgae-bacteria ratio**

Microalgae-bacteria consortium in the cocultures SWWx1 and SWWx2 was dominated by microalgae. This tendency is likely due to the strong affinity of *S. obliquus* for acetate. However, a significant dominance of microalgae over bacteria is often reported in HRAPs. Safi et al. (2016) reported that in HRAPs, the particulate carbon was not dominated by active heterotrophic components, including bacteria and grazers, and stated that a balanced HRAP contained >60 % of microalgae, <20 % of bacteria, and <3 % of grazers. Cromar and Fallowfield (1992) determined that microalgal biomass accounted for 40 % of the total dry weight of a sample from an HRAP fed with aerobically pre-treated pig slurry, with the remaining 60 % comprising organic detritus and bacteria. However, in the model where only bacteria were consuming the organic carbon, bacteria represented 78 % of the total biomass compared to 22 % for microalgae, which is not representative of most HRAPs. The model revealed here that the relatively high microalgae/bacteria ratio observed in HRAP cannot be reproduced using a model that considers only one microalgal specie, one bacteria specie and one organic carbon source consumable only by bacteria. Microalgal growth relies thus on more complex mechanisms than the ones considered in the model.

The dominance of one microorganism over another one, either in the simplified system such as the coculture investigated in the present study or in a real-scale HRAP, is also expected to

depend on the hydraulic retention time. Bacteria have a much shorter generation time than microalgae, thus they are favored by relatively short HRT compared to microalgae when cultivated in continuous mode. In contrast, a long HRT, as applied in HRAPs and in the experiments presented in this study, could disadvantage bacteria compared to microalgae. Modeling work designed to test the impact of dilution rate on microalgae-bacteria ratio showed very little effect of the dilution rate due to the dependence of microalgae on bacteria. This might be more relevant in HRAPs were interdependence between the microorganisms is expected during the daytime.

- **Dynamics along day-night cycles**

In photoautotrophic conditions, studies have reported microalgal biomass losses ranging from 6 to 20 % over a 10-hour night (Artu 2016, Hindersin et al. 2014). Similarly, a microalgal biomass loss of 1 % per hour was observed following a light transition from 765 to 75 μmol.m^{-2}.s^{-1} in a photoautotrophic culture of *Chlorella vulgaris* (Bonnanfant et al. 2021). However, in the present study where microalgae were grown in mixotrophy in the presence of acetate, a lower biomass loss of 5 % was observed over 10 hours of darkness. This result is consistent with the conclusions drawn in Chapter 4, where organic carbon was found to reduce algal biomass loss during the dark phase. However, this hypothesis is contradicted by the model predictions, which suggest similar biomass loss even when organic carbon is not consumed by microalgae.

Algal and bacterial biomass measurements present a significant uncertainty as both measurements are indirect. They rely on total dry weight and on bacterial count and the correlation establish with bacterial biomass. As suggested by the large error bars in the Figure 6.9, variations in algal and bacterial biomass along the day-night cycle are in the range of the measurement uncertainty. Consequently, this method does not enable the observation of significant diurnal variations in bacterial and algal biomass.

Online measurements revealed diurnal variations in dissolved oxygen, with levels dropping to 1 mg.L^{-1} at night and rising to 6 mg.L^{-1} a few hours after sunrise. These periods of darkness correspond to low DO concentrations, potentially leading to oxygen limitation for both microalgae and bacteria. However, due to the limited precision of algal and bacterial biomass

measurements, the effect of oxygen limitation at night on their biomass could not be clearly observed. In Peterborough HRAP, dissolved oxygen tends to be limiting at the end of the night as well, but it exceeds 20 mg.L^{-1} at midday. The lower dissolved oxygen concentration measured in the cocultures compared to a real-scale HRAP is likely due to the utilization of acetate as a carbon source, which is more easily assimilable than other compounds present in wastewater. This hypothesis is supported by Sforza et al. (2018), who reported higher oxygen demand in microalgae-bacteria consortium in synthetic wastewater when acetate was used as a carbon source compared to meat extract or peptone.

Similarly, dissolved inorganic carbon concentration varied diurnally. TIC concentration increased by 20 % (SWWx1) and 38 % (SWWx2) at night due to microalgal respiration in the dark and dropped during the first 3 hours after sunrise due to CO_2 fixation by photosynthesis. Le Gouic et al. (2021) estimated that microalgae were limited in inorganic carbon when TIC $<$ 1 mM, yet DIC was close to this value in the torus PBR experiments. Limitation by TIC was also confirmed by the model with an organic carbon supply of 260 mgC_{org}.L^{-1}. Dissolved inorganic carbon concentration in Peterborough HRAP during the day was 1.9 mM on average, but diurnal variations of TIC were not measured. Sutherland et al. (2021) reported that TIC varied from 1 mM at midday to 3 mM at the end of the night in a real-scale HRAP, which is in the range of the values obtained in the torus PBR in the present study.

Finally, there was no significant variations of organic carbon over the day-night cycle, suggesting that acetate consumption was not impacted by darkness or by light-dependant mechanisms (photoautotrophy). This result is coherent with the conclusions drawn in Chapter 5, where photoautotrophic and photoheterotrophic algal growth were found to occur independently.

In conclusion, similar dynamics were observed in the model and in the torus PBR experiments, which allowed the identification of limitation by TIC for microalgae. This suggests that CO_2 production by bacteria was not sufficient to cover algal needs in the torus PBR experiment. Even while predominantly consuming acetate as a carbon source, microalgae would still be sensitive to TIC limitation and would benefit from CO_2 production by bacteria.

• **Carbon and oxygen fate in the consortium**

The stoichiometric analysis coupled to a data reconciliation approach allowed an estimation of the contributions of each microorganism and growth mode to carbon and oxygen fate, which was a relevant approach given the redundancy of the information available. However, the elementary compositions of *S. obliquus* and *E. coli* used in this method were sourced from the literature and were not determined for the specific strains and experimental conditions applied in the cocultures. Moreover, the *E. coli* yield coefficient for acetate was also taken from the literature. For future studies, measuring the elemental composition and stoichiometric parameters of each microorganism, grown under conditions similar to those in the experiment, would be necessary.

The capacity of *S. obliquus* to utilize acetate as a carbon source suggests that microalgae did not mainly rely on bacteria for carbon. Indeed, photoautotrophic growth contributed only 8 % and 21 % to algal growth in SWWx1 and SWWx2 respectively. Nevertheless, in SWWx2, enhanced CO_2 produced by bacteria significantly enhanced photoautotrophic algal growth compared to SWWx1, suggesting that microalgae still benefit from bacterial production of CO_2, while competing with them for acetate. Microalgae and bacteria were in competition for acetate, however according to the stoichiometric analysis bacteria still produces CO_2 that is consumed by microalgae and microalgae still produces O_2 that is consumed by bacteria, suggesting a mutual benefit between microalgae and bacteria. In addition, the model, where organic carbon was consumed only by bacteria, showed that in these conditions the coculture partly improves total biomass compared to monoculture due to microalgae relying completely on bacteria for carbon supply in the model. Similarities in the behaviour of oxygen and CO_2 in the model and in the coculture on acetate allowed for the identification of a limitation by inorganic carbon in the coculture on acetate, even while acetate was the main carbon source for microalgae according to the stoichiometric analysis. Even while microalgae and bacteria were in competition for acetate, microalgal growth also partly relied on bacteria for the production of CO_2.

Furthermore, contradictory results on the necessity of adding external CO_2 to HRAP to cover microalgal needs are reported in the literature (Ruas et al. 2020, Shayesteh et al. 2021,

Young et al. 2019b). DIC concentrations measured in HRAP (Sutherland et al. 2021) exceed the concentration of 1 mM, below which microalgae would be limited by inorganic carbon (Le Gouic et al. 2021). Moreover, as explained in Chapter 4, light is often the limiting parameter to microalgal growth in HRAP. These elements suggest that sparging CO_2 in HRAP would present only limited benefits, especially considering the additional operational costs associated with this system. However, the capacity of microalgae to use organic carbon as a carbon source questions the fate of the CO_2 produced by bacteria and the efficiency of carbon removal by the biomass. Yet, in the present study, even while using an organic carbon source easily consumable by microalgae such as acetate, the net CO_2 production, which can be seen as the flux of non-utilized CO_2 lost in the gas and the liquid phase, is very low (0.01 $mol.m^{-3}.h^{-1}$), suggesting an efficient use of the inorganic carbon by the coculture. The optimisation of the carbon source and its affinity towards cultivated microorganisms emerges as a key factor in the efficiency of microalgae-bacteria consortium for wastewater treatment, providing crucial information about the necessity to add external CO_2 to the HRAP.

6.4.2 Relevance of using torus PBR to simulate HRAP

- **Choice of the carbon source**

Approximately 45 $mgC_{org}.L^{-1}$ was measured in Peterborough HRAP; however, the biodegradable fraction of the remaining organic carbon is unknown. As suggested in Chapter 4, further studies should focus on the characterisation of the main organic molecules present in wastewater and in the outlet of the HRAP as well as their availability for different microorganisms to evaluate the limitations of both microalgae and bacteria in organic carbon. In SWWx1, organic carbon was limiting in the coculture and led to a strong competition between *S. obliquus* and *E. coli* for acetate, which is unlikely to occur in real HRAP. In SWWx2, acetate concentration was doubled to observe the behaviour of the consortium in non-limiting organic carbon conditions, but microalgae dominated the consortium in both cases, highlighting that the low growth of *E. coli* was due to the fact that acetate is more suitable for *S. obliquus* than for *E. coli*. Moreover, the same experiment using glucose as the carbon source led to very low algal

growth and total biomass, with bacteria dominating the consortium. In the end, using only one organic carbon source led to domination of the consortium by the specie with the highest affinity for the substrate. For further research, the composition of the synthetic wastewater in laboratory experiments should be more representative of the biodegradability of the organic load in HRAP operated in real conditions. In wastewater, certain molecules as polysaccharides for example can only be consumed by bacteria, limiting microalgal heterotrophic growth and allowing heterotrophic bacteria to grow without competition on organic carbon with microalgae (Sforza et al. 2018), enhancing the contribution of autotrophic growth, the production of oxygen by microalgae, and of inorganic carbon by bacteria, which is beneficial for the symbiosis. Besides, organic compounds require more or less oxygen for their degradation. For example, pollutants like methane and methanol require more O_2 in the system than glucose to be degraded (Russel et al. 2020), influencing O_2 availability in the consortium and microalgae-bacteria interactions (Figure 6.17).

As part of a study investigating microalgae-bacteria gas exchanges in wastewater, Sforza et al. (2018) utilized a synthetic wastewater composed of 38 % acetate, 36 % meat extract and 26 % peptone. Despite the presence of simple (acetate) and complex (meat extract) compounds, the biological oxygen demand of the synthetic medium was higher than real wastewater, suggesting the biodegradability of the compounds utilized was not representative of real wastewater either. Prepared according to Nopens et al. (2001), the synthetic wastewater used by Robles et al. (2020) and Casagli et al. (2021) for feeding HRAP was more complex and comprised six different organic compounds: 31 % starch, 29 % milk powder, 15 % acetate, 13 % yeast extract, 7 % soy oil and 4 % peptone. The fraction of acetate is coherent with domestic wastewater composition reported by Huang et al. (2010), where volatile fatty acids represent 11 % of the total COD. With this medium, simple sugars are supplied by milk powder and proteins by peptone, milk powder and yeast and would represent respectively 10 % and 25 % of the organic load, which is coherent as well with the composition of domestic wastewater. In this synthetic wastewater, starch represents the organic fraction consumable by bacteria but not by microalgae. Again, the biodegradability of different groups of organic molecules by different groups of microorganisms

needs to be investigated to better understand the complexity of HRAP systems.

- **Light attenuation**

The Mean Rate of Photons Absorption in Peterborough HRAP was estimated around 6 μmol.g^{-1}.s^{-1}, considering an algal biomass concentration around 0.3 g.L^{-1}, a depth of 0.3 m and an average incident irradiance over 24 hours of 500 μmol.m^{-2}.s^{-1}, based on light measurements completed in summer. However, the MRAP was found much higher in the cocultures in the torus PBR, with 18 μmol.g^{-1}.s^{-1} in SWWx1 and 9 μmol.g^{-1}.s^{-1} in SWWx2 due to the lower reactor depth in the torus PBR. Higher biomass productivity and higher dissolved oxygen concentration were then expected in the torus PBR than in Peterborough HRAP due to higher light availability, however the opposite was observed. This result suggests that biomass productivity, oxygen, and carbon cycle rely on a more complex system than initially expected.

- **Conclusion on the relevance of using torus PBR**

The algal and bacterial biomass measurements lacked precision to reveal subtle variations in behaviour along the day-night cycle. However, online analysis of gas and liquid phases, facilitated by a well-mixed, controlled, and equipped torus PBR, provided valuable information on biomass dynamic response to light variations. In addition, Chapter 3 demonstrated that large-scale HRAPs are well-mixed and that oxygen, inorganic carbon, and organic carbon are not impacted by depth, width, or distance from the paddlewheel in a large-scale HRAP. Consequently, using a well-mixed PBR such as torus PBR to simulate HRAP remains relevant. However, the design of these laboratory-scale experiments reveals to follow a model that is too simplified to fully account for the phenomena actually involved in contributing to the effectiveness of an HRAP. Using acetate alone was inadequate for simulating wastewater organic load due to its high affinity with microalgae, which is not representative of microalgae's affinity with most of wastewater organic molecules. Moreover, different microalgae and bacteria species have varying affinities with organic molecules, making a consortium composed of a variety of microalgae and bacteria species more appropriate than a single microalgal and bacterial specie. Additionally, while the present study focused on the carbon cycle, the nitrogen cycle is maybe

also crucial for understanding microalgae-bacteria interactions. As demonstrated in Chapter 3, nitrifying bacteria that convert NH_4^+ (microalgae preferred nitrogen source) to NO_2^- and NO_3^- are significant in HRAP and could impact microalgal growth.

Analysis of the DO dynamics in the model and in the experimental cocultures, that turned out to be similar, revealed that the modeled and experimental cocultures were limited by TIC. This demonstrates that, in these models, TIC limitation occurs whether microalgae-bacteria ratio is in favour of microalgae or bacteria and whether organic carbon is consumed by microalgae and bacteria. Yet, DO dynamics observed in Peterborough HRAP showed no TIC limitation in the HRAP. The bell-shaped DO curve was typically associated with a limitation by light rather than TIC. Besides, the microalgae-bacteria ratio obtained in the model (low microalgae) was far from the ratio observed in HRAP, this being due to microalgae limited by TIC in the model and not in the HRAP. In conclusion, overly simplified systems like the model and the experiments in the torus using acetate or glucose are not fully suitable to simulate a complex system such as a HRAP. In the end, the system used to simulate HRAP should not be limited in TIC or in DO and present a microalgae proportion close to 2/3 of the biomass (Safi et al. 2016) to be considered representative.

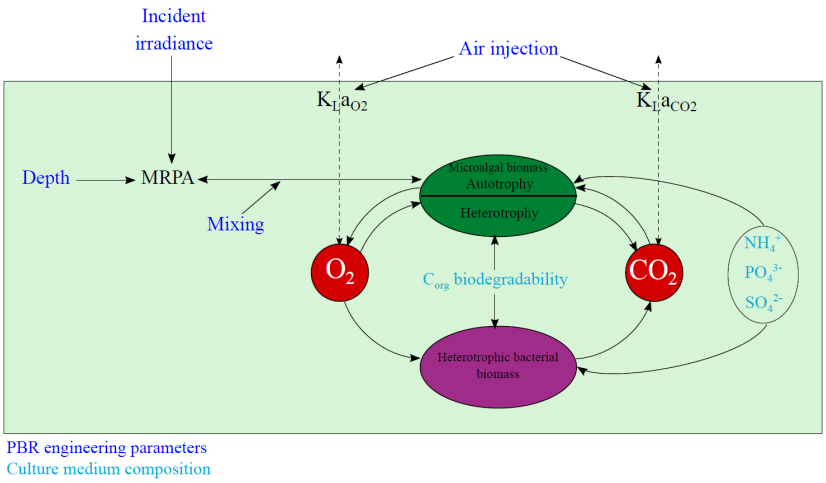

Figure 6.17 – Factors determined by experimental conditions influencing O_2, CO_2 and organic carbon availability in a laboratory PBR

6.5 Conclusion

Instead of a symbiotic interaction, microalgae and bacteria were found to compete for acetate, which favoured microalgae, while using glucose favoured only bacteria in the lab-scale experimental setup designed to study microalgae-bacteria interactions that could occur in an HRAP. Besides, no complete synergy could be observed in the model where organic carbon was consumed only by bacteria, which is the generally accepted mechanism. These results suggest that overly simplified systems like the model or the experiment in the torus using a sole organic carbon source, a sole microalgae strain and a sole bacteria strain did not permit recreation of the interactions as encountered in HRAP. This is supported by the observation that the total biomass productivity obtained in the torus was far from the productivity measured in Peterborough HRAP.

A portion of the phenomena necessary to fully explain this synergy is still to be explored. The synergy observed in HRAP seems to rely on a more complex system than a simple coculture, in which a variety of bacterial strains are able to degrade a variety of organic molecules as a result of their specific affinities. The level of simplification of the system turns out to be crucial while simulating large-scale HRAP systems in a laboratory photobioreactor. Both microalgal and bacterial populations (including nitrifiers) and organic carbon source should be complexified to enable accurate simulation of microalgae-bacterial interactions in HRAP.

Despite significant differences in the conditions between the laboratory-scale torus PBR and Peterborough HRAP, our results have enabled a better understanding of the nature of microalgae-bacteria interactions in a coculture under dynamic light conditions simulating solar conditions, demonstrating the relevance of the proposed approaches. While experiments with acetate demonstrated that microalgae contribute to organic load removal traditionally attributed solely to bacteria, this study also revealed that the choice of the organic carbon source was extremely relevant when studying microalgae-bacteria interactions, significant photoheterotrophic contribution being observed with acetate but not with glucose. Therefore, investigating the respective affinities of microalgae and bacteria towards various organic carbon sources present in HRAPs would be an interesting perspective toward a better understanding of HRAP functioning.

Nevertheless, both the torus PBR and modelling turned out to be relevant tools for studying interactions between microorganisms in HRAP system. As detailed in Chapter 4, a combination of controlled laboratory studies and outdoor large-scale operational high rate algal ponds should be conducted to comprehensively investigate the complex mechanisms involved.

Moving forward, while previous chapters focused on microalgae-bacteria interactions related to the removal of organic and mineral pollutants, Chapter 7 will address pathogen removal, another major issue in wastewater treatment. While oxygen is essential in microalgae-bacteria interactions, it also plays a crucial role in pathogen disinfection in HRAPs by enabling the production of Reactive Oxygen Species that damage microbial and viruses structure. Moreover, despite the well-mixed nature of the Peterborough HRAP, field measurements revealed a strong attenuation of solar radiations throughout the reactor depth, potentially impacting solar inactivation of pathogens. Chapter 7 will focus on the impact of microalgae on the solar inactivation of indicator viruses in HRAPs, with the perspective of improving pathogen removal efficiency in HRAP systems.

Highlights

- Photoheterotrophic contribution depends on the organic carbon source.
- In coculture in dynamic conditions, microalgal growth relies on bacterial production of CO_2.
- The model predicted similar dynamics to the ones observed in HRAP.
- Complex carbon source mixtures and algal and bacterial populations should be used to simulate HRAP more representatively.
- Further research should focus on the biodegradability of wastewater compounds by microalgae and bacteria.

Chapter 7

Impact of microalgae on indicator viruses solar inactivation in HRAP in the perspective of improving pathogens removal in HRAP systems

7.1 Introduction

Nowadays, pathogens removal constitutes the most crucial challenge of wastewater treatment worldwide. Pathogens conveyed by wastewater are responsible for diseases such as cholera, dysentery, typhoid, intestinal worm infections and polio. Poor wastewater pathogens removal contributes both to spreading those diseases and to enhancing antimicrobial resistance (World Health Organisation 2022). In classical wastewater treatment systems, pathogens are removed by tertiary treatments such as chlorination, UV irradiation or ozonation, when necessary (Lian et al. 2018). In High Rate Algal Ponds, pathogens can be removed by solar disinfection. Ultraviolet radiations from the sun generate photochemical modifications of microorganisms and viruses DNA and RNA, causing the inhibition of DNA replication and transcription and the interruption of cell division. Microalgae are generally highly resilient to UV damages due to

efficient biosynthesis of photoprotectant and antioxidant molecules, DNA repair mechanisms, migration through the water column and biofilm formation capacities (Rastogi et al. 2020). On the contrary, solar radiations significantly improve the inactivation of *E. coli*, MS2 virus, echovirus and norovirus compared to darkness. Park et al. (2021) reported that, in an outdoor pond, the inactivation of those pathogens was 10 times slower in darkness than when exposed to sunlight.

However, microorganisms and virus DNA can be repaired by a photolyase enzyme after irradiation, causing their regrowth (Putois 2012). Consequently, irradiation of wastewater by UV must be coupled to processes assisting pathogens inactivation. Bolton (2012) reported synergistic effects of dissolved oxygen, pH and sunlight in pathogen inactivation in Waste Stabilisation Ponds. Yet, algal biomass is higher in HRAP than in WSP, causing higher turbidity and reducing UV penetration throughout the 30 cm-depth wastewater column. However, pH and photosynthetically produced dissolved oxygen are also expected to be higher in HRAP than in WSP due to higher algal biomass and photosynthetic activity. Besides, the molecules present in the pond can also act as photosensitisers and contribute to disinfection process. Photosensitizers are light absorbing compounds that transfer their energy to other molecules leading to the formation of Reactive Oxygen Species that can damage microorganisms and virus membranes and capsid proteins. Photosensitisers are either exogenous, including humic substances, photosynthetic pigments and dissolved organic matter, or endogenous, including cells able to absorb wavelengths between 290 and 750 nm (Bolton et al. 2011). The effect of photosensitisers from wastewater coupled to high pH and DO on indicator microorganisms and viruses inactivation was reported as significant in the presence of UVA (Bolton 2012). However, the contribution of photosensitisers from microalgae compared to photosensitisers from wastewater is still poorly studied.

Besides, microalgae appeared to be the main contributor to absorbance in a 70 cm depth pond containing wastewater and microalgae (Bolton 2012). As mentioned in the Chapter 3, in Peterborough HRAP, both turbidity and chlorophyll *a* concentration were high, suggesting that microalgae would actually be the main contributor to attenuation of the suns' radiation along the pond depth. However, as reported in the Chapter 3, Peterborough HRAP also shows a very

high suspended solids concentration (1 $g.L^{-1}$) that would be composed of only approximately 30% of microalgae, the remaining fraction being organic detritus likely to be responsible for sun radiations attenuation. Moreover, inactivation by UV radiations was reported to be less efficient at higher suspended solids concentrations (Lazarova et al. 1999). While organic detritus impact pathogens inactivation by reducing sun radiations penetration in the pond, they would also favour the adsorption of viruses, protecting them from the radiations. In winter 2020, Peterborough HRAP exibited a log reduction value of 1 for coliphage viruses and 2.26 for *E. coli* along with an *E. coli* concentration of 3.68 $\log_{10}$MPN.$100ml^{-1}$ [1] in the outlet (Sam Butterworth and Howard Fallowfield, personnal communication), which complies with Australian regulations for irrigation of non food crops but not for irrigation of food crops or public gardens. The contribution of both wastewater and microalgae to sun radiation attenuation in Peterborough HRAP is then still unclear, as well as its direct effect on pathogens inactivation (Figure 7.1). Evaluating the impact of microalgae on pathogens inactivation would be useful for the design of a tertiary treatment system targeting pathogens and would contribute to the optimisation of pathogens removal in HRAP.

This study aims at determining the impact of microalgae and wastewater on inactivation process in terms of sun radiations attenuation and ROS production. Sun radiations include UVB (280-315 nm), UVA (315-400 nm) and visible light (400-800 nm). UVB, that cause direct damage to RNA, was reported to be the predominant mechanism associated with disinfection by sunlight (Lian et al. 2018), however UVB measurements in Peterborough HRAP showed that this range of radiation does not penetrate the pond surface due to high turbidity. Visible light experiences lower attenuation in the pond but generally show negligible effect on pathogens inactivation (Bolton 2012). The present study will then focus on the effect of UVA, that were detected in the volume of Peterborough HRAP and reported to enhance pathogens inactivation (Bolton 2012) but of which role is well less understood than UVB. In this study, irradiation of samples with UVA is completed in controlled and sterile conditions in a UVA cabinet.

Viruses constitute a major issue for public health, notably because only one of few viral

1. MPN = Most Probable Number

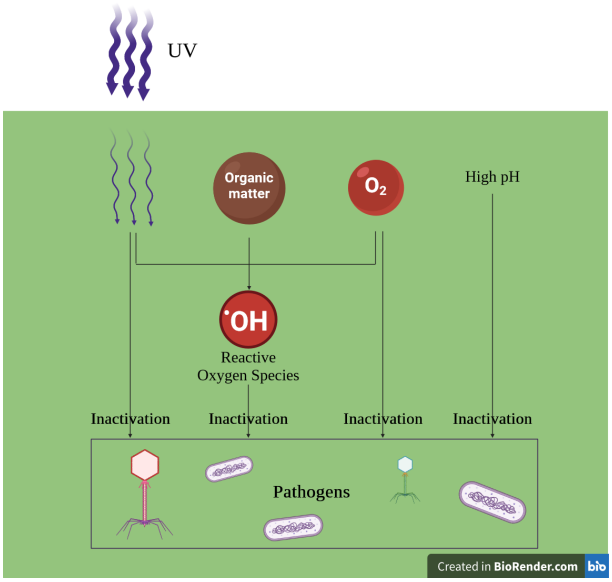

Figure 7.1 – Interactions of factors influencing disinfection in HRAP

particles can lead to an infection and because viruses are usually more resistant than bacteria to disinfecting agents. Viruses are found in very large quantities in HRAP. Hisee et al. (2020) reported a viral load of approximately $10^{9.5}$.ml^{-1} of virus-like particles and $10^{8.5}$.ml^{-1} of large virus-like particle in Kingston-on-Murray HRAP (South Australia). For those reasons, this study will focus on the inactivation of viruses.

The coliphage virus MS2, a widely used indicator for the presence of coliphages in wastewater, was chosen as the model pathogen. This F-RNA coliphage is used extensively to determine likely virus inactivation rates when validating disinfection rates of wastewater treatment systems. MS2 virus also presents a simple composition (Kuzmanovic et al. 2003), is non pathogenic, have similar resistance to antimicrobial agents to human pathogenic viruses (e.g., poliovirus, influenza A, and rhinovirus) and is easy of preparation and assay (Woo et al. 2010). This virus constitutes then an interesting model microorganism for studying inactivation in wastewater. MS2 is an icosahedral virus that belongs to the Leviviridae family. It is a non-enveloped and single stranded RNA virus of very small size (27 nm, Dedeo et al. (2011)). 32 pores of 2 nm each on the virus capside allow the diffusion of small molecules (Dedeo et al. 2011). MS2 also present a protein A for binding to

E. coli F-pilus (Zhong et al. 2016). MS2 infection of *E. coli* down regulates TCA cycle, altering bacterial cell growth and biosynthesis of the cell wall (Jain and Srivastava 2009).

Firstly, the contribution of both microalgae and wastewater to UVA attenuation through 30 cm depth and the impact on MS2 inactivation will be estimated in sterile 250 ml quartz-lid bottles. Secondly, the impact of exogenous photosensitisers from microalgae extract and wastewater and of endogenous photosensitisers from microalgal cells on MS2 inactivation under UVA irradiation will be investigated in sterile 250 ml quartz-lid bottles. In this part, L-histidine will be used to inhibit the inactivation effects of singlet oxygen produced from photosensitisers exposed to UV radiations (Méndez-Hurtado et al. 2012). The impact of each factor (UVA attenuation and the presence of photosensitisers) will be compared in order to determine if the presence of microalgae globally enhances or inhibits coliphage indictor viruses inactivation compared to wastewater. Thirdly, this statement will be verified by measuring MS2 inactivation in 30 cm depth wastewater columns in the presence or absence of microalgae.

7.2 Material and methods

- **Effect of UVA attenuation**

As illustrated in the Figure 7.2, the depth averaged UVA irradiances $G_{30cm_{RO}}$, $G_{30cm_{WW}}$ and $G_{30cm_{ALG}}$ were obtained by measuring UVA irradiance throughout a 30 cm-depth column of RO water, anaerobically pretreated wastewater and microalgae at a concentration close to microalgal biomass concentration in Peterborough HRAP, respectively. As explained in the Chapter 2, wastewater was sampled at the outlet of Peterborough HRAP and microalgae was isolated from Peterborough HRAP then grown in BBM until reaching chlorophyll *a* concentration measured in Peterborough HRAP. Incident irradiance was 22 $W.m^{-2}$, which corresponds to the average UVA irradiance measured over 3 days per months in winter between 2008 and 2011 on a roof in Old Reynella, South Australia (S35°5′56.3″ E138°32′25.9″) (Bolton 2012) and was then considered as the value of reference as Australian standards for HRAPs evaluation are based on winter performances.

To determine disinfection rate in optically clear water at the respective depth averaged

irradiances, $G_{30cm_{RO}}$, $G_{30cm_{WW}}$ and $G_{30cm_{ALG}}$ were then applied as incident UVA irradiances on 250 ml RO water inoculated with MS2 in quartz lid bottles. A sample was taken aseptically every 12 h during 50 h for MS2 concentration determination and calculation of inactivation rates. Each condition was tested in triplicates.

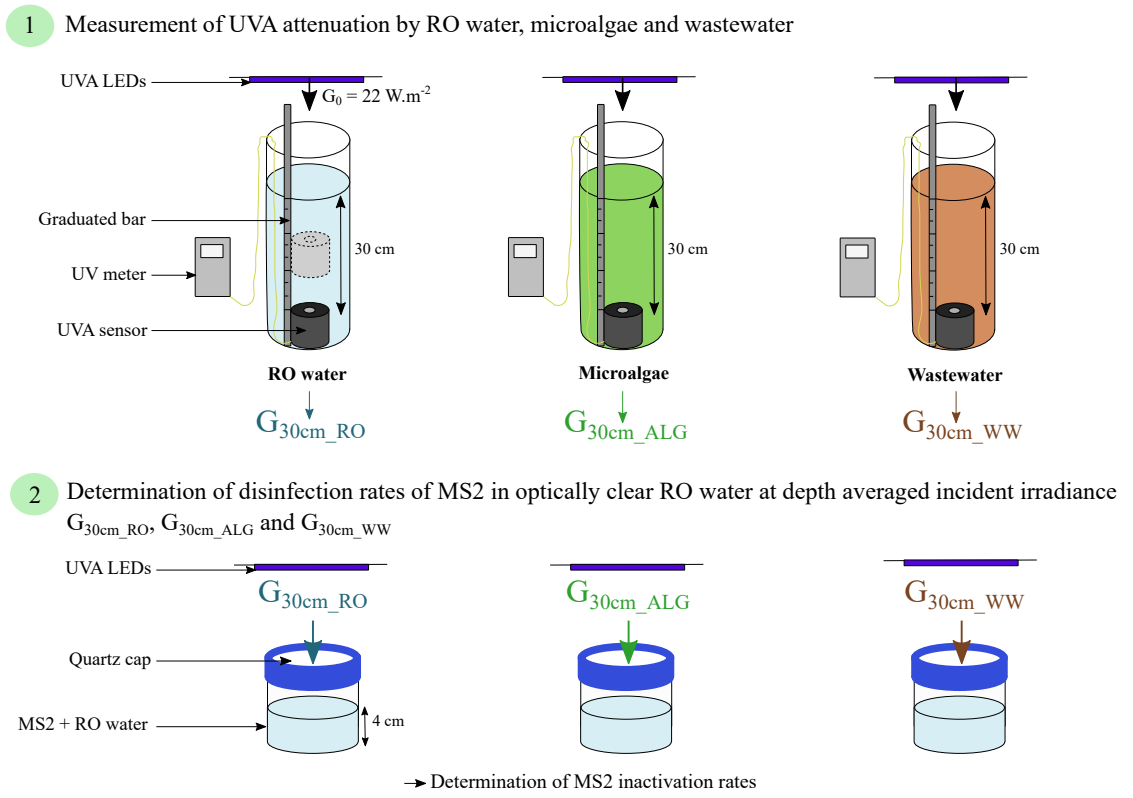

Figure 7.2 – Experimental plan for investigation of effect of UVA attenuation by microalgae and wastewater on MS2 inactivation by UVA

- **Effect of photosensitisers**

As illustrated in the Figure 7.4, MS2 was incubated in 250 ml of RO water, BBM, 0.45 μm filtered wastewater, microalgae extract (microalgae heated at 80°C then 0.45 μm filtered) and microalgae. The objective was to have same depth averaged irradiance for all substrates within a 4 cm depth i.e. $G_{4cm_{RO/BBM}} \approx G_{4cm_{WW}} \approx G_{4cm_{EXTR}} \approx G_{4cm_{ALG}}$. This required varying the incident UVA irradiance and in situ measurement of attenuation within a 4 cm depth of substrate above the measuring probe (as shown in Figure 7.3). Table 7.1 synthesises the UVA

irradiance values measured over the sample depth after determining the incident irradiance (in red) so the average UVA intensity (in bold) is approximately equal to 9 ± 0.5 W.m^{-2} in RO water, BBM, filtered wastewater, microalgae and microalgae extract.

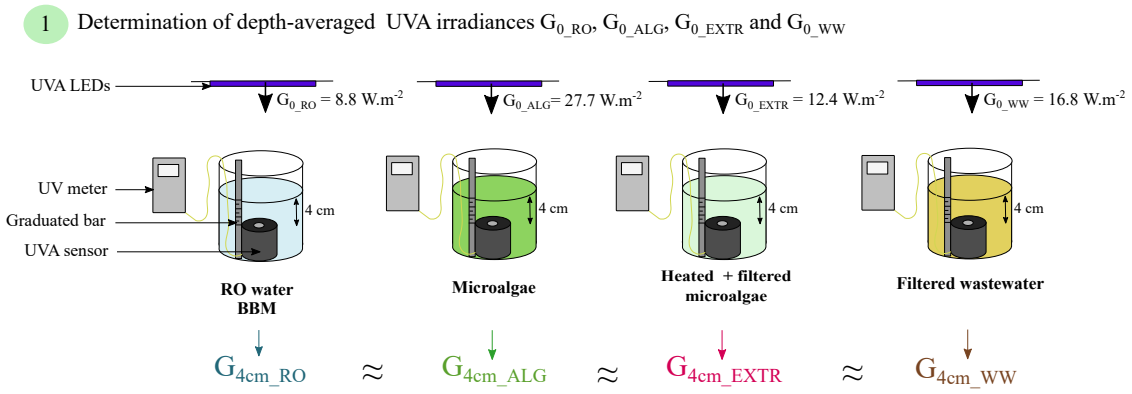

Figure 7.3 – Experimental plan for investigation of effect of ROS from microalgae and wastewater on MS2 inactivation by UVA - Determination of depth-averaged irradiance

Depth	**RO water and BBM**	**Microalgae**	**Microalgae extract**	**Filtered wastewater**
0 cm	8.8	27.7	12.4	16.8
1 cm	8.7	10.9	11.1	12.5
2 cm	8.3	3.8	8.6	8.8
3 cm	8.8	1.4	7.3	5.4
4 cm	8.8	0.3	6.4	3.9
Average	**8.7**	**8.8**	**9.2**	**9.5**

Table 7.1 – UVA irradiance (in W.m^{-2}) over 4 cm-depth RO water/BBM, microalgae, microalgae extract and filtered wastewater after adjusting incident UVA irradiance (at depth = 0 cm, in red) to obtain similar average irradiance over the 4 cm depth (in bold)

MS2 incubated in RO water, BBM, 0.45 μm filtered wastewater, microalgae extract and microalgae were irradiated (Figure 7.4) respectively with the previously obtained (Figure 7.3) depth averaged irradiances $G0_{RO}$, $G0_{BBM}$, $G0_{WW}$, $G0_{EXTR}$ and $G0_{ALG}$. Each experiment was completed in triplicate and with and without L-histidine. Added at a concentration of 20 mmol, L-histidine inhibits the effects of the ROS singlet oxygen produced by photosensitisers when irradiated with UV. As illustrated in Figure 7.5, the singlet oxygen binds to L-histidine and is

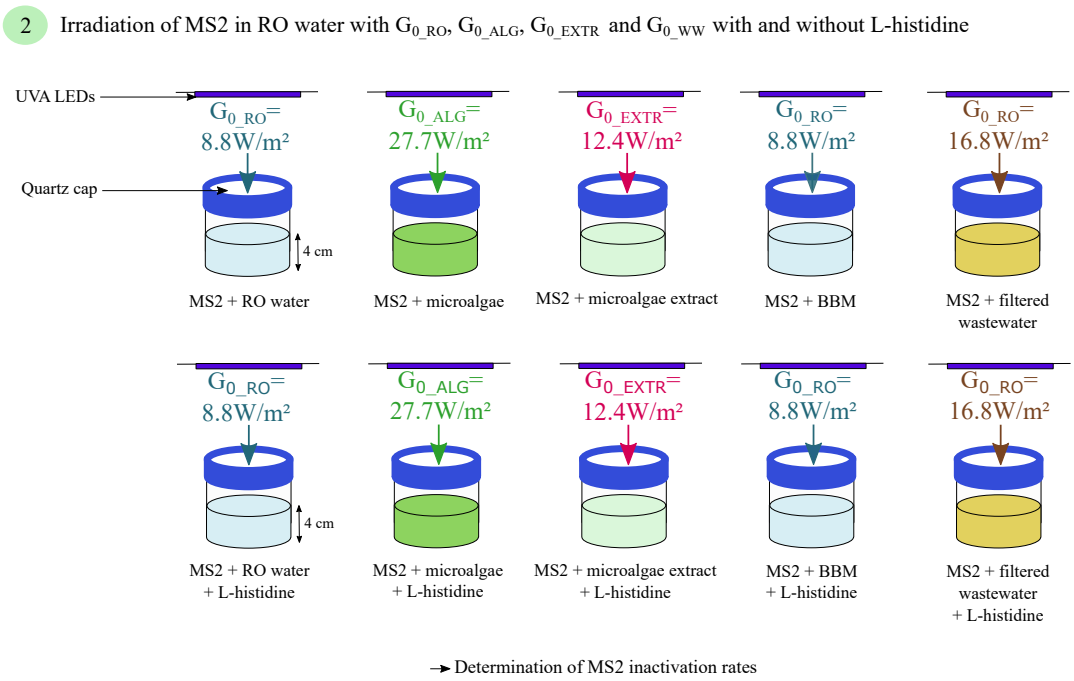

Figure 7.4 – Experimental plan for investigation of the effect of ROS from microalgae and wastewater on MS2 inactivation by UVA - Irradiation of MS2

consequently inefficient for the inactivation of microorganisms.

A sample was taken aseptically every 12 h during 50 h for MS2 concentration determination and calculation of inactivation rates. Singlet oxygen effect on MS2 inactivation was then deduced by difference from the inactivation rate obtained with and without L-histidine.

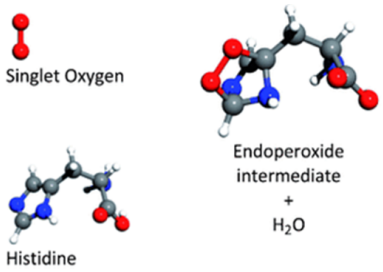

Figure 7.5 – Mode of action of L-histidine for the inhibition of the effects of singlet oxygen (Méndez-Hurtado et al. 2012)

Figure 7.6 details the components present in each medium and the associated photosensitisers. The purpose of this study is to estimate the impact of ROS from wastewater and microalgae

on MS2 inactivation, represented in brown and green in Figure 7.6. However, some components contained in the MS2 inoculum (organic molecules from the TSA agar plate) and in the BBM used for growing microalgae (nitrates and EDTA) are expected to act as photosensitisers and to contribute significantly to MS2 inactivation, leading to potential overestimation of the contribution of ROS to MS2 inactivation. Consequently, inactivation rates determined in RO water and in BBM constitute the baselines of the inactivation rates obtained in filtered wastewater and microalgae respectively.

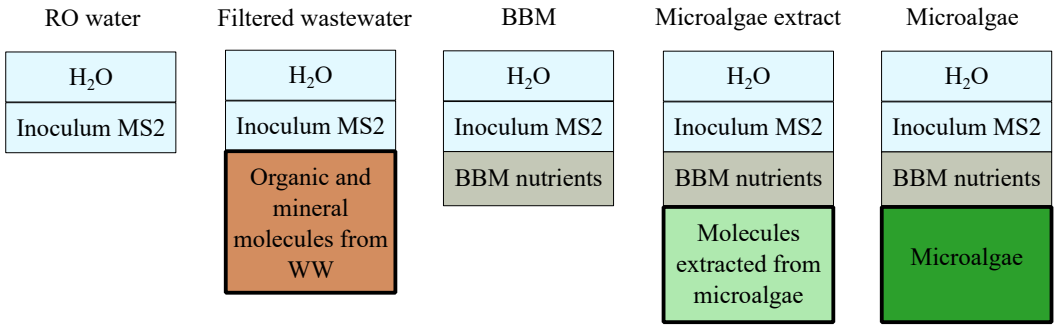

Figure 7.6 – Composition of the different media used in experiments investigating the effect of ROS from wastewater and microalgae on MS2 inactivation

While the global inactivation rate K_{TOT} is measured from the experiments without L-histidine, the inactivation rate K_{HST} is measured from the experiments with L-histidine where the effects of ROS are inhibited. The inactivation rate K_{ROS} attributable to ROS is then given by the following formula:

$$K_{ROS} = K_{TOT} - K_{HST} \tag{7.1}$$

- **Integration experiments:**

The third series of experiments aims at evaluating the global impact of microalgal cells on MS2 inactivation in a 30 cm depth wastewater column. As illustrated in the Figure 7.7, MS2 was inoculated in 30 cm depth anaerobically pretreated wastewater columns with and without microalgae and irradiated with UVA at $G_0 = 22$ W.m^{-2}. A sample was taken aseptically every

12 h during 50 h for MS2 concentration determination and calculation of inactivation rates. Each condition was tested in triplicates, with and without L-histidine.

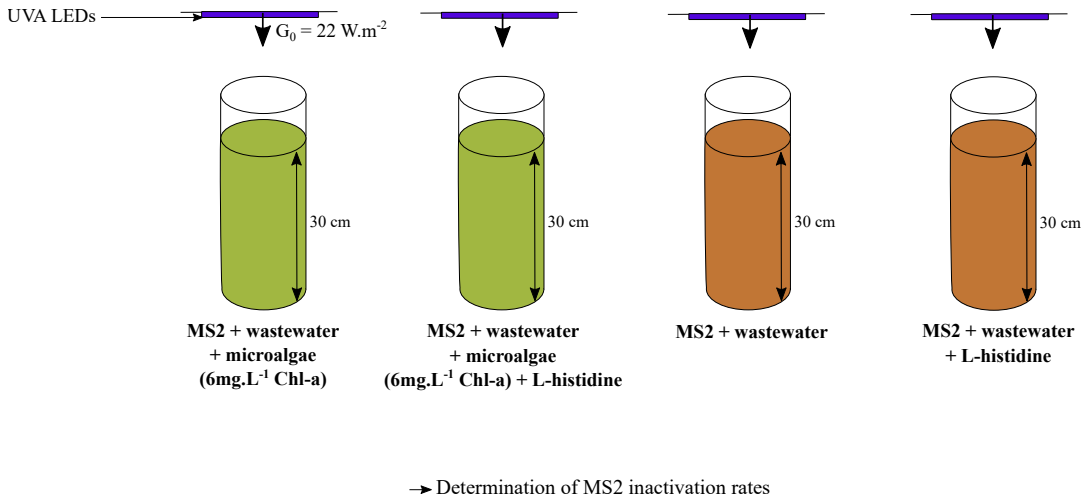

Figure 7.7 – Experimental plan for investigation of the effect of microalgae on MS2 inactivation in a 30 cm depth wastewater column

7.3 Results

7.3.1 Effect of UVA attenuation by wastewater and microalgae on MS2 inactivation

7.3.1.1 UVA attenuation by RO water, wastewater and microalgae

The Figure 7.8 shows the impact of depth on UVA intensity in RO water, wastewater and microalgae culture at an incident irradiance of 22 W.m^2. The strongest attenuation of UVA radiation was observed in the microalgae culture, where UVA radiation was completely absorbed below 6 cm depth. In wastewater, UVA radiations are completely attenuated below 9 cm depth, while in RO water UVA radiation was still detected (9 W.m^{-2}) at the bottom of the column. The depth averaged UVA irradiances were 12.9 W.m^{-2}, 2.5 W.m^{-2} and 2.1 W.m^{-2} in the 30 cm depth RO water, wastewater and microalgae columns respectively. Those values correspond to the average UVA intensities at which viruses would be exposed to in a 30 cm depth column of

RO water, wastewater and microalgae culture respectively.

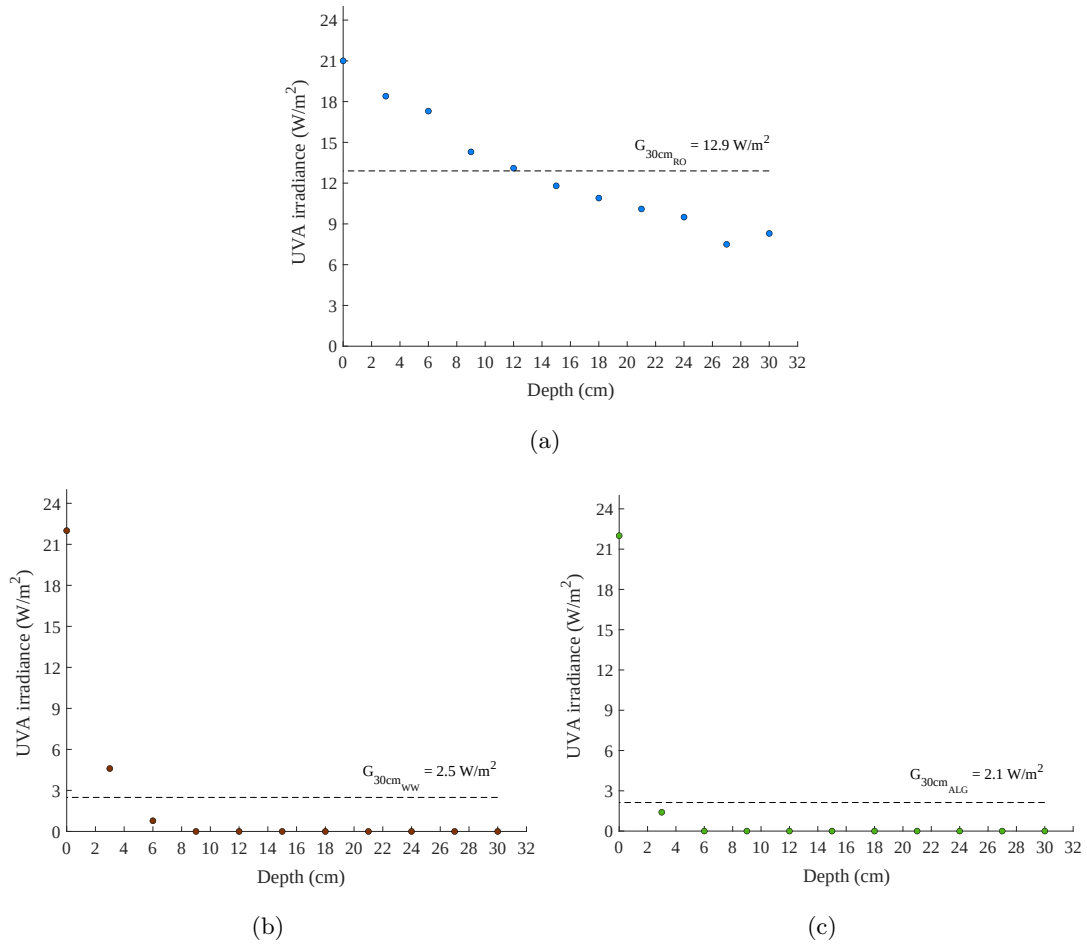

Figure 7.8 – UVA attenuation in a 30 cm-depth column of (a) RO water (b) anaerobically pretreated wastewater (c) microalgae culture. Dotted lines correspond to the averaged UVA irradiance.

7.3.1.2 MS2 inactivation rates under different UVA irradiances

The UVA intensities $G_{30cm_{RO}} = 12.9$ W.m^{-2}, $G_{30cm_{WW}} = 2.5$ W.m^{-2} and $G_{30cm_{ALG}} = 2.1$ W.m^{-2}, determined experimentally as described in the Section 7.3.1.1, were applied to RO water samples inoculated with MS2 to investigate the effect of UVA attenuation by wastewater and microalgae on MS2 inactivation. The inactivation rates are represented in the Figure 7.9. The changes in MS2 concentration over 50 h that were used for the calculation of the inactivation rates K are presented in the Appendix D.

The control experiment in darkness revealed a very low MS2 decay rate (0.0068 h^{-1}) in the absence of UVA radiations in RO water. This value is of the same order of magnitude as the MS2 inactivation rate of 0.005 h^{-1} measured in dark conditions in RO water by Bolton (2012). In comparison, the MS2 inactivation rate at UVA irradiances of $G_{30cm_{RO}}$ = 12.9 $W.m^{-2}$ was 0.084 h^{-1}, 0.043 h^{-1} for $G_{30cm_{WW}}$ = 2.5 $W.m^{-2}$ and 0.023 h^{-1} for $G_{30cm_{ALG}}$ = 2.1 $W.m^{-2}$. The turbidity attributable to wastewater or microalgae induced then respectively a reduction of 48.8% and 72.6% in the inactivation rate of MS2 compared to a clear medium such as RO water.

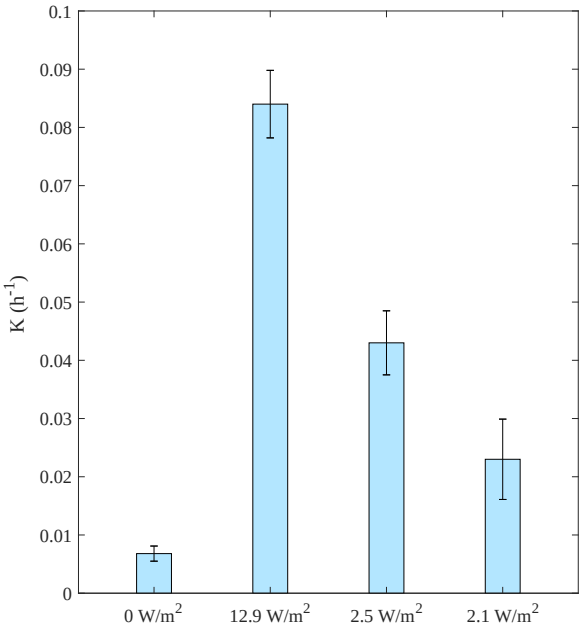

Figure 7.9 – MS2 inactivation rates K in h^{-1} obtained in RO water at UVA incident irradiances equivalent to the respective depth averaged irradiance obtained at an incident irradiance of 22 $W.m^{-2}$ within 30 cm-depth columns of RO water, wastewater and a microalgal suspension.

7.3.2 Effect of ROS from wastewater and microalgae on MS2 inactivation

MS2 inactivation in the presence of ROS (without L-histidine) and in the absence of ROS (with the addition of L-histidine) from wastewater and microalgae while irradiated with respective depth averaged UVA irradiances (Section 7.3.1.1) was investigated. The inactivation rates

are shown in the Figure 7.10. The evolution of MS2 concentration over 50 h that were used for the calculation of the inactivation rates K are presented in the Appendix D.

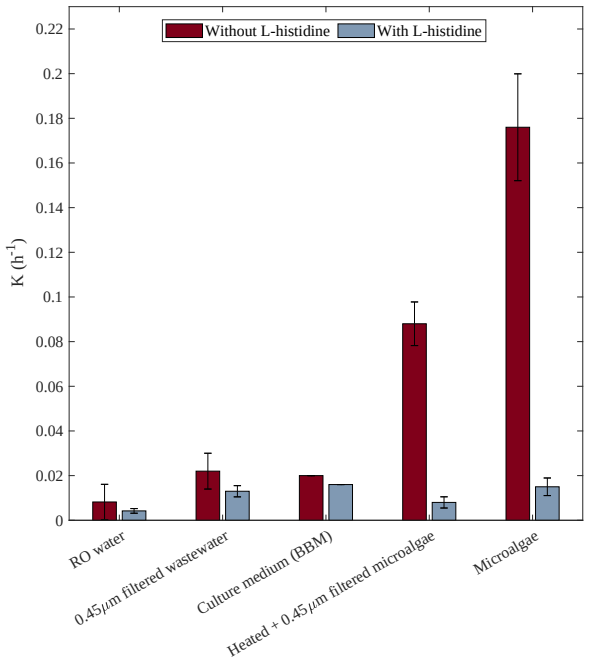

Figure 7.10 – MS2 inactivation rates K with and without L-histidine in RO water, 0.45 μm filtered wastewater, BBM, heated and 0.45 μm filtered microalgae culture and microalgae culture irradiated respectively with with adjusted UVA intensities $G0_{RO}$ = 8.8 W.m^{-2}, $G0_{WW}$ = 16.8 W.m^{-2}, $G0_{BBM}$ = 8.8 W.m^{-2}, $G0_{EXTR}$ = 12.4 W.m^{-2} and $G0_{ALG}$ = 27.7 W.m^{-2}

In RO water, the inactivation rate K was 0.0042 h^{-1} in the presence of L-histidine and 0.0082 h^{-1} in the absence of L-histidine. RO water is considered free of photosensitisers, consequently the inactivation rates with and without L-histidine were expected to be similar. However, traces of organic molecules from agar plates may be in the MS2 inoculum and could have acted as photosensitisers in this experiment. The contribution of ROS to MS2 inactivation in this experiment was, however, very low (0.0040 h^{-1}) and comparable with the dark inactivation rate (0.0068 h^{-1}), suggesting that UVA *per se* does not inactivate viruses efficiently and that a significant amount of photosensitiers are needed to produce ROS and damage the viral particles. In addition, as illustrated in the Figure 7.10, inactivation rates with L-histidine in RO water, wastewater, BBM, microalgae and microalgae extract were all similarly low compared to the

inactivation rates obtained without L-histidine, highlighting the major contribution of ROS to MS2 inactivation regardless of the medium.

The Figure 7.10 shows that the MS2 inactivation rate in filtered wastewater (0.022 h^{-1}) was higher than in RO water (0.0082 h^{-1}). Filtered wastewater contained a significant amount of organic carbon (65 $mgC_{org}.L^{-1}$) compared to RO water (Figure 7.11), suggesting that the higher inactivation rate in filtered wastewater was due to a higher production of ROS induced by the presence of organic molecules acting as photosensitisers in filtered wastewater.

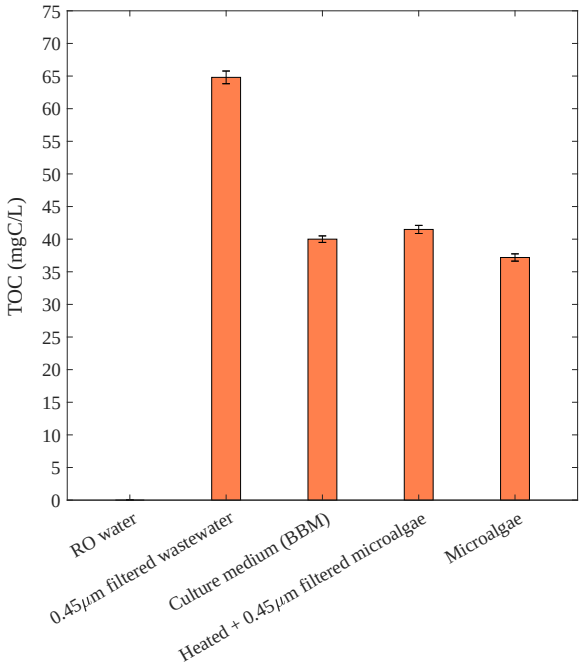

Figure 7.11 – Dissolved organic carbon in RO water, 0.45 μm filtered wastewater, BBM, heated and 0.45 μm filtered microalgae culture and microalgae culture

The highest MS2 inactivation rate (0.176 h^{-1}) was obtained in the presence of microalgal cells without L-histidine, even while the dissolved TOC in the microalgae medium, attributable to EDTA added to the BBM, was only 37 $mgC_{org}.L^{-1}$ (lower than in filtered wastewater). Here, MS2 inactivation by ROS was not correlated with dissolved organic carbon concentration, suggesting that microalgal cells themselves induce the production of singlet oxygen that significantly impact MS2 inactivation. The MS2 inactivation rate in microalgae extract, obtained by

heating then filtering at 0.45 μm a microalgae culture, reached 0.088 h^{-1}. This inactivation rate is half that measured in the presence of microalgal cells but four times higher than in filtered wastewater. This result suggests a significant impact of organic compounds contained inside the microalgal cells (pigments, carbohydrates...) on MS2 inactivation. The BBM used for growing microalgae contains nitrates, EDTA and traces of organic molecules from the MS2 inoculum which are expected to act as photosensitisers in the samples with microalgal cells and microalgae extract. However, the MS2 inactivtaion in BBM reached only 0.020 h^{-1}. The contribution of photosensitisers from BBM and MS2 inoculum to MS2 inactivation in the presence of microalgal cells and in microalgae extract was then estimated at 11% and 23% respectively (Figure 7.12). This result confirms that the high MS2 inactivation rates obtained in the presence of microalgal cells and in microalgae extract was mainly due to photosensitisers from microalgae and only little to the BBM in which they were suspended during the experiment. In the end, ROS mediated disinfection was the highest in the microalgal suspension, followed by the microalgae extract, the wastewater, the BBM and the RO water.

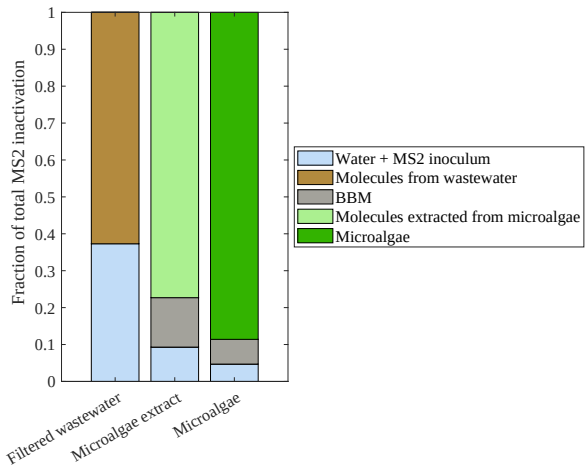

Figure 7.12 – Contribution of water + MS2 inoculum and BBM to the total MS2 inactivation (without L-histidine) in filtered wastewater, microalgae extract and microalgae experiments

The Figure 7.11 shows that TOC content in the microalgae extract (41 $mgC_{org}.L^{-1}$) is not significantly higher than in BBM (40 $mgC_{org}.L^{-1}$) or microalgae culture (37 $mgC_{org}.L^{-1}$), despite microalgae were heated at 80 °C. However, the very low quantity of organic molecules

extracted from microalgae induced a higher MS2 inactivation rate than the organic molecules from wastewater, despite the TOC content was higher in wastewater (65 $mgC_{org}.L^{-1}$).

7.3.3 Balance between positive and negative impact of microalgae and wastewater on MS2 inactivation

The two series of experiments presented above aimed at discriminating and evaluating the impact of microalgae and wastewater on MS2 inactivation through UV attenuation and ROS production.

The Figure 7.13 shows that the reduction of UVA penetration through the water column due to microalgae induced a reduction of -0.061 h^{-1} on the MS2 inactivation rate compared to the control with RO water. However, the production of ROS by microalgal cells induced an increase of +0.153 h^{-1} on the MS2 inactivation rate compared to the control with RO water. The negative impact of microalgae on MS2 inactivation rate due to the reduction of UVA penetration through the water column would then be significantly compensated by its inherent capacity to produce ROS that enhance MS2 inactivation.

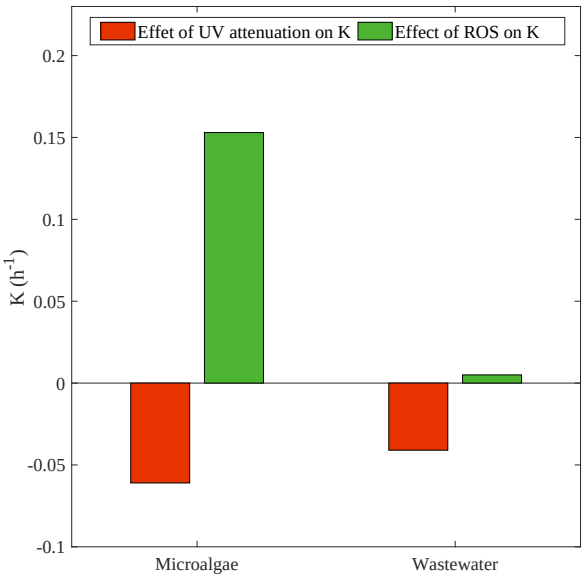

Figure 7.13 – Negative impact of microalgae and wastewater on inactivation rate due to UV attenuation (in red) and positive impact of microalgae and wastewater on inactivation rate due to ROS production (in green)

However, it is not the case for wastewater. The reduction of UVA penetration through the water column due to wastewater turbidity induced a reduction of -0.041 h^{-1} on the MS2 inactivation rate compared to the control with RO water. The production of ROS by photosensitisers found in wastewater induced an increase of +0.005 h^{-1} on the MS2 inactivation rate compared to the control with RO water. The negative impact of wastewater on MS2 inactivation rate due to the reduced UVA penetration through the water column would then not be compensated by the production of ROS attributable to wastewater organic molecules.

7.3.4 MS2 inactivation in a 30 cm depth wastewater column

The results presented in the previous section suggest that the presence of microalgae would globally enhance MS2 inactivation in wastewater, despite their strong contribution to UVA attenuation over a 30 cm depth water column. In order to confirm this hypothesis, 30 cm depth wastewater columns were inoculated with MS2, with and without microalgae and with and without L-histidine and placed under UVA radiations.

As illustrated in the Figure 7.14, MS2 inactivation rate was slightly higher in the wastewater column that did not contain microalgae (0.014 h^{-1}) than in the column with microalgae (0.010 h^{-1}). In addition, MS2 inactivation rates with and without L-histidine were very similar in both experiments (0.013 and 0.014 h^{-1} without microalgae; 0.012 and 0.010 h^{-1} with microalgae), suggesting a very low impact of ROS in MS2 inactivation in those experiments.

Measurement of UVA intensity along the depth of the columns with and without microalgae revealed that, in wastewater alone, UVA was completely attenuated below 9 cm depth, against 1 cm in wastewater added with microalgae (Figure 7.15). Consequently, 97% of the volume of the column containing microalgae was not irradiated by UVA. This observation could explain why the inactivation rates obtained in the UVA-irradiated 30 cm depth columns containing microalgae were only slightly higher than the inactivation rate obtained in darkness (0.0068 h^{-1}).

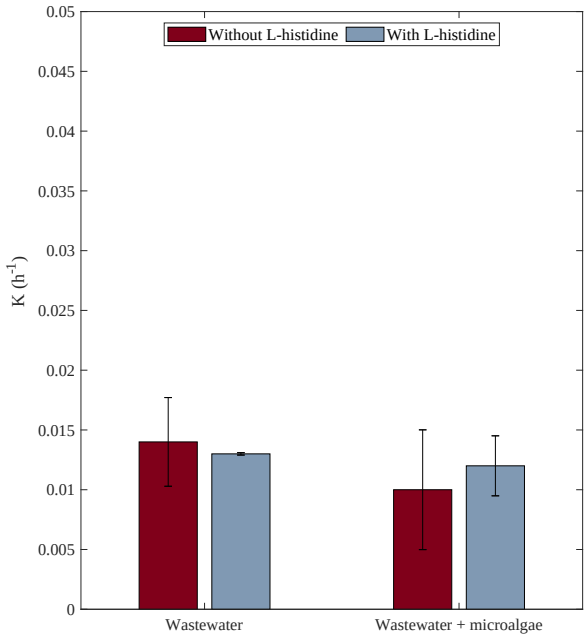

Figure 7.14 – MS2 inactivation rates K with and without L-histidine in wastewater and wastewater added with microalgae, irradiated with 22 W.m^{-2} UVA

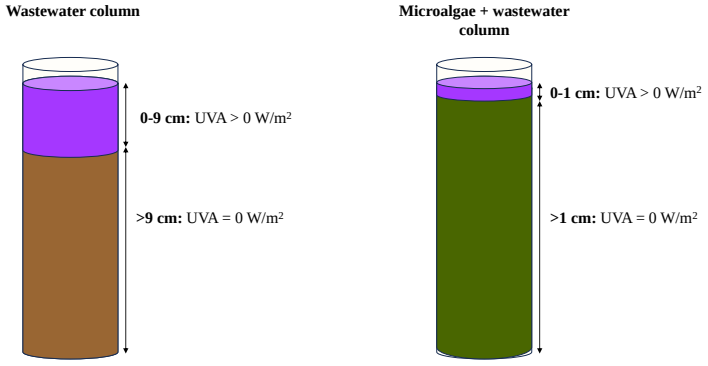

Figure 7.15 – UVA attenuation in 30 cm depth wastewater columns containing or not microalgae

7.4 Discussion

7.4.1 Effect of UVA attenuation

The experiment conducted in darkness confirmed that MS2 exhibited negligible decay rate over 50 h at 20°C in RO water. This confirms that significant MS2 decay observed when samples

were irradiated with UVA was actually due to UVA. UVA attenuation attributable to both microalgae and wastewater highly impacted MS2 inactivation, with 40% of the reduction in inactivation rate attributable to wastewater turbidity and 60% to microalgae turbidity. Note that as a single-stranded RNA virus (Dedeo et al. 2011), MS2 is less resistant to UV disinfection than double stranded RNA/DNA viruses that are able to repair their genome (Li et al. 2009). Further investigation should imply double stranded RNA/DNA viruses to validate the result on more resistant type of viruses.

7.4.2 Effect of ROS production

In RO water, filtered wastewater, BBM, microalgae and microalgae extract, the inactivation rates of viruses with L-histidine, that inhibits the effects of ROS, were close to inactivation rates measured in darkness. This result suggests that sole UVA does not permit to inactivate viruses. Rattanakul and Oguma (2017) also reported that UV treatment alone did not induce damage in the target genome and that MS2 was not removed. Indeed, Davies (2003) reported that viruses lack a bound chromophore within their protein structures that would act as an endogenous photosensitiser and permit inactivation in the absence of exogenous photosensitisers, explaining why MS2 would survive to sole UV treatment. However, the viral capside of MS2 is permeable and MS2 is sensitive to damages by ROS that cross the capside (Majiya et al. 2018), which was confirmed by the present study. Indeed, the MS2 inactivation rate was higher in filtered wastewater, BBM, microalgae and microalgae extract, all containing photosensitisers, than in RO water. However, inactivation rates in the media containing photosensitisers were also slightly higher than in RO water when L-histidine was added to the media, while L-histidine was supposed to inhibit ROS. L-histidine inhibits only one type of ROS, the singlet oxygen, which is the ROS most commonly formed. However, other forms such as hydroxyl radical HO• can also be present depending on the media and enhance MS2 inactivation even in the presence of L-histidine, which might explain the small differences in MS2 inactivation between the different media even in the presence of L-histidine.

Photosensitisers from wastewater induced only a slight increase in MS2 inactivation rate

compared to the control experiment in RO water. In contrast, a previous study reported that wastewater could produce significant concentrations of ROS (Dong and Rosario-Ortiz 2012), the main type of ROS produced by organic matter being singlet oxygen ($^1O_2$) and hydroxyl radical (HO•) (Niu et al. 2014). In wastewater, both organic carbon and nitrate can act as photosensitisers. Dong and Rosario-Ortiz (2012) reported that nitrates and organic carbon from wastewater presented similar capacity to form ROS by photolysis. In Peterborough HRAP, nitrates represent only 9.2 mgN.L^{-1}, against 36.7 mgC.L^{-1} for organic carbon. The main contributor to photosensitisers in Peterborough HRAP is then most likely organic carbon.

In contrast, microalgal cells attained a significantly higher MS2 inactivation rate than organic compounds in wastewater. This finding is consistent with a previous study (Niu and Croué 2019) that demonstrated that organic matter from algae (AOM) was an efficient photosensitiser that produced significantly more ROS than terrestrial sourced organic matter due to aromatic protein-like and soluble microbial substances found in AOM. Xinjie et al. 2019 reported that native pathogens from wastewater were inactivated both by ROS that were released by the microalgae and by high dissolved oxygen concentration. In addition, Cho et al. (2022) reported that NADPH oxidase, located on the algal cell surface structure of the marine genus *Chattonella sp.* (Raphidophyceae), could be responsible for the production of extracellular ROS production by this microalgae. These studies suggest that ROS could be produced not only by extracellular compounds released by microalgae but also through reactions occurring with the microalgal cell wall directly.

In the experiment with microalgae extract, the amount of TOC extracted from microalgae was very low, even while a first extraction test by heating microalgae at 80°C increased the dissolved TOC by more than 40%. The first extraction test was done on a microalgae sample in exponential phase of growth, while in this study microalgae was in a stationary phase, which might have increased the resistance of the cell wall to extraction by heating. However, MS2 inactivation rate in the microalgae extract was still much higher than in BBM and filtered wastewater, showing that the effect of ROS on inactivation is not necessarily correlated with the TOC content. The specific capacity of the molecules to act as photosensitisers might be of more

significant relevance. As well, molecules extracted from microalgae other than TOC could have acted as photosensitisers in this experiment (nitrogen species for example). A potential release of carotenoids with a protector effect against the oxidation of MS2 by ROS is also possible, but probably marginal regarding the low carotenoids content in microalgae (less than 1% of the total dry weight, Bonnanfant et al. (2021)). Further investigation should include a more efficient method for extracting TOC from microalgae, notably by using microalgae in their exponential phase.

Furthermore, one of the purposes of the present study was to investigate the impact of microalgae as a photosensitiser on MS2 inactivation. However, the presence of microalgal cells is often associated with high dissolved oxygen concentrations. Bolton (2012) demonstrated that increasing DO from 0 et 8.5 mg.L^{-1} did not have any effect on MS2 inactivation. While increasing the range of dissolved oxygen to 25 mg.L^{-1} would be relevant regarding the conditions observed in HRAP, dissolved oxygen was consequently not controlled in the samples in the present study. Moreover, dissolved oxygen was expected low as UVA radiations are not photosynthetically active radiations. Nevertheless, for future research, the significant capacity of microalgal cells to produce ROS should be confirmed by ensuring similar dissolved oxygen concentration than in the control.

Moreover, in the experiments aiming at exploring the effect of ROS from microalgae and wastewater on MS2 inactivation, the applied UVA irradiance was depth averaged according to the turbidity of the medium. Consequently, higher incident UVA intensity was applied on the samples with microalgae than on the samples with microalgae extract, filtered wastewater, BBM or RO water to compensate for the higher turbidity. Samples were continuously mixed using a shaking waterbath, however this system does not permit perfect mixing and slight sedimentation of microalgal cells was observed, which could have increased the exposition of viruses to UVA and led to potential over-estimation of the impact of microalgae on MS2 inactivation by ROS production. However, samples were re-homogenised every 12 h at the moment of sampling to reduce this risk. Adjusting incident UVA irradiances to compensate for medium turbidity was necessary to decorrelate the effects of UVA attenuation and ROS production on viruses inacti-

vation. This method is based on the average UVA intensity over the samples depth, however the samples are shaken but not perfectly mixed and surface effects can occur. Nevertheless, samples with microalgae extract presented a higher inactivation rate than filtered wastewater even while the incident UVA irradiance applied on the microalgae extract (12.4 $W.m^{-2}$) was lower than the incident UVA irradiance applied on the filtered wastewater (16.8 $W.m^{-2}$), showing that adjusted UVA incident irradiances did not erase the effect of ROS.

Finally, the constant exposition of samples to UVA radiations raises the question of the stability of the microalgae sample throughout the experiment. Yet, Rastogi et al. (2020) reported that microalgae were highly resilient to UV damages by means of repair mechanisms, anti-oxidant system, biosynthesis of UV protectants (mycosporine-like amino acids (MAAs), scytonemin (Scy), carotenoids and polyamines). However, in the sample with microalgae extract, their is a possibility that the chlorophyll and other pigments or organic compounds progressively degraded during the 50 h experiment. For further investigation, the main factors affecting viruses inactivation such as turbidity, chlorophyll, TOC, dissolved oxygen and pH should be measured along the experiment to ensure for consistency and conservation of the experimental conditions.

7.4.3 Impact of microalgae in 30 cm depth columns

Adding microalgae to a 30 cm depth wastewater column did not improve MS2 inactivation, which contradicts the hypothesis arising from the two first sets of experiments, where the negative impact of microalgae on MS2 inactivation rate due to the reduced UVA penetration appeared to be compensated by its inherent capacity to produce ROS. Yet, UVA measurement inside the column containing wastewater and microalgae revealed that UVA was completely attenuated below 1 cm depth only. It is important to note that ROS production is enhanced by UV radiations, yet microalgal capacity to form ROS cannot be expressed while UVA does not penetrate the column. The inter-dependance between UVA and ROS production explains why, in more realistic conditions, ROS production cannot necessarily compensate UVA attenuation.

In addition, non-filtered wastewater was used in the experiments in the columns. The very low MS2 inactivation rate measured in the columns compared to the first two sets of experiments

might also be due to suspended solids offering protection to viruses against UVA, even in the surface area where UVA radiations are still detected (Brahmi et al. 2010). This phenomenon is representative of what happens in HRAP, but this cofounding factor was not considered in the two first sets of experiments. In addition, even while UVA measurements in the field in Peterborough HRAP showed similar conditions as in the columns (UVA radiations were fully attenuated below 0.5-1 cm depth, see Chapter 3), the columns were not stirred (except every 12 h before sampling) while Peterborough is well-mixed. Inactivation might have been underestimated in the columns compared to HRAP. However, note that the reverse phenomenon was reported by Park et al. (2021), where higher removal rates where obtained in the presence of suspended solids due to the absorption of viruses on solid particles.

To conclude, the strong inherent capacity of microalgae to produce ROS that successfully improves the inactivation of viruses suggests that the implementation of a thin-film system as a tertiary treatment downstream the HRAP could enhance the penetration of sun radiations and the production of ROS by microalgae for improving pathogens disinfection. Hawley and Fallowfield (2016) reported encouraging results using an inclined pond wall with a culture depth of a few millimeters only. While the model system permitted a significant enhancement of MS2 inactivation compared to normal pond conditions, the operation of the system on the field did not observe a significant improvement of pathogens removal. Further research should then focus on the constraints raised by the operation of those thin-film systems targeting pathogens removal in real conditions. Indeed, thin-film systems present a very low depth that could impact turbulence and potentially reduce the contact between viruses and microalgae, thus limiting the efficiency of the process. Nevertheless, thin film system increase the MRPA associated with high oxygen production that could possibly favour disinfection through oxidative stress. The number of viral particles decreased from 10^5 to 0 in only 30 h in the presence of microalgal cells in the experiments in the UV cabinet, which means that the retention time in the thin film system could be relatively short, from a few hours to 2 days depending on the level of disinfection wanted. This constitutes an important point regarding implementation of such a system at large scale. HRT in thin film systems should indeed be short in order to treat significant volumes of

wastewater despite the low depth.

7.5 Conclusion

Both microalgae and wastewater compounds contribute significantly to UVA attenuation in a 30 cm depth HRAP. While photosensitisers from wastewater permit only a slight enhancement of MS2 inactivation rate compared to RO water, microalgae showed a strong inherent capacity to produce ROS that improved MS2 inactivation. However, microalgae did not improve MS2 inactivation in 30 cm depth wastewater columns. Indeed, 97% of the column was not irradiated by UVA due to the very high turbidity, inhibiting ROS production by microalgae. Previous studies have suggested separating microalgae from the water for tertiary treatment of wastewater targeting pathogens removal, however the present study demonstrated that microalgae could greatly enhance MS2 inactivation by ROS, when UVA penetration was sufficient. This result suggests that thin-layer systems including microalgae for tertiary treatment of wastewater could favour both UV penetration and ROS production by microalgae for improving pathogens removal. Enhancement of HRAP performances in terms of pathogens removal is necessary for reaching water quality standards for reusing the treated water for the irrigation of a wider range of crops, including food crops.

This study confirms the relevance of efficient vertical mixing raised in the Chapter 3, not only for improving light availability for microalgae but also for permitting exposition of viruses to UV radiations.

Highlights

- The contribution of ROS from wastewater to MS2 inactivation was very low.
- When UVA penetration is sufficient, microalgae play a major role in MS2 inactivation by ROS.
- Thin-film systems could be considered as tertiary treatments targeting pathogens removal.

GENERAL CONCLUSION

Classical wastewater treatment methods such as activated sludge have significant economic, energetic and environmental impacts due to the high power consumption, the associated greenhouse gas production and the sludge production. Alternative, sustainable and low-energy consuming treatment methods such as utilizing microalgae in HRAP are increasingly being considered as alternatives. Nevertheless, gaps persist in the literature regarding microalgae-bacteria interactions concerning carbon sources and oxygen dynamics in HRAP.

Contribution of the thesis for understanding microalgae-bacteria interactions in HRAP

This thesis proposed an integrative approach involving different study systems to investigate microalgae-bacteria consortia in high-rate algal ponds, thereby shedding light on the relevance of using laboratory photobioreactors to investigate interactions dynamics in large-scale HRAPs.

The 3D characterization of the large-scale HRAP in Peterborough revealed a serpentine 1 km length HRAP was well-mixed, with homogeneous wastewater chemical and microbial composition. Key indicators of microalgal and bacterial activity such as dissolved oxygen, organic carbon and inorganic carbon were uniformly distributed throughout the pond. Oxygen required for organic carbon degradation by bacteria was photosynthetically produced and efficiently mixed by the paddlewheel within the pond. Overall, essential substrates for microalgal and bacterial growth were consistently available across the length, depth, and width of the HRAP.

The assumption that organic carbon is solely consumed by bacteria in HRAPs has been widely discussed in the literature. Cross-referencing wastewater composition with microalgae's affinity for organic molecules revealed that a small fraction (10-15 %) of the organic molecules

present in wastewater may be assimilable by microalgae. This fraction is likely higher after pretreatment of the wastewater in an anaerobic pond, where volatile fatty acids easily assimilable by microalgae are produced. This suggests that photoheterotrophic and chemoheterotrophic growth of microalgae could be significant and potentially playing a relevant role in interactions with bacteria.

Given the complex trophic interactions within microalgae-bacteria consortia, a study employing laboratory-scale controlled conditions with online measurements throughout day-night cycles coupled with theoretical investigation using a model was chosen to provide a better understanding of microalgae-bacteria interactions. Cultivation of *S. obliquus* in photoautotrophy, photoheterotrophy and mixotrophy revealed that organic carbon utilized by microalgae from wastewater alone was insufficient to meet their needs, necessitating intrinsic CO_2 from bacterial respiration. This study also revealed that oxygen production by microalgae needed for bacterial growth relied on available inorganic carbon. Significantly, co-cultivation of *S. obliquus* and *E. coli* using acetate as a carbon source demonstrated unexpected strong competition for acetate instead of expected symbiosis. Stoichiometric analysis demonstrated that acetate was predominately consumed by microalgae and that photoheterotrophy was the main growth mode of *S. obliquus*. In contrast, in the simulations where exclusively bacteria were consuming the organic carbon and in cocultures using glucose, bacteria dominated the culture while microalgal growth was minimal. These findings show that the contribution of photoheterotrophy in the microalgae-bacteria consortia depends on the carbon source used. Moreover, similarities in oxygen and CO_2 dynamics between the model and cocultures on acetate suggested that microalgal growth in these conditions was impacted by inorganic carbon limitations even while acetate was the main carbon source for microalgae, according to the stoichiometric analysis. Despite competition for acetate between microalgae and bacteria, bacterial CO_2 production also impacted microalgal growth. Consequently, dissolved oxygen then consumed by bacteria was also dependant on CO_2, which is coherent with the results issued from the cultures of *S. obliquus* in photoautotrophy, photoheterotrophy and mixotrophy.

However, overly simplified systems such as models or experiments using single organic car-

bon sources, microalgal strains and bacteria strains did not recreate the symbiosis expected in HRAPs. As shown in our results, affinity towards carbon sources was found highly relevant in the exchanges then created between populations. Future studies are then recommended to employ complex mixtures of carbon sources and mixed populations of algae and bacteria to better simulate HRAP conditions.

Notwithstanding, the torus PBR and simplified microalgal-bacterium consortia turned out to be relevant tools for studying HRAP behaviour. On one hand, online measurements provided key information on O_2 and CO_2 dynamics throughout day-night cycles. On another hand, while one hypothesis of this work questioned the representativeness of well-mixed lab-scale experiments like those carried out in the the torus PBR compared to potential heterogeneous large-scale raceways, 3D characterisation of the Peterborough HRAP indicated excellent mixing. This justified the use of well-mixed lab PBRs such as the torus PBR to simulate real-scale systems. This research demonstrated that a coupled kinetic and radiative model turned out to be a valuable tool for understanding O_2, CO_2, algal and bacterial biomass dynamics throughout day-night cycles. Although the model in our thesis was over-simplified compared to HRAP conditions and could be consolidated, dissolved oxygen concentrations were found in agreement with measurements conducted in HRAP. The trends were however different and highlighted a limitation by TIC in the model while HRAP appeared to be limited by light. This tends then to emphasize that hypotheses and underlying phenomena assumed in our model were close to the actual functioning of HRAP (i.e. organic carbon is consumed predominantly by bacteria), but that complex underlying phenomena involved in the carbon fate in microalgae-bacteria consortium are still to be elucidated (i.e. the absence of limitation by TIC in HRAP which is expected to be associated with more complex synergistic mechanisms).

Moreover, modeling HRAP behaviour and its performances in terms of pollutant and pathogen removal is extremely complex, requiring consideration of hydrodynamics, light and gas transfer, microbial interactions with pollutants and disinfection mechanisms. These factors are generally studied independently while this research developed and evaluated an integrative laboratory approach to better understand physical, chemical and biological interactions in HRAPs.

Penetration of solar radiations in the Peterborough HRAP was very low, questioning the relative impact of microalgae on solar disinfection. Finally, lab experiments conducted in UV cabinet on MS2 inactivation revealed that microalgae not only played a major role in trophic interactions with bacteria but also significantly contributed to disinfection mechanisms by producing ROS when exposed to UV radiation.

Research perspectives

The present work raised a few issues that could be considered as perspectives for future research.

First, 3D characterisation of Peterborough suggested that nitrifiers could possibly be affected by turbulence and mixing. Further investigations are needed to clarify associations amongst mixing, turbulence, flocs size, nitrification and denitrification in micro anaerobic zones within flocs. Nitrification was a significant process in Peterborough HRAP. Furthermore, nitrifiers potentially compete with microalgae for TIC and their impact on the carbon fate of an HRAP needs to be better understood. This work also raised the issue of the impact of suspended solids transferred from the anaerobic pond into the HRAP. Suspended solids impact light availability for microalgae, oxygen and inorganic carbon availability for nitrifying bacteria and UV penetration responsible for pathogens disinfection. The design of anaerobic ponds could be improved to avoid short circuiting that would cause the discharge of excessive suspended solids directly into the HRAP.

The chemical composition of anaerobically pre-treated wastewater considering main groups of molecules (poly-di-mono saccharides, VFA, lipids, proteins...) and their affinity with different groups of microorganisms (microalgae, different strains of heterotrophic bacteria, denitrifying bacteria...) should be characterised. Once the availability of the main groups of organic molecules found in pre-treated wastewater for microorganisms is determined, the lab experiments can be complexified by establishing a representative synthetic wastewater and selecting different strains representative of the main trophic groups of microorganisms encountered in HRAP. A consequence of increasing the complexity of the system is that more advanced technologies for

monitoring and analysis such as flow cytometry or genomic analysis will be required instead of non-selective methods such as dry weight or agar plates. This would permit precise estimations of the evolution of the biomass for each strain.

Also, identifying kinetic parameters for microalgae in photoheterotrophy and chemoheterotrophy would be necessary in order to include photoheterotrophy and chemoheterotrophy in the model. Knowing that a more complex system will be considered, kinetic parameters of different types of bacteria on different substrates should also be identified. Combining lab experiments and modeling would then enable an estimate of the relative contribution of microalgal photoheterotrophy/chemoheterotrophy to carbon and oxygen balance. This might provide insight for the optimisation of the carbon source, with a final aim of avoiding costly CO_2 injections in the pond. Besides, further research in real conditions is needed. Large scale HRAPs present additional constraints that laboratory photobioreactors can mitigate. Therefore, a combination of laboratory-controlled studies, which evaluate the relevance of different factors within the system, and outdoor, large scale operational HRAPs should be conducted to comprehensively investigate the complex mechanisms involved in HRAPs.

Finally, highlighting of the key role of microalgae in disinfection process through ROS production suggests that thin film systems targeting pathogens removal should be further explored.

Research perspectives

- Correlations between mixing, turbulence, flocs, micro-anaerobic zones, O_2/CO_2 and nitrification.
- Characterisation of organic molecules and their affinity with microorganisms.
- Complexification of lab experiments and models in terms of organic molecules and populations.
- Exploration of the interest of a thin film system targeting pathogens disinfection.

Towards low tech wastewater treatment systems: different levels of acceptance worldwide

Beyond the scientific issues raised throughout this thesis, working both in France and in South Australia prompted consideration of the obstacles to the implementation of HRAP at large scale worldwide. In South Australia, HRAPs were adopted as wastewater treatment systems in Peterborough, Kingston-on-Murray, and soon in Barrossa valley. New Zealand have also implemented large-scale HRAP treating real wastewater in Cambridge and Christchurch. In contrast, in France, HRAP were not adopted at all as wastewater treatment systems. The very different level of acceptance of HRAP among countries though presenting similar level of development raise the question.

Of course, the climate in Mediterranean regions of France and Europe is less favourable for growing microalgae than in Australia. However, high dissolved oxygen concentrations were measured in Peterborough HRAP even in winter on a cloudy day, demonstrating that microalgae are able to keep the pond oversaturated in oxygen even with low light. On the contrary, one of the main differences between France and Australia is the density of population, with 124 inhabitants/km^2 in France against 3 inhabitants/km^2 in Australia (The World Bank 2021). Sparsely populated countries such as Australia are definitely more adapted for implementing large-scale HRAP than countries with a denser population such as France. In addition, it is problematic in France to question the replacement of systems such as activated sludge that, in the end, seems efficient. Moreover, the operation of HRAP does not require costly high-tech equipment, which might present a too low financial interest for companies. France and Australia also experience different level of pressure on the water resource due to the different climate, which causes diverging behaviours regarding water management. In France, only 1% of the wastewater is reused for irrigation, against 40% in South Australia. France has set an objective of 10% of water reuse before 2030, which suggests that the intensification of global warming and water stress might accelerate the adoption of wastewater treatment using microalgae in France.

Adopting low-cost wastewater treatment systems in developing countries can also be chal-

lenging. There are numerous examples of attempts of implementation of high-tech wastewater treatment solutions in developing countries by developed countries. In most of cases, the lack of technical and financial local means does not permit a long-lasting functioning of the wastewater treatment system implemented, which is rapidly unused because it is too expensive to run and maintain with the local means. Low-tech solutions requiring low energy and low maintenance such as HRAP are much more appropriate in these cases and should be considered worldwide.

Appendix A

Culture medium composition

Raw formula	Concentration (g/L)
$NaNO_3$	1.5
$MgSO_4$, $7H_2O$	0.23
$CaCl_2$, $2H_2O$	0.025
Additive 1	1 ml
Additive 2	1 ml
$EDTANa_2$, $2H_2O$	0.050
$FeSO_4$, $7H_2O$	0.014
K_2HPO_4	0.150
KH_2PO_4	0.123
$NaHCO_3$	1.26

Table A.1 – Composition of BBM-nitrate medium

Raw formula	Concentration (g/L)
$ZnSO_4$, $7H_2O$	0.222
$Co(NO_3)_2$, $6H_2O$	0.044
$CuSO_4$	0.079
H_3BO_3	2.86
$MnCl_2$, $4H_2O$	1.81

Table A.2 – Composition of additive 1

Raw formula	Concentration (g/L)
Na_2MoO_4	0.22

Table A.3 – Composition of additive 2

Raw formula	Concentration (g/L)
KH_2PO_4	15
NaCl	2.5
Na_2HPO_4	33.9
NH_4Cl	5

Table A.4 – Composition of M9 medium for *E. coli* cultivation

Raw formula	Concentration for SWWx1 (g/L)	Concentration for SWWx2 (g/L)
NH_4Cl	0.3	0.6
$MgSO_4$, $7H_2O$	0.2	0.4
$CaCl_2$, $2H_2O$	0.074	0.148
Additive 1	1 ml	2 ml
Additive 2	1 ml	2 ml
$NaCH_3COOH$	0.44	0.88
$EDTANa_2$, $2H_2O$	0.050	0.1
$FeSO_4$, $7H_2O$	0.014	0.028
KH_2PO_4	0.063	0.126

Table A.5 – Composition of synthetic wastewater, classical (SWWx1) and concentrated (SWWX2)

Appendix B

Schumpe coefficients for the effect of salinity on O_2 solubility

$\mathbf{H}_i$	**Value**
$\mathrm{H}_i - NH4$	-0.704
$\mathrm{H}_i - Cl$	0.8466
$\mathrm{H}_i - Mg$	-0.3014
$\mathrm{H}_i - SO4$	0.4592
$\mathrm{H}_i - Ca$	0.3026
$\mathrm{H}_i - K$	-0.5894
$\mathrm{H}_i - HPO4$	0.477
$\mathrm{H}_i - H2PO4$	0.997
$\mathrm{H}_i - Na$	-0.5688
$\mathrm{H}_i - HCO3$	1.076

Table B.1 – Schumpe coefficients H_i at 23°C for each ion

Appendix C

UVA INTENSITY VARIATION IN THE WATERBATH

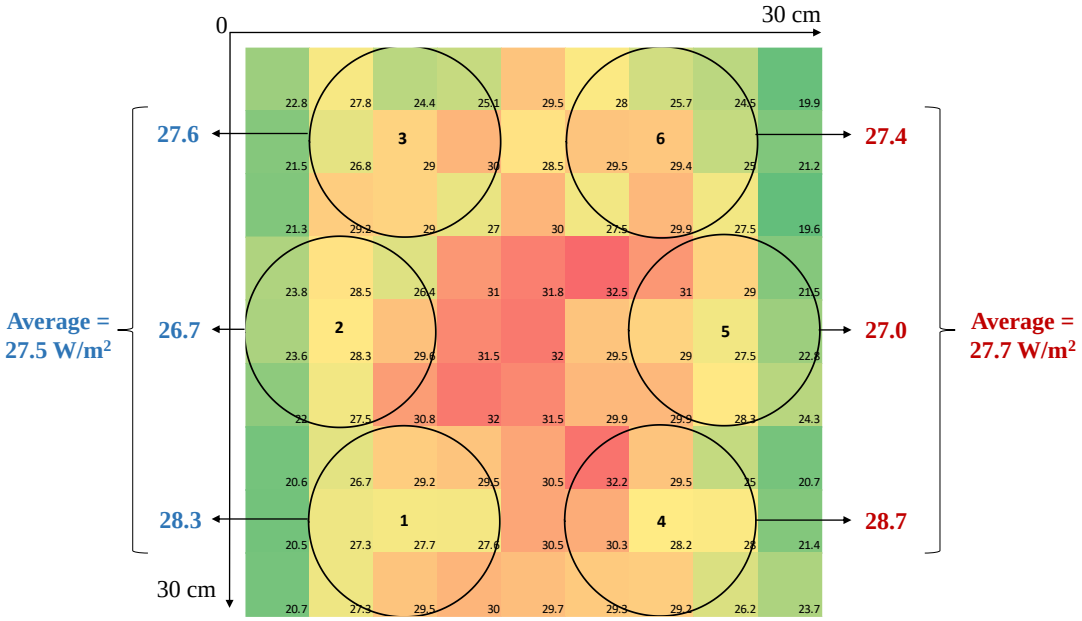

Figure C.1 – UVA intensity variation in the waterbath inside the UV cabinet and position of the 6 samples

Appendix D

MS2 CONCENTRATION CURVES

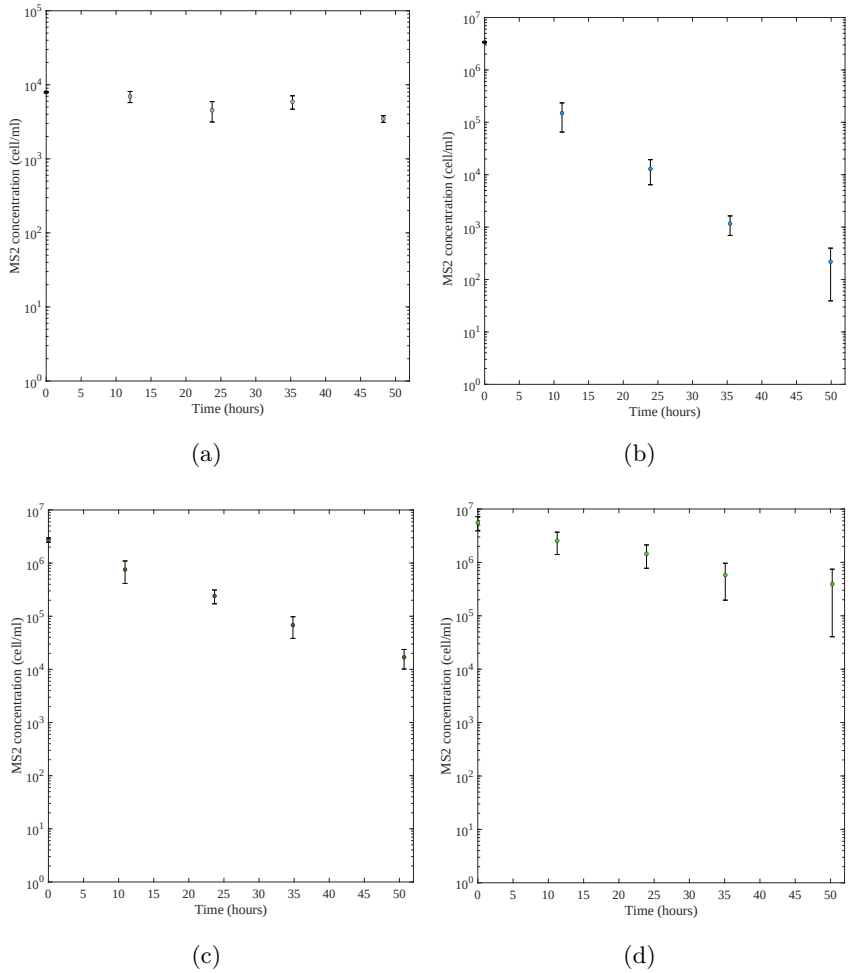

Figure D.1 – MS2 concentration over 50h irradiated with (a) G_{dark} = 0 W.m^{-2}, (b) $G_{mean_{RO}}$ = 12.9 W.m^{-2}, (c) $G_{mean_{WW}}$ = 2.5 W.m^{-2}, (d) $G_{mean_{algae}}$ = 2.1 W.m^{-2}

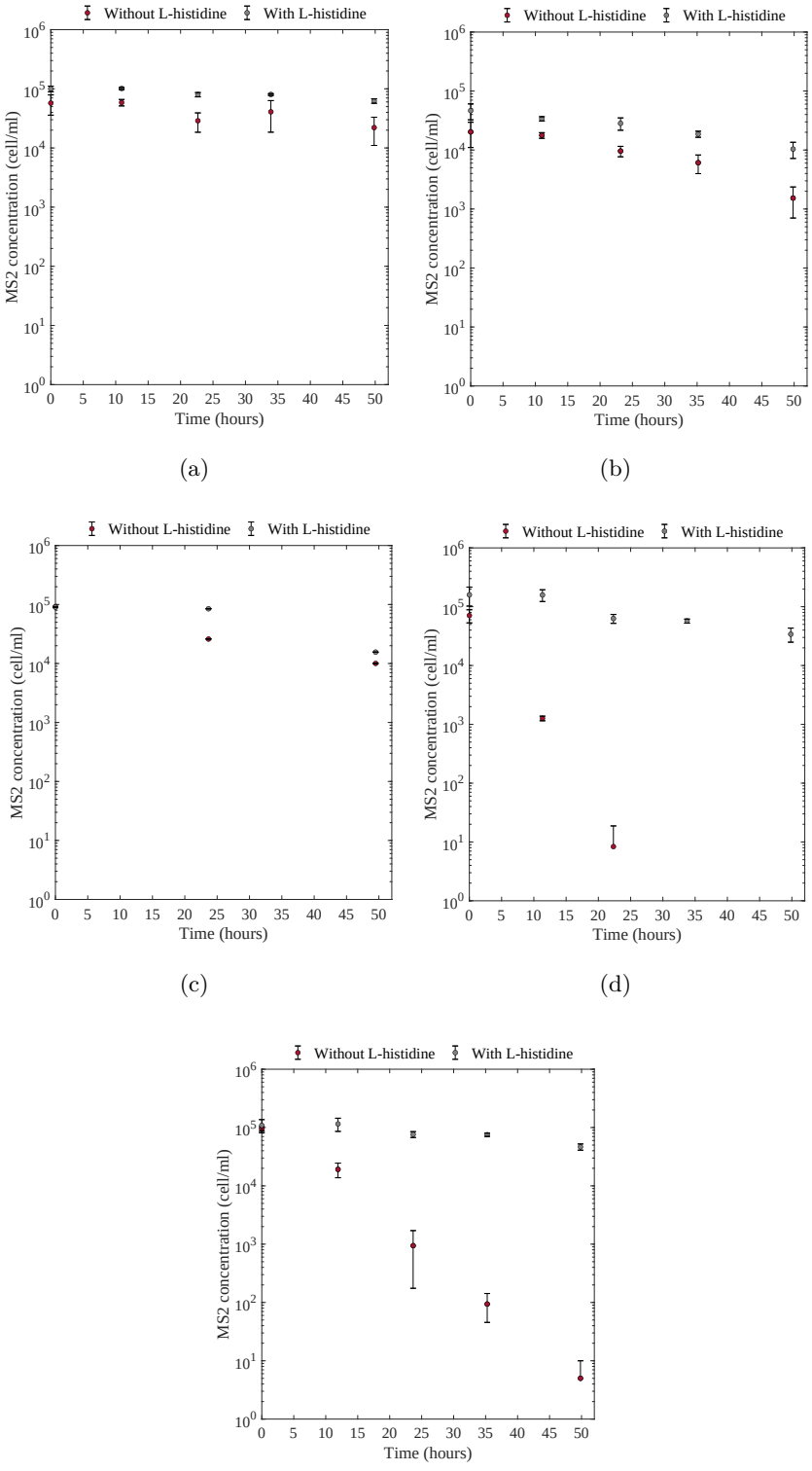

Figure D.2 – MS2 concentration over 50h in (a) RO water, $G_{0_{RO}} = 8.8$ W.m^{-2}, (b) Filtered wastewater, $G_{0_{WW}} = 16.8$ W.m^{-2}, (c) BBM, $G_{0_{BBM}} = 8.8$ W.m^{-2}, (d) Microalgae extract, $G_{0_{EXTR}} = 12.4$ W.m^{-2}, (e) Microalgae, $G_{0_{ALG}} = 27.7$ W.m^{-2}

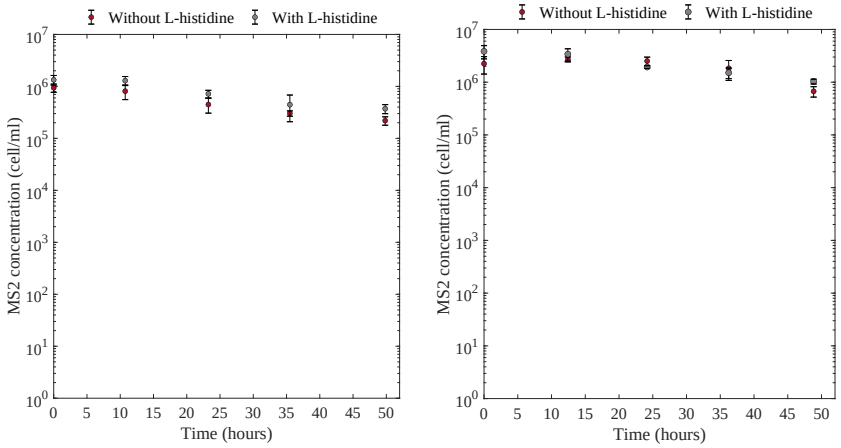

(a) (b)

Figure D.3 – MS2 concentration over 50h under $G_0 = 22$ W.m^{-2} in a 30-cm depth column of (a) Wastewater (b) Wastewater + microalgae

BIBLIOGRAPHY

Abeliovich, A., and D. Weisman, 1978, « Role of heterotrophic nutrition in growth of the alga Scenedesmus obliquus in high-rate oxidation ponds », *Applied and Environmental Microbiology* 35 (*1*): 32–37, ISSN: 00992240, https://doi.org/10.1128/aem.35.1.32-37.1978.

Abert Vian, M., C. Dejoye Tanzi, and F. Chemat, 2013, « Techniques conventionelles et innovantes, et solvants alternatifs pour l'extraction des lipides de micro-organismes », *OCL - Oilseeds and fats, crops and lipids* 20 (*6*), ISSN: 22576614, https://doi.org/10.1051/ocl/2013032.

Abiusi, F., R. H. Wijffels, and M. Janssen, 2020, « Doubling of Microalgae Productivity by Oxygen Balanced Mixotrophy », *ACS Sustainable Chemistry and Engineering* 8 (*15*): 6065–6074, ISSN: 21680485, https://doi.org/10.1021/acssuschemeng.0c00990.

Abreu, A. P., R. C. Morais, J. A. Teixeira, and J. Nunes, 2022, « A comparison between microalgal autotrophic growth and metabolite accumulation with heterotrophic, mixotrophic and photoheterotrophic cultivation modes », *Renewable and Sustainable Energy Reviews* 159 (*September 2021*), ISSN: 18790690, https://doi.org/10.1016/j.rser.2022.112247.

Acheson, D., 2009, *Elementary Fluid Dynamics,* Oxford App, Clarendon Press, ISBN: 0-19-859679-0.

AERM, 2007, *Procédés d'épuration des petites collectivités du bassin Rhin-Meuse,* technical report.

Agarwal, A., K. M. Shaikh, K. Gharat, P. P. Jutur, R. A. Pandit, and A. M. Lali, 2019, « Investigating the modulation of metabolites under high light in mixotrophic alga Asteracys sp. using a metabolomic approach », *Algal Research* 43 (*April*): 101646, ISSN: 22119264, https://doi.org/10.1016/j.algal.2019.101646, https://doi.org/10.1016/j.algal.2019.101646.

Akissa, P., and B. Inrgref, 1992, « Réutilisation agricole des eaux usées », *Agridoc,* 1–4.

Alkhamis, Y., and J. G. Qin, 2013, « Cultivation of Isochrysis galbana in phototrophic, heterotrophic, and mixotrophic conditions », *BioMed Research International* 2013, ISSN: 23146133, https://doi.org/10.1155/2013/983465.

Álvarez-González, A., E. Uggetti, L. Serrano, G. Gorchs, M. Escolà Casas, V. Matamoros, E. Gonzalez-Flo, and R. Díez-Montero, 2023, « The potential of wastewater grown microalgae for agricultural purposes: Contaminants of emerging concern, heavy metals and pathogens assessment », *Environmental Pollution* 324 (*November 2022*), ISSN: 18736424, https://doi.org/10.1016/j.envpol.2023.121399.

Álvarez-González, A., E. Uggetti, L. Serrano, G. Gorchs, I. Ferrer, and R. Díez-Montero, 2022, « Can microalgae grown in wastewater reduce the use of inorganic fertilizers? », *Journal of Environmental Management* 323 (*September*), ISSN: 10958630, https://doi.org/10.1016/j.jenvman.2022.116224.

Andersen, K. B., and K. Von Meyenburg, 1980, « Are growth rates of Escherichia coli in batch cultures limited by respiration? », *Journal of Bacteriology* 144 (*1*): 114–123, ISSN: 00219193, https://doi.org/10.1128/jb.144.1.114-123.1980.

Andruleviciute, V., V. Makareviciene, V. Skorupskaite, and M. Gumbyte, 2014, « Biomass and oil content of Chlorella sp., Haematococcus sp., Nannochloris sp. and Scenedesmus sp. under mixotrophic growth conditions in the presence of technical glycerol », *Journal of Applied Phycology* 26 (*1*): 83–90, ISSN: 09218971, https://doi.org/10.1007/s10811-013-0048-x.

APHA, 1981, « Standard Methods for the Examination of Water and Wastewater », *American Public Health Association.*

Arashiro, L. T., I. Ferrer, D. P. Rousseau, S. W. Van Hulle, and M. Garfí, 2019, « The effect of primary treatment of wastewater in high rate algal pond systems: Biomass and bioenergy recovery », *Bioresource Technology* 280 (*November 2018*): 27–36, ISSN: 18732976, https://doi.org/10.1016/j.biortech.2019.01.096, https://doi.org/10.1016/j.biortech.2019.01.096.

Arashiro, L. T., N. Montero, I. Ferrer, F. G. Acién, C. Gómez, and M. Garfí, 2018, « Life cycle assessment of high rate algal ponds for wastewater treatment and resource recovery », *Science of the Total Environment* 622-623:1118–1130, ISSN: 18791026, https://doi.org/10.1016/j.scitotenv.2017.12.051, https://doi.org/10.1016/j.scitotenv.2017.12.051.

Arauzo, M., and M. Valladolid, 2003, « Short-term harmful effects of unionised ammonia on natural populations of Moina micrura and Brachionus rubens in a deep waste treatment pond », *Water Research* 37 (*11*): 2547–2554, ISSN: 00431354, https://doi.org/10.1016/S0043-1354(03)00023-X.

ARMCANZ, 1997, « National Water Quality Management Strategy: Australian Guidelines for Sewerage Systems - Effluent Management », 46, ISSN: 1038 7072, http://www.environment.gov.au/water/publications/quality/pubs/sewerage-systems-effluent-man-paper11.pdf.

Artu, A., 2016, « Etude et optimisation de la culture de microalgues en photobioréacteurs solaires », PhD thesis, Universite de Nantes, https://doi.org/10.13140/RG.2.2.23498.41924, http://www.theses.fr/2016NANT4019.

Assemany, P. P., M. L. Calijuri, E. d. A. d. Couto, M. H. B. de Souza, N. C. Silva, A. d. F. Santiago, and J. d. S. Castro, 2015, « Algae/bacteria consortium in high rate ponds: Influence of solar radiation on the phytoplankton community », *Ecological Engineering* 77:154–162, ISSN: 09258574, https://doi.org/10.1016/j.ecoleng.2015.01.026, http://dx.doi.org/10.1016/j.ecoleng.2015.01.026.

Ayers, R., and D. Westcot, 1985, *Water quality for agriculture,* technical report.

Azema, N., M. F. Pouet, C. Berho, and O. Thomas, 2002, « Wastewater suspended solids study by optical methods », *Colloids and Surfaces A: Physicochemical and Engineering Aspects* 204 (*1-3*): 131–140, ISSN: 09277757, https://doi.org/10.1016/S0927-7757(02)00006-7.

Bankston, E., Q. Wang, and B. T. Higgins, 2020, « Algae support populations of heterotrophic, nitrifying, and phosphate-accumulating bacteria in the treatment of poultry litter anaerobic digestate », *Chemical Engineering Journal* 398 (*May*): 125550, ISSN: 13858947, https://doi.org/10.1016/j.cej.2020.125550, https://doi.org/10.1016/j.cej.2020.125550.

Baroukh, C., J. P. Steyer, O. Bernard, and B. Chachuat, 2016, « Dynamic Flux Balance Analysis of the Metabolism of Microalgae under a Diurnal Light Cycle », *IFAC-PapersOnLine* 49 (*7*): 791–796, ISSN: 24058963, https://doi.org/10.1016/j.ifacol.2016.07.285, http://dx.doi.org/10.1016/j.ifacol.2016.07.285.

Barraqué, B., 2014, « For a history of the water and sanitation services in Europe and North America », *Flux* 97-98 (*4*): 4–15, ISSN: 11542721, https://doi.org/10.3917/flux.097.0004.

Basu, S., A. S. Roy, K. Mohanty, and A. K. Ghoshal, 2013a, « Enhanced CO2 sequestration by a novel microalga: Scenedesmus obliquus SA1 isolated from bio-diversity hotspot region of Assam, India », *Bioresource Technology* 143:369–377, ISSN: 18732976, https://doi.org/10.1016/j.biortech.2013.06.010, http://dx.doi.org/10.1016/j.biortech.2013.06.010.

Basu, S., A. S. Roy, K. Mohanty, and A. K. Ghoshal, 2013b, « Enhanced CO2 sequestration by a novel microalga: Scenedesmus obliquus SA1 isolated from bio-diversity hotspot region of Assam, India », *Bioresource Technology* 143:369–377, ISSN: 18732976, https://doi.org/10.1016/j.biortech.2013.06.010, http://dx.doi.org/10.1016/j.biortech.2013.06.010.

Beccerra-Celis, G., 2009, « Proposition de stratégies de commande pour la culture de microalgue dans un photobioréacteur continu », PhD thesis.

Bello, M., P. Ranganathan, and F. Brennan, 2017, « Dynamic modelling of microalgae cultivation process in high rate algal wastewater pond », *Algal Research* 24:457–466, ISSN: 22119264, https://doi.org/10.1016/j.algal.2016.10.016, http://dx.doi.org/10.1016/j.algal.2016.10.016.

Benchokroun, S., B. Imziln, and L. Hassani, 2003, « Solar inactivation of mesophilic Aeromonas by exogenous photooxidation in high-rate algal pond treating waste water », *Journal of Applied Microbiology* 94 (*3*): 531–538, ISSN: 13645072, https://doi.org/10.1046/j.1365-2672.2003.01867.x.

Benedetti, M., V. Vecchi, S. Barera, and L. Dall'Osto, 2018, « Biomass from microalgae: The potential of domestication towards sustainable biofactories », *Microbial Cell Factories* 17 (*1*): 1–18, ISSN: 14752859, https://doi.org/10.1186/s12934-018-1019-3, https://doi.org/10.1186/s12934-018-1019-3.

Benemann, J., J. Weissman, B. Koopman, D. Eisenberg, R. Goebel, and W. J. Oswald, 1978, *Large-scale freshwater micralgal biomass production for fuel and fertilizer,* technical report, U.S. Department of Energy Fuels from Biomass Systems.

Berben, T., L. Overmars, D. Y. Sorokin, and G. Muyzer, 2019, « Diversity and distribution of sulfur oxidation-related genes in thioalkalivibrio, a genus of chemolithoautotrophic and haloalkaliphilic sulfur-oxidizing bacteria », *Frontiers in Microbiology* 10 (*160*), ISSN: 1664302X, https://doi.org/10.3389/fmicb.2019.00160.

Bird, P., 1992, « The urban waste water treatment directive », *Institution of Water Officers Journal* 28 (*4*): 14–15, ISSN: 09620311.

Bolton, N., N. J. Cromar, P. Hallsworth, and H. J. Fallowfield, 2010, « A review of the factors affecting sunlight inactivation of micro-organisms in waste stabilisation ponds: Preliminary results for enterococci », *Water Science and Technology* 61 (*4*): 885–890, ISSN: 02731223, https://doi.org/10.2166/wst.2010.958.

Bolton, N., N. Cromar, N. Buchanan, and H. Fallowfield, 2011, « Sunlight attenuation may be predicted by turbidity in waste stabilisation ponds and environmental waters », 2010.

Bolton, N., 2012, « Photoinactivation of indicator micro-organisms and adenovirus in sunlit waters », PhD thesis, Flinders University.

Bonnanfant, M., H. Marec, B. Jesus, J. L. Mouget, and J. Pruvost, 2021, « Investigation of the photosynthetic response of Chlorella vulgaris to light changes in a torus-shape photobioreactor », *Applied Microbiology and Biotechnology* 105 (*23*): 8689–8701, ISSN: 14320614, https://doi.org/10.1007/s00253-021-11636-w, https://doi.org/10.1007/s00253-021-11636-w.

Bonnanfant, M., 2020, « Étude des mécanismes de conversion photosynthétique de lénergie lumineuse par Chlorella vulgaris en photobioréacteur solaire », PhD thesis, Université de Nantes.

Bonnanfant, M., B. Jesus, J. Pruvost, J. L. Mouget, and D. A. Campbell, 2019, « Photosynthetic electron transport transients in Chlorella vulgaris under fluctuating light », *Algal Research* 44 (*November*): 101713, ISSN: 22119264, https://doi.org/10.1016/j.algal.2019.101713, https://doi.org/10.1016/j.algal.2019.101713.

Borowitzka, M. A., and N. R. Moheimani, 2013, *Algae for Biofuels and Energy,* Springer, ISBN: 9789400754782.

Bouarab, L., A. Dauta, and M. Loudiki, 2004, « Heterotrophic and mixotrophic growth of Micractinium pusillum Fresenius in the presence of acetate and glucose:effect of light and acetate gradient concentration », *Water Research* 38 (*11*): 2706–2712, ISSN: 00431354, https://doi.org/10.1016/j.watres.2004.03.021.

Boutin, C., and S. Prost-Boucle, 2012, « Les zones de rejet végétalisées », *Sciences Eaux & Territoires* Numéro 9 (*4*): 36–43, ISSN: 2109-3016, https://doi.org/10.3917/set.009.0004.

Brahmi, M., N. H. Belhadi, H. Hamdi, and A. Hassen, 2010, « Modeling of secondary treated wastewater disinfection by UV irradiation: Effects of suspended solids content », *Journal of Environmental Sciences* 22 (*8*): 1218–1224, ISSN: 10010742, https://doi.org/10.1016/S1001-0742(09)60241-2, http://dx.doi.org/10.1016/S1001-0742(09)60241-2.

Breuer, G., P. P. Lamers, D. E. Martens, R. B. Draaisma, and R. H. Wijffels, 2013, « Effect of light intensity, pH, and temperature on triacylglycerol (TAG) accumulation induced by nitrogen starvation in Scenedesmus obliquus », *Bioresource Technology* 143:1–9, ISSN: 18732976, https://doi.org/10.1016/j.biortech.2013.05.105, http://dx.doi.org/10.1016/j.biortech.2013.05.105.

Buchanan, N., P. Young, N. J. Cromar, and H. J. Fallowfield, 2018a, « Comparison of the treatment performance of a high rate algal pond and a facultative waste stabilisation pond operating in rural South Australia », *Water Science and Technology* 78 (*1*): 3–11, ISSN: 02731223, https://doi.org/10.2166/wst.2018.201.

Buchanan, N. A., P. Young, N. J. Cromar, and H. J. Fallowfield, 2018b, « Performance of a high rate algal pond treating septic tank effluent from a community wastewater management scheme in rural South Australia », *Algal Research* 35 (*September*): 325–332, ISSN: 22119264, https://doi.org/10.1016/j.algal.2018.08.036.

Cai, L., and T. Zhang, 2013, « Detecting human bacterial pathogens in wastewater treatment plants by a high-throughput shotgun sequencing technique », *Environmental Science and Technology* 47 (*10*): 5433–5441, ISSN: 0013936X, https://doi.org/10.1021/es400275r.

Canziani, R., 2010, *Biomass activity measurements Part 1 Microbiology and wastewater characterisation,* technical report.

Casagli, F., G. Zuccaro, O. Bernard, J. P. Steyer, and E. Ficara, 2021, « ALBA: A comprehensive growth model to optimize algae-bacteria wastewater treatment in raceway ponds », *Water Research* 190:116734, ISSN: 18792448, https://doi.org/10.1016/j.watres.2020.116734, https://doi.org/10.1016/j.watres.2020.116734.

Cébron, A., 2004, « Nitrification, bacteries nitrifiantes et emissions de N2O - La Seine en aval de Paris », PhD thesis, Paris VI - Pierre et Marie Curie.

Cecchin, M., 2020, « Study of Molecular Mechanisms to Increase Carbon Use Efficiency in Microalgae », PhD thesis, Universita' Degli Studi Di Verona.

Cecchin, M., S. Benfatto, F. Griggio, A. Mori, S. Cazzaniga, N. Vitulo, M. Delledonne, and M. Ballottari, 2018, « Molecular basis of autotrophic vs mixotrophic growth in Chlorella sorokiniana », *Scientific Reports* 8 (*1*): 1–13, ISSN: 20452322, https://doi.org/10.1038/s41598-018-24979-8, http://dx.doi.org/10.1038/s41598-018-24979-8.

Chambonniere, P., J. Bronlund, and B. Guieysse, 2020, « Escherichia coli removal during domestic wastewater treatment in outdoor high rate algae ponds: Long-term performance and mechanistic implications », *Water Science and Technology* 82 (*6*): 1166–1175, ISSN: 19969732, https://doi.org/10.2166/wst.2020.233.

Chipasa, K. B., and K. Mdrzycka, 2006, « Behavior of lipids in biological wastewater treatment processes », *Journal of Industrial Microbiology and Biotechnology* 33 (*8*): 635–645, ISSN: 13675435, https://doi.org/10.1007/s10295-006-0099-y.

Chislock, M. F., E. Doster, R. A. Zitomer, and A. E. Wilson, 2013, « Eutrophication: Causes, Consequences, and Controls in Aquatic Ecosystems », *Nature Education Knowledge* 4(4):10, https://www.nature.com/scitable/knowledge/library/eutrophication-causes-consequences-and-controls-in-aquatic-102364466/.

Chiu, P. H., K. Soong, and C. N. N. Chen, 2016, « Cultivation of two thermotolerant microalgae under tropical conditions: Influences of carbon sources and light duration on biomass and lutein productivity in four seasons », *Bioresource Technology* 212:190–198, ISSN: 18732976, https://doi.org/10.1016/j.biortech.2016.04.045, http://dx.doi.org/10.1016/j.biortech.2016.04.045.

Cho, K., M. Ueno, Y. Liang, D. Kim, and T. Oda, 2022, « Generation of Reactive Oxygen Species (ROS) by Harmful Algal Bloom (HAB)-Forming Phytoplankton and Their Potential Impact on Surrounding Living Organisms », *Antioxidants* 11 (*2*), ISSN: 20763921, https://doi.org/10.3390/antiox11020206.

Collos, Y., and P. J. Harrison, 2014, « Acclimation and toxicity of high ammonium concentrations to unicellular algae », *Marine Pollution Bulletin* 80 (*1-2*): 8–23, ISSN: 0025326X, https://doi.org/10.1016/j.marpolbul.2014.01.006.

Cook, S., M. Hall, and A. Gregory, 2012, *Energy use in the prevision and consumption of urban water in Australia: an update,* technical report, CSIRO Water for a Healthy Country Flagship, Australia.

Corpuz, M. V. A., A. Buonerba, G. Vigliotta, T. Zarra, F. Ballesteros, P. Campiglia, V. Belgiorno, G. Korshin, and V. Naddeo, 2020, « Viruses in wastewater: occurrence, abundance and detection methods », *Science of the Total Environment* 745:140910, ISSN: 18791026, https://doi.org/10.1016/j.scitotenv.2020.140910, https://doi.org/10.1016/j.scitotenv.2020.140910.

Corsi, S. R., M. A. Borchardt, S. K. Spencer, P. E. Hughes, and A. K. Baldwin, 2014, « Human and bovine viruses in the Milwaukee River watershed: Hydrologically relevant representation and relations with environmental variables », *Science of the Total Environment* 490:849–860, ISSN: 18791026, https://doi.org/10.1016/j.scitotenv.2014.05.072, http://dx.doi.org/10.1016/j.scitotenv.2014.05.072.

Craggs, R., J. Park, D. Sutherland, and S. Heubeck, 2015, « Economic construction and operation of hectare-scale wastewater treatment enhanced pond systems », *Journal of Applied Phycology* 27 (*5*): 1913–1922, ISSN: 15735176, https://doi.org/10.1007/s10811-015-0658-6.

Craggs, R., D. Sutherland, and H. Campbell, 2012, « Hectare-scale demonstration of high rate algal ponds for enhanced wastewater treatment and biofuel production », *Journal of Applied Phycology* 24 (*3*): 329–337, ISSN: 09218971, https://doi.org/10.1007/s10811-012-9810-8.

Craggs, R. J., A. Zwart, J. W. Nagels, and R. J. Davies-Colley, 2004, « Modelling sunlight disinfection in a high rate pond », *Ecological Engineering* 22 (*2*): 113–122, ISSN: 09258574, https://doi.org/10.1016/j.ecoleng.2004.03.001.

Cromar, N. J., and H. J. Fallowfield, 1992, « Separation of components of the biomass from high rate algal ponds using PercollR density gradient centrifugation », *Journal of Applied Phycology* 4 (*2*): 157–163, ISSN: 09218971, https://doi.org/10.1007/BF02442464.

Cromar, N. J., and H. J. Fallowfield, 1997, « Effect of nutrient loading and retention time on performance of high rate algal ponds », *Journal of Applied Phycology* 9 (*4*): 301–309, ISSN: 09218971, https://doi.org/10.1023/A:1007917610508.

Cromar, N. J., and H. J. Fallowfield, 2003, « Use of image analysis of determine algal and bacterial biomass in a high rate algal pond following Percollő fractionation », *Water Science and Technology* 48 (*2*): 53–60, ISSN: 02731223, https://doi.org/10.2166/wst.2003.0084.

Curtis, T. P., D. D. Mara, N. G. Dixo, and S. A. Silva, 1994, « Light penetration in waste stabilization ponds », *Water Research* 28 (*5*): 1031–1038, ISSN: 00431354, https://doi.org/10.1016/0043-1354(94)90188-0.

Daneshvar, E., L. Antikainen, E. Koutra, M. Kornaros, and A. Bhatnagar, 2018, « Investigation on the feasibility of Chlorella vulgaris cultivation in a mixture of pulp and aquaculture effluents: Treatment of wastewater and lipid extraction », *Bioresource Technology* 255 (*November 2017*): 104–110, ISSN: 18732976, https://doi.org/10.1016/j.biortech.2018.01.101, https://doi.org/10.1016/j.biortech.2018.01.101.

Davies, M. J., 2003, « Singlet oxygen-mediated damage to proteins and its consequences », *Biochemical and Biophysical Research Communications* 305 (*3*): 761–770, ISSN: 0006291X, https://doi.org/10.1016/S0006-291X(03)00817-9.

Dedeo, M. T., D. T. Finley, and M. B. Francis, 2011, « Chapter 8 - Viral Capsids as Self-Assembling Templates for New Materials », *in Progress in Molecular Biology and Translational Science,* 353–392, https://doi.org/https://doi.org/10.1016/B978-0-12-415906-8.00002-9.

Delfosse, P., 2014, « Microbiologie de la Digestion Anaérobie », *Ecobiogaz. Journée de formation à la méthanisation.,* number figure 1, 61.

Demory, D., C. Combe, P. Hartmann, A. Talec, E. Pruvost, R. Hamouda, F. Souillé, et al., 2018, « How do microalgae perceive light in a high-rate pond? Towards more realistic Lagrangian experiments », *Royal Society Open Science* 5 (*5*), ISSN: 20545703, https://doi.org/10.1098/rsos.180523.

Deng, X., B. Chen, C. Xue, D. Li, X. Hu, and K. Gao, 2019, « Biomass production and biochemical profiles of a freshwater microalga Chlorella kessleri in mixotrophic culture: Effects of light intensity and photoperiodicity », *Bioresource Technology* 273 (*2*): 358–367, ISSN: 18732976, https://doi.org/10.1016/j.biortech.2018.11.032.

Deronzier, G., and J.-m. Choubert, 2004, *Traitement du phosphore dans les petites stations dépuration à boues activées,* technical report.

Deronzier, G., S. Schétrite, Y. Racault, J.-P. Canler, A. Liénard, A. Héduit, and P. Duchène, 2001, *Traitement de l'azote dans les stations d'épuration biologique des petites collectivités,* 25:79, ISBN: 2110928522.

Deutsch, J.-C., and M. Vullierme, 2003, « L'évolution des techniques », *Flux* 52-53:17–26.

Diab, S., M. Kochba, and Y. Avnimelech, 1993, « Nitrification pattern in a fluctuating anaerobic-aerobic pond environment », *Water Research* 27 (*9*): 1469–1475, ISSN: 00431354, https://doi.org/10.1016/0043-1354(93)90027-F.

Dong, M. M., and F. L. Rosario-Ortiz, 2012, « Photochemical formation of hydroxyl radical from effluent organic matter », *Environmental Science and Technology* 46:3788–3794, ISSN: 15205851, https://doi.org/10.1021/es2043454.

Duan, Y., X. Guo, J. Yang, M. Zhang, and Y. Li, 2020, « Nutrients recycle and the growth of Scenedesmus obliquus in synthetic wastewater under different sodium carbonate concentrations », *Royal Society Open Science* 7 (*1*), ISSN: 20545703, https://doi.org/10.1098/rsos.191214.

Ebeling, J. M., M. B. Timmons, and J. J. Bisogni, 2006, « Engineering analysis of the stoichiometry of photoautotrophic, autotrophic, and heterotrophic removal of ammonia-nitrogen in aquaculture systems », *Aquaculture* 257 (*1-4*): 346–358, ISSN: 00448486, https://doi.org/10.1016/j.aquaculture.2006.03.019, http://dx.doi.org/10.1016/j.aquaculture.2006.03.019.

Edmundson, S. J., and M. H. Huesemann, 2015, « The dark side of algae cultivation: Characterizing night biomass loss in three photosynthetic algae, Chlorella sorokiniana, Nannochloropsis salina and Picochlorum sp. », *Algal Research* 12:470–476, ISSN: 22119264, https://doi.org/10.1016/j.algal.2015.10.012, http://dx.doi.org/10.1016/j.algal.2015.10.012.

El Hamouri, B., J. Jellal, H. Outabiht, B. Nebri, K. Khallayoune, A. Benkerroum, A. Hajli, and R. Firadi, 1995, *The performance of a high rate algal pond in the moroccan climate.*

El Hamouri, B., A. Rami, and J. L. Vasel, 2003, « The reasons behind the performance superiority of a high rate algal pond over three facultative ponds in series », *Water Science and Technology* 48 (*2*): 269–276, ISSN: 02731223, https://doi.org/10.2166/wst.2003.0130.

El Hamouri, B., 2009, « Rethinking natural, extensive systems for tertiary treatment purposes: The high-rate algae pond as an example », *Desalination and Water Treatment* 4 (*1-3*): 128–134, ISSN: 19443986, https://doi.org/10.5004/dwt.2009.367.

El Ouarghi, H., E. Praet, H. Jupsin, and J. L. Vasel, 2003, « Comparison of oxygen and carbon dioxide balances in HRAP (high-rate algal ponds) », *Water Science and Technology* 48 (*2*): 277–281, ISSN: 02731223, https://doi.org/10.2166/wst.2003.0131.

Eme, C., and C. Boutin, 2015, « Composition des eaux usées domestiques par source d'émission à l'échelle de l'habitation - Etude bibliographique », 90.

Evans, R. A., N. J. Cromar, and H. J. Fallowfield, 2005, « Performance of a pilot-scale high rate algal pond system treating abattoir wastewater in rural South Australia: Nitrification and denitrification », *Water Science and Technology* 51 (*12*): 117–124, ISSN: 02731223, https://doi.org/10.2166/wst.2005.0443.

Fallahi, A., F. Rezvani, H. Asgharnejad, E. Khorshidi, N. Hajinajaf, and B. Higgins, 2021, « Interactions of microalgae-bacteria consortia for nutrient removal from wastewater: A review », *Chemosphere* 272, ISSN: 18791298, https://doi.org/10.1016/j.chemosphere.2021.129878.

Fallowfield, H. J., and M. K. Garrett, 1985, « The treatment of wastes by algal culture », *Journal of Applied Bacteriology* 59:187S–205S, ISSN: 13652672, https://doi.org/10.1111/j.1365-2672.1985.tb04900.x.

Fallowfield, H. J., P. Young, M. J. Taylor, N. Buchanan, N. Cromar, A. Keegan, and P. Monis, 2018, « Independent validation and regulatory agency approval for high rate algal ponds to treat wastewater from rural communities », *Environmental Science: Water Research and Technology* 4 (*2*): 195–205, ISSN: 20531419, https://doi.org/10.1039/c7ew00228a, http://dx.doi.org/10.1039/C7EW00228A.

Fan, H., X. Liu, H. Wang, Y. Han, L. Qi, and H. Wang, 2017, « Oxygen transfer dynamics and activated sludge floc structure under different sludge retention times at low dissolved oxygen concentrations », *Chemosphere* 169:586–595, ISSN: 18791298, https://doi.org/10.1016/j.chemosphere.2016.10.137.

Fan, J., X. Zhang, X. Du, and Z. Cai, 2022, « Insights into activated sludge/Chlorella consortia under dark condition compared with light condition », *Water Science and Technology* 86 (*8*): 1915–1926, ISSN: 19969732, https://doi.org/10.2166/wst.2022.322.

Farkas, K., D. I. Walker, E. M. Adriaenssens, J. E. McDonald, L. S. Hillary, S. K. Malham, and D. L. Jones, 2020, « Viral indicators for tracking domestic wastewater contamination in the aquatic environment », *Water Research* 181:115926, ISSN: 18792448, https://doi.org/10.1016/j.watres.2020.115926, https://doi.org/10.1016/j.watres.2020.115926.

Fernández del Olmo, P., F. G. Acién, and J. M. Fernández-Sevilla, 2021, « Analysis of productivity in raceway photobioreactor using computational fluid dynamics particle tracking coupled to a dynamic photosynthesis model », *Bioresource Technology* 334, ISSN: 18732976, https://doi.org/10.1016/j.biortech.2021.125226.

Flores-Salgado, G., F. Thalasso, G. Buitrón, M. Vital-Jácome, and G. Quijano, 2021, « Kinetic characterization of microalgal-bacterial systems: Contributions of microalgae and heterotrophic bacteria to the oxygen balance in wastewater treatment », *Biochemical Engineering Journal* 165 (*September 2020*), ISSN: 1873295X, https://doi.org/10.1016/j.bej.2020.107819.

Foladori, P., S. Petrini, and G. Andreottola, 2020, « How suspended solids concentration affects nitrification rate in microalgal-bacterial photobioreactors without external aeration », *Heliyon* 6 (*1*): e03088, ISSN: 24058440, https://doi.org/10.1016/j.heliyon.2019.e03088, https://doi.org/10.1016/j.heliyon.2019.e03088.

Folsom, J. P., and R. P. Carlson, 2015, « Physiological, biomass elemental composition and proteomic analyses of Escherichia coli ammoniumlimited chemostat growth, and comparison with iron- and glucose-limited chemostat growth », *Microbiology (United Kingdom)* 161 (*8*): 1659–1670, ISSN: 14652080, https://doi.org/10.1099/mic.0.000118.

Fuentes, J. L., I. Garbayo, M. Cuaresma, Z. Montero, M. González-Del-Valle, and C. Vílchez, 2016, « Impact of microalgae-bacteria interactions on the production of algal biomass and associated compounds », *Marine Drugs* 14 (*5*), ISSN: 16603397, https://doi.org/10.3390/md14050100.

Galès, A., A. Bonnafous, C. Carré, V. Jauzein, E. Lanouguère, E. Le Floc'h, J. Pinoit, et al., 2019, « Importance of ecological interactions during wastewater treatment using High Rate Algal Ponds under different temperate climates », *Algal Research* 40 (*June*), ISSN: 22119264, https://doi.org/10.1016/j.algal.2019.101508.

Ganjegunte, G., A. Ulery, G. Niu, and Y. Wu, 2017, « Effects of treated municipal wastewater irrigation on soil properties, switchgrass biomass production and quality under arid climate », *Industrial Crops and Products* 99:60–69, ISSN: 09266690, https://doi.org/10.1016/j.indcrop.2017.01.038, http://dx.doi.org/10.1016/j.indcrop.2017.01.038.

Gao, P., L. Guo, M. Gao, Y. Zhao, C. Jin, and Z. She, 2022, « Regulation of carbon source metabolism in mixotrophic microalgae cultivation in response to light intensity variation », *Journal of Environmental Management* 302 (*PB*): 114095, ISSN: 10958630, https://doi.org/10.1016/j.jenvman.2021.114095, https://doi.org/10.1016/j.jenvman.2021.114095.

Gao, P., L. Guo, Y. Zhao, C. Jin, Z. She, and M. Gao, 2021, « Enhancing microalgae growth and product accumulation with carbon source regulation: New perspective for the coordination between photosynthesis and aerobic respiration », *Chemosphere* 278:130435, ISSN: 18791298, https://doi.org/10.1016/j.chemosphere.2021.130435, https://doi.org/10.1016/j.chemosphere.2021.130435.

García, J., R. Mujeriego, and M. Hernández-Mariné, 2000, « High rate algal pond operating strategies for urban wastewater nitrogen removal », *Journal of Applied Phycology* 12 (*3-5*): 331–339, ISSN: 09218971, https://doi.org/10.1023/a:1008146421368.

García-Galán, M. J., L. Arashiro, L. H. Santos, S. Insa, S. Rodríguez-Mozaz, D. Barceló, I. Ferrer, and M. Garfí, 2020, « Fate of priority pharmaceuticals and their main metabolites and transformation products in microalgae-based wastewater treatment systems », *Journal of Hazardous Materials* 390 (*November 2019*): 121771, ISSN: 18733336, https://doi.org/10.1016/j.jhazmat.2019.121771, https://doi.org/10.1016/j.jhazmat.2019.121771.

Garcia-Moscoso, J. L., A. Teymouri, and S. Kumar, 2015, « Kinetics of peptides and arginine production from microalgae (Scenedesmus sp.) by flash hydrolysis », *Industrial and Engineering Chemistry Research* 54 (*7*): 2048–2058, ISSN: 15205045, https://doi.org/10.1021/ie5047279.

Garfí, M., L. Flores, and I. Ferrer, 2017, « Life Cycle Assessment of wastewater treatment systems for small communities: Activated sludge, constructed wetlands and high rate algal ponds », *Journal of Cleaner Production* 161:211–219, ISSN: 09596526, https://doi.org/10.1016/j.jclepro.2017.05.116, http://dx.doi.org/10.1016/j.jclepro.2017.05.116.

Gerba, C. P., 2000, « Assessment of Enteric Pathogen Shedding by Bathers during Recreational Activity and its Impact on Water Quality », *Quantitative microbiology* 2:55–68, https://doi.org/https://doi.org/10.1023/A:1010000230103.

Godos, I. d., S. Blanco, P. A. García-Encina, E. Becares, and R. Muñoz, 2009, « Long-term operation of high rate algal ponds for the bioremediation of piggery wastewaters at high loading rates », *Bioresource Technology* 100 (*19*): 4332–4339, ISSN: 09608524, https://doi.org/10.1016/j.biortech.2009.04.016, http://dx.doi.org/10.1016/j.biortech.2009.04.016.

Golmohammadi, R., K. Valegård, K. Fridborg, and L. Liljas, 1993, « The refined structure of bacteriophage MS2 at 2.8 A resolution », *Journal of Molecular Biology,* number 234, 620–639.

Gomes, L. A., R. F. Gonçalves, M. F. Martins, and C. N. Sogari, 2023, « Assessing the suitability of solar dryers applied to wastewater plants: A review », *Journal of Environmental Management* 326 (*June 2022*), ISSN: 10958630, https://doi.org/10.1016/j.jenvman.2022.116640.

Grama, B. S., S. N. Agathos, and C. S. Jeffryes, 2016, « Balancing Photosynthesis and Respiration Increases Microalgal Biomass Productivity during Photoheterotrophy on Glycerol », *ACS Sustainable Chemistry and Engineering* 4 (*3*): 1611–1618, ISSN: 21680485, https://doi.org/10.1021/acssuschemeng.5b01544.

Gris, B., T. Morosinotto, G. M. Giacometti, A. Bertucco, and E. Sforza, 2014, « Cultivation of Scenedesmus obliquus in photobioreactors: Effects of light intensities and light-dark cycles on growth, productivity, and biochemical composition », *Applied Biochemistry and Biotechnology* 172 (*5*): 2377–2389, ISSN: 15590291, https://doi.org/10.1007/s12010-013-0679-z.

Grobbelaar, J. U., 1994, « Turbulence in mass algal cultures and the role of light/dark fluctuations », *Journal of Applied Phycology* 6 (*3*): 331–335, ISSN: 09218971, https://doi.org/10.1007/BF02181947.

Guardia, M. J., and E. G. Calvo, 2001, « Modeling of Escherichia coli growth and acetate formation under different operational conditions », *Enzyme and Microbial Technology* 29 (*6-7*): 449–455, ISSN: 01410229, https://doi.org/10.1016/S0141-0229(01)00413-6.

Gutiérrez, R., I. Ferrer, A. González-Molina, H. Salvadó, J. García, and E. Uggetti, 2016a, « Microalgae recycling improves biomass recovery from wastewater treatment high rate

algal ponds », *Water Research* 106:539–549, ISSN: 18792448, https://doi.org/10.1016/j.watres.2016.10.039.

Gutiérrez, R., I. Ferrer, E. Uggetti, C. Arnabat, H. Salvadó, and J. García, 2016b, « Settling velocity distribution of microalgal biomass from urban wastewater treatment high rate algal ponds », *Algal Research* 16:409–417, ISSN: 22119264, https://doi.org/10.1016/j.algal.2016.03.037, http://dx.doi.org/10.1016/j.algal.2016.03.037.

Gutiérrez-Alfaro, S., J. J. Rueda-Márquez, J. A. Perales, and M. A. Manzano, 2018, « Combining sun-based technologies (microalgae and solar disinfection) for urban wastewater regeneration », *Science of the Total Environment* 619-620:1049–1057, ISSN: 18791026, https://doi.org/10.1016/j.scitotenv.2017.11.110, https://doi.org/10.1016/j.scitotenv.2017.11.110.

Hall, D. O., and K. K. Rao, 1992, *Photosynthesis Sixth edition,* Cambridge, 29–41, ISBN: 0521428068, http://www.cup.org.

Hargreaves, J., 2013, « Biofloc production systems for aquaculture », *Stoneville, MS: Southern Regional Aquaculture Center,* number 4503, 1–12.

Hawley, A. L., and H. J. Fallowfield, 2016, « Inclusion of pond walls to enhance solar exposure and pathogen removal », number March, 1–10.

Heredia, V., J. Legrand, and J. Pruvost, 2022, « Microalgal biofuels: Pathways towards a positive energy balance », *Energy Conversion and Management* 267 (*March*): 115929, ISSN: 01968904, https://doi.org/10.1016/j.enconman.2022.115929, https://doi.org/10.1016/j.enconman.2022.115929.

Hernández, D., B. Riaño, M. Coca, M. Solana, A. Bertucco, and M. C. García-González, 2016, « Microalgae cultivation in high rate algal ponds using slaughterhouse wastewater for biofuel applications », *Chemical Engineering Journal* 285:449–458, ISSN: 13858947, https://doi.org/10.1016/j.cej.2015.09.072.

Hindersin, S., M. Leupold, M. Kerner, and D. Hanelt, 2014, « Key parameters for outdoor biomass production of Scenedesmus obliquus in solar tracked photobioreactors », *Journal of Applied Phycology* 26 (*6*): 2315–2325, ISSN: 15735176, https://doi.org/10.1007/s10811-014-0261-2.

Hiremath, P., P. Bannigidad, and S. S. Yelgond, 2012, « Identification of Flagellated or Fimbriated Bacterial Cells using Digital Image Processing Techniques », *International Journal of Computer Applications* 59 (*12*): 12–16, https://doi.org/10.5120/9599-4223.

Hisee, A. R., M. Hisee, J. C. McKerral, S. R. Rosenbauer, J. S. Paterson, J. G. Mitchell, and H. J. Fallowfield, 2020, « Changes of viral and prokaryote abundances in a high rate algal pond using flow cytometry detection », *Water Science and Technology* 82 (*6*): 162–1669, ISSN: 19969732, https://doi.org/10.2166/wst.2020.379.

Hodaifa, G., M. E. Martínez, and S. Sánchez, 2010, « Influence of temperature on growth of Scenedesmus obliquus in diluted olive mill wastewater as culture medium », *Engineering in Life Sciences* 10 (*3*): 257–264, ISSN: 16180240, https://doi.org/10.1002/elsc.201000005.

Huang, K. X., B. D. Mao, M. M. Lu, D. Z. Chen, J. Qiu, and F. Gao, 2024, « Effect of external acetate added in aquaculture wastewater on mixotrophic cultivation of microalgae, nutrient removal, and membrane contamination in a membrane photobioreactor », *Journal of Envi-*

ronmental Management 349 (*September 2023*): 119391, ISSN: 10958630, https://doi.org/10.1016/j.jenvman.2023.119391, https://doi.org/10.1016/j.jenvman.2023.119391.

Huang, M., Y. M. Li, and G. W. Gu, 2010, « Chemical composition of organic matters in domestic wastewater », *Desalination* 262 (*1-3*): 36–42, ISSN: 00119164, https://doi.org/10.1016/j.desal.2010.05.037, http://dx.doi.org/10.1016/j.desal.2010.05.037.

Incropera, F. P., and K. G. Privoznik, 1979, « Radiative property measurements for selected water suspensions », *Water Resources Research* 15 (*1*): 85–89, ISSN: 19447973, https://doi.org/10.1029/WR015i001p00085.

Inostroza, C., A. Solimeno, J. García, J. M. Fernández-Sevilla, and F. G. Acién, 2021, « Improvement of real-scale raceway bioreactors for microalgae production using Computational Fluid Dynamics (CFD) », *Algal Research* 54 (*February*), ISSN: 22119264, https://doi.org/10.1016/j.algal.2021.102207.

IPCC, 2023, « Climate Change 2023: Synthesis Report. Contribution of Working Groups I, II and III to the Sixth Assessment Report of the Intergovernmental Panel on Climate Change », https://doi.org/10.59327/IPCC/AR6-9789291691647, https://www.unep.org/resources/report/climate-change-2023-synthesis-report.

IWA, 2016, *Total water delivered for households in 2016,* https://waterstatistics.iwa-network.org/graph/VG90YWwgV2F0ZXIgRGVsaXZlcmVkIGZvciBIb3VzZUhvbGRzIChtsy9jYXBpdGEveWVhcik/100/2016.

Jacob-Lopes, E., M. I. Queiroz, and L. Q. Zepka, 2020, *Pigments from microalgae handbook,* Springer, ISBN: 9783030509712, https://doi.org/10.1007/978-3-030-50971-2.

Jacob-Lopes, E., C. H. G. Scoparo, L. M. C. F. Lacerda, and T. T. Franco, 2009, « Effect of light cycles (night/day) on CO2 fixation and biomass production by microalgae in photobioreactors », *Chemical Engineering and Processing: Process Intensification* 48 (*1*): 306–310, ISSN: 02552701, https://doi.org/10.1016/j.cep.2008.04.007.

Jain, R., and R. Srivastava, 2009, « Metabolic investigation of host/pathogen interaction using MS2-infected Escherichia coli », *BMC Systems Biology* 3, ISSN: 17520509, https://doi.org/10.1186/1752-0509-3-121.

Kandilian, R., A. Soulies, J. Pruvost, B. Rousseau, J. Legrand, and L. Pilon, 2016, « Simple method for measuring the spectral absorption cross-section of microalgae », *Chemical Engineering Science* 146:357–368, ISSN: 00092509, https://doi.org/10.1016/j.ces.2016.02.039, http://dx.doi.org/10.1016/j.ces.2016.02.039.

Kang, J. H., H. G. Namgung, J. I. Cho, S. S. Yoo, B. J. Lee, and H. W. Ji, 2020, « Removal of hydrogen sulfide in septic tanks for treating black water via an immobilized media of sulfur-oxidizing bacteria », *International Journal of Environmental Research and Public Health* 17 (*3*), ISSN: 16604601, https://doi.org/10.3390/ijerph17030684.

Kazbar, A., G. Cogne, B. Urbain, H. Marec, B. Le-Gouic, J. Tallec, H. Takache, A. Ismail, and J. Pruvost, 2019, « Effect of dissolved oxygen concentration on microalgal culture in photobioreactors », *Algal Research* 39 (*June 2018*): 101432, ISSN: 22119264, https://doi.org/10.1016/j.algal.2019.101432, https://doi.org/10.1016/j.algal.2019.101432.

Kazbar, A., 2019, « Etude de l'impact de la concentration en oxygene dissous et la presence d'une fraction sombre sur la performance des photobioreacteurs », PhD thesis, Université de Nantes.

Khaire, P., 2020, *A Peek into the History of Wastewater Treatment,* https://organicabiotech.com/a-peek-into-the-history-of-wastewater-treatment/.

Kim, B. H., J. E. Choi, K. Cho, Z. Kang, R. Ramanan, D. G. Moon, and H. S. Kim, 2018, « Influence of water depth on microalgal production, biomass harvest, and energy consumption in high rate algal pond using municipal wastewater », *Journal of Microbiology and Biotechnology* 28 (*4*): 630–637, ISSN: 17388872, https://doi.org/10.4014/jmb.1801.01014.

Koch, H., M. A. van Kessel, and S. Lücker, 2019, « Complete nitrification: insights into the ecophysiology of comammox Nitrospira », *Applied Microbiology and Biotechnology* 103 (*1*): 177–189, ISSN: 14320614, https://doi.org/10.1007/s00253-018-9486-3.

Kohlheb, N., M. van Afferden, E. Lara, Z. Arbib, M. Conthe, C. Poitzsch, T. Marquardt, and M. Y. Becker, 2020, « Assessing the life-cycle sustainability of algae and bacteria-based wastewater treatment systems: High-rate algae pond and sequencing batch reactor », *Journal of Environmental Management* 264 (*February*): 110459, ISSN: 10958630, https://doi.org/10.1016/j.jenvman.2020.110459, https://doi.org/10.1016/j.jenvman.2020.110459.

Krimech, A., M. Helamieh, M. Wulf, I. Krohn, U. Riebesell, O. Cherifi, L. Mandi, and M. Kerner, 2022, « Differences in adaptation to light and temperature extremes of Chlorella sorokiniana strains isolated from a wastewater lagoon », *Bioresource Technology* 350 (*March*): 126931, ISSN: 18732976, https://doi.org/10.1016/j.biortech.2022.126931, https://doi.org/10.1016/j.biortech.2022.126931.

Kumar, V., and S. M. Jain, 2014, « Plants and algae species: Promising renewable energy production source », *Emirates Journal of Food and Agriculture* 26 (*8*): 679–692, ISSN: 20790538, https://doi.org/10.9755/ejfa.v26i8.18364.

Kuzmanovic, D. A., I. Elashvili, C. Wick, C. O'Connell, and S. Krueger, 2003, « Bacteriophage MS2: Molecular weight and spatial distribution of the protein and RNA components by small-angle neutron scattering and virus counting », *Structure* 11 (*11*): 1339–1348, ISSN: 09692126, https://doi.org/10.1016/j.str.2003.09.021.

Lachmann, S. C., T. Mettler-Altmann, A. Wacker, and E. Spijkerman, 2019, « Nitrate or ammonium: Influences of nitrogen source on the physiology of a green alga », *Ecology and Evolution* 9 (*3*): 1070–1082, ISSN: 20457758, https://doi.org/10.1002/ece3.4790.

Lacroux, J., E. Trably, N. Bernet, J. P. Steyer, and R. van Lis, 2020, « Mixotrophic growth of microalgae on volatile fatty acids is determined by their undissociated form », *Algal Research* 47 (*March*): 101870, ISSN: 22119264, https://doi.org/10.1016/j.algal.2020.101870, https://doi.org/10.1016/j.algal.2020.101870.

Lane, A. E., and J. E. Burris, 1981, « Effects of Environmental pH on the Internal pH of Chlorella pyrenoidosa, Scenedesmus quadricauda, and Euglena mutabilis », *Plant Physiology* 68 (*2*): 439–442, ISSN: 0032-0889, https://doi.org/10.1104/pp.68.2.439.

Lazarova, V., P. Savoye, M. L. Janex, E. R. Blatchley, and M. Pommepuy, 1999, « Advanced wastewater disinfection technologies: State of the art and perspectives », *Water Science and*

Technology 40 (*4-5*): 203–213, ISSN: 02731223, https://doi.org/10.1016/S0273-1223(99)00502-8.

Le Borgne, F., and J. Pruvost, 2013, « Investigation and modeling of biomass decay rate in the dark and its potential influence on net productivity of solar photobioreactors for microalga Chlamydomonas reinhardtii and cyanobacterium Arthrospira platensis », *Bioresource Technology* 138:271–276, ISSN: 18732976, https://doi.org/10.1016/j.biortech.2013.03.056.

Le Gouic, B., H. Marec, J. Pruvost, and J. F. Cornet, 2021, « Investigation of growth limitation by CO2 mass transfer and inorganic carbon source for the microalga Chlorella vulgaris in a dedicated photobioreactor », *Chemical Engineering Science* 233:116388, ISSN: 00092509, https://doi.org/10.1016/j.ces.2020.116388, https://doi.org/10.1016/j.ces.2020.116388.

Le Gouic, B., 2013, « Analyse et optimisation de l'apport de carbone en photobioréacteur », PhD thesis, Nantes Université.

Legifrance, 2021, *Arrêté du 21 juillet 2015, dernière mise à jour le 1er janvier 2021,* https://www.legifrance.gouv.fr/loda/id/JORFTEXT000031052756/2021-01-06/.

Legifrance, 2023, *Arrêté du 18 décembre 2023 relatif aux conditions de production et d'utilisation des eaux usées traitées pour l'irrigation de cultures.,* https://www.legifrance.gouv.fr/jorf/id/JORFTEXT000048679665.

Legrand, J., A. Artu, J. Cornet, J. Dauchet, C. Dussap, M. Janssen, R. Kandilian, et al., 2016, *Advances in Chemical Engineering - Photobioreaction engineering,* edited by G. Marin, volume 48, ISBN: 978-0-12-803661-7.

Lester, J., 2001, « Sewage and Sewage Sludge Treatment », *in Pollution: Causes, Effects and Control,* 113–144, ISBN: 978-1-84755-171-9.

LGA, 2020, « High Rate Algal Pond (HRAP) Design Guideline - an element in CWMS Wastewater Treatment Trains », number January, 0–24.

Li, D., A. Z. Gu, M. He, H. C. Shi, and W. Yang, 2009, « UV inactivation and resistance of rotavirus evaluated by integrated cell culture and real-time RT-PCR assay », *Water Research* 43 (*13*): 3261–3269, ISSN: 00431354, https://doi.org/10.1016/j.watres.2009.03.044, http://dx.doi.org/10.1016/j.watres.2009.03.044.

Li, L., S. Zhang, G. Li, and H. Zhao, 2012, « Determination of chemical oxygen demand of nitrogenous organic compounds in wastewater using synergetic photoelectrocatalytic oxidation effect at TiO2 nanostructured electrode », *Analytica Chimica Acta* 754:47–53, ISSN: 00032670, https://doi.org/10.1016/j.aca.2012.10.008.

Li, M., L. Gao, and L. Lin, 2015, « Specific growth rate, colonial morphology and extracellular polysaccharides (EPS) content of Scenedesmus obliquus grown under different levels of light limitation », *Annales de Limnologie* 51 (*4*): 329–334, ISSN: 2100000X, https://doi.org/10.1051/limn/2015033.

Li, T., F. Yang, J. Xu, H. Wu, J. Mo, L. Dai, and W. Xiang, 2020, « Evaluating differences in growth, photosynthetic efficiency, and transcriptome of Asterarcys sp. SCS-1881 under autotrophic, mixotrophic, and heterotrophic culturing conditions », *Algal Research* 45 (*June 2019*): 101753, ISSN: 22119264, https://doi.org/10.1016/j.algal.2019.101753, https://doi.org/10.1016/j.algal.2019.101753.

Li, T., H. Kirchhoff, M. Gargouri, J. Feng, A. B. Cousins, P. T. Pienkos, D. R. Gang, and S. Chen, 2016, « Assessment of photosynthesis regulation in mixotrophically cultured microalga Chlorella sorokiniana », *Algal Research* 19:30–38, ISSN: 22119264, https://doi.org/10.1016/j.algal.2016.07.012, http://dx.doi.org/10.1016/j.algal.2016.07.012.

Li, T., Y. Zheng, L. Yu, and S. Chen, 2014, « Mixotrophic cultivation of a Chlorella sorokiniana strain for enhanced biomass and lipid production », *Biomass and Bioenergy* 66:204–213, ISSN: 09619534, https://doi.org/10.1016/j.biombioe.2014.04.010, http://dx.doi.org/10.1016/j.biombioe.2014.04.010.

Li, X., M. Song, Z. Yu, C. Wang, J. Sun, K. Su, N. Liu, Y. Mou, and T. Lu, 2022, « Comparison of heterotrophic and mixotrophic Chlorella pyrenoidosa cultivation for the growth and lipid accumulation through acetic acid as a carbon source », *Journal of Environmental Chemical Engineering* 10 (*1*), ISSN: 22133437, https://doi.org/10.1016/j.jece.2021.107054.

Li, Y., D. Si, W. Wang, S. Xue, W. Shang, Z. Chi, C. Li, C. Hao, G. Govindjee, and Y. Shi, 2023, « Light-driven CO2 assimilation by photosystem II and its relation to photosynthesis », *Chinese Journal of Catalysis* 44:117–126, ISSN: 18722067, https://doi.org/10.1016/S1872-2067(22)64170-6, http://dx.doi.org/10.1016/S1872-2067(22)64170-6.

Lian, Y., L. Mai, N. Cromar, N. Buchanan, H. Fallowfield, and X. Li, 2018, « MS2 coliphage and E. Coli UVB inactivation rates in optically clear water: Dose, dose rate and temperature dependence », *Water Science and Technology* 78 (*10*): 2228–2238, ISSN: 02731223, https://doi.org/10.2166/wst.2018.509.

Lin, C. Y., M. L. T. Nguyen, and C. H. Lay, 2017, « Starch-containing textile wastewater treatment for biogas and microalgae biomass production », *Journal of Cleaner Production* 168:331–337, ISSN: 09596526, https://doi.org/10.1016/j.jclepro.2017.09.036, https://doi.org/10.1016/j.jclepro.2017.09.036.

Lin, K., C. R. Schulte, and L. C. Marr, 2020, « Survival of MS2 and Φ6 viruses in droplets as a function of relative humidity, pH, and salt, protein, and surfactant concentrations », *PLoS ONE* 15 (*12 December*): 1–18, ISSN: 19326203, https://doi.org/10.1371/journal.pone.0243505, http://dx.doi.org/10.1371/journal.pone.0243505.

Lin, T. S., and J. Y. Wu, 2015, « Effect of carbon sources on growth and lipid accumulation of newly isolated microalgae cultured under mixotrophic condition », *Bioresource Technology* 184:100–107, ISSN: 18732976, https://doi.org/10.1016/j.biortech.2014.11.005, http://dx.doi.org/10.1016/j.biortech.2014.11.005.

Liu, M., J. Lv, C. Qin, H. Zhang, L. Wu, W. Guo, C. Guo, and J. Xu, 2022, « Chemical fingerprinting of organic micropollutants in different industrial treated wastewater effluents and their effluent-receiving river », *Science of the Total Environment* 838 (*May*), ISSN: 18791026, https://doi.org/10.1016/j.scitotenv.2022.156399.

Lotter, L. H., and M. Murphy, 1985, « The identification of heterotrophic bacteria in an activated sludge plant with particular reference to polyphosphate accumulation », *Water SA* 11 (*4*): 179–184, ISSN: 03784738.

Louten, J., 2016, *Virus structure and classification,* 1–9, 1, ISBN: 9780128009475.

Lürling, M., 2003, « Phenotypic plasticity in the green algae Desmodesmus and Scenedesmus with special reference to the induction of defensive morphology », *Annales de Limnologie* 39 (*2*): 85–101, ISSN: 00034088, https://doi.org/10.1051/limn/2003014.

Luther, M., and C. J. Soeder, 1991, « 1-naphthalenesulfonic acid and sulfate as sulfur sources for the green ALGA Scenedesmus obliquus », *Water Research* 25 (*3*): 299–307, ISSN: 00431354, https://doi.org/10.1016/0043-1354(91)90009-F.

Majiya, H., O. O. Adeyemi, N. J. Stonehouse, and P. Millner, 2018, « Photodynamic inactivation of bacteriophage MS2: The A-protein is the target of virus inactivation », *Journal of Photochemistry and Photobiology B: Biology* 178 (*November 2017*): 404–411, ISSN: 18732682, https://doi.org/10.1016/j.jphotobiol.2017.11.032, https://doi.org/10.1016/j.jphotobiol.2017.11.032.

Manhaeghe, D., T. Blomme, S. W. Van Hulle, and D. P. Rousseau, 2020, « Experimental assessment and mathematical modelling of the growth of Chlorella vulgaris under photoautotrophic, heterotrophic and mixotrophic conditions », *Water Research* 184:116152, ISSN: 18792448, https://doi.org/10.1016/j.watres.2020.116152, https://doi.org/10.1016/j.watres.2020.116152.

Marcilhac, C., 2014, « Étude des conditions de culture d'un écosystème complexe microalgues / bactéries : application au développement d'un procédé d'extraction-valorisation des nutriments issus des digestats », PhD thesis, Rennes 1, https://tel.archives-ouvertes.fr/tel-01127525/.

Martens, D., 2005, « Denitrification », *in Encyclopedia of Soils in the Environment,* 378–382, USDA Agricultural Research Service, Tucson, AZ, USA.

MassWWP, 2001, « Standard Operating Procedure Lakes-6 for pH and Alkalinity ».

Matamoros, V., R. Gutiérrez, I. Ferrer, J. García, and J. M. Bayona, 2015, « Capability of microalgae-based wastewater treatment systems to remove emerging organic contaminants: A pilot-scale study », *Journal of Hazardous Materials* 288:34–42, ISSN: 18733336, https://doi.org/10.1016/j.jhazmat.2015.02.002, http://dx.doi.org/10.1016/j.jhazmat.2015.02.002.

Mehrabadi, A., R. Craggs, and M. M. Farid, 2015, « Wastewater treatment high rate algal ponds (WWT HRAP) for low-cost biofuel production », *Bioresource Technology* 184:202–214, ISSN: 18732976, https://doi.org/10.1016/j.biortech.2014.11.004, http://dx.doi.org/10.1016/j.biortech.2014.11.004.

Mehrabadi, A., M. M. Farid, and R. Craggs, 2016, « Variation of biomass energy yield in wastewater treatment high rate algal ponds », *Algal Research* 15:143–151, ISSN: 22119264, https://doi.org/10.1016/j.algal.2016.02.016, http://dx.doi.org/10.1016/j.algal.2016.02.016.

Méndez-Hurtado, J., R. Lõpez, D. Suárez, and M. I. Menéndez, 2012, « Theoretical study of the oxidation of histidine by singlet oxygen », *Chemistry - A European Journal* 18 (*27*): 8437–8447, ISSN: 09476539, https://doi.org/10.1002/chem.201103680.

Mendoza, J. L., M. R. Granados, I. de Godos, F. G. Acién, E. Molina, C. Banks, and S. Heaven, 2013, « Fluid-dynamic characterization of real-scale raceway reactors for microalgae production », *Biomass and Bioenergy* 54:267–275, ISSN: 09619534, https://doi.org/10.1016/j.biombioe.2013.03.017.

Mitra, D., J. (van Leeuwen, and B. Lamsal, 2012, « Heterotrophic/mixotrophic cultivation of oleaginous Chlorella vulgaris on industrial co-products », *Algal Research* 1 (*1*): 40–48, ISSN: 22119264, https://doi.org/10.1016/j.algal.2012.03.002.

Molnar, C., and J. Gair, 2015, *Concepts of Biology 1st Canadian Edition,* BCcampus, ISBN: 978-1-989623-98-5, https://opentextbc.ca/biology/.

Montemezzani, V., I. C. Duggan, I. D. Hogg, and R. J. Craggs, 2016, « Zooplankton community influence on seasonal performance and microalgal dominance in wastewater treatment High Rate Algal Ponds », *Algal Research* 17:168–184, ISSN: 22119264, https://doi.org/10.1016/j.algal.2016.04.014, http://dx.doi.org/10.1016/j.algal.2016.04.014.

Montemezzani, V., I. C. Duggan, I. D. Hogg, and R. J. Craggs, 2017, « Control of zooplankton populations in a wastewater treatment High Rate Algal Pond using overnight CO2 asphyxiation », *Algal Research* 26 (*March*): 250–264, ISSN: 22119264, https://doi.org/10.1016/j.algal.2017.08.004, http://dx.doi.org/10.1016/j.algal.2017.08.004.

Moulin, L., F. Richard, S. Stefania, M. Goulet, S. Gosselin, A. Gonçalves, V. Rocher, C. Paffoni, and A. Dumètre, 2010, « Contribution of treated wastewater to the microbiological quality of Seine River in Paris », *Water Research* 44 (*18*): 5222–5231, ISSN: 00431354, https://doi.org/10.1016/j.watres.2010.06.037.

Moulin, S., D. Rozen-Rechels, and M. Stankovic, 2013, « Traitement des eaux usées ».

Murwanashyaka, T., L. Shen, Z. Yang, J. S. Chang, E. Manirafasha, T. Ndikubwimana, C. Chen, and Y. Lu, 2020, « Kinetic modelling of heterotrophic microalgae culture in wastewater: Storage molecule generation and pollutants mitigation », *Biochemical Engineering Journal* 157 (*September 2019*): 107523, ISSN: 1873295X, https://doi.org/10.1016/j.bej.2020.107523, https://doi.org/10.1016/j.bej.2020.107523.

Mussgnug, J. H., V. Klassen, A. Schlüter, and O. Kruse, 2010, « Microalgae as substrates for fermentative biogas production in a combined biorefinery concept », *Journal of Biotechnology* 150 (*1*): 51–56, ISSN: 01681656, https://doi.org/10.1016/j.jbiotec.2010.07.030, http://dx.doi.org/10.1016/j.jbiotec.2010.07.030.

Mutanda, T., S. Karthikeyan, and F. Bux, 2011, « The utilization of post-chlorinated municipal domestic wastewater for biomass and lipid production by Chlorella spp. under batch conditions », *Applied Biochemistry and Biotechnology* 164 (*7*): 1126–1138, ISSN: 02732289, https://doi.org/10.1007/s12010-011-9199-x.

Nair, A., and S. Chakraborty, 2020, « Synergistic effects between autotrophy and heterotrophy in optimization of mixotrophic cultivation of Chlorella sorokiniana in bubble-column photobioreactors », *Algal Research* 46 (*December 2019*): 101799, ISSN: 22119264, https://doi.org/10.1016/j.algal.2020.101799, https://doi.org/10.1016/j.algal.2020.101799.

Natural Resource Management Ministerial Council, 2006, « Overview of the Australian guidelines for water recycling: Managing health and environment risks ».

Nazari, L., S. Sarathy, D. Santoro, D. Ho, M. Ray, and C. Xu, 2018, « 3 - Recent advances in energy recovery from wastewater sludge », *in Direct Thermochemical Liquefaction for Energy Applications,* edited by Lasse Rosendahl, 67–100, ISBN: 978-0-08-101029-7, https://doi.org/https://doi.org/10.1016/C2015-0-06012-9.

Nelson, K. L., B. J. Cisneros, G. Tchobanoglous, and J. L. Darby, 2004, « Sludge accumulation, characteristics, and pathogen inactivation in four primary waste stabilization ponds in central Mexico », *Water Research* 38 (*1*): 111–127, ISSN: 00431354, https://doi.org/10.1016/j.watres.2003.09.013.

Nirmalakhandan, N., T. Selvaratnam, S. M. Henkanatte-Gedera, D. Tchinda, I. S. Abeysiriwardana-Arachchige, H. M. Delanka-Pedige, S. P. Munasinghe-Arachchige, Y. Zhang, F. O. Holguin, and P. J. Lammers, 2019, « Algal wastewater treatment: Photoautotrophic vs. mixotrophic processes », *Algal Research* 41 (*May*): 101569, ISSN: 22119264, https://doi.org/10.1016/j.algal.2019.101569, https://doi.org/10.1016/j.algal.2019.101569.

Niu, X. Z., and J. P. Croué, 2019, « Photochemical production of hydroxyl radical from algal organic matter », *Water Research* 161:11–16, ISSN: 18792448, https://doi.org/10.1016/j.watres.2019.05.089.

Niu, X. Z., C. Liu, L. Gutierrez, and J. P. Croué, 2014, « Photobleaching-induced changes in photosensitizing properties of dissolved organic matter », *Water Research* 66:140–148, ISSN: 18792448, https://doi.org/10.1016/j.watres.2014.08.017.

Noble, R. T., I. M. Lee, and K. C. Schiff, 2004, « Inactivation of indicator micro-organisms from various sources of faecal contamination in seawater and freshwater », *Journal of Applied Microbiology* 96 (*3*): 464–472, ISSN: 13645072, https://doi.org/10.1111/j.1365-2672.2004.02155.x.

Nopens, I., C. Capalozza, and P. A. Vanrolleghem, 2001, *Technical report : Stability analysis of a synthetic municipal wastewater,* technical report.

Nordio, R., E. Rodríguez-Miranda, F. Casagli, A. Sánchez-Zurano, J. L. Guzmán, and G. Acién, 2024, « ABACO-2: a comprehensive model for microalgae-bacteria consortia validated outdoor at pilot-scale », *Water Research* 248 (*October 2023*): 120837, ISSN: 00431354, https://doi.org/10.1016/j.watres.2023.120837.

Norvill, Z. N., A. Shilton, and B. Guieysse, 2016, « Emerging contaminant degradation and removal in algal wastewater treatment ponds: Identifying the research gaps », *Journal of Hazardous Materials* 313:291–309, ISSN: 18733336, https://doi.org/10.1016/j.jhazmat.2016.03.085, http://dx.doi.org/10.1016/j.jhazmat.2016.03.085.

NRMMC, 2006, *Australian guidelines for water recycling: managing health and environmental risk (phase 1),* technical report, https://www.susana.org/_resources/documents/default/2-1533-waterrecyclingguidelines-02nov06.pdf.

Ofori, S., A. Pukáová, I. Riková, and J. Wanner, 2021, « Treated wastewater reuse for irrigation: Pros and cons », *Science of the Total Environment* 760, ISSN: 18791026, https://doi.org/10.1016/j.scitotenv.2020.144026.

Oviedo, J. A., R. Muñoz, A. Donoso-Bravo, O. Bernard, F. Casagli, and D. Jeison, 2022, « A half-century of research on microalgae-bacteria for wastewater treatment », *Algal Research* 67 (*May*), ISSN: 22119264, https://doi.org/10.1016/j.algal.2022.102828.

Owusu-Agyeman, I., B. Bedaso, C. Laumeyer, C. Pan, A. Malovanyy, C. Baresel, E. Plaza, and Z. Cetecioglu, 2023, « Volatile fatty acids production from municipal waste streams and use as a carbon source for denitrification: The journey towards full-scale application and revealing key microbial players », *Renewable and Sustainable Energy Reviews* 175 (*December*

2022): 113163, ISSN: 18790690, https://doi.org/10.1016/j.rser.2023.113163, https://doi.org/10.1016/j.rser.2023.113163.

Paing, J., B. Picot, and J. P. Sambuco, 2003, « Emission of H2S and mass balance of sulfur in anaerobic ponds », *Water Science and Technology* 48 (*2*): 227–234, ISSN: 02731223, https://doi.org/10.2166/wst.2003.0125.

Park, J. B., R. J. Craggs, and A. N. Shilton, 2011, « Wastewater treatment high rate algal ponds for biofuel production », *Bioresource Technology* 102 (*1*): 35–42, ISSN: 09608524, https://doi.org/10.1016/j.biortech.2010.06.158, http://dx.doi.org/10.1016/j.biortech.2010.06.158.

Park, J. B., R. J. Craggs, and A. N. Shilton, 2013, « Enhancing biomass energy yield from pilot-scale high rate algal ponds with recycling », *Water Research* 47 (*13*): 4422–4432, ISSN: 18792448, https://doi.org/10.1016/j.watres.2013.04.001, http://dx.doi.org/10.1016/j.watres.2013.04.001.

Park, J. B., L. Weaver, R. Davies-Colley, R. Stott, W. Williamson, M. Mackenzie, E. McGill, S. Lin, J. Webber, and R. J. Craggs, 2021, « Comparison of faecal indicator and viral pathogen light and dark disinfection mechanisms in wastewater treatment pond mesocosms », *Journal of Environmental Management* 286 (*October 2020*): 112197, ISSN: 10958630, https://doi.org/10.1016/j.jenvman.2021.112197, https://doi.org/10.1016/j.jenvman.2021.112197.

Parker, N., M. Schneegurt, A.-H. T. Tu, P. Lister, and B. M. Forster, 2016, « Cellular respiration », *in Microbiology,* OpenStax, https://openstax.org/books/microbiology/pages/1-introduction.

Passos, F., M. Hernández-Mariné, J. García, and I. Ferrer, 2014, « Long-term anaerobic digestion of microalgae grown in HRAP for wastewater treatment. Effect of microwave pretreatment », *Water Research* 49, ISSN: 18792448, https://doi.org/10.1016/j.watres.2013.10.013.

Patel, A., E. Krikigianni, U. Rova, P. Christakopoulos, and L. Matsakas, 2022, « Bioprocessing of volatile fatty acids by oleaginous freshwater microalgae and their potential for biofuel and protein production », *Chemical Engineering Journal* 438 (*March*): 135529, ISSN: 13858947, https://doi.org/10.1016/j.cej.2022.135529, https://doi.org/10.1016/j.cej.2022.135529.

Patel, A. K., J. M. Joun, M. E. Hong, and S. J. Sim, 2019, « Effect of light conditions on mixotrophic cultivation of green microalgae », *Bioresource Technology* 282 (*March*): 245–253, ISSN: 18732976, https://doi.org/10.1016/j.biortech.2019.03.024, https://doi.org/10.1016/j.biortech.2019.03.024.

Pavlostathis, S., 2011, « 6.31 - Kinetics and Modeling of Anaerobic Treatment and Biotransformation Processes », *in Comprehensive Biotechnology (Second Edition) Volume 6,* edited by M. Moo-Young, 385–397, ISBN: 978-0-08-088504-9.

Pereira, E. G., M. A. Martins, M. D. S. Mendes, L. B. Mendes, and A. N. Nesi, 2017, « Outdoor cultivation of Scenedesmus obliquus BR003 in stirred tanks by airlift », *Engenharia Agricola* 37 (*5*): 1041–1055, ISSN: 18094430, https://doi.org/10.1590/1809-4430-Eng.Agric.v37n5p1041-1055/2017.

Pham, L. A., J. Laurent, P. Bois, and A. Wanko, 2020, « A coupled RTD and mixed-order kinetic model to predict high rate algal pond wastewater treatment under different operational conditions: Performance assessment and sizing application », *Biochemical Engineering*

Journal 162 (*July*): 107709, ISSN: 1873295X, https://doi.org/10.1016/j.bej.2020.107709, https://doi.org/10.1016/j.bej.2020.107709.

Picot, B., A. Bahlaoui, S. Moersidik, B. Baleux, and J. Bontoux, 1992, « Comparison of the purifying efficiency of high rate algal pond with stabilization pond », *Water Science and Technology* 25 (*12*): 197–206, ISSN: 02731223, https://doi.org/10.2166/wst.1992.0351.

Picot, B., H. El Halouani, C. Casellas, S. Moersidik, and J. Bontoux, 1991, « Nutrient Removal By High Rate Pond System in a Mediterranean climate (France) », *Water Science and Technology* 23 (*1963*): 1535–1541, ISSN: 0273-1223, http://apps.webofknowledge.com/full_record.do?product=UA&search_mode=GeneralSearch&qid=23&SID=V2IMBjjRAI6C1fmi39b&page=1&doc=2.

Pignolet, O., S. Jubeau, C. Vaca-Garcia, and P. Michaud, 2013, « Highly valuable microalgae: Biochemical and topological aspects », *Journal of Industrial Microbiology and Biotechnology* 40 (*8*): 781–796, ISSN: 13675435, https://doi.org/10.1007/s10295-013-1281-7.

Plouviez, M., P. Chambonnière, A. Shilton, M. A. Packer, and B. Guieysse, 2019, « Nitrous oxide (N2O) emissions during real domestic wastewater treatment in an outdoor pilot-scale high rate algae pond », *Algal Research* 44 (*March*): 101670, ISSN: 22119264, https://doi.org/10.1016/j.algal.2019.101670, https://doi.org/10.1016/j.algal.2019.101670.

Pobernik, M., L. Trauner, A. Leis, and A. Lobnik, 2008, « Improvements to the quality of underground water by introducing carbon dioxide », *Acta Geotechnica Slovenica* 5 (*2*): 51–62, ISSN: 18540171.

Pooja, K., V. Priyanka, B. C. S. Rao, and V. Raghavender, 2022, « Cost-effective treatment of sewage wastewater using microalgae Chlorella vulgaris and its application as bio-fertilizer », *Energy Nexus* 7 (*May*): 100122, ISSN: 27724271, https://doi.org/10.1016/j.nexus.2022.100122, https://doi.org/10.1016/j.nexus.2022.100122.

Popa, D. G., C. Lupu, D. Constantinescu-Aruxandei, and F. Oancea, 2022, « Humic Substances as Microalgal BiostimulantsImplications for Microalgal Biotechnology », *Marine Drugs* 20 (*5*): 1–27, ISSN: 16603397, https://doi.org/10.3390/md20050327.

Poughon, L., C. G. Dussap, and J. B. Gros, 1999, « Dynamic model of a nitrifying fixed bed column: Simulation of the biomass distribution of Nitrosomonas and Nitrobacter and of transient behaviour of the column », *Bioprocess Engineering* 20 (*3*): 209–221, ISSN: 0178515X, https://doi.org/10.1007/s004490050583.

Price, G. D., D. Sültemeyer, B. Klughammer, M. Ludwig, and M. R. Badger, 1998, « The functioning of the CO2 concentrating mechanism in several cyanobacterial strains: A review of general physiological characteristics, genes, proteins, and recent advances », *Canadian Journal of Botany* 76 (*6*): 973–1002, ISSN: 00084026, https://doi.org/10.1139/b98-081.

Pruvost, J., J. F. Cornet, F. Le Borgne, V. Goetz, and J. Legrand, 2015, « Theoretical investigation of microalgae culture in the light changing conditions of solar photobioreactor production and comparison with cyanobacteria », *Algal Research* 10:87–99, ISSN: 22119264, https://doi.org/10.1016/j.algal.2015.04.005, http://dx.doi.org/10.1016/j.algal.2015.04.005.

Pruvost, J., J. F. Cornet, and L. Pilon, 2012, *Large-scale production of algal biomass: Photobioreactors,* 41–66, Springer, https://doi.org/10.1007/978-3-319-12334-9{_}3.

Pruvost, J., B. Le Gouic, and J. F. Cornet, 2022, « Kinetic Modeling of CO2 Biofixation by Microalgae and Optimization of Carbon Supply in Various Photobioreactor Technologies », *ACS Sustainable Chemistry and Engineering* 10 (*38*): 12826–12842, ISSN: 21680485, https://doi.org/10.1021/acssuschemeng.2c03927.

Putois, T., 2012, « Etude du traitement de désinfection des eaux de refroidissement par le couplage H2O2/UV : Application à une tour aéroréfrigérante ».

Quilbé, R., C. Serreau, S. Wicherek, C. Bernard, Y. Thomas, and J.-P. Oudinet, 2005, « Nutrient transfer by runoff from sewage sludge amended soil under simulated rainfall », *Environmental Monitoring and Assessment,* 177–190.

Rastogi, R. P., D. Madamwar, H. Nakamoto, and A. Incharoensakdi, 2020, « Resilience and self-regulation processes of microalgae under UV radiation stress », *Journal of Photochemistry and Photobiology C: Photochemistry Reviews* 43:100322, ISSN: 13895567, https://doi.org/10.1016/j.jphotochemrev.2019.100322, https://doi.org/10.1016/j.jphotochemrev.2019.100322.

Rattanakul, S., and K. Oguma, 2017, « Analysis of Hydroxyl Radicals and Inactivation Mechanisms of Bacteriophage MS2 in Response to a Simultaneous Application of UV and Chlorine », *Environmental Science and Technology* 51 (*1*): 455–462, ISSN: 15205851, https://doi.org/10.1021/acs.est.6b03394.

Ravndal, K. T., E. Opsahl, A. Bagi, and R. Kommedal, 2018, « Wastewater characterisation by combining size fractionation, chemical composition and biodegradability », *Water Research* 131:151–160, ISSN: 18792448, https://doi.org/10.1016/j.watres.2017.12.034, https://doi.org/10.1016/j.watres.2017.12.034.

Rawat, I., R. Ranjith Kumar, and F. Bux, 2016, « Phycoremediation by High-Rate Algal Ponds (HRAPs) », *Biotechnological Applications of Microalgae,* 51–75, https://doi.org/10.1201/b14920.

Renou, S., J. G. Givaudan, S. Poulain, F. Dirassouyan, and P. Moulin, 2008, « Landfill leachate treatment: Review and opportunity », *Journal of Hazardous Materials* 150 (*3*): 468–493, ISSN: 03043894, https://doi.org/10.1016/j.jhazmat.2007.09.077.

Robles, Á., G. Capson-Tojo, A. Galès, M. V. Ruano, B. Sialve, J. Ferrer, and J. P. Steyer, 2020, « Microalgae-bacteria consortia in high-rate ponds for treating urban wastewater: Elucidating the key state indicators under dynamic conditions », *Journal of Environmental Management* 261 (*February*), ISSN: 10958630, https://doi.org/10.1016/j.jenvman.2020.110244.

Roeva, O., T. Pencheva, S. Tzonkov, and B. Hitzmann, 2015, « Functional state modelling of cultivation processes: Dissolved oxygen limitation state », *International Journal Bioautomation* 19 (*September 2016*): S93–S112, ISSN: 13142321.

Rogers, K., 2011, « Bacterial Morphology and Reproduction », *in Bacteria and viruses,* Britannica Educational Publishing, ISBN: 978-1-61530-376-2.

Rolfsson, Ó., S. Middleton, I. W. Manfield, S. J. White, B. Fan, R. Vaughan, N. A. Ranson, et al., 2016, « Direct Evidence for Packaging Signal-Mediated Assembly of Bacteriophage MS2 », *Journal of Molecular Biology* 428 (*2*): 431–448, ISSN: 10898638, https://doi.org/10.1016/j.jmb.2015.11.014, http://dx.doi.org/10.1016/j.jmb.2015.11.014.

Rosenwinkel, K. H., D. Weichgrebe, H. Meyer, and D. Wendler, 2001, « Suspended solids from industrial and municipal origins », *Ecotoxicology and Environmental Safety* 50 (*2*): 135–142, ISSN: 01476513, https://doi.org/10.1006/eesa.2001.2082.

Ruan, Z., and M. Giordano, 2017, « The use of NH4+ rather than NO3 affects cell stoichiometry, C allocation, photosynthesis and growth in the cyanobacterium Synechococcus sp. UTEX LB 2380, only when energy is limiting », *Plant Cell and Environment* 40 (*2*): 227–236, ISSN: 13653040, https://doi.org/10.1111/pce.12858.

Ruas, G., S. L. Farias, P. G. Scarcelli, M. L. Serejo, and M. A. Boncz, 2020, « The effect of CO2 addition and hydraulic retention time on pathogens removal in HRAPs », *Water Science and Technology* 82 (*6*): 1184–1192, ISSN: 19969732, https://doi.org/10.2166/wst.2020.255.

Russel, M., Q. Meixue, M. A. Alam, L. Lifen, M. Daroch, C. Blaszczak-Boxe, and G. Kumar Gupta, 2020, « Investigating the potentiality of Scenedesmus obliquus and Acinetobacter pittii partnership system and their effects on nutrients removal from synthetic domestic wastewater », *Bioresource Technology* 299 (*September 2019*): 122571, ISSN: 18732976, https://doi.org/10.1016/j.biortech.2019.122571, https://doi.org/10.1016/j.biortech.2019.122571.

Ryu, W.-S., 2017, « Virus Life Cycle », *in Molecular Virology of Human Pathogenic Viruses,* 31–45, 1, ISBN: 9780128008386, https://doi.org/10.1016/b978-0-12-800838-6.00003-5.

Safi, K. A., J. B. Park, and R. J. Craggs, 2016, « Partitioning of wastewater treatment high rate algal pond biomass and particulate carbon », *Algal Research* 19:77–85, ISSN: 22119264, https://doi.org/10.1016/j.algal.2016.07.017.

Sebastian, S., and K. V. Nair, 1984, « Total removal of coliforms and E. coli from domestic sewage by high-rate pond mass culture of Scenedesmus obliquus », *Environmental Pollution. Series A, Ecological and Biological* 34 (*3*): 197–206, ISSN: 01431471, https://doi.org/10.1016/0143-1471(84)90116-8.

Sekomo, C. B., D. P. Rousseau, S. A. Saleh, and P. N. Lens, 2012, « Heavy metal removal in duckweed and algae ponds as a polishing step for textile wastewater treatment », *Ecological Engineering* 44:102–110, ISSN: 09258574, https://doi.org/10.1016/j.ecoleng.2012.03.003, http://dx.doi.org/10.1016/j.ecoleng.2012.03.003.

Sforza, E., M. Pastore, A. Spagni, and A. Bertucco, 2018, « Microalgae-bacteria gas exchange in wastewater: how mixotrophy may reduce the oxygen supply for bacteria », *Environmental Science and Pollution Research* 25 (*28*): 28004–28014, ISSN: 16147499, https://doi.org/10.1007/s11356-018-2834-0.

Shayesteh, H., A. Vadiveloo, P. A. Bahri, and N. R. Moheimani, 2021, « Can CO2 addition improve the tertiary treatment of anaerobically digested abattoir effluent (ADAE) by Scenedesmus sp. (Chlorophyta)? », *Algal Research* 58 (*May*): 102379, ISSN: 22119264, https://doi.org/10.1016/j.algal.2021.102379, https://doi.org/10.1016/j.algal.2021.102379.

Shi, W., L. Wang, D. P. Rousseau, and P. N. Lens, 2010, « Removal of estrone, 17α-ethinylestradiol, and 17SS-estradiol in algae and duckweed-based wastewater treatment systems », *Environmental Science and Pollution Research* 17 (*4*): 824–833, ISSN: 09441344, https://doi.org/10.1007/s11356-010-0301-7.

Shishlyannikov, S. M., I. V. Klimenkov, Y. D. Bedoshvili, I. S. Mikhailov, and A. G. Gorshkov, 2014, « Effect of mixotrophic growth on the ultrastructure and fatty acid composition of the diatom Synedra acus from Lake Baikal », *Journal of Biological Research (Greece)* 21 (*1*): 1–8, ISSN: 22415793, https://doi.org/10.1186/2241-5793-21-15.

Shoener, B. D., S. M. Schramm, F. Béline, O. Bernard, C. Martínez, B. G. Plósz, S. Snowling, et al., 2019a, « Microalgae and cyanobacteria modeling in water resource recovery facilities: A critical review », *Water Research X* 2, ISSN: 25899147, https://doi.org/10.1016/j.wroa.2018.100024.

Shoener, B. D., S. M. Schramm, F. Béline, O. Bernard, C. Martínez, B. G. Plósz, S. Snowling, et al., 2019b, « Microalgae and cyanobacteria modeling in water resource recovery facilities: A critical review », *Water Research X* 2, ISSN: 25899147, https://doi.org/10.1016/j.wroa.2018.100024.

Shu, W., Q. Zhang, J. Audet, Z. Li, P. Leng, Y. Qiao, C. Tian, et al., 2024, « Non-negligible N2O emission hotspots: Rivers impacted by ion-adsorption rare earth mining », *Water Research* 251 (*August 2023*): 121124, ISSN: 18792448, https://doi.org/10.1016/j.watres.2024.121124, https://doi.org/10.1016/j.watres.2024.121124.

Sialve, B., and J. Steyer, 2013, « Les microalgues, promesses et defis », *Innovation Agronomiques* 26:101–116.

Sim, S. J., J. Joun, M. E. Hong, and A. K. Patel, 2019, « Split mixotrophy: A novel cultivation strategy to enhance the mixotrophic biomass and lipid yields of Chlorella protothecoides », *Bioresource Technology* 291 (*June*): 121820, ISSN: 18732976, https://doi.org/10.1016/j.biortech.2019.121820, https://doi.org/10.1016/j.biortech.2019.121820.

Simkin, A. J., 2019, « Genetic engineering for global food security: Photosynthesis and biofortification », *Plants* 8 (*12*), ISSN: 22237747, https://doi.org/10.3390/plants8120586.

Smith, R. T., K. Bangert, S. J. Wilkinson, and D. J. Gilmour, 2015, « Synergistic carbon metabolism in a fast growing mixotrophic freshwater microalgal species Micractinium inermum », *Biomass and Bioenergy* 82:73–86, ISSN: 09619534, https://doi.org/10.1016/j.biombioe.2015.04.023, http://dx.doi.org/10.1016/j.biombioe.2015.04.023.

Soleimani, H., B. Mansouri, A. Kiani, and A. Khalid, 2023, « Ecological risk assessment and heavy metals accumulation in agriculture soils irrigated with treated wastewater effluent , river water , and well water combined with chemical fertilizers », *Heliyon* 9 (*3*), ISSN: 2405-8440, https://doi.org/10.1016/j.heliyon.2023.e14580, https://doi.org/10.1016/j.heliyon.2023.e14580.

Solimeno, A., and J. García, 2019, « Microalgae and bacteria dynamics in high rate algal ponds based on modelling results: Long-term application of BIO_ALGAE model », *Science of the Total Environment* 650:1818–1831, ISSN: 18791026, https://doi.org/10.1016/j.scitotenv.2018.09.345, https://doi.org/10.1016/j.scitotenv.2018.09.345.

Solimeno, A., L. Parker, T. Lundquist, and J. García, 2017, « Integral microalgae-bacteria model (BIO_ALGAE): Application to wastewater high rate algal ponds », *Science of the Total Environment* 601-602:646–657, ISSN: 18791026, https://doi.org/10.1016/j.scitotenv.2017.05.215, http://dx.doi.org/10.1016/j.scitotenv.2017.05.215.

Song, M., and H. Pei, 2018, « The growth and lipid accumulation of Scenedesmus quadricauda during batch mixotrophic/heterotrophic cultivation using xylose as a carbon source », *Bioresource Technology* 263 (*May*): 525–531, ISSN: 18732976, https://doi.org/10.1016/j.biortech.2018.05.020, https://doi.org/10.1016/j.biortech.2018.05.020.

Souliès, A., 2014, « Contribution à l'étude hydrodynamique et à la modélisatio des photobioréacteurs à haute productivité volumique », *Thèse de Doctorat en génie procédées France.*

Steichen, P., 2011, « Lévolution du droit de lassainissement en France : une mise aux normes sous contrainte », *Les Cahiers de droit* 51 (*3-4*): 567–593, ISSN: 0007-974X, https://doi.org/10.7202/045724ar.

Su, K., M. Song, Z. Yu, C. Wang, J. Sun, X. Li, N. Liu, Y. Mou, and T. Lu, 2021, « The effect of volatile fatty acids on the growth and lipid properties of two microalgae strains during batch heterotrophic cultivation », *Chemosphere* 283 (*April*), ISSN: 18791298, https://doi.org/10.1016/j.chemosphere.2021.131204.

Su, Y., A. Mennerich, and B. Urban, 2012, « Synergistic cooperation between wastewater-born algae and activated sludge for wastewater treatment: Influence of algae and sludge inoculation ratios », *Bioresource Technology* 105:67–73, ISSN: 09608524, https://doi.org/10.1016/j.biortech.2011.11.113, http://dx.doi.org/10.1016/j.biortech.2011.11.113.

SUEZ, *Degrillage,* https://www.suezwaterhandbook.fr/procedes-et-technologies/pretraitements/degrillage-tamisage-dilaceration/degrillage.

Sun, J., and H. Simsek, 2017, « Bioavailability of wastewater derived dissolved organic nitrogen to green microalgae Selenastrum capricornutum, Chlamydomonas reinhardtii, and Chlorella vulgaris with/without presence of bacteria », *Journal of Environmental Sciences (China)* 57:346–355, ISSN: 18787320, https://doi.org/10.1016/j.jes.2016.12.017, http://dx.doi.org/10.1016/j.jes.2016.12.017.

Sutherland, D. L., V. Montemezzani, C. Howard-Williams, M. H. Turnbull, P. A. Broady, and R. J. Craggs, 2015, « Modifying the high rate algal pond light environment and its effects on light absorption andphotosynthesis », *Water Research* 70:86–96, ISSN: 18792448, https://doi.org/10.1016/j.watres.2014.11.050, http://dx.doi.org/10.1016/j.watres.2014.11.050.

Sutherland, D. L., J. Park, S. Heubeck, P. J. Ralph, and R. J. Craggs, 2020, « Size matters Microalgae production and nutrient removal in wastewater treatment high rate algal ponds of three different sizes », *Algal Research* 45 (*November 2019*): 101734, ISSN: 22119264, https://doi.org/10.1016/j.algal.2019.101734, https://doi.org/10.1016/j.algal.2019.101734.

Sutherland, D. L., J. Park, P. J. Ralph, and R. Craggs, 2021, « Ammonia, pH and dissolved inorganic carbon supply drive whole pond metabolism in full-scale wastewater high rate algal ponds », *Algal Research* 58 (*April*): 102405, ISSN: 22119264, https://doi.org/10.1016/j.algal.2021.102405, https://doi.org/10.1016/j.algal.2021.102405.

Sutherland, D. L., M. H. Turnbull, P. A. Broady, and R. J. Craggs, 2014a, « Effects of two different nutrient loads on microalgal production, nutrient removal and photosynthetic efficiency in pilot-scale wastewater high rate algal ponds », *Water Research* 66:53–62, ISSN: 18792448, https://doi.org/10.1016/j.watres.2014.08.010, http://dx.doi.org/10.1016/j.watres.2014.08.010.

Sutherland, D. L., M. H. Turnbull, and R. J. Craggs, 2014b, « Increased pond depth improves algal productivity and nutrient removal in wastewater treatment high rate algal ponds », *Water Research* 53:271–281, ISSN: 18792448, https://doi.org/10.1016/j.watres.2014.01.025, http://dx.doi.org/10.1016/j.watres.2014.01.025.

Sutherland, D. L., M. H. Turnbull, and R. J. Craggs, 2017, « Environmental drivers that influence microalgal species in fullscale wastewater treatment high rate algal ponds », *Water Research* 124:504–512, ISSN: 18792448, https://doi.org/10.1016/j.watres.2017.08.012, http://dx.doi.org/10.1016/j.watres.2017.08.012.

The World Bank, 2021, *Population density (people per sq. km of land area) - Australia, France,* https://data.worldbank.org/indicator/EN.POP.DNST?end=2021&locations=AU-FR&start=1961&view=chart.

Tuser, C., 2021, *What is Activated Sludge?,* https://www.wwdmag.com/sludge-and-biosolids/article/10939479/what-is-activated-sludge.

UE, 2019, *Règlement UE 2019/1009 du parlement européen et du conseil du 5 juin 2019 sur les fertilisants.*

Unnithan, V. V., A. Unc, and G. B. Smith, 2014, « Mini-review: A priori considerations for bacteria-algae interactions in algal biofuel systems receiving municipal wastewaters », *Algal Research* 4 (*1*): 35–40, ISSN: 22119264, https://doi.org/10.1016/j.algal.2013.11.009, http://dx.doi.org/10.1016/j.algal.2013.11.009.

Urbain, B., 2017, « Elaboration of a biochemically-based structured model for the growth of eukaryotic microalgae in photobioreactors - Application to the unicellular green algae Chlamydomonas reinhardtii ».

Vargas, G., A. Donoso-Bravo, C. Vergara, and G. Ruiz-Filippi, 2016, « Assessment of microalgae and nitrifiers activity in a consortium in a continuous operation and the effect of oxygen depletion », *Electronic Journal of Biotechnology* 23:63–68, ISSN: 07173458, https://doi.org/10.1016/j.ejbt.2016.08.002, http://dx.doi.org/10.1016/j.ejbt.2016.08.002.

Vassalle, L., I. Ferrer, F. Passos, C. R. M. Filho, and M. Garfí, 2023, « Nature-based solutions for wastewater treatment and bioenergy recovery: A comparative Life Cycle Assessment », *Science of the Total Environment* 880 (*March*), ISSN: 18791026, https://doi.org/10.1016/j.scitotenv.2023.163291.

Vassalle, L., A. Sunyer-Caldú, M. S. Díaz-Cruz, L. T. Arashiro, I. Ferrer, M. Garfí, and M. J. García-Galán, 2020, « Behavior of UV filters, UV blockers and pharmaceuticals in high rate algal ponds treating urban wastewater », *Water (Switzerland)* 12 (*10*): 1–17, ISSN: 20734441, https://doi.org/10.3390/w12102658.

Vaxelaire, J., N. Roche, and C. Pkost, 1995, « Oxygen transfer in activated sludge surface-aerated process », *Environmental Technology (United Kingdom)* 16 (*3*): 279–285, ISSN: 1479487X, https://doi.org/10.1080/09593331608616270.

Vergine, P., C. Salerno, A. Libutti, L. Beneduce, G. Gatta, G. Berardi, and A. Pollice, 2017, « Closing the water cycle in the agro-industrial sector by reusing treated wastewater for irrigation », *Journal of Cleaner Production* 164:587–596, ISSN: 09596526, https://doi.org/10.1016/j.jclepro.2017.06.239.

Voltolina, D., H. Gómez-Villa, and G. Correa, 2005, « Nitrogen removal and recycling by Scenedesmus obliquus in semicontinuous cultures using artificial wastewater and a simulated light and temperature cycle », *Bioresource Technology* 96 (*3*): 359–362, ISSN: 09608524, https://doi.org/10.1016/j.biortech.2004.04.004.

Vonshak, A., S. M. Cheung, and F. Chen, 2000, « Mixotrophic growth modifies the response of Spirulina (Arthrospira) platensis (Cyanobacteria) cells to light », *Journal of Phycology* 36 (*4*): 675–679, ISSN: 00223646, https://doi.org/10.1046/j.1529-8817.2000.99198.x.

Vymazal, J., 2011, « Constructed Wetlands for Wastewater Treatment: Five decades of experience », *Environmental Science and Technology* 45:61–69, https://doi.org/10.1021/es101403q.

Wainaina, S., 2021, « Chapter Seven - Microbial Conversion of Food Waste: Volatile Fatty Acids Platform », *in Current Developments in Biotechnology and Bioengineering,* 205–233, https://doi.org/https://doi.org/10.1016/B978-0-12-819148-4.00007-5.

Wang, H., V. Rudolph, and Z. Zhu, 2008, « Sewage Sludge Technologies », chapter Earth Syst *in Encyclopedia of Ecology,* 3227–3242, https://doi.org/10.1016/B978-008045405-4.00078-1.

Wang, S. H. Ho, C. L. Cheng, W. Q. Guo, D. Nagarajan, N. Q. Ren, D. J. Lee, and J. S. Chang, 2016, « Perspectives on the feasibility of using microalgae for industrial wastewater treatment », *Bioresource Technology* 222:485–497, ISSN: 18732976, https://doi.org/10.1016/j.biortech.2016.09.106, http://dx.doi.org/10.1016/j.biortech.2016.09.106.

Wang, X., Z. H. Qin, T. B. Hao, G. B. Ye, J. H. Mou, S. Balamurugan, X. Y. Bin, et al., 2022, « A combined light regime and carbon supply regulation strategy for microalgae-based sugar industry wastewater treatment and low-carbon biofuel production to realise a circular economy », *Chemical Engineering Journal* 446 (*P4*): 137422, ISSN: 13858947, https://doi.org/10.1016/j.cej.2022.137422, https://doi.org/10.1016/j.cej.2022.137422.

Wang, Y., W. Guo, H. W. Yen, S. H. Ho, Y. C. Lo, C. L. Cheng, N. Ren, and J. S. Chang, 2015, « Cultivation of Chlorella vulgaris JSC-6 with swine wastewater for simultaneous nutrient/COD removal and carbohydrate production », *Bioresource Technology* 198:619–625, ISSN: 18732976, https://doi.org/10.1016/j.biortech.2015.09.067, http://dx.doi.org/10.1016/j.biortech.2015.09.067.

Ward, B. B., D. J. Arp, and M. G. Klotz, 2011, « Nitrification: an introduction and overview of the state of the field », *in Nitrification,* edited by American Society for Microbiology Press, ISBN: 1555814816, 9781555814816.

Wegelin, M., S. Canonica, K. Mechsner, T. Fleischmann, F. Pesaro, and A. Metzler, 1994, « Solar water disinfection: Scope of the process and analysis of radiation experiments », *Aqua: Journal of Water Supply Research and Technology* 43 (*3*): 154–169, ISSN: 00037214.

Woo, M. H., Y. M. Hsu, C. Y. Wu, B. Heimbuch, and J. Wander, 2010, « Method for contamination of filtering facepiece respirators by deposition of MS2 viral aerosols », *Journal of Aerosol Science* 41 (*10*): 944–952, ISSN: 00218502, https://doi.org/10.1016/j.jaerosci.2010.07.003, http://dx.doi.org/10.1016/j.jaerosci.2010.07.003.

World Health Organisation, 2022, *Sanitation,* https://www.who.int/news-room/fact-sheets/detail/sanitation.

Xinjie, W., N. Xin, C. Qilu, X. Ligen, Z. Yuhua, and Z. Qifa, 2019, « Vetiver and Dictyosphaerium sp. co-culture for the removal of nutrients and ecological inactivation of pathogens in swine wastewater », *Journal of Advanced Research* 20:71–78, ISSN: 20901232, https://doi.org/10.1016/j.jare.2019.05.004, https://doi.org/10.1016/j.jare.2019.05.004.

Xu, X., W. Wang, Y. Zhang, Q. Meng, T. Huang, and W. Zhang, 2023, « Analysis on the properties of hydrolyzed amino acids in typical municipal sludge », *Environmental Science and Pollution Research* 30 (*21*): 60760–60767, ISSN: 16147499, https://doi.org/10.1007/s11356-023-26794-9, https://doi.org/10.1007/s11356-023-26794-9.

Yalin, D., H. A. Craddock, S. Assouline, E. Ben Mordechay, A. Ben-Gal, N. Bernstein, R. M. Chaudhry, et al., 2023, « Mitigating risks and maximizing sustainability of treated wastewater reuse for irrigation », *Water Research X* 21 (*July*), ISSN: 25899147, https://doi.org/10.1016/j.wroa.2023.100203.

Yan, Z., Z. Zhou, X. Sang, and H. Wang, 2018, « Water replenishment for ecological flow with an improved water resources allocation model », *Science of the Total Environment* 643:1152–1165, ISSN: 18791026, https://doi.org/10.1016/j.scitotenv.2018.06.085, https://doi.org/10.1016/j.scitotenv.2018.06.085.

Ye, Y., S. Ma, H. Peng, Y. Huang, W. Zeng, A. Xia, X. Zhu, and Q. Liao, 2023, « Insight into the comprehensive effect of carbon dioxide, light intensity and glucose on heterotrophic-assisted phototrophic microalgae biofilm growth: A multifactorial kinetic model », *Journal of Environmental Management* 325 (*PB*): 116582, ISSN: 10958630, https://doi.org/10.1016/j.jenvman.2022.116582, https://doi.org/10.1016/j.jenvman.2022.116582.

Young, P., N. Buchanan, and H. J. Fallowfield, 2016, « Inactivation of indicator organisms in wastewater treated by a high rate algal pond system », *Journal of Applied Microbiology* 121 (*2*): 577–586, ISSN: 13652672, https://doi.org/10.1111/jam.13180.

Young, P., M. Taylor, and H. J. Fallowfield, 2017, « Mini-review: high rate algal ponds, flexible systems for sustainable wastewater treatment », *World Journal of Microbiology and Biotechnology* 33 (*6*): 1–13, ISSN: 15730972, https://doi.org/10.1007/s11274-017-2282-x.

Young, P., M. J. Taylor, N. Buchanan, J. Lewis, and H. J. Fallowfield, 2019a, « Case study on the effect continuous CO2 enrichment, via biogas scrubbing, has on biomass production and wastewater treatment in a high rate algal pond », *Journal of Environmental Management* 251 (*August*): 109614, ISSN: 10958630, https://doi.org/10.1016/j.jenvman.2019.109614, https://doi.org/10.1016/j.jenvman.2019.109614.

Young, P., M. J. Taylor, N. Buchanan, J. Lewis, and H. J. Fallowfield, 2019b, « Case study on the effect continuous CO2 enrichment, via biogas scrubbing, has on biomass production and wastewater treatment in a high rate algal pond », *Journal of Environmental Management* 251 (*August*): 109614, ISSN: 10958630, https://doi.org/10.1016/j.jenvman.2019.109614, https://doi.org/10.1016/j.jenvman.2019.109614.

Zema, D. A., G. Bombino, S. Andiloro, and S. M. Zimbone, 2012, « Irrigation of energy crops with urban wastewater: Effects on biomass yields, soils and heating values », *Agricultural Water Management* 115:55–65, ISSN: 03783774, https://doi.org/10.1016/j.agwat.2012.08.009, http://dx.doi.org/10.1016/j.agwat.2012.08.009.

Zeng, J., Z. Wang, and G. Chen, 2021, « Biological characteristics of energy conversion in carbon fixation by microalgae », *Renewable and Sustainable Energy Reviews* 152 (*January*): 111661, ISSN: 18790690, https://doi.org/10.1016/j.rser.2021.111661, https://doi.org/10.1016/j.rser.2021.111661.

Zhang, H., W. Gong, L. Bai, R. Chen, W. Zeng, Z. Yan, G. Li, and H. Liang, 2020, « Aeration-induced CO2 stripping, instead of high dissolved oxygen, have a negative impact on algaebacteria symbiosis (ABS) system stability and wastewater treatment efficiency », *Chemical Engineering Journal* 382 (*June 2019*): 122957, ISSN: 13858947, https://doi.org/10.1016/j.cej.2019.122957, https://doi.org/10.1016/j.cej.2019.122957.

Zhang, Z., D. Sun, K. W. Cheng, and F. Chen, 2021, « Investigation of carbon and energy metabolic mechanism of mixotrophy in Chromochloris zofingiensis », *Biotechnology for Biofuels* 14 (*1*): 14–36, ISSN: 17546834, https://doi.org/10.1186/s13068-021-01890-5, https://doi.org/10.1186/s13068-021-01890-5.

Zhang, Z., D. Sun, T. Wu, Y. Li, Y. Lee, J. Liu, and F. Chen, 2017, « The synergistic energy and carbon metabolism under mixotrophic cultivation reveals the coordination between photosynthesis and aerobic respiration in Chlorella zofingiensis », *Algal Research* 25 (*April*): 109–116, ISSN: 22119264, https://doi.org/10.1016/j.algal.2017.05.007, http://dx.doi.org/10.1016/j.algal.2017.05.007.

Zhao, G., T. Sun, D. Wang, S. Chen, Y. Ding, Y. Li, G. Shi, et al., 2023a, « Treated wastewater and weak removal mechanisms enhance nitrate pollution in metropolitan rivers », *Environmental Research* 231 (*P2*): 116182, ISSN: 10960953, https://doi.org/10.1016/j.envres.2023.116182, https://doi.org/10.1016/j.envres.2023.116182.

Zhao, X., S. Lu, X. Guo, R. Wang, M. Li, C. Fan, and H. Wu, 2023b, « Effects of disturbance modes and carbon sources on the physiological traits and nutrient removal performance of microalgae (S. obliquus) for treating low C/N ratio wastewater », *Chemosphere,* https://doi.org/https://doi.org/10.1016/j.chemosphere.2023.140672, https://doi.org/10.1016/j.chemosphere.2023.140672.

Zhao, X., K. Kumar, M. A. Gross, T. E. Kunetz, and Z. Wen, 2018, « Evaluation of revolving algae biofilm reactors for nutrients and metals removal from sludge thickening supernatant in a municipal wastewater treatment facility », *Water Research* 143:467–478, ISSN: 18792448, https://doi.org/10.1016/j.watres.2018.07.001, https://doi.org/10.1016/j.watres.2018.07.001.

Zhong, Q., A. Carratala, S. Nazarov, R. C. Guerrero-Ferreira, L. Piccinini, V. Bachmann, P. G. Leiman, and T. Kohn, 2016, « Genetic, Structural, and Phenotypic Properties of MS2 Coliphage with Resistance to ClO2 Disinfection », *Environmental Science and Technology* 50 (*24*): 13520–13528, ISSN: 15205851, https://doi.org/10.1021/acs.est.6b04170.

Titre : Vers une meilleure compréhension des interactions cinétiques entre les microalgues et les bactéries - Du laboratoire à un high rate algal pond à grande échelle

Mot clés : high rate algal pond, photobioréacteur, carbone, oxygène, mixotrophie

Résumé : Les high rate algal ponds (HRAP) sont des systèmes de traitement des eaux usées peu énergivores où les microalgues produisent l'oxygène pour la dégradation aérobie de la matière organique par les bactéries. Cette thèse propose une approche intégrative impliquant différents systèmes d'étude pour étudier les interactions au sein du consortium microalgues-bactéries dans de tels sytèmes. L'hypothèse selon laquelle le carbone organique est consommé uniquement par les bactéries a été discuté dans la littérature, soulevant l'hypothèse d'une croissance microalgale hétérotrophe significative impactant potentiellement les interactions avec les bactéries. Au regard de la complexité des interactions trophiques dans le consortium microalgues-bactéries, une étude en photobioréacteur (PBR) de laboratoire en conditions contrôlées utilisant de l'acétate comme source de carbone organique et couplée à une approche de modélisation a été conduite. Ces outils se sont avérés sursimplifiés, cependant ce travail a révélé que les interactions entre les microalgues et les bactéries en high rate algal pond pourraient être plus complexes qu'une simple synergie reposant sur des échanges d'O_2 et de CO_2. Par ailleurs, les microalgues ont joué un rôle majeur non seulement dans les interactions trophiques avec les bactéries mais également dans les méchanismes de désinfection par la production d'espèces réactives à l'oxygène.

Title: Towards a better understanding of kinetic interactions between microalgae and bacteria - From lab to large-scale high rate algal pond

Keywords: high rate algal pond, photobioreactor, carbon, oxygen, mixotrophy

Abstract: High rate algal ponds (HRAP) are low-energy consuming wastewater treatment systems where microalgae provide the oxygen to bacteria for aerobic degradation of organic matter. This thesis propose an integrative approach involving different study systems to investigate interactions within the microalgae-bacteria consortium in high rate algal ponds. The assumption that organic carbon is consumed solely by bacteria in HRAP has been discussed in the literature, raising the hypothesis that heterotrophic growth of microalgae could be relevant and potentially impacting the interactions with bacteria. Considering the complexity of trophic interactions inside the microalgae-bacteria consortium, a study in laboratory photobioreactor in controlled conditions using acetate as the organic carbon source and coupled to a modeling approach was conducted. These tools turned out to be oversimplified, however this work revealed that interactions between microalgae and bacteria in high-rate algal ponds would be more complex than a simple synergy relying on O_2 and CO_2 exchanges. Besides, microalgae played a major role not only in trophic interactions with bacteria but also in disinfection mechanisms through Reactive Oxygen Species production.